

Chapter 0

Power System System Control Engineering

Measurement / control selection series

Takayuki Ishizaki, Takahiro Kawaguchi, Kenichi Kawabe

Preface

May 2022Takayuki Ishizaki

In Japan, the Great East Japan Earthquake of 2011 triggered the start of electric power system reform. In 2012, the following year, the Ministry of Education, Culture, Sports, Science and Technology (MEXT) launched the "Creation and Integration of Theories and Fundamental Technologies for the Construction of Distributed and Cooperative Energy Management Systems" as a project-type research project by the Japan Science and Technology Agency (JST). The authors, Ishizaki and Kawaguchi, are researchers who participated in the project, specializing in systems and control engineering, and were engaged in the research and development of renewable energy as a main power source.

The impetus for writing this book came from our own experience of the "high barriers to entry for power system R&D" in the above project. At the beginning of the project, we were complete amateurs in the field of power systems. We started learning the basics of related fields to conduct our research, but we could not understand most of the things that we should have been familiar with in systems and control engineering, such as differential equations and optimization, in the context of power system engineering. The reason for this was that power system engineering is a practical academic discipline that emphasizes the reality of power systems, while systems control engineering is a mathematical discipline with its origins in mathematics, and thus has very different academic values and styles. This difference in awareness of the underlying issues is also thought to be a factor that hinders practical communication between researchers in systems and control engineering and those in power system engineering. As our daily research activities revealed this hindsight, we came to strongly feel the necessity of bridging the gap between the disciplines.

This book is intended for students, researchers, and engineers in the field of systems and control who wish to work on research and development of power systems with the purpose of:

- To be able to understand the structural and mathematical basis of power systems in the language of systems and control engineering

- To be able to independently build a numerical simulation environment for power system analysis and control

Specifically, for the former purpose, the configuration and characteristics of power systems are explained using basic concepts such as equations of state, equilibrium points, stability, and feedback in systems and control engineering. The prerequisite knowledge required for this course is linear algebra, dynamical systems theory, and AC circuit theory from liberal arts courses at universities. For the latter purpose, in addition to illustrating scripts for running numerical simulations, the fundamentals of object-oriented thinking and programming techniques that describe the entire complex power system as a group of modules divided by function will be explained. A power system is not a single mechanical system, but a synthesis of a wide variety of elements and many decision makers. Therefore, the numerical simulation environment should be modularized accordingly. A distributed development environment structured into a group of modules is also very useful as a common base for aggregating the knowledge of multiple people. Although this document assumes implementation in MATLAB, the core ideas should be applicable to other programming languages as well.

Finally, it should be noted that all authors have made every effort to ensure that the descriptions throughout this document are as accurate as possible. In particular, the author, Kawabe, checked the terminology and wording related to power systems from a professional perspective in power system engineering. In addition, students and collaborators in the authors' laboratories pointed out errors and unclear descriptions, and the authors have worked hard to improve the manuscript. The authors would like to thank Masahiro Ito, Taku Nishino, Miki Taya, Yota Kimura, Yoshihito Kinoshita, Yoshiyuki Onishi, Taichi Ichimura, Kentaro Oda, and Hirohiro Kawano for their significant contributions in writing and improving the manuscript.

We hope that this book will be a catalyst for new learning for those involved in systems and control engineering and help support the future of electric power systems.

Contents

1	Introduction	9
1.1	Control of electrical power system	9
1.1.1	Importance of interdisciplinary integration aimed at power system reform	9
1.1.2	Objective of this book	10
1.1.3	Characteristics of this book	11
1.2	How to use this book	11
1.2.1	Overall structure	11
1.2.2	Published numerical simulation codes and supplementary material	12
1.2.3	Mathematical notations	12
2	Mathematical model of electrical power systems	15
2.1	Foundation of AC circuit theory	15
2.1.1	Circuit elements	15
2.1.2	Instantaneous value and effective value	16
2.1.3	Phasor representation	17
2.1.4	Impedance and admittance	18
2.2	Admittance matrix: representation of interaction between connected devices	19
2.2.1	Fundamentals of modeling of power grids	19
2.2.2	Power grid model with capacitance to ground	23
2.2.3	Mathematical properties of the admittance matrix	24
2.3	Mathematical model of synchronous generators	25
2.3.1	Classification of generator models based on the level of detail	25
2.3.2	Mathematical expression of the one-axis model	26
2.3.3	Kron reduction of a generator bus	30
2.3.4	Derivation of the Kuramoto-type oscillator model	37
2.3.5	Single machine infinite bus system model	40

2.3.6	Mathematical properties of the admittance matrix with reduced generator bus	41
2.3.7	Mathematical model of salient pole synchronous generators	42
2.4	Mathematical model of load	46
2.4.1	Relational expression of current and voltage according to load characteristics	46
2.4.2	Kron reduction of load bus bar	47
2.4.3	Mathematical properties of the admittance matrix with reduced load bus bar	49
	Mathematical Supplement	52
3	Numerical simulation of the electrical power system model	57
3.1	Calculation of time response of an electrical power system	57
3.1.1	Challenges in calculating time response	57
3.1.2	Calculation steps	58
3.2	Numerical analysis of steady-state in power flow calculation	59
3.2.1	Outline of the power flow calculation	60
3.2.2	Numerical Search Method for Steady-State Power Flow ..	63
3.2.3	The relationship between the admittance matrix and transmission loss	66
3.3	The steady state of generators achieving desired power supply	68
3.3.1	The steady state of generators that achieves a desired supply of electric power	69
3.3.2	Load Parameters for Achieving Desired Power Consumption	70
3.3.3	mathematical relationship between generator internal state and input/output	71
3.4	Time Response Calculation of Power System Model	76
3.4.1	Initial Value Response	77
3.4.2	Response to Parameter Variations of the Load Model	79
3.4.3	Response to ground fault	80
3.5	Synchronization of bus bar voltage in a steady power flow distribution	84
3.6	Implementation of Power Flow Calculation	92
3.6.1	Solving Algebraic Equations	92
3.6.2	Simple implementation of power flow calculation	94
3.6.3	Implementation of Power Flow Calculation using Separated Modules	97
3.7	Implementation method for time response calculation of power system models	103
3.7.1	Simple implementation of time response calculations for power system models	107
3.7.2	Implementation method for time response calculation using a group of partitioned modules	110

Contents	7
Mathematical Appendix	123
4 Steady-state stability analysis of power system models	125
4.1 Stability analysis based on linear approximation	126
4.1.1 Approximate linearization of the power system model ..	126
4.1.2 Stability analysis of approximate linear models	129
4.2 stability analysis of approximate linear models using numerical calculations	131
4.2.1 Implementation of approximate linearization using a group of partitioned modules	131
4.2.2 Numerical analysis of small signal stability	136
4.3 Mathematical stability analysis of the linearized model [‡]	139
4.3.1 Small signal stability of the linearized model	139
4.3.2 Passivity of approximate linear models	141
4.3.3 Analysis of small signal stability based on passivity [‡] ..	147
4.3.4 Necessary conditions for the approxiamte linear model to be passive [‡]	156
4.3.5 Necessary condition for the steady-state stability of the approximate linear model [‡]	165
Mathematical Appendix	169
5 Stabilization control of power system models	171
5.1 Frequency stabilization control	171
5.1.1 Automatic generation control using broadcast-type PI controller	171
5.1.2 Numerical simulation of frequency stabilization control .	175
5.2 Mathematical stability analysis of frequency stabilization control system	178
5.2.1 Power system model under consideration	178
5.2.2 Equilibrium-independent passivity of power system models	180
5.2.3 Stability analysis of frequency stabilization control system	188
5.3 Transient stability control	194
5.3.1 Decentralized control of generators with excitation system	194
5.3.2 Standard Automatic Voltage Regulator model	194
5.3.3 Control effectiveness of AVR	199
5.3.4 Power System Stabilizer	202
5.3.5 Control Effect of Power System Stabilization Device ..	204
5.4 PSS based on the retrofit control theory	205
5.4.1 Power system model used in the design of PSS	205
5.4.2 PSS design based on the retrofit control theory	209
6 Numerical simulation examples of a large-scale model	215
6.1 Power system model under consideration	215
6.1.1 IEEE68 bus system model	215

6.1.2	Data sheet for power flow calculation	216
6.1.3	Load model	216
6.2	Frequency stability analysis for load fluctuations	217
6.2.1	Load fluctuation settings	217
6.2.2	When the machine input and field input of the generator are constant	217
6.2.3	Case where the Mechanical Input is Constant	217
6.2.4	Case where machine input is controlled by an automatic generation controller	219
6.3	Transient stability analysis for bus ground faults	220
6.3.1	Setting of ground fault	220
6.3.2	Effect of power system stabilizers bassed on retrofit control theory	221
	References	223
	References	223

Chapter 1

Introduction

In this Chapter, the objectives, characteristics and instructions of how to use this book will be explained. The mathematical notation used in this book will also be summarized.

1.1 Control of electrical power system

1.1.1 Importance of interdisciplinary integration aimed at power system reform

In Japan, the reformation of the power system began with the Great East Japan Earthquake in March 2011, and the full-scale introduction of renewable energy, such as solar, wind and geothermal power took place after the full liberalization of the electricity retail market in April 2016. Furthermore, in October 2020, Japan pledged to achieve carbon neutrality by 2050 as a matter of national policy. Thus, improvements to the existing energy supply system and maximization of the use of renewable energy are strongly required. To achieve such an ambitious goal, technologies related to energy generation, as well as digital technologies, such as telecommunications, must be fully utilized to create a smart grid that improves the operation of power systems and to control supply and demand of renewable energy, where power supply fluctuates with weather.

A power system is a large-scale system that consists of the interaction of events and phenomena on a wide range of spatio-temporal scales. Specifically, the operation of actual power systems is influenced not only by the properties of electromechanical devices and facilities, such as generators and transmission lines, but also by natural phenomena, such as weather condition and natural disasters, and human-related activities, such as electricity demand by the consumers, and commercial activities of power generation, transmission and distribution companies.

Therefore, the reformation of current power systems should be supported by the expertise of various academic fields in addition to energy-related fields. For instance, notions of economics are essential for designing a fair market system capable of adding value to the planned and observed values of energy supply and demand, and at the same time avoiding monopoly formation. In addition, to manage the uncertainties of renewable energy generation, it is imperative to develop methods to plan supply and demand and to forecast power generation from these resources. For this purpose, notions of mathematical optimization and statistics are fundamental. Finally, expertise in feedback control methods is essential for improving system stability against disturbances such as load fluctuations and ground faults.

In summary, the design and operation of power systems require expertise of various research fields. This academic diversity will lead to challenging yet attractive research and development topics.

1.1.2 Objective of this book

Control systems engineering is an interdisciplinary field that covers many areas of science, such as control theory, information theory, data science, systems engineering and mathematical optimization, and it is expected to contribute to the research and development of power systems. However, since power systems are complex systems composed by a wide range of devices and phenomena, it is often very challenging for beginners to get an overview of the whole system. This difficulty hinders the contribution of experts in other areas in research and development of power systems. This book attempts to tackle this problem by providing an introduction and an overview of power systems.

By explaining modeling, numerical simulation, control system design and mathematical analysis for power systems will be explained from a viewpoint of network system analysis and control, this book aims to make students and researchers in the field of system control to be able to:

- understand the structure of power systems and mathematical foundation in the language of control systems engineering, and
- build a numerical simulation environment for analysis and control of power systems on their own.

For this purpose, the structure and characteristics of power systems will be explained by using fundamental concepts of control systems engineering, such as state-space representation, equilibrium point, stability and feedback control. In addition, the numerical simulation environment will be conducted based on the foundations of object-oriented programming, describing the entire complex power system as classes and methods and providing code examples for easier understanding.

1.1.3 Characteristics of this book

Review English in this section There are many good books, both in Japanese and other languages, on electrical power systems. Characteristics of this book compared to these books are as follows:

- one can follow this book without a background in electromagnetism, and
- the structure and characteristics of power systems as a network system are clearly described.

For example, a standard book on electrical power system engineering assumes that one has knowledge on three-phase electric power and electromagnetic induction, and focuses on the explanation of electromagnetic phenomena inside of each generator and so on. Meanwhile, as far as the authors are aware, there are few if any books that clearly explain the dynamic characteristics and structures of the whole system when multiple generators are connected via a power grid from the viewpoint of control systems engineering. In addition, while a model in which multiple generators are connected in a power grid is used to analyze power transmission distribution, known as power flow calculation, in system stability discussions, different models are often introduced depending on the topic of discussions (e.g., single machine infinite bus system models, models consisting of only one generator). This makes it difficult for novice learners who are unfamiliar with electrical power system engineering to see the link between explained topics and gain a comprehensive view of the entire power system. Considering these situations, this book presents essential basics for students, researchers, and technologists in the field of system control to “understand” the structure and characteristics of power systems “based on system theory.”

As discussed above, various academic knowledge is required to design and operate power systems. With the help of the information in this book, we hope that challenging and attractive research and development targets will be used as one of the benchmark models in the field of system control.

1.2 How to use this book

1.2.1 Overall structure

Review English in this section This book introduces mathematical models of electrical power systems in Chapter 2, then explains the steps for numerical simulation of the electrical power system model in Chapter 3. This is followed by discussions of the stability of the electrical power system model in Chapter 4 and control methods to improve the system stability in Chapter 5. Finally, in Chapter 6, we present the results of numerical simulations using a large-scale electrical power system model.

This book assumes that readers will follow from Chapter 2 to Chapter 6 in that order. However, readers who aim to perform numerical simulations on their own can skip Sections with “†” in the title. These Sections primarily describe development topics that are useful in understanding the mathematical structure of the electrical power system model. Since this book focuses on explanations of the basics of electrical power system analysis, topics related to new energy, such as solar power, wind power, and batteries are not presented. Please refer to [1] for these topics.

1.2.2 Published numerical simulation codes and supplementary material

Review English in this section The numerical simulations described in this document were created with a Matlab program called GUILDA (Grid & Utility Infrastructure Linkage Dynamics Analyzer), which is being developed mainly by the authors. and can be freely extended by users. The programs used for the numerical simulations in this book are also available. For details, please refer to the web page of this book by Corona Inc. for more details. Color versions of the figures in this book are also provided. Translated with www.DeepL.com/Translator (free version)

1.2.3 Mathematical notations

Real numbers and complex numbers are expressed as \mathbb{R} and \mathbb{C} , respectively. Real vectors with n dimensions are expressed as \mathbb{R}^n , while real matrices with dimensions $n \times m$ are expressed as $\mathbb{R}^{n \times m}$. The same style of notation is used for complex vectors and matrices. In addition, the imaginary unit is expressed as j , and bold font is used for complex scalars, vectors and matrices.

A vector in which all elements are one is expressed as $\mathbb{1}$. A diagonal matrix that has real scalar, c_1, \dots, c_n , as diagonal elements is expressed as $(c_i)_{i \in \{1, \dots, n\}}$. When it is clear from the context, subscripts are omitted and the diagonal matrix is simply expressed as $\text{diag}(c_i)$. The same applies to complex numbers. In addition, the inverse matrix of a nonsingular complex matrix Z is expressed as Z^{-1} .

The transposed matrix of real matrix A is expressed as A^\top . The real and imaginary parts of a complex matrix Z are expressed as $\text{Re}[Z]$ and $i[Z]$, respectively. In other words, for an arbitrary complex matrix Z :

$$Z = \text{Re}[Z] + j\text{i}[Z]$$

In addition, the conjugate of a complex matrix Z is expressed as \bar{Z} , and the conjugate of its transpose is expressed as Z^* . In other words:

$$\bar{Z} = \text{Re}[Z] - j\text{i}[Z], \quad Z^* = (\text{Re}[Z])^\top - j(\text{i}[Z])^\top$$

The absolute value of a complex scalar z is expressed as $|z|$, while its argument is expressed as $\angle z$. In other words, $z = |z|e^{j\angle z}$.

When complex symmetric matrix $Z = Z^*$ is positive definite, it is written as $Z > 0$. When Z is positive semi-definite, it is written as $Z \geq 0$. Similarly, negative definite and negative semi-definite are expressed with inequality signs of the opposite direction.

COFFEE BREAK

Singularity of matrix: A square matrix A is said to be **regular**(nonsingular) if it has an inverse A^{-1} such that:

$$AA^{-1} = I$$

The above condition is true if and only if the determinant of A is non-zero.

Positive and negative definiteness of matrices: For a given complex vector x , a square matrix A is said to be **positive semi-definite** if the following relationship is true:

$$x^*Ax \geq 0$$

Additionally, A is **positive definite** if $x \neq 0$ and:

$$x^*Ax > 0$$

The definition of semi-negative and negative definiteness are similar, with the only difference being the sign of the inequality. A necessary and sufficient condition for a complex symmetric matrix A to be positive semi-definite is that all its eigenvalues are non-negative. Similarly, a necessary and sufficient condition for A to be positive definite is that all its eigenvalues are strictly positive.

The null space of real matrix $A \in \mathbb{R}^{n \times m}$, $\ker A$, is defined as:

$$\ker A := \{x \in \mathbb{R}^m : Ax = 0\}$$

where the symbol “:=” means that the term on the right side of the symbol defines the term on its left side. The null space of a complex matrix $Z \in \mathbb{C}^{n \times m}$ is similarly defined as:

$$\ker Z := \{x \in \mathbb{C}^m : Zx = 0\}$$

Moreover, given a set of real vectors $v_1, \dots, v_m \in \mathbb{R}^n$, the linear space formed by all the vectors that can be written as linear combination of vectors v_1, \dots, v_m is defined as:

$$\text{span}\{v_1, \dots, v_m\} := \{c_1v_1 + \dots + c_mv_m : (c_1, \dots, c_m) \in \mathbb{R} \times \dots \times \mathbb{R}\}$$

Finally, the Euclidean norm of a real vector $x \in \mathbb{R}^n$ is represented by $\|x\|$. In other words:

$$\|x\| := \sqrt{|x_1|^2 + \dots + |x_n|^2}$$

where the x_i is the i th element of x .

Please note that, in this book, standard symbols in control systems and electrical power system engineering might overlap. For example, in control systems engineering, “ G ” is often used to represent a system, whereas in electrical power system engineering, it is commonly used to express conductance. Unless there is a concern about misunderstanding of the context, overlaps between these symbols will not be discussed.

Chapter 2

Mathematical model of electrical power systems

In this Chapter, we explain the mathematical model of electrical power systems. In summary, we show that the dynamics of synchronous generators can be described by differential equations, and loads can be described by algebraic equations. Therefore, by combining both the equations of loads and synchronous generators, the entire electrical power system can be expressed as nonlinear differential-algebraic equations.

The current Chapter is structured as follows. First, in Section 2.1, we introduce to the basic concept of impedance and admittance of circuit elements and phasor representation of current and voltage in AC circuits. Next, in Section 2.2, we introduce the concept of nodal admittance matrix, which is a mathematical model of power grids. In Sections 2.3 and 2.4, mathematical models for generators and loads are explained. Specifically, in Section 2.3, we show that the model of a power grid composed only by generators can be expressed as a nonlinear ordinary differential equation through Kron reduction of the generator buses. The behavior of such an ordinary differential equation system is shown through a numerical simulation.

2.1 Foundation of AC circuit theory

2.1.1 Circuit elements

The basic circuit elements used in mathematical modeling of electrical power systems include resistors, inductors and capacitors. The relationship between terminal voltage and terminal current of each element is presented as follows:

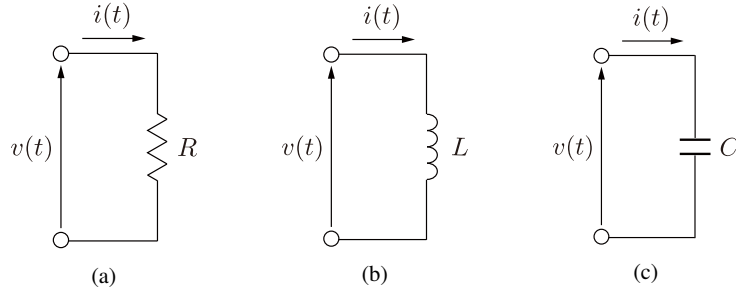


Fig. 2.1 Basic circuit of resistors, inductors, and capacitors.

- (a) **Resistor:** For the resistor with resistance $R [\Omega]$ shown in 2.1(a), the following relationship holds between the terminal voltage $v [V]$ and terminal current $i [A]$:

$$v(t) = Ri(t) \quad (2.1)$$

where $R \geq 0$.

- (b) **Inductor:** For the inductor with inductance $L [H]$ shown in 2.1(b), the following relationship holds between the terminal voltage and terminal current:

$$v(t) = L \frac{di}{dt}(t) \quad (2.2)$$

where $L \geq 0$.

- (c) **Capacitor:** For the capacitor with capacitance $C [F]$ shown in 2.1(c), the following relationship holds between the terminal voltage and terminal current:

$$i(t) = C \frac{dv}{dt}(t) \quad (2.3)$$

where $C \geq 0$.

2.1.2 Instantaneous value and effective value

- (a) **Instantaneous value:** The instantaneous value of an AC quantity is an expression of this quantity in function of time t . For example, for a sinusoidal alternating voltage, its instantaneous value can be expressed by:

$$v(t) = V_m \sin(\omega t + \phi) \quad (2.4)$$

where V_m [V] is the voltage amplitude, ω [rad/s] is the angular frequency, and ϕ [rad] is the phase. The sine wave period T [s] is expressed as follows using ω :

$$T := \frac{2\pi}{\omega} \quad (2.5)$$

Frequency f [Hz] is expressed as its reciprocal $f := \frac{1}{T}$. Due to the characteristics of the elements presented in Section 2.1, when the instantaneous value of voltage is a sine wave, the instantaneous value of the current also becomes a sine wave.

- (b) **Effective value:** The effective value of an AC quantity corresponds to the square root of the average of the square of the values over a period of time T . Because of this definition, the effective value is also called **RMS value** (root mean square value). For example, for the resistor in 2.1(a), the average electric power consumed in one period can be calculated as follows:

$$\frac{1}{T} \int_t^{t+T} v(\tau)i(\tau)d\tau = \frac{1}{R} \left(\underbrace{\frac{V_m}{\sqrt{2}}}_{V_e} \right)^2 \quad (2.6)$$

where V_e is the **effective value** of voltage. The effective value of the current is defined in the same manner. Since the average electric power can be described simply by using the effective value of voltage and current, the effective value is often used to perform calculations for AC circuit. The effective value is also used for the phasor representation of voltage and current introduced below.

2.1.3 Phasor representation

The AC voltage waveform of Equation 2.4 can be represented in the complex plane as in Figure 2.2. In this case, $v(t)$ is expressed by the following equation:

$$v(t) = i \left[V_m e^{j(\omega t + \phi)} \right] \quad (2.7)$$

In an electrical power system, the angular frequency ω can be considered constant and equal to the reference angular speed. Under this assumption, the voltage $v(t)$ of Equation 2.7 can be uniquely expressed by the phase ϕ , which can be derived from ωt and the amplitude V_m . Then, by using the effective value as an expression of the amplitude, we can obtain:

$$V := V_e e^{j\phi} \quad (2.8)$$

This is called the **phasor representation** of voltage. When an electrical power system is in a steady state, the phasor V is constant. In other words, the absolute value $|V| = V_e$ and phase $\angle V = \phi$ are constant. On the other hand, when an electrical

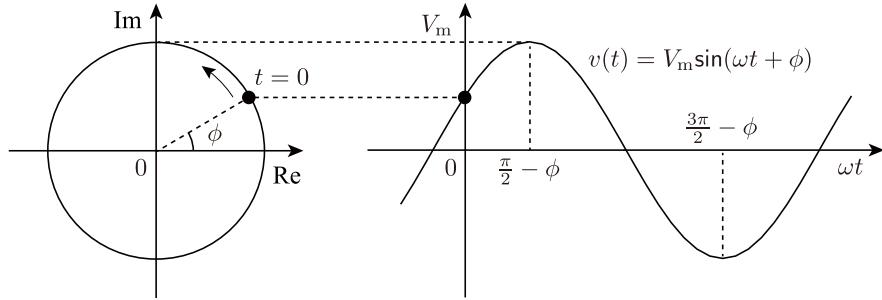


Fig. 2.2 Complex plane representation of AC voltage

power system is in a transient state, the temporal changes of $|V|$ and $\angle V$ have to be analyzed. The definition for the current phasor I is the same.

2.1.4 Impedance and admittance

The concept of impedance Z [Ω] arises when expressing the relationship between voltage and current using the phasor representation explained in Section 2.1.3. It is equivalent to the resistance in DC circuits, and corresponds to an opposition to alternating current. For the typical circuit elements presented in Section 2.1, the phasor representations of their terminal voltage and current V, I respect the following relationship.

$$V = ZI \quad (2.9)$$

The impedance of resistors, inductors and capacitors are, respectively:

$$Z_R := R, \quad Z_L := j\omega L, \quad Z_C := \frac{1}{j\omega C}$$

Please note that the characteristics of components such as synchronous generators and power converters may not be expressed using only constant impedances.

The real part of impedance is called **resistance** and the imaginary part is called **reactance**. As standard symbols, R [Ω] is used for resistance and X [Ω] is used for reactance. In other words:

$$Z = R + jX$$

The reciprocal Z^{-1} of impedance is called **admittance**. As a standard symbol, Y [S] is used. In addition, the real part of admittance is called **conductance** and the imaginary part is called **susceptance**. As a standard symbol, G [S] is used for conductance and B [S] is used for susceptance. In other words:

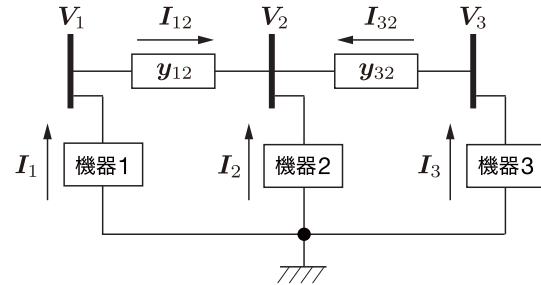


Fig. 2.3 Power system model composed of three bus bars

$$Y = G + jB$$

The reading of each physical unit presented so far is, V: volt, A: ampere, Ω : ohm, H: henry, F: farad, rad: radian, s: second, Hz: hertz, and S: siemens.

2.2 Admittance matrix: representation of interaction between connected devices

2.2.1 Fundamentals of modeling of power grids

In this section we derive the **admittance matrix** of a power grid, which expresses the interaction between the devices connected to an electrical power system

We derive the **admittance matrix** of a power grid that shows the interaction of equipment connected to an electrical power system using a basic transmission line model. The admittance matrix is derived from Ohm's law and Kirchhoff's laws for each bus bar and the transmission lines that connect them. Depending on the literature, the bus bar may also be called a **node** or **bus**. In this book, the bus bar is shown with a thick line in the diagram of an electrical power system. The bus bar is a conductor where the end of the transmission line has been collected. The thin line that connects the bus bar represents the transmission line.

Example 2.1 Admittance matrix of a power grid

Let us consider a simple electrical power system consisting of three bus bars as shown in Fig. 2.3. Assume that to each bus there is a device connected. In this book, the word "device" refers to synchronous generators and loads.¹ In addition, in an electrical power system model circuit such as that shown in 2.3, the connection to ground is often omitted for simplification.

¹ In this book, we analyze only load and generators, however, when considering solar generators, wind generators and batteries, these are also classified as "devices".

Below, the voltage phasor of bus bar i with respect to the ground is expressed as $\mathbf{V}_i \in \mathbb{C}$, and the current phasor flowing from the device to the bus bar i is expressed as $\mathbf{I}_i \in \mathbb{C}$. The voltage and current phasors are unknown variables, therefore it is necessary to find an equation governed by the power grid that establishes a relationship between the current phasor $(\mathbf{I}_1, \mathbf{I}_2, \mathbf{I}_3)$ and the current phasor $(\mathbf{V}_1, \mathbf{V}_2, \mathbf{V}_3)$ of the bus bars. For this purpose, we define the admittance matrix of the power grid.

The admittance of a transmission line that connects bus bars i and j is expressed as $y_{ij} \in \mathbb{C}$, with y_{ij} being known variables for every pair of bus bars ij . Additionally, the current phasor that flows in each transmission line is expressed as $\mathbf{I}_{ij} \in \mathbb{C}$, where y_{ij} and y_{ji} are equal. In addition, the sign for \mathbf{I}_{ij} is positive for an arbitrarily determined direction, and $\mathbf{I}_{ji} = -\mathbf{I}_{ij}$ are equal. The current phasor of this transmission line is an intermediate variable that describes the physical relationship of the current phasor and voltage phasor of the bus bars. Specifically, if the sign of the current phasor is defined positive for the direction indicated by the arrows in Fig. 2.3, the following relationship can be obtained by applying the Ohm's law:

$$\mathbf{I}_{12} = \mathbf{y}_{12}(\mathbf{V}_1 - \mathbf{V}_2), \quad \mathbf{I}_{32} = \mathbf{y}_{32}(\mathbf{V}_3 - \mathbf{V}_2)$$

According to Kirchhoff's first law (current law), since the sum of all current on each bus bar is 0, the following relationship is obtained for bus bar 1 to bus bar 3.

$$\mathbf{I}_1 - \mathbf{I}_{12} = 0, \quad \mathbf{I}_2 + \mathbf{I}_{12} + \mathbf{I}_{32} = 0, \quad \mathbf{I}_3 - \mathbf{I}_{32} = 0$$

Note that Kirchhoff's first law states that the sum of inflow currents and the sum of outflow currents are equal at the point where an electric circuit branches. By replacing the variables \mathbf{I}_{ij} by the previously calculated relationship $\mathbf{I}_i = \mathbf{y}_{ij}(\mathbf{V}_1 - \mathbf{V}_2)$, we can find the following vectorized version of the Ohm's law:

$$\begin{bmatrix} \mathbf{I}_1 \\ \mathbf{I}_2 \\ \mathbf{I}_3 \end{bmatrix} = \begin{bmatrix} \mathbf{y}_{12} & -\mathbf{y}_{12} & 0 \\ -\mathbf{y}_{12} & \mathbf{y}_{12} + \mathbf{y}_{32} & -\mathbf{y}_{32} \\ 0 & -\mathbf{y}_{32} & \mathbf{y}_{32} \end{bmatrix} \begin{bmatrix} \mathbf{V}_1 \\ \mathbf{V}_2 \\ \mathbf{V}_3 \end{bmatrix} \quad (2.10)$$

The complex matrix obtained in this manner is the admittance matrix of the power grid. Since each transmission line is usually expressed as a circuit with an equivalent resistance and inductance, the real part (conductance) of the admittance of the transmission line \mathbf{y}_{ij} is non-negative, and the imaginary part (susceptance) is non-positive. Specifically, the imaginary part is usually negative (non-zero).

Below, we consider an electrical power system connected with N bus bars. Then, the admittance matrix $\mathbf{Y} \in \mathbb{C}^{N \times N}$ of the power grid gives the following relationship to the current phasor $(\mathbf{I}_1, \dots, \mathbf{I}_N)$ and voltage phasor $(\mathbf{V}_1, \dots, \mathbf{V}_N)$ of the bus bars.

$$\begin{bmatrix} \mathbf{I}_1 \\ \vdots \\ \mathbf{I}_N \end{bmatrix} = \underbrace{\begin{bmatrix} \mathbf{Y}_{11} & \cdots & \mathbf{Y}_{1N} \\ \vdots & \ddots & \vdots \\ \mathbf{Y}_{N1} & \cdots & \mathbf{Y}_{NN} \end{bmatrix}}_{\mathbf{Y}} \begin{bmatrix} \mathbf{V}_1 \\ \vdots \\ \mathbf{V}_N \end{bmatrix} \quad (2.11)$$

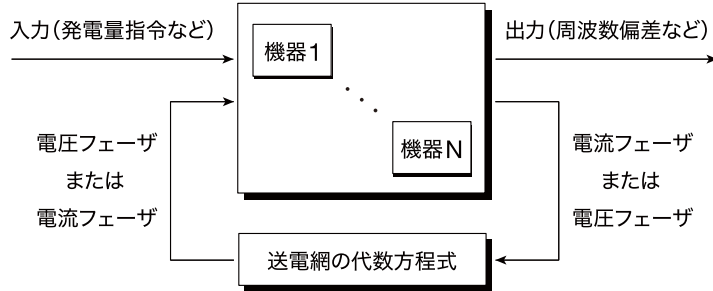


Fig. 2.4 Schematic diagram of a power system model

Equation 2.11 can be considered a mathematical model of the power grid that expresses interactions between inputs and outputs of devices connected to a bus bar. Specifically, if we consider the voltage phasor V_i as the output from the device i to the electrical power system, and current phasor I_i as the input from the electrical power system to the device i , I_i can be expressed as a linear combination of output from the other devices:

$$I_i = Y_{i1}V_1 + \cdots + Y_{iN}V_N$$

The real part and imaginary parts of the admittance matrix are called the **conductance matrix** and **susceptance matrix**, respectively.

The simultaneous equations 2.11 provide partial information about the current and voltage phasors of the bus bars, such that the current and voltage phasors of each bus bar, (I_1, \dots, I_N) and (V_1, \dots, V_N) , cannot be uniquely determined. To uniquely determine the steady and transient behaviors of the current and voltage phasors of every bus bar, the local relationship between I_i and V_i of each bus bar must be separately determined.

This localized relationship expresses the characteristics of the devices connected to the bus bars and can be considered mathematical models that express the input-output relationship of each device. Specific mathematical models of synchronous generators and loads will be described in detail in Section 2.3 and beyond.

$$\begin{bmatrix} V_1 \\ \vdots \\ V_N \end{bmatrix} = \underbrace{\begin{bmatrix} Z_{11} & \cdots & Z_{1N} \\ \vdots & \ddots & \vdots \\ Z_{N1} & \cdots & Z_{NN} \end{bmatrix}}_Z \begin{bmatrix} I_1 \\ \vdots \\ I_N \end{bmatrix} \quad (2.12)$$

If the admittance matrix Y in Equation 2.11 is nonsingular, $Z = Y^{-1}$, however Y is not always nonsingular. For example, if the admittance matrix of Equation 2.10 is not nonsingular, the following holds:

$$V_1 = V_2 = V_3 \quad \implies \quad I_1 = I_2 = I_3 = 0$$

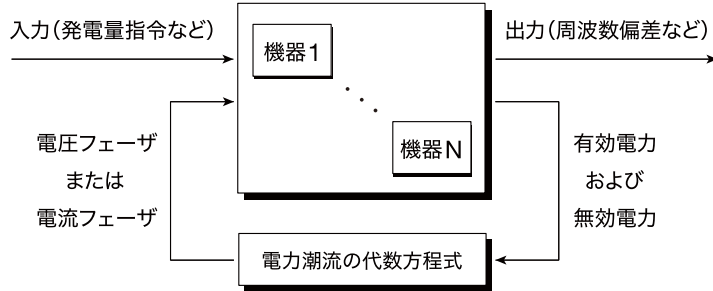


Fig. 2.5 Schematic diagram of a power system model

The singularity of this admittance matrix indicates that when all current phasors of each bus bar are zero, all voltage phasors are the same; however, this value cannot be uniquely determined. Nevertheless, there is rarely any need to pay attention to the singularity of the admittance matrix within the scope of general analysis.

In addition, active power $P_i \in \mathbb{R}$ and reactive power $Q_i \in \mathbb{R}$ provided from device i to bus bar i are defined by:

$$P_i := \operatorname{Re} [\bar{V}_i \bar{I}_i], \quad Q_i := \operatorname{Im} [\bar{V}_i \bar{I}_i]$$

In other words, the following relationship holds between active power, reactive power, bus bar voltage phasor, and bus bar current phasor.

$$P_i + jQ_i = \bar{V}_i \bar{I}_i \quad (2.13)$$

Then, by rearranging Equation 2.11, it is possible to obtain a power system model in which the active and reactive power supplied to the bus bar is the output of the device.

$$\begin{aligned} P_i &= \sum_{j=1}^N \operatorname{Re} [\bar{Y}_{ij} V_i \bar{V}_j] & i \in \{1, \dots, N\} \\ Q_i &= \sum_{j=1}^N \operatorname{Im} [\bar{Y}_{ij} V_i \bar{V}_j] \end{aligned} \quad (2.14)$$

Equation 2.14 is a simultaneous equation that expresses the electric power flow in each bus bar. Figures 2.4 and 2.5 are equivalent electrical power system models, but they can be used alternatively according to the analysis purpose.

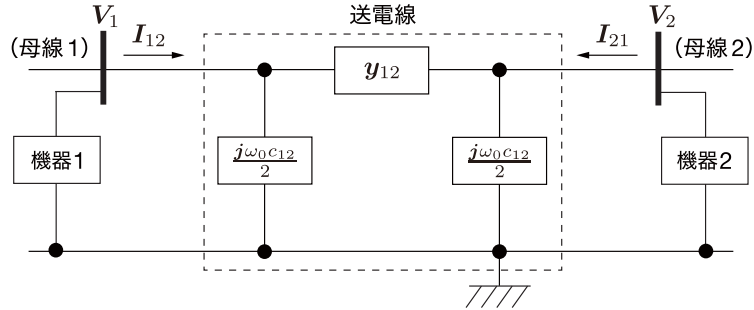


Fig. 2.6 π -type circuit model of a transmission line with ground capacitance
(Transmission lines with end points at bus bars 1 and 2)

2.2.2 Power grid model with capacitance to ground

In short transmission lines, the model from the example 2.1 can be used; however, in medium transmission lines that exceed 50 km, the capacitance to ground (capacitance component) created between the transmission lines and the ground cannot be ignored.

When the capacitance to ground, a transmission line is often represented as a π -type equivalent circuit as shown in Figure 2.6. In Figure 2.6, a transmission line connecting the bus bars 1 and 2 is shown, where ω_0 is the system frequency and c_{12} is the capacitance to ground. Using this representation of transmission line, the admittance of the power grid is obtained as follows.

Example 2.2 Admittance matrix for the transmission line in a π -type circuit

For an electrical power system similar to Example 2.1, let's derive the admittance matrix when the transmission line is expressed by a π -type equivalent circuit. First, let's consider the relationship of the current phasors I_{12} , I_{21} , flowing from the bus bars, and the voltage phasors V_1 , V_2 of the bus bars of a transmission line with bus bars 1 and 2 as end points, as illustrated in Figure 2.6. Then, please note that, unlike in Example 2.1, I_{21} is different from $-I_{12}$. If the current flowing through the transmission line with admittance y_{12} from left to right is expressed as I'_{12} , the following equations are obtained from the Kirchhoff's laws:

$$I_{12} = \frac{j\omega_0 c_{12}}{2} V_1 + I'_{12}, \quad \frac{j\omega_0 c_{12}}{2} V_2 = I_{21} + I'_{12}$$

Moreover, by using the Ohm's law:

$$I'_{12} = y_{12}(V_1 - V_2)$$

By replacing I'_{12} and rearranging the equations, we obtain:

$$\begin{bmatrix} \mathbf{I}_{12} \\ \mathbf{I}_{21} \end{bmatrix} = \begin{bmatrix} \mathbf{y}_{12} + \frac{j\omega_0 c_{12}}{2} & -\mathbf{y}_{12} \\ -\mathbf{y}_{12} & \mathbf{y}_{12} + \frac{j\omega_0 c_{12}}{2} \end{bmatrix} \begin{bmatrix} \mathbf{V}_1 \\ \mathbf{V}_2 \end{bmatrix}$$

The following is true for the transmission line that uses bus bar 2 and bus bar 3 as end points:

$$\begin{bmatrix} \mathbf{I}_{32} \\ \mathbf{I}_{23} \end{bmatrix} = \begin{bmatrix} \mathbf{y}_{32} + \frac{j\omega_0 c_{32}}{2} & -\mathbf{y}_{32} \\ -\mathbf{y}_{32} & \mathbf{y}_{32} + \frac{j\omega_0 c_{32}}{2} \end{bmatrix} \begin{bmatrix} \mathbf{V}_3 \\ \mathbf{V}_2 \end{bmatrix}$$

Therefore, by using:

$$\mathbf{I}_1 - \mathbf{I}_{12} = 0, \quad \mathbf{I}_2 - \mathbf{I}_{21} - \mathbf{I}_{23} = 0, \quad \mathbf{I}_3 - \mathbf{I}_{32} = 0$$

The admittance matrix of the power grid can be obtained as:

$$\begin{bmatrix} \mathbf{I}_1 \\ \mathbf{I}_2 \\ \mathbf{I}_3 \end{bmatrix} = \begin{bmatrix} \mathbf{y}_{12} + \frac{j\omega_0 c_{12}}{2} & -\mathbf{y}_{12} & 0 \\ -\mathbf{y}_{12} & \mathbf{y}_{12} + \mathbf{y}_{32} + \frac{j\omega_0(c_{12}+c_{32})}{2} & -\mathbf{y}_{32} \\ 0 & -\mathbf{y}_{32} & \mathbf{y}_{32} + \frac{j\omega_0 c_{32}}{2} \end{bmatrix} \begin{bmatrix} \mathbf{V}_1 \\ \mathbf{V}_2 \\ \mathbf{V}_3 \end{bmatrix}$$

This is consistent with Equation 2.10 when c_{12} and c_{32} are zero.

2.2.3 Mathematical properties of the admittance matrix

In this book, we assume power grids that are connected; in other words, there is at least one route connecting two arbitrarily chosen bus bar. For unconnected power grids, the connected parts can be independently discussed. In Figure 2.7a, the nodes (circles) correspond to the bus bars and the edges (black lines) correspond to the transmission lines.

In the power grid model of Example 2.1 where the capacitance to ground is ignored, the admittance matrix is expressed as $\mathbf{Y}_0 \in \mathbb{C}^{N \times N}$. The real and imaginary parts of \mathbf{Y}_0 ; in other words, the conductance and susceptance matrices, are expressed as:

$$G_0 := \text{Re}[\mathbf{Y}_0], \quad B_0 := \text{Im}[\mathbf{Y}_0]$$

These matrices have the following properties. First, the sum of elements in all row vectors of these matrices is equal to zero. This is expressed by the following equations, where $\mathbf{1} \in \mathbb{R}^N$ is a vector which all elements are equal to one:

$$\mathbf{Y}_0 \mathbf{1} = 0 \iff G_0 \mathbf{1} = 0, \quad B_0 \mathbf{1} = 0 \quad (2.15a)$$

Furthermore, since the conductance is non-negative and the susceptance is negative in each transmission line, the conductance matrix is positive semi-definite and the susceptance matrix is negative semi-definite; in other words:

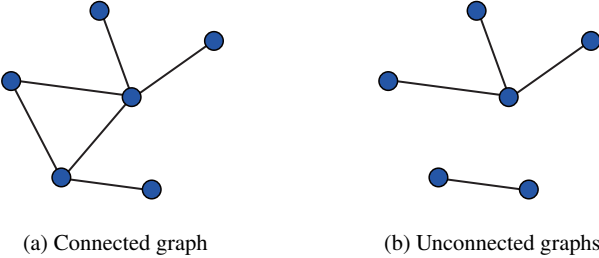


Fig. 2.7 Connected and disconnected graphs (Connected graph and unconnected graph)

$$G_0 = G_0^T \geq 0, \quad B_0 = B_0^T \leq 0 \quad (2.15b)$$

Specifically, based on the fact that the connectivity of the power grid and the susceptance of the transmission line are non-zero, the multiplicity of the zero eigenvalue of B_0 is derived to be 1. This can also be expressed as:

$$\ker B_0 = \text{span}\{\mathbf{1}\} \quad (2.15c)$$

Under the graph theory perspective, $-B_0$ is called a **graph Laplacian** of a strongly connected weighted undirected graph. The multiplicity of the zero eigenvalue in a graph Laplacian being 1 is a requirement for the corresponding undirected graph to be strongly connected [2].

Furthermore, when considering a π -type equivalent circuit for the transmission lines like in Example 2.2, a non-negative value is added to the diagonal element of the susceptance matrix B_0 . In other words, the admittance matrix for the power grid model in Examples 2.1 and 2.2 is expressed as:

$$Y = G_0 + j(B_0 + \text{diag}(b_i)_{i \in \{1, \dots, N\}}) \quad (2.16)$$

where b_i is a non-negative constant equivalent to capacitance to ground, and the conductance G_0 and the susceptance B_0 matrices satisfy Equation (2.15).

2.3 Mathematical model of synchronous generators

2.3.1 Classification of generator models based on the level of detail

In electrical power system engineering, different synchronous generator models with different levels of detail, such as the consideration of the field and damper windings, have been used to analyze the stability of electrical power systems [4, 5, 8, 9]. Here, we present four types of models.

- (a) Park model** The Park model, also called **complete model**, is a model with a high level of details that considers the change in magnetic flux in the stator and field and damper windings. It consists of a two-dimensional linear differential equation (swing equation) that expresses the mechanical dynamic characteristics of the rotor of the generator, and a five to seven-dimensional nonlinear differential equation that expresses the magnetic flux changes in the stator, field winding, and damper winding. The dimension of the latter differential equation that expresses changes in magnetic flux varies based on the number of windings to consider and the setting of variables.

The active and reactive power, which represent the electrical output of a generator, are nonlinear functions of the internal state of the generator. The models used in Japanese works consider a type of damper winding on the d-axis and two types of damper windings on the q-axis in addition to field winding on the d-axis [8]. When there is only one type of damper winding on the q-axis, if the constant is set appropriately, there are no issues in terms of practical use.

- (b) Two-axis model** It is a model that approximates the differential equations to the algebraic equation, assuming that the time constants of the dynamic response of the magnetic flux change in the stator and damper winding are sufficiently small [9, Section 5.4]. It consists of a two-dimensional swing equation and a two-dimensional nonlinear differential equation expressing the magnetic flux change in the field and damper windings. Generally, the dynamic response of the magnetic flux change in the stator and damper winding are sufficiently fast; thus, the behavior of the Park model is generally well simplified.

- (c) One-axis model** In contrast to the two-axis model, the one-axis model, also called **transient model**, is obtained under the assumption that the time constant of the magnetic flux change in the damper winding is sufficiently small [10-12]. It consists of a two-dimensional swing equation and a one-dimensional nonlinear differential equation that expresses the magnetic flux change in the field winding. In this book, we use a one-axis model to perform analysis. The process of deriving a one-axis model from the Park model is explained in [3, Section 5] and [4, Section 4.15].

- (d) Classical model** It is a model that ignores the magnetic flux changes in the field and damper windings. It consists of a two-dimensional linear swing equation and the active and reactive power are nonlinear functions of the internal states of the generator. This model is currently widely used to analyze the oscillatory and synchronization phenomena of electrical power systems [10-14].

2.3.2 Mathematical expression of the one-axis model

- (1) Expressing the relationship of current and voltage with the internal state of the generator as an intermediate variable**

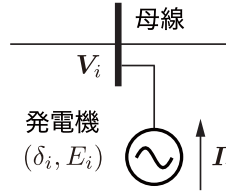


Fig. 2.8 Generator connected to bus bar

If the interval voltage of a generator i connected to a bus bar i is E_i , and the rotor angle relative to a coordinate system that rotates with angular speed ω_0 is δ_i , the following relationship holds for the voltage phasor V_i of the bus bar i and for the current phasor I_i flowing from the generator to the bus bar i :

$$I_i = \frac{1}{jX'_i} (E_i e^{j\delta_i} - V_i) \quad (2.17a)$$

where X'_i is the transient reactance of the generator. Figure 2.8 illustrates the bus bar and current and voltage phasors. The connection to ground is omitted from the figure.

δ_i and E_i in Equation 2.17a are intermediate variables representing the internal state of the generator i , and they provide with a dynamic relationship between I_i and V_i . In other words, from the perspective of control systems engineering, Equation 2.17a uses δ_i and E_i as internal states, and can be interpreted as an “output equation” of a generator i , when I_i is the output from the generator to the electrical power system and V_i is the input from the electrical power system to the generator. Alternatively, we can consider V_i as the output and I_i as the input. Details will be discussed later. By multiplying both sides of the Equation 2.17a with $e^{-j\delta}$ and evaluating its real and imaginary parts separately, we find:

$$\begin{aligned} |V_i| \sin(\delta_i - \angle V_i) &= X'_i |I_i| \cos(\delta_i - \angle I_i), \\ |V_i| \cos(\delta_i - \angle V_i) &= E_i - X'_i |I_i| \sin(\delta_i - \angle I_i) \end{aligned} \quad (2.17b)$$

Active power P_i provided from the generator i to the bus bar i and can be expressed as:

$$\begin{aligned} P_i &= \operatorname{Re} [V_i \bar{I}_i] \\ &= \operatorname{Re} [|V_i| e^{-j(\delta_i - \angle V_i)} |I_i| e^{-j(\delta_i - \angle I_i)}] \\ &= |V_i| |I_i| \cos(\delta_i - \angle V_i) \cos(\delta_i - \angle I_i) \\ &\quad + |V_i| |I_i| \sin(\delta_i - \angle V_i) \sin(\delta_i - \angle I_i) \end{aligned}$$

Similarly, reactive power Q_i can be expressed as:

$$\begin{aligned} Q_i &= i \left[V_i \bar{I}_i \right] \\ &= |V_i| |I_i| \cos(\delta_i - \angle V_i) \sin(\delta_i - \angle I_i) \\ &\quad - |V_i| |I_i| \sin(\delta_i - \angle V_i) \cos(\delta_i - \angle I_i) \end{aligned}$$

Thus, by replacing the current phasor using the Equation 2.17b, the following can be obtained:

$$\begin{aligned} P_i &= \frac{E_i |V_i|}{X'_i} \sin(\delta_i - \angle V_i), \\ Q_i &= \frac{E_i |V_i|}{X'_i} \cos(\delta_i - \angle V_i) - \frac{|V_i|^2}{X'_i} \end{aligned} \quad (2.18)$$

These expressions indicate that the active and reactive power are function of the difference between the rotor angle δ_i and the voltage angle $\angle V_i$ of the bus bar. In typical electrical power system operation, the difference between δ_i and $\angle V_i$ is small; thus, the following approximation holds:

$$P_i \simeq \frac{E_i |V_i|}{X'_i} (\delta_i - \angle V_i), \quad Q_i \simeq \frac{|V_i|}{X'_i} (E_i - |V_i|)$$

The above equations indicate that a difference between δ_i and $\angle V_i$ mainly contributes to the active power, while a difference between E_i and $|V_i|$ contributes to the reactive power.

When the voltage phasor is the input, Equations (2.17) and 2.18 can be interpreted as an equivalent deformation of the output equation of the generator under the definition of active power and reactive power in Equation 2.13. Similarly, if the voltage phasor is cancelled, an output equation, when current phasor is the input, is obtained as:

$$\begin{aligned} P_i &= E_i |I_i| \cos(\delta_i - \angle I_i), \\ Q_i &= E_i |I_i| \sin(\delta_i - \angle I_i) - X'_i |I_i|^2 \end{aligned} \quad (2.19)$$

(2) Relational expression of current and voltage in dynamic characteristics of a generator

The swing equation that describes the mechanical dynamics of a synchronous generator is given as follows:

$$\begin{cases} \dot{\delta}_i &= \omega_0 \Delta \omega_i \\ M_i \Delta \dot{\omega}_i &= -D_i \Delta \omega_i - P_i + P_{\text{mechi}} \end{cases} \quad (2.20a)$$

where, $\Delta \omega_i$ is the frequency deviation from the system frequency, ω_0 , M_i is the inertia coefficient, D_i is the damping factor, and P_{mechi} is the mechanical torque.

In addition, as a differential equation that expresses the attenuation of magnetic flux, the electromagnetic dynamics of the synchronous generator are given as follows:

$$\tau_i \dot{E}_i = -\frac{X_i}{X'_i} E_i + \left(\frac{X_i}{X'_i} - 1 \right) |V_i| \cos(\delta_i - \angle V_i) + V_{\text{field}i} \quad (2.20\text{b})$$

where, τ_i is the time constant of the field circuit, X_i is the synchronous reactance, and $V_{\text{field}i}$ is the field voltage. From the viewpoint of system control, mechanical torque P_{mechi} and field voltage $V_{\text{field}i}$ become external inputs. Generally, $X_i > X'_i$ holds.

Summarizing the above, if the voltage magnitude and angle ($|V_i|, \angle V_i$) are considered inputs from the bus bar i to the generator i , the following equations become the state-space equation that expresses the dynamic characteristics of the generator:

$$\begin{cases} \dot{\delta}_i &= \omega_0 \Delta \omega_i \\ M_i \Delta \dot{\omega}_i &= -D_i \Delta \omega_i - P_i + P_{\text{mechi}} \\ \tau_i \dot{E}_i &= -\frac{X_i}{X'_i} E_i + \left(\frac{X_i}{X'_i} - 1 \right) |V_i| \cos(\delta_i - \angle V_i) + V_{\text{field}i} \end{cases} \quad (2.21\text{a})$$

and the active power P_i is given by Equation 2.18. The magnitude and angle of the current phasor can be derived from Equation 2.17b as follows:

$$\begin{aligned} |\mathbf{I}_i| &= \sqrt{\left\{ \frac{|V_i|}{X'_i} \sin(\delta_i - \angle V_i) \right\}^2 + \left\{ \frac{E_i}{X'_i} - \frac{|V_i|}{X'_i} \cos(\delta_i - \angle V_i) \right\}^2}, \\ \angle \mathbf{I}_i &= \delta_i - \arctan \left(\frac{E_i - |V_i| \cos(\delta_i - \angle V_i)}{|V_i| \sin(\delta_i - \angle V_i)} \right) \end{aligned} \quad (2.21\text{b})$$

At this time, the current phasor is considered the output from generator i to the bus bar i . As discussed above, based on the definition of Equation 2.13, a set of active power and reactive power of Equation 2.18, (P_i, Q_i) , can be considered as an output that is mathematically equivalent to $(|\mathbf{I}_i|, \angle \mathbf{I}_i)$.

Similarly, the magnitude and angle of the current phasor can be considered inputs from the bus bar i to the generator i . In this case, the following equation becomes the state-space equation that expresses the dynamic characteristics of the generator.

$$\begin{cases} \dot{\delta}_i &= \omega_0 \Delta \omega_i \\ M_i \Delta \dot{\omega}_i &= -D_i \Delta \omega_i - P_i + P_{\text{mechi}} \\ \tau_i \dot{E}_i &= -E_i - (X_i - X'_i) |\mathbf{I}_i| \sin(\delta_i - \angle \mathbf{I}_i) + V_{\text{field}i} \end{cases} \quad (2.22\text{a})$$

where the active power P_i is expressed as in Equation 2.19. In addition, the magnitude and angle of the voltage phasor can be derived from Equation 2.17b as follows:

$$\begin{aligned} |V_i| &= \sqrt{\{X'_i|\mathbf{I}_i| \cos(\delta_i - \angle \mathbf{I}_i)\}^2 + \{E_i - X'_i|\mathbf{I}_i| \sin(\delta_i - \angle \mathbf{I}_i)\}^2}, \\ \angle V_i &= \delta_i - \arctan\left(\frac{X'_i|\mathbf{I}_i| \cos(\delta_i - \angle \mathbf{I}_i)}{E_i - X'_i|\mathbf{I}_i| \sin(\delta_i - \angle \mathbf{I}_i)}\right) \end{aligned} \quad (2.22b)$$

In this context, the voltage phasor is regarded as an output from the generator to the bus bar. The set of active power and reactive power of Equation 2.19, (P_i, Q_i) , can also be considered as an output that is mathematically equivalent to $(|V_i|, \angle V_i)$.

The unit of each variable is as follows: the unit for rotor angle δ_i , voltage phasor angle $\angle V_i$, and current phasor angle $\angle \mathbf{I}_i$ of the bus bar is [rad]. Frequency deviation $\Delta\omega_i$, internal voltage E_i , absolute value of voltage phasor $|V_i|$, absolute value of current phasor $|\mathbf{I}_i|$, active power P_i , active power Q_i , mechanical torque $P_{\text{mech}i}$, and field voltage $V_{\text{field}i}$ are divided by their reference value and, thus are dimensionless values divided by their reference value. Their unit is [pu], which means "per unit". If the system frequency is 50 [Hz], ω_0 is set as 100π . Therefore, the unit of $\omega_0\Delta\omega_i$ is [rad/s].

(3) Relationship with the classical model

With the above one-axis model, the dynamic characteristics of the internal voltage of the generator E_i are taken into consideration. However, in the classical model, this internal voltage is assumed to be constant. Specifically, the following is assumed for the differential equation of internal voltage E_i in Equations (2.20) and (2.21):

- Synchronous reactance X_i and transient reactance X'_i are equal, and
- Field voltage $V_{\text{field}i}$ is constant.

Then, if we denote the constant value of the field voltage as V_i^* , the stationary solution of the differential equation in Equation 2.20b is $E_i(t) = V_i^*$. In other words, the internal voltage E_i becomes V_i^* , which is constant. For the deeper understanding of the classical model in electrical power system analysis, please refer to [4, Section 2.11].

2.3.3 Kron reduction of a generator bus

In this Section, we analyze an electrical power system model, where the synchronous generator as equipment is connected to each bus bar. Then, if a set of generator buses is expressed as \mathcal{I}_G , the number of generator buses $|\mathcal{I}_G|$ is equal to the total number of bus bars N . The model for the entire electrical power system is described as a "differential algebraic equation system", where generators described by Equation 2.21a are combined with Equation 2.21b following the input-output relationship of the algebraic equation of Equation 2.11.

COFFEE BREAK

Differential algebraic equation system: it is a system that described by differential algebraic equations and algebraic equations as follows:

$$\begin{cases} \dot{x}_1 &= f_1(x_1, x_2) \\ 0 &= f_2(x_1, x_2) \end{cases}$$

where x_1 is the state of the differential equation and x_2 is the state of the algebraic equation. For example, in a system where generator models of Equation (2.21) are combined with the algebraic equation of the power grid of Equation 2.12, the vector with the internal state of all generators, $\delta_i \Delta\omega_i, E_i$, is x_1 , while x_2 is the vector which contains all bus voltage phasor variables, $|V_i|$ and $\angle V_i$. When the algebraic equation has a solution for x_2 , the solution is expressed as $x_2 = h(x_1)$. By substituting $x_2 = h(x_1)$ into the differential equation we get the following ordinary differential equation system that describes the behavior of x_1 :

$$\dot{x}_1 = f_1(x_1, h(x_1))$$

The goal of this section is to equivalently transform the system of differential algebraic equations via current and voltage phasors of the generator bus bar ($|V_i|, \angle V_i$) $_{i \in \mathcal{I}_G}$ into a system of ordinary differential equations described only by the state variables of the generators, by expressing all voltage phasors as functions of the generator state variables $(\delta_i, E_i)_{i \in \mathcal{I}_G}$. This transformation is called **Kron reduction** of the generator bus and the steps for performing it are as follows:

- (a) Replace the current phasor in the Equation 2.17a using the algebraic equation representing the power grid in Equation 2.11. Then, express the voltage phasor $(V_i)_{i \in \mathcal{I}_G}$ as a function of the generator state variables $(\delta_i, E_i)_{i \in \mathcal{I}_G}$.
- (b) Rewrite the phasors using the Euler's identity:

$$e^{j\delta_i} \bar{V}_i = |V_i| \cos(\delta_i - \angle V_i) + j|V_i| \sin(\delta_i - \angle V_i)$$

and rewrite the term of trigonometric function related to V_i included in the model by the state variables $(\delta_i, E_i)_{i \in \mathcal{I}_G}$.

First, let us consider step (a). If the output equation of Equation 2.17a is expressed as a vector:

$$\begin{bmatrix} I_1 \\ \vdots \\ I_N \end{bmatrix} = \text{diag}\left(\frac{1}{jX'_i}\right) \left(\text{diag}\left(e^{j\delta_i}\right) \begin{bmatrix} E_1 \\ \vdots \\ E_N \end{bmatrix} - \begin{bmatrix} V_1 \\ \vdots \\ V_N \end{bmatrix} \right)$$

Using the algebraic equation of the power grid expressed by Equation 2.11, and solving the resulting equation for the voltage phasor, the following is obtained:

$$\begin{bmatrix} V_1 \\ \vdots \\ V_N \end{bmatrix} = \left(\text{diag} \left(\frac{1}{jX'_i} \right) + Y \right)^{-1} \text{diag} \left(\frac{e^{j\delta_i}}{jX'_i} \right) \begin{bmatrix} E_1 \\ \vdots \\ E_N \end{bmatrix} \quad (2.23)$$

In this manner, the voltage phasor $(V_i)_{i \in \mathcal{I}_G}$ of the bus bars is equivalently expressed by the state variables of generators $(\delta_i, E_i)_{i \in \mathcal{I}_G}$. Next, let us consider step (b). If the voltage phasor of the bus bar is expressed in the polar form:

$$V_i = |V_i| e^{j\angle V_i}$$

Then, by multiplying both sides of Equation 2.23 by $\text{diag}(\frac{e^{-j\delta_i}}{X'_i})$ and taking the complex conjugate, we get:

$$\begin{bmatrix} \frac{|V_1|}{X'_1} e^{j(\delta_1 - \angle V_1)} \\ \vdots \\ \frac{|V_N|}{X'_N} e^{j(\delta_N - \angle V_N)} \end{bmatrix} = \text{diag} \left(e^{j\delta_i} \right) \Gamma^{-1} \text{diag} \left(e^{-j\delta_i} \right) \begin{bmatrix} E_1 \\ \vdots \\ E_N \end{bmatrix} \quad (2.24)$$

where $\Gamma \in \mathbb{C}^{N \times N}$ is a complex square matrix defined by:

$$\Gamma := \text{diag}(X'_i) - j \text{diag}(X'_i) \bar{Y} \text{diag}(X'_i) \quad (2.25)$$

In Equation 2.24, if the (i, j) th element of Γ^{-1} is expressed as γ_{ij}^{-1} , then:

$$\text{diag} \left(e^{j\delta_i} \right) \Gamma^{-1} \text{diag} \left(e^{-j\delta_i} \right) = \begin{bmatrix} \gamma_{11}^{-1} e^{j(\delta_1 - \delta_1)} & \cdots & \gamma_{1N}^{-1} e^{j(\delta_1 - \delta_N)} \\ \vdots & \ddots & \vdots \\ \gamma_{N1}^{-1} e^{j(\delta_N - \delta_1)} & \cdots & \gamma_{NN}^{-1} e^{j(\delta_N - \delta_N)} \end{bmatrix}$$

Thus, the real part and imaginary part of the (i, j) th element can be written as:

$$\begin{aligned} \text{Re} \left[\gamma_{ij}^{-1} e^{j(\delta_i - \delta_j)} \right] &= -B_{ij}^{\text{red}} \cos(\delta_i - \delta_j) - G_{ij}^{\text{red}} \sin(\delta_i - \delta_j), \\ \text{Im} \left[\gamma_{ij}^{-1} e^{j(\delta_i - \delta_j)} \right] &= -B_{ij}^{\text{red}} \sin(\delta_i - \delta_j) + G_{ij}^{\text{red}} \cos(\delta_i - \delta_j) \end{aligned}$$

where the reduced conductance and susceptance matrices are defined as:

$$G_{ij}^{\text{red}} := \text{Im} \left[\gamma_{ij}^{-1} \right], \quad B_{ij}^{\text{red}} := -\text{Re} \left[\gamma_{ij}^{-1} \right] \quad (2.26)$$

In addition, the reduced admittance matrix Y^{red} is defined as:

$$Y_{ij}^{\text{red}} := G_{ij}^{\text{red}} + jB_{ij}^{\text{red}}$$

This is equal to defining as follows using the above complex matrix Γ^{-1} :

$$\mathbf{Y}^{\text{red}} := -j\mathbf{I}^{-1} \quad (2.27)$$

Then, Equation 2.23 can be rewritten as:

$$\begin{aligned} \frac{|\mathbf{V}_i|}{X'_i} \cos(\delta_i - \angle \mathbf{V}_i) &= - \sum_{j=1}^N E_j \{ B_{ij}^{\text{red}} \cos(\delta_i - \delta_j) + G_{ij}^{\text{red}} \sin(\delta_i - \delta_j) \}, \\ \frac{|\mathbf{V}_i|}{X'_i} \sin(\delta_i - \angle \mathbf{V}_i) &= - \sum_{j=1}^N E_j \{ B_{ij}^{\text{red}} \sin(\delta_i - \delta_j) - G_{ij}^{\text{red}} \cos(\delta_i - \delta_j) \} \end{aligned} \quad (2.28)$$

Please note that this equation associates the voltage phasor with the variation of the rotor angle $\delta_i - \delta_j$ and internal voltage E_i . Therefore, a differential algebraic equation model of an electrical power system, in which the generator model of Equation (2.21) is combined by the simultaneous equation of Equation 2.11, can be equivalently expressed as a simultaneous ordinary differential equation system related to all $i \in \mathcal{I}_G$.

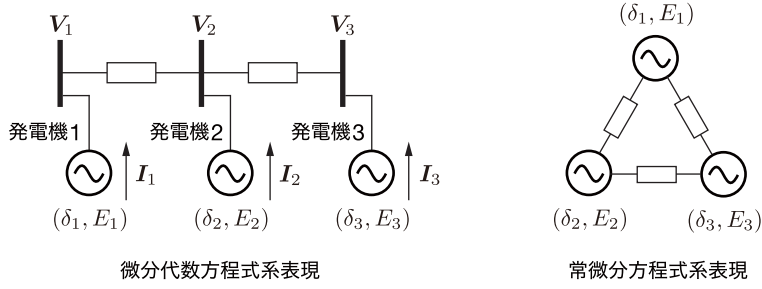
$$\begin{aligned} \dot{\delta}_i &= \omega_0 \Delta \omega_i \\ M_i \Delta \dot{\omega}_i &= -D_i \Delta \omega_i - f_i(\delta, E) + P_{\text{mech}_i} \quad i \in \mathcal{I}_G \\ \tau_i \dot{E}_i &= -\frac{X_i}{X'_i} E_i + (X_i - X'_i) g_i(\delta, E) + V_{\text{field}_i} \end{aligned} \quad (2.29)$$

However, δ and E are column vectors corresponding to nonlinear interactions between generators. Defining $\delta_{ij} := \delta_i - \delta_j$:

$$\begin{aligned} f_i(\delta, E) &:= -E_i \sum_{j=1}^N E_j (B_{ij}^{\text{red}} \sin \delta_{ij} - G_{ij}^{\text{red}} \cos \delta_{ij}) \\ g_i(\delta, E) &:= - \sum_{j=1}^N E_j (B_{ij}^{\text{red}} \cos \delta_{ij} + G_{ij}^{\text{red}} \sin \delta_{ij}) \end{aligned} \quad (2.30)$$

Based on Equation 2.29, the behavior of a generator i is only impacted by the relative difference of rotor argument of the remaining generators $(\delta_j)_{j \in \mathcal{I}_G \setminus \{i\}}$. Furthermore, by comparing with Equation 2.22a, we can see that $f_i(\delta, E)$ of Equation 2.29 corresponds to the active power P_i output by the generators. If the real part of the admittance matrix \mathbf{Y} is zero, in other words, if the conductance of all transmission lines is zero (equivalent resistance equal to zero), the reduced conductance G_{ij}^{red} also becomes 0 for all (i, j) . As it will be discussed in Section 3.2.1, this is equivalent to a lossless transmission of active power in the power grid.

In addition, although the admittance matrix \mathbf{Y} is a sparse matrix that reflects the graph structure of the power grid, the reduced admittance matrix \mathbf{Y}^{red} in Equation 2.29 is usually not a sparse matrix. Therefore, note that the system of ordinary differential equations in Equation 2.29 has a coupled structure in which the internal states

**Fig. 2.9** Changes in bond structure due to Kron reduction

of all generators interact closely. Let's confirm this fact with numerical examples along with the behavior of the electrical power system model.

COFFEE BREAK

Sparse and dense matrices: A matrix with many 0 elements is called a **sparse matrix**. In contrast, a matrix with almost no 0 elements is called a **dense matrix**. However, how many 0 elements are necessary to call a matrix sparse matrix depends on the context. The inverse matrix of a sparse matrix that is not diagonal is usually a dense matrix.

Table 2.1 Physical constants of the generator model

i	M_i [s]	D_i [pu]	τ_i [s]	X_i [pu]	X'_i [pu]
1	100	10	5.14	1.569	0.936
2	18	10	5.90	1.651	0.911
3	12	10	8.97	1.220	0.667

Table 2.2 Steady-state values of external inputs and internal states of the generator

i	P_{mech}^* [pu]	V_{filed}^* [pu]	δ_i^* [rad]	$\Delta\omega_i^*$ [pu]	E_i^* [pu]
1	-0.5623	1.5132	0.4656	0	1.4363
2	0.8832	2.2216	1.0903	0	1.8095
3	-0.3160	0.9198	0.6067	0	1.1030

Example 2.3 Behavior of an electrical power system model with a reduced generator bus

Let us consider an electrical power system model consisting of three bus bars as discussed in Example 2.1. Moreover, a synchronous generator is connected to each

bus bar and modeled as the one-axis generator model discussed in Section 2.3.2. Then, the electrical power system model can be drawn as the left picture in Figure 2.9. The values of the physical constants of the generators are chosen as in 2.1. Since the system frequency is set to 60 [Hz], the value of ω_0 is 120π .

The admittance of the two transmission lines is set as:

$$y_{12} = 1.3652 - j11.6041, \quad y_{23} = 1.9422 - j10.5107 \quad (2.31)$$

In this manner, the admittance matrix of the power grid in Equation 2.10 can be obtained. Then, the real and imaginary parts of the reduced admittance matrix \mathbf{Y}^{red} can be calculated according to Equation 2.27.

$$\begin{aligned} G^{\text{red}} &= \begin{bmatrix} 0.0073 & 0.0005 & -0.0079 \\ 0.0005 & 0.0041 & -0.0046 \\ -0.0079 & -0.0046 & 0.0125 \end{bmatrix}, \\ B^{\text{red}} &= \begin{bmatrix} -0.3716 & -0.3167 & -0.3800 \\ -0.3167 & -0.3550 & -0.4260 \\ -0.3800 & -0.4260 & -0.6933 \end{bmatrix} \end{aligned}$$

Therefore, both reduced conductance and susceptance matrices are dense. This dense structure corresponds to the right image of 2.9.

Next, let us calculate the time response of the ordinary differential equation system model of Equation 2.29. In the following, the initial value response is obtained when the mechanical power and the magnetic field, which are external inputs, are fixed to constants. In this example, we assume that the steady-state values of the external inputs and internal states of the power system model are obtained in advance using the steady-state calculation method that will be described in Section ???. Specifically, the input mechanical power and magnetic field are set to the constant values shown in the first and second columns of Table 2.2. In this case, the steady-state values of the internal states of the power system are given in columns 3 to 5 of Table 2.2.

These steady values are one of the solutions that satisfy the following simultaneous equations:

$$\begin{aligned} 0 &= -f_i(\delta^\star, E^\star) + P_{\text{mech}i}^\star \\ 0 &= -\frac{X_i}{X'_i} E_i^\star + (X_i - X'_i) g_i(\delta^\star, E^\star) + V_{\text{field}i}^\star \quad i \in \{1, 2, 3\} \end{aligned}$$

where δ^\star and E^\star are vectors composed by δ_i^\star and E_i^\star and the functions f_i and g_i are defined by Equation 2.30.

First, let us consider a situation in which the steady-state value is perturbed and set as initial value. In other words:

$$\begin{bmatrix} \delta_1(0) \\ \delta_2(0) \\ \delta_3(0) \end{bmatrix} = \begin{bmatrix} \delta_1^\star + \frac{\pi}{6} \\ \delta_2^\star \\ \delta_3^\star \end{bmatrix}, \quad \begin{bmatrix} E_1(0) \\ E_2(0) \\ E_3(0) \end{bmatrix} = \begin{bmatrix} E_1^\star + 0.1 \\ E_2^\star \\ E_3^\star \end{bmatrix} \quad (2.32)$$

where the initial value of the frequency deviation is 0. Then, the time response of the electrical power system model is shown in 2.10.

From this figure, it can be seen that after the angular frequency deviation and rotor deflection angle oscillate for about 15 seconds, they asymptotically converge to the original steady state. However, since the behavior of the rotor angle is only affected by the relative difference among generators, the convergence value of the rotor angle is shifted from the original steady state value by a constant. In other words, for a certain constant c_0 :

$$\lim_{t \rightarrow \infty} \delta_i(t) = \delta_i^* + c_0, \quad \forall i \in \{1, 2, 3\}$$

For any value of c_0 , the steady value is essentially equivalent. The voltage phasor of the bus bar shown in Figure 2.10 can be calculated independently of the internal state of the generators by using the Equation 2.23. Similarly, the active and reactive power can be calculated independently using Equation 2.19. Furthermore, since the frequency deviation is equal to 5×10^{-3} [pu] times the system frequency, it is equal to 0.3 [Hz].

Next, let us consider a case where the value of an external input is perturbed. Specifically, let us consider a perturbation in the mechanical power of generator 1.

$$\begin{bmatrix} P_{\text{mech}1}(t) \\ P_{\text{mech}2}(t) \\ P_{\text{mech}3}(t) \end{bmatrix} = \begin{bmatrix} P_{\text{mech}1}^* + 0.05 \\ P_{\text{mech}2}^* \\ P_{\text{mech}3}^* \end{bmatrix}$$

Figure 2.11 shows the time response of the electrical power system model under this condition. The initial value is set to be the same as in Equation 2.32. In addition, the phase of the rotor angle and the bus voltage phasor are the remainder of the division by π . In this case, it can be seen that the angular frequency deviation does not become 0 in the steady state, and the integral of the rotor angle changes constantly. Figure 2.12 shows the time response of the electrical power system model when field voltage of generator 1 is similarly perturbed:

$$\begin{bmatrix} V_{\text{filed}1}(t) \\ V_{\text{filed}2}(t) \\ V_{\text{filed}3}(t) \end{bmatrix} = \begin{bmatrix} V_{\text{filed}1}^* + 0.5 \\ V_{\text{filed}2}^* \\ V_{\text{filed}3}^* \end{bmatrix}$$

Similarly, in this situation the frequency deviation in a steady state does not become 0. Therefore, to calculate the time response of an electrical power system model, not only the initial values, but also the external inputs, such as mechanical power and field voltage, must be set to appropriate values.

Since Equation 2.29 is an ordinary differential equation system model, it is possible to numerically simulate its behavior by using differential equation solvers in MATLAB. However, as shown in Example 2.3, unless the value of the mechanical power and the field voltage are set appropriately, the frequency deviation of each generator does not converge to 0 in the steady state, and the rotor argument constantly deviates from the reference. Thus, to perform a numerical simulation that is

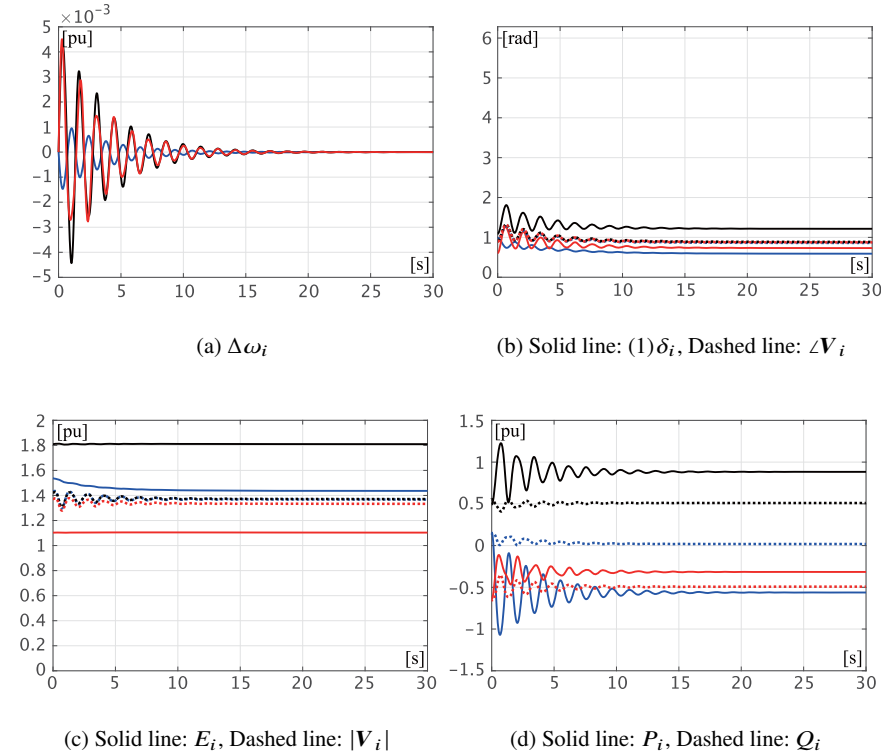


Fig. 2.10 System time response for perturbed initial value
 ((Blue: Bus 1, Black: Bus 2, Red: Bus 3))

realistically meaningful, a method to calculate valid equilibrium points and initial values is necessary. These details will be explained in Chapter 3.

2.3.4 Derivation of the Kuramoto-type oscillator model

By applying Kron reduction of generator bus to the classical model explained in Section 2.3.2, a Kuramoto-type oscillator model can be derived.

Specifically, if we assume that the value of synchronous and transient reactances, X_i and X'_i , are equal, and that the field voltage $V_{\text{field}i}$ is constant and equal to V_i^* , the internal voltage E_i is constant and equal to V_i^* . Therefore, the model of an electrical power system with synchronous generators connected to each bus bar is expressed by the following ordinary differential equation.

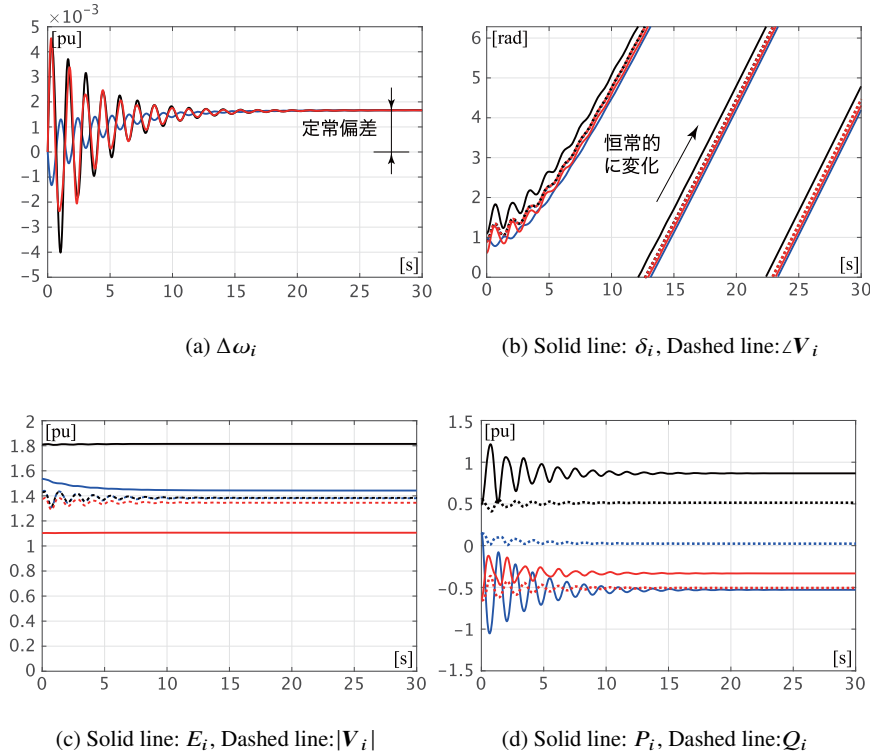


Fig. 2.11 System time response when perturbation is applied to the mechanical power
(Blue: Bus 1, Black: Bus 2, Red: Bus 3)

$$\begin{aligned} \dot{\delta}_i &= \omega_0 \Delta\omega_i \\ M_i \Delta\dot{\omega}_i &= -D_i \Delta\omega_i - \hat{f}_i(\delta) + P_{\text{mechi}} \end{aligned} \quad i \in \mathcal{I}_G \quad (2.33)$$

However, the nonlinear term is given by:

$$\hat{f}_i(\delta) := -V_i^* \sum_{j=1}^N V_j^* \left(B_{ij}^{\text{red}} \sin \delta_{ij} - G_{ij}^{\text{red}} \cos \delta_{ij} \right)$$

The function $\hat{f}_i(\delta)$ expresses the active power of a generator i . An electrical power system mode whose transmission lines have zero conductance, that is $G_{ij}^{\text{red}} = 0$, is occasionally used.

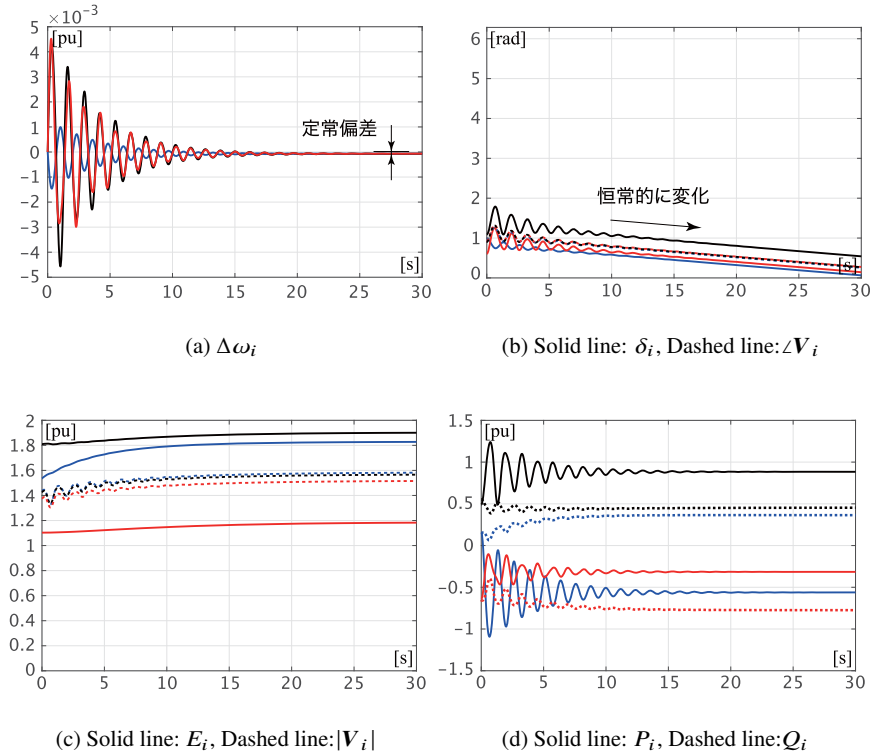


Fig. 2.12 System time response when perturbation is applied to the field voltage
(Blue: Bus 1, Black: Bus 2, Red: Bus 3)

COFFEE BREAK

Kuramoto model:

The following differential equation system comprising of N oscillators moving on the circumference is called **Kuramoto model**.

$$\dot{\theta}_i = \omega_i - \frac{K}{N} \sum_{j=1}^N \sin(\theta_i - \theta_j), \quad i = 1, \dots, N$$

In this context, ω_i is a constant representing the intrinsic angular velocity of the oscillator i , and K is a constant representing the coupling strength. In general, when the coupling strength K is sufficiently large compared to the magnitude of the inhomogeneity of the intrinsic angular speeds $\omega_1, \dots, \omega_N$, the angular speeds of the oscillator, $\dot{\theta}_1, \dots, \dot{\theta}_N$, are asymptotically synchronized.

The Kuramoto model has been analyzed mainly in the field of physics as a mathematical model describing the synchronization phenomena of nonlinear

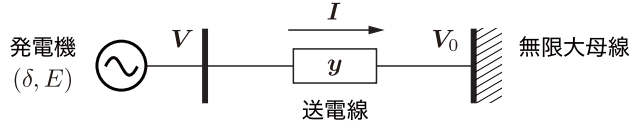


Fig. 2.13 Single machine infinity bus system model

oscillators, and is known to have a wide range of applications [5, 6]. The non-linear second-order oscillator model with inertial is also applied to the analysis of synchronization in power systems [7–10].

2.3.5 Single machine infinite bus system model

The **single machine infinite bus system model** is a simplified electrical power system model that is often used in basic mathematical analysis of electrical power systems, such as in [?, Section 1.3] and [?, Section 6.3, Section 8.3]. It is an electrical power system model consisting of a generator, a transmission line, and an infinite bus bar as shown in Figure 2.13. The infinite bus bar is interpreted as a rough approximation of the entire electrical power system, except for the generator of interest, as a "fixed voltage source".

Specifically, we assume that voltage phasor of the infinite bus bar V_0 is maintained as constant regardless the internal state of the generator. In other words, considering a transmission loss of electric power, the active and reactive power generated by the generator are assumed to be consumed each moment, without excess or deficiency, by the infinite bus bar.

In the following, we only focus on one generator, so we omit the subscript i and denote the variables of the generator and the generator bus. For the dynamic characteristics of the generator expressed in Equation (2.21), the voltage phasor V and current phasor I of a generator bus have the following relationship:

$$I = y(V - V_0)$$

This is an algebraic equation that determines the input-output relationship of the generator and the electrical power system. For reference, let us derive an ordinary differential equation model from the Kron reduction of the single machine infinite bus bar system when the resistance of the transmission line is 0 and the reactance x . In other words, the admittance of the transmission line is:

$$y = \frac{1}{jx}$$

Specifically, following the same procedure as of the Kron reduction of a generator bus in Section 2.3.3, the following two equations are used to replace the current and voltage phasors of the generator bus.

$$\mathbf{I} = \frac{1}{jx}(\mathbf{V} - \mathbf{V}_0), \quad \mathbf{I} = \frac{1}{jX'}(Ee^{j\delta} - \mathbf{V})$$

By substituting the voltage phasor and reorganizing the equation, the following is obtained:

$$|\mathbf{I}|e^{j(\delta-\angle\mathbf{I})} = -\frac{E - |\mathbf{V}_0|e^{j\delta}}{j(X' + x)}$$

However, without loss of generality, $\angle\mathbf{V} = 0$ with respect to the phase of the infinite bus voltage phasor. Therefore, by replacing the current phasor into Equation 2.22a, the expression of the ordinary differential equation system is obtained as follows:

$$\begin{aligned}\dot{\delta} &= \omega_0 \Delta\omega \\ M\Delta\dot{\omega} &= -D\Delta\omega - \frac{E|\mathbf{V}_0|}{X'+x} \sin\delta + P_{\text{mech}} \\ \tau\dot{E} &= -\frac{X+x}{X'+x}E + \frac{X-X'}{X'+x}|\mathbf{V}_0| \cos\delta + V_{\text{field}}\end{aligned}$$

Similarly, from Equation 2.19 the active and reactive power supplied from the generator to the bus bar can be calculated as follows:

$$P = \frac{E|\mathbf{V}_0| \sin\delta}{X'+x}, \quad Q = \frac{xE^2 + (X'-x)E|\mathbf{V}_0| \cos\delta - X'|\mathbf{V}_0|^2}{(X'+x)^2}$$

In practice, since electrical power systems consist of multiple generators, the single machine infinite bus system model is not usually used in this book. The introduction of this model only serves as a reference.

2.3.6 Mathematical properties of the admittance matrix with reduced generator bus

Below, we mathematically discuss the existence and definiteness of the reduced admittance matrix \mathbf{Y}^{red} of Equation 2.27. Let us remember that when the capacitance to ground can be ignored, the conductance matrix G_0 is positive semi-definite and the susceptance matrix B_0 is negative definite. Moreover, the reduced conductance and susceptance matrices, which correspond to the real and imaginary parts of \mathbf{Y}^{red} are expressed as follows:

$$G^{\text{red}} := \text{Re}[\mathbf{Y}^{\text{red}}], \quad B^{\text{red}} := \text{Im}[\mathbf{Y}^{\text{red}}] \quad (2.34)$$

Then, the following facts hold.

Theorem 2.1 (Existence and definiteness of the reduced admittance matrix)

If the following is true for the admittance matrix $\mathbf{Y} \in \mathbb{C}^{N \times N}$ of Equation 2.16:

$$b_i X'_i \leq 1, \quad \forall i \in \mathcal{I}_G \quad (2.35)$$

and at the same time for at least one generator bus the inequality in Equation 2.35 is strict, then $\boldsymbol{\Gamma}$ of Equation 2.25 is nonsingular. Moreover, for the admittance matrix \mathbf{Y}^{red} of Equation 2.27, the reduced conductance matrix G^{red} is positive semi-definite, and the reduced susceptance matrix B^{red} is negative definite.

Proof By using the Mathematical Supplement 2.1 at the end of this chapter, we prove the singularity of $\boldsymbol{\Gamma}$ of Equation 2.25. From the definition, if M and N are the real and imaginary parts of $\boldsymbol{\Gamma}$, respectively, then:

$$\begin{aligned} M &:= \text{diag}(X'_i(1 - b_i X'_i)) - \text{diag}(X'_i) B_0 \text{diag}(X'_i), \\ N &:= -\text{diag}(X'_i) G_0 \text{diag}(X'_i) \end{aligned}$$

Here, since B_0 in Equation 2.16 is negative semi-definite, M is at least positive semi-definite if Equation 2.35 holds. If $b_i X'_i < 1$ for at least one $i \in \mathcal{I}_G$, then

$$\underbrace{\ker \text{diag}(X'_i) B_0 \text{diag}(X'_i)}_{\text{span}\{\text{diag}(1/X'_i)\mathbf{1}\}} \not\subseteq \ker \text{diag}(X'_i(1 - b_i X'_i))$$

and M is positive definite.

Therefore, since N is symmetric, $M + NM^{-1}N$ is positive definite. This implies that $M + NM^{-1}N$ is non-singular. Also, since N is negative semi-definite from the relation in Equation 2.15b, from the Mathematical Supplement 2.2 at the end of the chapter, it can be shown that the real part of $\boldsymbol{\Gamma}^{-1}$ is positive definite and the imaginary part is negative semi-definite. Therefore, the real part G^{red} of \mathbf{Y}^{red} is positive semi-definite and the imaginary part B^{red} is negative definite. \square

Inequality in Equation 2.35 is a sufficient condition for $\boldsymbol{\Gamma}$ to be nonsingular. However, if $b_i X'_i = 1$ for all generator buses, $\boldsymbol{\Gamma}$ is no longer nonsingular. If all b_i are sufficiently small; in other words, if the capacitance to ground of each transmission line can be ignored as in the Example 2.1, Equation 2.35 holds. Then, the reduced conductance matrix G^{red} , the real part of \mathbf{Y}^{red} , is positive semi-definite. The imaginary part, the reduced susceptance matrix B^{red} , is negative definite. For this reason, the definiteness of the admittance matrix is invariable to the Kron reduction.

2.3.7 Mathematical model of salient pole synchronous generators

Let us consider a salient pole synchronous generator model that incorporates the difference in reactance between the d and q axes [11–14]. Specifically, let us consider a situation where Equation 2.17b is as follows:

$$\begin{aligned} |\mathbf{V}_i| \sin(\delta_i - \angle \mathbf{V}_i) &= X_{qi} |\mathbf{I}_i| \cos(\delta_i - \angle \mathbf{I}_i), \\ |\mathbf{V}_i| \cos(\delta_i - \angle \mathbf{V}_i) &= E_i - X'_{di} |\mathbf{I}_i| \sin(\delta_i - \angle \mathbf{I}_i) \end{aligned} \quad (2.36)$$

where X'_{di} is the transient reactance of the d-axis. If X'_{di} and X_{qi} are equal X'_i , Equation 2.36 is consistent with Equation 2.17b.

When cancelling the current phasor using Equation 2.36, the active and reactive power are expressed as:

$$\begin{aligned} P_i &= \frac{|\mathbf{V}_i| E_i}{X'_{di}} \sin(\delta_i - \angle \mathbf{V}_i) \\ &\quad - \left(\frac{1}{X'_{di}} - \frac{1}{X_{qi}} \right) |\mathbf{V}_i|^2 \sin(\delta_i - \angle \mathbf{V}_i) \cos(\delta_i - \angle \mathbf{V}_i), \\ Q_i &= \frac{|\mathbf{V}_i| E_i}{X'_{di}} \cos(\delta_i - \angle \mathbf{V}_i) \\ &\quad - |\mathbf{V}_i|^2 \left(\frac{\cos^2(\delta_i - \angle \mathbf{V}_i)}{X'_{di}} + \frac{\sin^2(\delta_i - \angle \mathbf{V}_i)}{X_{qi}} \right) \end{aligned} \quad (2.37)$$

Similarly, if the voltage phasor is cancelled, the following is obtained:

$$\begin{aligned} P_i &= E_i |\mathbf{I}| \cos(\delta_i - \angle \mathbf{I}_i) \\ &\quad - (X'_{di} - X_{qi}) |\mathbf{I}_i|^2 \sin(\delta_i - \angle \mathbf{I}_i) \cos(\delta_i - \angle \mathbf{I}_i), \\ Q_i &= E_i |\mathbf{I}_i| \sin(\delta_i - \angle \mathbf{I}_i) \\ &\quad - |\mathbf{I}_i|^2 \{ X'_{di} \sin^2(\delta_i - \angle \mathbf{I}_i) + X_{qi} \cos^2(\delta_i - \angle \mathbf{I}_i) \} \end{aligned} \quad (2.38)$$

Similar to Equation 2.21, by combining the swing equation with the electromagnetic dynamics, the following can be obtained.

$$\begin{aligned} \dot{\delta}_i &= \omega_0 \Delta \omega_i \\ M_i \Delta \dot{\omega}_i &= -D_i \Delta \omega_i - P_i + P_{\text{mechi}} \\ \tau_i \dot{E}_i &= -\frac{X_{di}}{X'_{di}} E_i + \left(\frac{X_{di}}{X'_{di}} - 1 \right) |\mathbf{V}_i| \cos(\delta_i - \angle \mathbf{V}_i) + V_{\text{field}i} \end{aligned} \quad (2.39a)$$

However, for active power P_i , the expression of Equation 2.37 is used. Here, the voltage phasor is regarded as an input from the electrical power system to the generator i . In addition, from Equation 2.36, the current phasor can be regarded as an output from the generator to the electrical power system:

$$\begin{aligned} |\mathbf{I}_i| &= \sqrt{\left\{ \frac{|V_i|}{X_{qi}} \sin(\delta_i - \angle V_i) \right\}^2 + \left\{ \frac{E_i}{X'_{di}} - \frac{|V_i|}{X'_{di}} \cos(\delta_i - \angle V_i) \right\}^2}, \\ \angle \mathbf{I}_i &= \delta_i - \arctan \left(\frac{\frac{E_i}{X'_{di}} - \frac{|V_i|}{X'_{di}} \cos(\delta_i - \angle V_i)}{\frac{|V_i|}{X_{qi}} \sin(\delta_i - \angle V_i)} \right) \end{aligned} \quad (2.39b)$$

Similarly, if the current phasor is regarded as an input from the electrical power system to the generator i , the state space representation of the dynamic characteristics of the generator becomes the following:

$$\begin{aligned} \dot{\delta}_i &= \omega_0 \Delta \omega_i \\ M_i \Delta \dot{\omega}_i &= -D_i \Delta \omega_i - P_i + P_{\text{mechi}} \\ \tau_i \dot{E}_i &= -E_i - (X_{di} - X'_{di}) |\mathbf{I}_i| \sin(\delta_i - \angle \mathbf{I}_i) + V_{\text{field}i} \end{aligned} \quad (2.40a)$$

where P_i is calculated through Equation 2.38.

Moreover, the voltage phasor obtained from Equation 2.36, is an output from the generator to the electrical power system:

$$\begin{aligned} |V_i| &= \sqrt{\{X_{qi} |\mathbf{I}_i| \cos(\delta_i - \angle \mathbf{I}_i)\}^2 + \{E_i - X'_{di} |\mathbf{I}_i| \sin(\delta_i - \angle \mathbf{I}_i)\}^2}, \\ \angle V_i &= \delta_i - \arctan \left(\frac{X_{qi} |\mathbf{I}_i| \cos(\delta_i - \angle \mathbf{I}_i)}{E_i - X'_{di} |\mathbf{I}_i| \sin(\delta_i - \angle \mathbf{I}_i)} \right) \end{aligned} \quad (2.40b)$$

This salient pole generator model is consistent with the generator model discussed in Section 2.3.2 by assuming that X'_{di} and X_{qi} are equal to X'_i and replacing X_{di} with X_i . The relationship, $X_{di} > X_{qi} > X'_{di}$ usually holds between these reactances.

COFFEE BREAK

Relationship between generator models: The relationship between the 2-axis, 1-axis and classical models is related to the magnitude of the time constant of the electromagnetic dynamics representing the flux variation. The state-space equation of the 2-axis model when the voltage phasor of the bus is regarded as the input is:

$$\begin{cases} \dot{\delta}_i &= \omega_0 \Delta \omega_i \\ M_i \Delta \dot{\omega}_i &= -D_i \Delta \omega_i - P_i + P_{\text{mechi}} \\ \tau_{di} \dot{E}_{qi} &= -\frac{X_{di}}{X'_{di}} E_{qi} + \left(\frac{X_{di}}{X'_{di}} - 1 \right) V_{qi} + V_{\text{field}i} \\ \tau_{qi} \dot{E}_{di} &= -\frac{X_{qi}}{X'_{qi}} E_{di} + \left(\frac{X_{qi}}{X'_{qi}} - 1 \right) V_{di} \end{cases}$$

where X'_{qi} is the transient reactance of the q axis.

$$V_{di} := |V_i| \sin(\delta_i - \angle V_i), \quad V_{qi} := |V_i| \cos(\delta_i - \angle V_i)$$

Additionally, the output active and reactive power are expressed by the following

equations:

$$\begin{cases} P_i &= \frac{E_{qi}}{X'_{di}} \mathbf{V}_{di} - \frac{E_{di}}{X'_{qi}} \mathbf{V}_{qi} + \left(\frac{1}{X'_{qi}} - \frac{1}{X'_{di}} \right) \mathbf{V}_{di} \mathbf{V}_{qi}, \\ Q_i &= \frac{E_{qi}}{X'_{di}} \mathbf{V}_{qi} + \frac{E_{di}}{X'_{qi}} \mathbf{V}_{di} - \left(\frac{\mathbf{V}_{di}^2}{X'_{qi}} + \frac{\mathbf{V}_{qi}^2}{X'_{di}} \right) \end{cases}$$

Note that the state variables of the internal voltage have increased to two, E_{di} and E_{qi} . This two-axis model matches the salient pole one-axis model asymptotically if the time constant τ_{qi} is small enough. Specifically, assuming that τ_{qi} is 0, the state variable E_{di} satisfies the following relationship over time.

$$0 = -\frac{X_{qi}}{X'_{qi}} E_{di} + \left(\frac{X_{qi}}{X'_{qi}} - 1 \right) \mathbf{V}_{di}$$

Then, the active power and the active power are given by:

$$\begin{cases} P_i &= \frac{E_{qi}}{X'_{di}} \mathbf{V}_{di} + \left(\frac{1}{X_{qi}} - \frac{1}{X'_{di}} \right) \mathbf{V}_{di} \mathbf{V}_{qi}, \\ Q_i &= \frac{E_{qi}}{X'_{di}} \mathbf{V}_{qi} - \left(\frac{\mathbf{V}_{di}^2}{X_{qi}} + \frac{\mathbf{V}_{qi}^2}{X'_{di}} \right) \end{cases}$$

Therefore, the dynamic characteristics of the generator model match those of the salient pole type uniaxial model. Furthermore, in the limit when the time constant τ_{di} is small enough:

$$\begin{cases} P_i &= \frac{V_{\text{field}i}}{X_{di}} \mathbf{V}_{di} + \left(\frac{1}{X_{qi}} - \frac{1}{X_{di}} \right) \mathbf{V}_{di} \mathbf{V}_{qi}, \\ Q_i &= \frac{V_{\text{field}i}}{X_{di}} \mathbf{V}_{qi} - \left(\frac{\mathbf{V}_{di}^2}{X_{qi}} + \frac{\mathbf{V}_{qi}^2}{X_{di}} \right) \end{cases}$$

In particular, assuming the non-salient rotor type, that is, X_{di} and X_{qi} are equal X_i , and the field input $V_{\text{field}i}$ is constant and equal to V_i^\star , the above equations become:

$$P_i = \frac{V_i^\star |V_i|}{X_i} \sin(\delta_i - \angle \mathbf{V}_i), \quad Q_i = \frac{V_i^\star |V_i|}{X_i} \cos(\delta_i - \angle \mathbf{V}_i) - \frac{|\mathbf{V}_i|^2}{X_i}$$

This matches the classic model. For the detailed derivation process, refer to [3, Section 5].

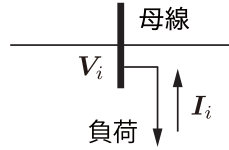


Fig. 2.14 Load connected to bus bar

2.4 Mathematical model of load

2.4.1 Relational expression of current and voltage according to load characteristics

With regard to static load models, **constant impedance model**, **constant power model**, and **constant current model** or combinations of them are often used. These are all static models described by algebraic equations with respect to the current and voltage phasors. Let us assume that voltage phasor of a bus bar i connected with a load is V_i and the current phasor flowing from the load to the bus bar is I_i (2.14). Then, the constant impedance model is given by the following relationship:

$$I_i = -\frac{V_i}{z_{\text{load}i}^*} \quad (2.41a)$$

where, $z_{\text{load}i}^* \in \mathbb{C}$ is a constant expressing the impedance of the load.

The negative sign on the right side of Equation 2.41a indicates the load is grounded and the direction of the flow of the current phasor I_i from the load to the bus bar i is defined as positive. Specifically:

$$I_i = \frac{1}{z_{\text{load}i}^*} (0 - V_i)$$

Incandescent lamps and electric heaters are common devices that can be expressed by the constant impedance model.

The constant current model is expressed by the following relationship, where $I_{\text{load}i}^* \in \mathbb{C}$ is a constant current phasor.

$$I_i = I_{\text{load}i}^* e^{j\angle V_i} \quad (2.41b)$$

In other words, the following is true for the magnitude $|I_{\text{load}i}^*|$ and phase $\angle I_{\text{load}i}^*$:

$$|I_i| = |I_{\text{load}i}^*|, \quad \angle I_i = \angle I_{\text{load}i}^* + \angle V_i$$

The constant power model is given by the following relationship:

$$I_i = \frac{P_{\text{load}i}^* - jQ_{\text{load}i}^*}{\bar{V}_i} \quad (2.41c)$$

where $P_{\text{load}_i}^* \in \mathbb{R}$ and $Q_{\text{load}_i}^* \in \mathbb{R}$ are constant active and reactive power supplied to the bus bar i . This is derived by considering the complex conjugate of:

$$P_{\text{load}_i}^* + jQ_{\text{load}_i}^* = \mathbf{V}_i \bar{\mathbf{I}}_i$$

Power converters can be represented as constant-current models or constant power model, depending on their characteristics.

Depending on the purpose of the analysis, a dynamic load model might be used. Please see [15, Section 7.1.2] for further details.

2.4.2 Kron reduction of load bus bar

Even when there are generators and multiple types of loads connected in a power system, a mathematical model of the system can be obtained by defining the relationship between the current and voltage phasors of each device using Equations 2.21 and 2.41 and combining them with Equation 2.11. In this case, the constant impedance model in Equation 2.41a gives a linear relationship between the current and voltage phasors. On the other hand, the constant-current model in Equation 2.41b and the constant-power model in Equation 2.41c provide nonlinear relationships for current and voltage phasors, which generally makes mathematical analysis of the resulting power system model difficult. Let us illustrate this fact with the following example.

Example 2.4 Kron reduction of load bus bar

Let us assume that in the electrical power system of the Example 2.1, the generators are represented by devices 1 and 2, and the load is represented by device 3. The relationship between current and voltage phasors and the admittance matrix of the power grid is given by Equation 2.10. First, let us consider the case where the load is given by the constant impedance model. If $\mathbf{z}_{\text{load}3}^*$ is the impedance of the load, the following Equation can be obtained:

$$\mathbf{I}_3 = -\frac{\mathbf{V}_3}{\mathbf{z}_{\text{load}3}^*}$$

If this is substituted into Equation 2.10 to cancel \mathbf{I}_3 :

$$\begin{bmatrix} \mathbf{I}_1 \\ \mathbf{I}_2 \\ 0 \end{bmatrix} = \begin{bmatrix} \mathbf{y}_{12} & -\mathbf{y}_{12} & 0 \\ -\mathbf{y}_{12} & \mathbf{y}_{12} + \mathbf{y}_{32} & -\mathbf{y}_{32} \\ 0 & -\mathbf{y}_{32} & \mathbf{y}_{32} + \frac{1}{\mathbf{z}_{\text{load}3}^*} \end{bmatrix} \begin{bmatrix} \mathbf{V}_1 \\ \mathbf{V}_2 \\ \mathbf{V}_3 \end{bmatrix} \quad (2.42)$$

Please note that with the equation on the third row the voltage phasor \mathbf{V}_3 can be written in function of the voltage phasor \mathbf{V}_2 of the generator bus. Specifically:

$$\mathbf{V}_3 = \left(\mathbf{y}_{32} + \frac{1}{\mathbf{z}_{\text{load}3}^*} \right)^{-1} \mathbf{y}_{32} \mathbf{V}_2$$

In addition, by replacing \mathbf{V}_3 using the above expression, the relationship between the current and voltage phasors of the generator bus bar group becomes:

$$\begin{bmatrix} \mathbf{I}_1 \\ \mathbf{I}_2 \end{bmatrix} = \mathbf{Y}_{\text{Kron}} \begin{bmatrix} \mathbf{V}_1 \\ \mathbf{V}_2 \end{bmatrix}$$

The reduced admittance matrix of the load bus bar is obtained as:

$$\mathbf{Y}_{\text{Kron}} := \begin{bmatrix} \mathbf{y}_{12} & -\mathbf{y}_{12} \\ -\mathbf{y}_{12} & \mathbf{y}_{12} + \mathbf{y}_{32} \end{bmatrix} - \begin{bmatrix} 0 \\ \mathbf{y}_{32} \end{bmatrix} \left(\mathbf{y}_{32} + \frac{1}{z_{\text{load3}}^*} \right)^{-1} \begin{bmatrix} 0 & \mathbf{y}_{32} \end{bmatrix}$$

Therefore, if the load is given as a constant impedance model, the load busbar and its variables can be eliminated by considering $\mathbf{Y}_{\text{Kron}} \in \mathbb{C}^{2 \times 2}$ as the admittance matrix of the new power grid, and the system can be equivalently transformed into a system of differential algebraic equations with only the generator connected to the busbar.

Next, let us consider a situation where the load is given as the constant current model. Let us assume that current phasor flows from the load to bus bar 3:

$$\mathbf{I}_3 = \mathbf{I}_{\text{load3}}^* e^{j\angle \mathbf{V}_3}$$

Then, following the same procedure as for the constant impedance model, and replacing \mathbf{I}_3 and \mathbf{V}_3 in Equation 2.10, the following is obtained:

$$\begin{bmatrix} \mathbf{I}_1 \\ \mathbf{I}_2 \end{bmatrix} = \mathbf{Y}'_{\text{Kron}} \begin{bmatrix} \mathbf{V}_1 \\ \mathbf{V}_2 \end{bmatrix} + \begin{bmatrix} 0 \\ -\mathbf{y}_{32} \end{bmatrix} \mathbf{y}_{32}^{-1} \mathbf{I}_{\text{load3}}^* e^{j\angle \mathbf{V}_3}$$

where:

$$\mathbf{Y}'_{\text{Kron}} := \begin{bmatrix} \mathbf{y}_{12} & -\mathbf{y}_{12} \\ -\mathbf{y}_{12} & \mathbf{y}_{12} + \mathbf{y}_{32} \end{bmatrix} - \begin{bmatrix} 0 \\ \mathbf{y}_{32} \end{bmatrix} \mathbf{y}_{32}^{-1} \begin{bmatrix} 0 & \mathbf{y}_{32} \end{bmatrix}$$

This means that, if the load is given as the constant current model, the relationship between the current and voltage phasors of the generators is affine. However, the phase $\angle \mathbf{V}_3$ of the voltage phasor of the load bus bar also has an impact on the current phasor of the generators. Generally, the phase $\angle \mathbf{V}_3$ of the voltage phasor is a nonlinear function of the voltage phasor \mathbf{V}_3 .

Finally, let us consider a case wherein the load is given as the constant power model. When constant active power P_{load3}^* and reactive power Q_{load3}^* are supplied from the load to bus bar 3, the following relationship holds:

$$\mathbf{I}_3 = \frac{P_{\text{load3}}^* - jQ_{\text{load3}}^*}{\overline{\mathbf{V}}_3}$$

Since this is a nonlinear relationship of \mathbf{I}_3 and \mathbf{V}_3 , to cancel \mathbf{V}_3 from Equation 2.10, nonlinear calculation is necessary. Specifically, \mathbf{V}_3 is given as a solution for the quadratic equation related to complex variables:

$$\mathbf{y}_{32} \mathbf{V}_3 \overline{\mathbf{V}}_3 - \mathbf{y}_{32} \mathbf{V}_2 \overline{\mathbf{V}}_3 - P_{\text{load3}}^* + jQ_{\text{load3}}^* = 0$$

Therefore, if the load of the constant power model is included in an electrical power system model, it is usually difficult to cancel the load bus bar through equivalent transformation.

As shown in Example 2.4, if the load is given as a static model expressed by Equation (2.41), the current phasor and voltage phasor of some or all load bus bars can be equivalently cancelled through algebraic calculation. This operation is called **Kron reduction of the load bus bar**. Specifically, when the load is given as the constant impedance model, Kron reduction of the load bus bar corresponds to reducing the dimension of the admittance matrix of the power grid by mathematically equivalent calculation.

If there is no device connected to the bus bar, such as a generator or load, we can assume a constant impedance model load with an infinite absolute value of $z_{\text{load}i}^*$ connected to bus i in Equation 2.41a. This is equivalent to a virtual connection of a constant-current model load in which the current phasor between the load and the bus is always zero. Therefore, the above-described Kron reduction of the load bus bar allows for equivalent cancellation of bus bars without device.

2.4.3 Mathematical properties of the admittance matrix with reduced load bus bar

Let us analyze properties that hold for Kron reduction of the load bus bar when all loads are given by the constant impedance model. First, the procedure for Kron reduction in Example 2.4 is shown as a general form when the number of generator and load buses is arbitrary. The subscripts set of generator buses is \mathcal{I}_G and the subscripts set of load bus bars is \mathcal{I}_L . Without loss of generality, the number of generator buses is assumed to be inferior to that of load buses. In other words:

$$\mathcal{I}_G = \{1, \dots, n\}, \quad \mathcal{I}_L = \{n+1, \dots, n+m\}$$

where n and m are numbers of generator buses and load bus bars, respectively. By definition, $n+m$ is equal to the total number of bus bars N .

Let $\mathbf{I}_G \in \mathbb{C}^n$ be the vector of current phasors of all generator buses, and $\mathbf{V}_G \in \mathbb{C}^n$ be the vector of voltage phasors. Similarly, the vector of current phasors of all load buses is expressed as $\mathbf{I}_L \in \mathbb{C}^m$, and the vector of voltage phasors is expressed as $\mathbf{V}_L \in \mathbb{C}^m$. Then, the relationship between all current and voltage phasors with respect to the admittance matrix $\mathbf{Y} \in \mathbb{C}^{N \times N}$ of the power grid is:

$$\begin{bmatrix} \mathbf{I}_G \\ \mathbf{I}_L \end{bmatrix} = \underbrace{\begin{bmatrix} \mathbf{Y}_{GG} & \mathbf{Y}_{GL} \\ \mathbf{Y}_{LG} & \mathbf{Y}_{LL} \end{bmatrix}}_{\mathbf{Y}} \begin{bmatrix} \mathbf{V}_G \\ \mathbf{V}_L \end{bmatrix} \quad (2.43)$$

Here, the relationship between the current phasor and the voltage phasor determined by the load in the constant impedance model is expressed using the admittance:

$$\mathbf{I}_L = -\text{diag}(\mathbf{y}_{\text{load}_i}^*)_{i \in \mathcal{I}_L} \mathbf{V}_L$$

Although $\mathbf{y}_{\text{load}_i}^*$ is defined as a reciprocal of $\mathbf{z}_{\text{load}_i}^*$ in Equation 2.41a and must have a non-zero value, since this is an expression of bus bars with no equipment connected, formally, $\mathbf{y}_{\text{load}_i}^*$ is allowed to be 0. Substituting it in Equation 2.43 to cancel \mathbf{V}_L , the followed is obtained.

$$\mathbf{I}_G = \underbrace{\left\{ \mathbf{Y}_{GG} - \mathbf{Y}_{GL} (\mathbf{Y}_{LL} + \text{diag}(\mathbf{y}_{\text{load}_i}^*)_{i \in \mathcal{I}_L})^{-1} \mathbf{Y}_{LG} \right\}}_{\mathbf{Y}_{\text{Kron}}} \mathbf{V}_G \quad (2.44)$$

Note that in general, if the load consumes active and reactive power with respect to the admittance of the load, then the following holds as in transmission lines.

$$\text{Re}[\mathbf{y}_{\text{load}_i}^*] \geq 0, \quad \text{Im}[\mathbf{y}_{\text{load}_i}^*] \leq 0, \quad \forall i \in \mathcal{I}_L \quad (2.45)$$

In addition, the conductance and susceptance matrices obtained by Kron reduction of the load bus, which are the real and imaginary parts of \mathbf{Y}_{Kron} , are expressed as:

$$G_{\text{Kron}} := \text{Re}[\mathbf{Y}_{\text{Kron}}], \quad B_{\text{Kron}} := \text{i}[\mathbf{Y}_{\text{Kron}}]$$

This introduces the following fact:

Theorem 2.2 (Properties of the Kron-reduced admittance matrix) *For the admittance matrix $\mathbf{Y} \in \mathbb{C}^{N \times N}$ of Equation 2.16, by dividing the block matrix of Equation 2.43, $\mathbf{Y}_{\text{Kron}} \in \mathbb{C}^{n \times n}$ of Equation 2.44 can be obtained, corresponding to the admittance matrix of the system after the Kron reduction of the load bus bars. Additionally, the admittance $\mathbf{y}_{\text{load}_i}^*$ of each load satisfies Equation 2.45. Then, the reduced conductance matrix G_{Kron} is positive semi-definite, and the reduced susceptance matrix B_{Kron} is symmetric. Furthermore, if the following is true for the generator buses:*

$$b_i = 0, \quad \forall i \in \mathcal{I}_G \quad (2.46a)$$

And the following is true for load bus bars:

$$\text{Im}[\mathbf{y}_{\text{load}_i}^*] + b_i \leq 0, \quad \forall i \in \mathcal{I}_L \quad (2.46b)$$

where b_i is a non-negative constant equivalent to the capacitance to ground of Equation 2.16, B_{Kron} is negative semidefinite.

Specifically, if the inequality of Equation 2.46b strictly holds for at least one load bus bar, then B_{Kron} is negative definite.

Proof Using Lemma 2.3 of the Mathematical Supplement at the end of the chapter, let us define:

$$\mathbf{Y}' := \begin{bmatrix} \mathbf{Y}_{GG} & \mathbf{Y}_{GL} \\ \mathbf{Y}_{LG} & \mathbf{Y}_{LL} + \text{diag}(\mathbf{y}_{\text{load}_i}^*)_{i \in \mathcal{I}_L} \end{bmatrix}$$

Since Equations 2.15b and 2.45 hold, the real part of $j\mathbf{Y}'$ is symmetric, and the imaginary part is positive semidefinite. Therefore, Lemma 2.3 shows that the real part of $j\mathbf{Y}_{\text{Kron}}$ is symmetric and the imaginary part is semi-positive. This implies that the real part of \mathbf{Y}_{Kron} , G_{Kron} , is positive semidefinite and the imaginary part, B_{Kron} , is symmetric.

Moreover, when Equation 2.46 holds, the imaginary part of \mathbf{Y}' is negative semidefinite, which by the Lemma 2.3 implies that B_{Kron} is negative semidefinite. Similarly, if Equation 2.46b holds strictly for at least one load bus bar, then \mathbf{Y}' and B_{Kron} are negative definite.

Theorem 2.2 shows that, if all loads are given by the constant impedance model, the conductance and susceptance matrix of related to the admittance matrix of Equation 2.16 remain positive semidefinite and symmetric, respectively, even if the load bus bars were Kron reduced. Therefore, it can be similarly applied to the electrical power system model, in which the generator buses and load bus bars in Section 2.3.3 are Kron reduced. Theorem 2.2 shows a case where all load bus bars are Kron reduced simultaneously. However, the same fact is shown when only some of load bus bars are Kron reduced.

As discussed above, while the definiteness of the admittance matrix is invariable to Kron reduction, the "element signs" of the real and imaginary parts are not necessarily invariable. Let us confirm this with the next Example.

Example 2.5 Sign change of the admittance matrix by Kron reduction of bus bars

Regarding the admittance matrix \mathbf{Y}_0 when the ground capacitance in Equation 2.15 is negligible, the conductance matrix G_0 is positive semidefinite and the susceptance matrix B_0 is negative semidefinite. Then, the diagonal and non-diagonal elements of G_0 are non-negative and non-positive, respectively, and the diagonal and non-diagonal elements of B_0 are non-positive and non-negative, respectively. For example, let bus 1 and bus 2 be the generator bus, bus 3 be the load bus. Then, the load bus admittance and the power grid admittance matrix are:

$$\mathbf{y}_{\text{load}_3}^* = \alpha - j\beta, \quad \mathbf{Y} = \gamma \underbrace{\begin{bmatrix} 1 & -1 & 0 \\ -1 & 1 & 0 \\ 0 & 0 & 0 \end{bmatrix}}_{G_0} + j \underbrace{\begin{bmatrix} -2 & 1 & 1 \\ 1 & -2 & 1 \\ 1 & 1 & -2 \end{bmatrix}}_{B_0}$$

where α , β , and γ are non-negative constants. Please note that the signs of the real and imaginary parts of the load bus admittance of are the same as the signs of the diagonal element of the admittance matrix.

By Kron reducing the load bus bar, the reduced admittance matrix of Equation 2.44 becomes:

$$\mathbf{Y}_{\text{Kron}} = \underbrace{\gamma \begin{bmatrix} 1 & -1 \\ -1 & 1 \end{bmatrix} + \frac{\alpha}{\alpha^2 + (2+\beta)^2} \begin{bmatrix} 1 & 1 \\ 1 & 1 \end{bmatrix}}_{G_{\text{Kron}}} \\ + j \underbrace{\left(\begin{bmatrix} -2 & 1 \\ 1 & -2 \end{bmatrix} + \frac{2+\beta}{\alpha^2 + (2+\beta)^2} \begin{bmatrix} 1 & 1 \\ 1 & 1 \end{bmatrix} \right)}_{B_{\text{Kron}}}$$

Here, for arbitrary non-negative constants, α , β , and γ , the diagonal element of G_{Kron} is non-negative and the diagonal and non-diagonal elements of B_{Kron} are negative and positive, respectively. However, the non-diagonal element of G_{Kron} is positive when:

$$\gamma < \frac{\alpha}{\alpha^2 + (2+\beta)^2}$$

Thus, when the load bus bar is Kron reduced, the sign of the non-diagonal elements of the admittance matrix is not always invariable. The diagonal elements are invariable because of the positive semidefinite nature of G_0 and the negative semidefinite nature of B_0 .

A change of sign of an off-diagonal element can occur when the conductance and susceptance are both non-zero for the load or transmission line connected to the bus bar being Kron reduced. For example, in the above case, the admittance of the load is a pure imaginary number when $\alpha = 0$ and the admittance of the transmission line connected to bus bar 3; in other words, the elements of the third column and the third row of \mathbf{Y} , are all pure imaginary. In such a case, it can be shown that there is no sign change of the elements of the conductance and susceptance matrices.

The above-described Kron reduction has been known as a mathematical operation related to the derivation of an equivalent circuit [16]. Specifically, in the analysis of an electrical power system, it is applied to power flow calculations explained in Section 3.1. Kron reduction has also been applied in graph theory, and has interesting mathematical properties [17].

Mathematical Supplement

Lemma 2.1 *Assume that the real matrix M is regular. Then, for real matrix N , the necessary and sufficient condition for $M + jN$ to be regular is that $M + NM - 1N$ is regular.*

Proof First, the fact that $M + jN$ is regular is equivalent to the fact that there exist certain real square matrices P and Q such that $(M+jN)(P+jQ) = I$. If we rearrange these two equations for the real and imaginary parts, we get:

$$\underbrace{\begin{bmatrix} M & -N \\ N & M \end{bmatrix}}_L \begin{bmatrix} P & -Q \\ Q & P \end{bmatrix} = I \quad (2.47)$$

This means that the regularity of $M + jN$ is equivalent to the regularity of L . Furthermore, using the properties of the determinant of block matrices:

$$\det L = \det M \det(M + NM^{-1}N)$$

From the assumption that $\det M \neq 0$, the regularity of L is equivalent to the regularity of $M + NM^{-1}N$. Then, the lemma is proven to be true. \square

Lemma 2.2 *Let the real part of the complex matrix Z be positive definite. If the imaginary part of Z is symmetric, then the real part of Z^{-1} is positive definite and the imaginary part is symmetric. In particular, if the imaginary part of Z is positive semidefinite, then the imaginary part of Z^{-1} is negative semidefinite. Also, if the imaginary part of Z is positive definite, the imaginary part of Z^{-1} is negative definite.*

Proof Let $Z = M + jN$, where M is a real positive definite matrix and N is a symmetric matrix. Let P be the real part of Z^{-1} and Q be its imaginary part. From the Lemma 2.1, $M + NM^{-1}N$ is positive definite and therefore Z is regular. Therefore

$$(M + jN)(P + jQ) = I$$

The equations for the real and imaginary parts of L are equivalent to the Equation 2.47. This means that the diagonal and off-diagonal blocks of the inverse of L are P and Q . From the properties of the inverse of block matrices:

$$L^{-1} = \begin{bmatrix} (M + NM^{-1}N)^{-1} & M^{-1}N(M + NM^{-1}N)^{-1} \\ -(M + NM^{-1}N)^{-1}NM^{-1} & (M + NM^{-1}N)^{-1} \end{bmatrix}$$

Therefore,

$$P = (M + NM^{-1}N)^{-1}, \quad Q = -M^{-1}N(M + NM^{-1}N)^{-1}$$

From the assumption that N is symmetric and M is positive definite, P is positive definite. Also, using the positive definite matrix $\sqrt{M^{-1}}$ such that $M^{-1} = \sqrt{M^{-1}}\sqrt{M^{-1}}$, Q is

$$Q = -\sqrt{M^{-1}} \underbrace{\sqrt{M^{-1}}N\sqrt{M^{-1}} \left(I + (\sqrt{M^{-1}}N\sqrt{M^{-1}})^2 \right)^{-1}}_X \sqrt{M^{-1}}$$

where $\sqrt{M^{-1}}N\sqrt{M^{-1}}$ is symmetric, so it can be diagonalized by the orthogonal matrix V and

$$X = V\Lambda \left(I + \Lambda^2 \right)^{-1} V^\top$$

However, Λ is a real diagonal matrix of eigenvalues of $\sqrt{M^{-1}}N\sqrt{M^{-1}}$. From this, since X is symmetric, Q is also symmetric. Furthermore, if N is semi-definite, then Λ is also semi-definite, and if N is positive, then Λ is also positive. Therefore, if N is semi-positive definite, then Q is semi-negative definite, and if N is positive definite, then Q is negative definite. From the above, the subject follows. \square

Lemma 2.3 *Let M and N be symmetric real matrices, which are partitioned into block matrices as follows:*

$$\begin{bmatrix} \mathbf{Z}_{11} & \mathbf{Z}_{12} \\ \mathbf{Z}_{21} & \mathbf{Z}_{22} \end{bmatrix} := \underbrace{\begin{bmatrix} M_{11} & M_{12} \\ M_{12}^\top & M_{22} \end{bmatrix}}_M + j \underbrace{\begin{bmatrix} N_{11} & N_{12} \\ N_{12}^\top & N_{22} \end{bmatrix}}_N \quad (2.48)$$

Let \mathbf{Z}_S denote $\mathbf{Z}_{11} - \mathbf{Z}_{12}\mathbf{Z}_{22}^{-1}\mathbf{Z}_{21}$. Moreover, assume that M is positive semi-definite and M_{22} is positive definite. Then the real part of \mathbf{Z}_S is positive semi-definite, and the imaginary part of \mathbf{Z}_S is symmetric. In particular, if N is positive semi-definite, then the imaginary part of \mathbf{Z}_S is also positive semi-definite. Furthermore, if N is positive definite, then the imaginary part of \mathbf{Z}_S is positive definite. Finally, if M is positive definite, then the real part of \mathbf{Z}_S is positive definite.

Proof Let us denote the matrix on the left-hand side of Equation 2.48 as \mathbf{Z} . First, if M is positive definite, then the real part of \mathbf{Z}_S is positive definite and the imaginary part is symmetric. Now, due to the positive definiteness of M_{22} , Lemma 2.1 implies that \mathbf{Z}_{22} is nonsingular. Hence by the property of the inverse of a block matrix, \mathbf{Z}_S^{-1} coincides with the upper left block of \mathbf{Z}^{-1} . Here, Lemma 2.2 implies that the real part of \mathbf{Z}^{-1} is positive definite and the imaginary part is symmetric. This means that the real part of \mathbf{Z}_S^{-1} is positive definite and the imaginary part is symmetric. Thus, by applying Lemma 2.2 to \mathbf{Z}_S^{-1} , we show the positive definiteness of the real part and the symmetry of the imaginary part of \mathbf{Z}_S .

Next, consider the case where M is positive semi-definite and N is symmetric. First, show that both the real and imaginary parts of \mathbf{Z}_S are symmetric. Now, since the real part M_{22} of \mathbf{Z}_{22} is positive definite and the imaginary part N_{22} is symmetric, both real and imaginary parts of \mathbf{Z}_{22}^{-1} are symmetric. Therefore,

$$\begin{aligned} \text{Re}[\mathbf{Z}_S] &= \text{Re}[\mathbf{Z}_{11}] - \text{Re}[\mathbf{Z}_{12}] \text{Re}[\mathbf{Z}_{22}^{-1}] \text{Re}[\mathbf{Z}_{21}] \\ &\quad + i[\mathbf{Z}_{12}]i[\mathbf{Z}_{22}^{-1}] \text{Re}[\mathbf{Z}_{21}] + i[\mathbf{Z}_{12}] \text{Re}[\mathbf{Z}_{22}^{-1}]i[\mathbf{Z}_{21}] \\ &\quad + \text{Re}[\mathbf{Z}_{12}]i[\mathbf{Z}_{22}^{-1}]i[\mathbf{Z}_{21}] \\ &= M_{11} - M_{12} \text{Re}[\mathbf{Z}_{22}^{-1}]M_{12}^\top + N_{12}i[\mathbf{Z}_{22}^{-1}]M_{12}^\top + N_{12} \text{Re}[\mathbf{Z}_{22}^{-1}]N_{12}^\top \\ &\quad + M_{12}i[\mathbf{Z}_{22}^{-1}]N_{12}^\top \end{aligned}$$

From this we see that the real part of \mathbf{Z}_S is symmetric. Similarly,

$$\begin{aligned} i[\mathbf{Z}_S] = & N_{11} + N_{12}i[\mathbf{Z}_{22}^{-1}]N_{12}^T - N_{12}\operatorname{Re}[\mathbf{Z}_{22}^{-1}]M_{12}^T \\ & - M_{12}i[\mathbf{Z}_{22}^{-1}]M_{12}^T - M_{12}\operatorname{Re}[\mathbf{Z}_{22}^{-1}]N_{12}^T \end{aligned}$$

From this we see that the imaginary part of \mathbf{Z}_S is also symmetric.

When M in Equation 2.48 is positive semi-definite, \mathbf{Z} is not always nonsingular and therefore \mathbf{Z}^{-1} may not exist. In what follows, for any $\epsilon > 0$:

$$\mathbf{Z}^+ := \begin{bmatrix} \mathbf{Z}_{11} + \epsilon I & \mathbf{Z}_{12} \\ \mathbf{Z}_{21} & \mathbf{Z}_{22} + \epsilon I \end{bmatrix}$$

The real part of $M + \epsilon I$, is positive definite. If N is positive semi-definite, then for any $\epsilon > 0$, the real part of the following matrix is positive definite, and its imaginary part is positive semi-definite:

$$\mathbf{Z}_S^+ := \mathbf{Z}_{11} + \epsilon I - \mathbf{Z}_{12}(\mathbf{Z}_{22} + \epsilon I)^{-1}\mathbf{Z}_{21}$$

Moreover, expanding $(\mathbf{Z}_{22} + \epsilon I)^{-1}$ using the auxiliary theorem of the inverse matrix the following is obtained.

$$\mathbf{Z}_S^+ = \mathbf{Z}_S + \underbrace{\epsilon \left\{ I + \mathbf{Z}_{12}\mathbf{Z}_{22}^{-1}(I + \epsilon\mathbf{Z}_{22}^{-1})^{-1}\mathbf{Z}_{22}^{-1}\mathbf{Z}_{21} \right\}}_{\Delta(\epsilon)}$$

As mentioned above, since the real and imaginary parts of \mathbf{Z}_S^+ and \mathbf{Z}_S are symmetric, the real and imaginary parts of $\Delta(\epsilon)$ are also symmetric.

Next, we show that if the imaginary part of \mathbf{Z}_S^+ is positive semi-definite, then the imaginary part of \mathbf{Z}_S is also positive semi-definite. Note that the same argument can be applied to the real part. For this purpose, we define:

$$\mathcal{X} := \{x : x^T i[\Delta(\epsilon)]x > 0, \quad \forall \epsilon > 0\}$$

From this definition of \mathcal{X} , for any x chosen arbitrarily $x \notin \mathcal{X}$, there exists some $\epsilon_0 > 0$ such that:

$$x^T i[\Delta(\epsilon_0)]x \leq 0$$

Therefore, since the imaginary part of \mathbf{Z}_S^+ is positive semi-definite, we have:

$$x^T i[\mathbf{Z}_S]x + x^T i[\Delta(\epsilon_0)]x \geq 0$$

This leads to the following for all $x \notin \mathcal{X}$:

$$x^T i[\mathbf{Z}_S]x \geq 0 \tag{2.49}$$

Furthermore, we prove the contrapositive that if the imaginary part of \mathbf{Z}_S^+ is not positive semi-definite, then Equation 2.49 does not hold for all $x \in \mathcal{X}$. That is, if there exists an $x \in \mathcal{X}$ such that

$$x^T i[\mathbf{Z}_S]x < 0 \tag{2.50}$$

then we show that the imaginary part of \mathbf{Z}_S^+ is not positive semi-definite.

Now, noting that the imaginary part of $\Delta(\epsilon)$ approaches to zero as $\epsilon \rightarrow 0$, if Equation 2.50 holds for some $x \in X$, then there exists some ϵ_0 such that:

$$x^T i[\mathbf{Z}_S]x + x^T i[\Delta(\epsilon_0)]x < 0$$

This means that the imaginary part of \mathbf{Z}_S^+ is not positive semi-definite. From these facts, we can conclude that the imaginary part of \mathbf{Z}_S is positive semi-definite.

Finally, we show that if N is positive definite, then the imaginary part of \mathbf{Z}_S is positive definite. For this purpose, we can use the fact that the real part of the following matrix is positive definite and its imaginary part is symmetric.

$$-j\mathbf{Z} = N - jM$$

Applying the results for the case when the real part of $-j\mathbf{Z}$ is positive definite, we can conclude that the real part of $-j\mathbf{Z}_S$ is positive definite, which means that the imaginary part of \mathbf{Z}_S is positive definite. \square

Chapter 3

Numerical simulation of the electrical power system model

In this chapter, we will explain numerical simulation methods for power system models described by nonlinear differential algebraic equation systems. We will also provide guidelines for building a structured numerical simulation environment.

The chapter is organized as follows. First, in Section 3.1, we will explain the difficulty of calculating the time response of power system models. Next, in section 3.2, we will describe the process of power flow calculation, which numerically explores the equilibrium state of power system models. In section 3.3, we will discuss how to determine the steady-state values of internal states of generators and constants of load models that are consistent with the steady-state values of bus voltages and power determined by power flow calculation.

In section 3.4, we will explain the calculation methods for time responses to changes in initial conditions, load fluctuations, and ground faults, and illustrate the calculation of time responses. Finally, in section 3.5, we will discuss synchronism phenomena of bus voltages in steady-state power flow states from an advanced perspective, and analyze them mathematically.

3.1 Calculation of time response of an electrical power system

3.1.1 Challenges in calculating time response

In Chapter 2, we explained that the mathematical model of the entire power system, including generator and load models coupled with transmission line models, is described by a system of nonlinear differential algebraic equations. Therefore, the time response of the power system model can be obtained by numerically integrating these equations with appropriate initial values and external inputs. However, when performing numerical simulations of the power system model, it is necessary to consider specific characteristics of the power system, such as:

- If external inputs are not properly set, the demand and supply will not be in equilibrium, and the steady-state value of the frequency deviation will not be zero, causing the rotor angle of the generator to continue to change.
- There are an infinite number of combinations of external input values that result in zero steady-state value for frequency deviation. Therefore, it is necessary to specify realistic external input values.
- The values of the voltage phase and current phase of the bus bar group must be determined so that they are consistent as dependent variables with respect to the state variables of the generator group.

Therefore, simply using the differential-algebraic equation solver that is standardly implemented in MATLAB is not sufficient to accurately execute numerical simulations of the power system. This is one of the factors that makes the calculation of the time response of the power system model difficult.

3.1.2 Calculation steps

The standard calculation procedure for the time response of a power system model described by nonlinear differential algebraic equations is divided into the following three steps:

- (A) To specify the power system state in a steady state where supply and demand are balanced, calculate the values of the phase angle and voltage of all buses in the steady state using the admittance matrix determined from the transmission network.
 - (B) Calculate the steady-state values of the internal voltage and rotor angle of each generator, the external input values to the generator, and the impedance value of each load, so that they are consistent with the steady-state values of the bus current phase and voltage phase determined in Step A.
 - (C) Using the power system state where supply and demand are balanced calculated in Steps A and B as the initial value, calculate the time response under various disturbances of different magnitudes such as giving perturbations to the internal state of the generator, grounding the voltage of the bus, or changing the parameter values of the load.

From the viewpoint of system control engineering, Step A can be understood as "determining one equilibrium point to perform numerical analysis from among an infinite number of equilibrium points." As described in Section 3.3, when the steady-state values of the phase angle and voltage of all buses are given, there must exist steady-state values of the internal state of the generator, external input values to the generator, and the load parameter values that realize them. Therefore, calculating the steady-state values of the phase angle and voltage of all buses is equivalent to calculating the equilibrium point of the power system model represented by differential

algebraic equations. In power system engineering, this process is called the **power flow calculation**.

It should be noted that calculating the steady-state values of the internal state of the generator, external input values, and the load parameter values in Step B is an indirect procedure of determining the mathematical model of the load from the results of the power flow calculation in Step A. For example, if you want to set the load connected to a certain bus as a constant impedance model, you need to reverse calculate the impedance value of the load using the current phase of the bus calculated by the power flow calculation divided by the voltage phase. If setting load model parameters as desired values, in Step C, the time response to load parameter fluctuations is calculated while changing the load parameters to desired values.

Finally, in Step C, the time response of the electrical power system model is calculated under various conditions depending on the purpose. For example, if the external input to each generator and load parameter calculated in Steps A and B are set as constants in the model, and the time response is calculated with the initial value appropriate for generators, the internal state of the generators asymptotically converges to the steady state calculated in Step B over time. However, to set valid initial values such that asymptotic convergence is established, as in Steps A and B, the equilibrium point that serves as the reference for the analysis must be calculated first. The calculated equilibrium point must be stable in an appropriate sense.

3.2 Numerical analysis of steady-state in power flow calculation

In this Section, we describe an overview of power flow calculation to numerically search the steady-state of the power system, as explained in Step A of Section 3.1.2 and the implementation method using MATLAB.

Given the admittance matrix \mathbf{Y} , the distribution of current and voltage phasors of the busbar group that satisfies the following relationship is referred to as the **power flow distribution** at time t .

$$\begin{bmatrix} \mathbf{I}_1(t) \\ \vdots \\ \mathbf{I}_N(t) \end{bmatrix} = \underbrace{\begin{bmatrix} Y_{11} & \cdots & Y_{1N} \\ \vdots & \ddots & \vdots \\ Y_{N1} & \cdots & Y_{NN} \end{bmatrix}}_{\mathbf{Y}} \begin{bmatrix} \mathbf{V}_1(t) \\ \vdots \\ \mathbf{V}_N(t) \end{bmatrix} \quad (3.1)$$

$$(|\mathbf{I}_1(t)|, \angle \mathbf{I}_1(t), |\mathbf{V}_1(t)|, \angle \mathbf{V}_1(t), \dots, |\mathbf{I}_N(t)|, \angle \mathbf{I}_N(t), |\mathbf{V}_N(t)|, \angle \mathbf{V}_N(t)) \quad (3.2)$$

Each current and voltage phasors changes with time, and from the laws of physics of current and voltage, these must satisfy Equation 3.1 at any arbitrary time t .

Power flow calculation is a computational process to find "one of the steady-state power flow distributions". A steady-state power flow distribution refers to the condi-

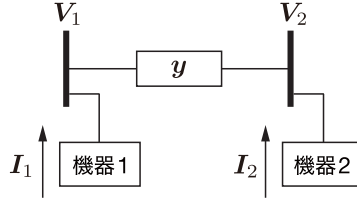


Fig. 3.1 Power system model consisting of two bus bars

tion that all the buses satisfy the following for given constant current phasors \mathbf{I}_i^* and voltage phasors \mathbf{V}_i^* .

$$\mathbf{I}_i(t) = \mathbf{I}_i^*, \quad \mathbf{V}_i(t) = \mathbf{V}_i^*, \quad \forall t \geq 0$$

Using the definitions of active power and reactive power supplied to the bus bars in the following equation, the current phasors can be eliminated.

$$P_i(t) + jQ_i(t) = \mathbf{V}_i(t)\bar{\mathbf{I}}_i(t) \quad (3.3)$$

Thus, the system of equations in Equation 3.1 is equivalent to:

$$\begin{aligned} P_1(t) + jQ_1(t) &= \sum_{j=1}^N \bar{Y}_{1j} |\mathbf{V}_1(t)| |\mathbf{V}_j(t)| e^{j(\angle \mathbf{V}_1(t) - \angle \mathbf{V}_j(t))} \\ &\vdots \\ P_N(t) + jQ_N(t) &= \sum_{j=1}^N \bar{Y}_{Nj} |\mathbf{V}_N(t)| |\mathbf{V}_j(t)| e^{j(\angle \mathbf{V}_N(t) - \angle \mathbf{V}_j(t))} \end{aligned} \quad (3.4)$$

Therefore, depending on the context, the distribution of active power, reactive power, and voltage phasors satisfying Equation 3.4 is referred to as the power flow distribution at time t .

$$(P_1(t), Q_1(t), |\mathbf{V}_1(t)|, \angle \mathbf{V}_1(t), \dots, P_N(t), Q_N(t), |\mathbf{V}_N(t)|, \angle \mathbf{V}_N(t)) \quad (3.5)$$

3.2.1 Outline of the power flow calculation

Let us explain the characteristics of the power flow calculation using a simple example consisting of two bus bars.

Example 3.1 Power flow calculation of a two bus bar power system model

Let us consider an electrical power system consisting of two bus bars, as shown in Figure 3.1. We assume that each bus is connected to either a load or a generator, but in power flow calculations, it is not necessary to specify the type of device connected.

The admittance of a transmission line that connects two bus bars is denoted by $y \in \mathbb{C}$. When using the basic transmission line model, the voltage and current phasors at the buses are related by:

$$\begin{bmatrix} I_1^* \\ I_2^* \end{bmatrix} = \begin{bmatrix} y & -y \\ -y & y \end{bmatrix} \begin{bmatrix} V_1^* \\ V_2^* \end{bmatrix} \quad (3.6)$$

However, to indicate that these values are in a steady-state, they are marked with a "★". Here, by eliminating the current phasors using the relationship in Equation 3.3, we obtain a system of equations equivalent to Equation 3.6 in terms of steady-state active power, reactive power, and voltage phasors as follows:

$$\begin{aligned} P_1^* + jQ_1^* &= \bar{y} \left(|V_1^*|^2 - |V_1^*||V_2^*|e^{j(\angle V_1^* - \angle V_2^*)} \right) \\ P_2^* + jQ_2^* &= \bar{y} \left(|V_2^*|^2 - |V_1^*||V_2^*|e^{j(\angle V_2^* - \angle V_1^*)} \right) \end{aligned} \quad (3.7a)$$

The objective of the power flow calculation is to determine the following set of values that satisfy the above simultaneous equations.

$$(P_1^*, Q_1^*, |V_1^*|, \angle V_1^*, P_2^*, Q_2^*, |V_2^*|, \angle V_2^*)$$

We denote the conductance and susceptance of a transmission line as:

$$g := \text{Re}[y], \quad b := \text{Im}[y]$$

Then, considering the real and imaginary parts of Equation 3.7a, we obtain a system of four equations:

$$\begin{aligned} P_1^* &= g|V_1^*|^2 - g|V_1^*||V_2^*|\cos\angle V_{12}^* - b|V_1^*||V_2^*|\sin\angle V_{12}^* \\ P_2^* &= g|V_2^*|^2 - g|V_1^*||V_2^*|\cos\angle V_{21}^* - b|V_1^*||V_2^*|\sin\angle V_{21}^* \\ Q_1^* &= -b|V_1^*|^2 + b|V_1^*||V_2^*|\cos\angle V_{12}^* - g|V_1^*||V_2^*|\sin\angle V_{12}^* \\ Q_2^* &= -b|V_2^*|^2 + b|V_1^*||V_2^*|\cos\angle V_{21}^* - g|V_1^*||V_2^*|\sin\angle V_{21}^* \end{aligned} \quad (3.7b)$$

where $\angle V_{ij}^*$ represents $\angle V_i^* - \angle V_j^*$.

The phase of the voltage phasor is only meaningful in terms of the difference value; thus, the number of variables that must be practically determined is seven. Therefore, there are three variables of freedom in Equation 3.7b. To determine these, one can choose appropriate values for the three variables ($|V_1^*|$, $|V_2^*|$, $\angle V_{12}^*$). This allows us to calculate the remaining variables (P_1^* , P_2^* , Q_1^* , Q_2^*)

However, with this method, while the voltage phase of each bus can be set to any value, it is not possible to set the power supplied or consumed by each bus to any value. That is, it is not possible to specify which bus is a load bus that consumes power, or which bus is a generator bus that supplies power. Therefore, in order to

perform numerical simulations with realistic settings, it is often necessary to properly determine the voltage phase values to achieve the specified active and reactive power values.

For example, let us consider finding the ($|V_1^*|$, $|V_2^*|$, $\angle V_{12}^*$) that realize balanced active power supplied to the bus as:

$$P_1^* = 1, \quad P_2^* = -1 \quad (3.8)$$

This corresponds to determining the voltage phase distribution when the device connected to bus 1 and bus 2 both supply and consume active power, respectively, with both having a value of 1 in a steady-state condition. By adding the equations in Equation 3.7b with respect to P_1^* and P_2^* , we obtain:

$$\begin{aligned} 0 &= g \left\{ |V_1^*|^2 + |V_2^*|^2 - 2|V_1^*||V_2^*| \cos \angle V_{12}^* \right\} \\ &= g \left\{ (|V_1^*| - |V_2^*|)^2 + 2|V_1^*||V_2^*|(1 - \cos \angle V_{12}^*) \right\} \end{aligned}$$

Note that in realistic power flow conditions, the phase difference in voltage phase between the buses, $\angle V_{12}^*$, is within the range of $\pm \frac{\pi}{2}$. Moreover, it should be noted that if the phase angle difference of the generator or the voltage phase difference of the bus exceeds the range of $\pm \frac{\pi}{2}$, the slope of the sine function will be inverted, resulting in an unrealistic transmission characteristic of active power.

From this, if the conductance g of the transmission line, which is the real part of y , is not equal to zero, then the voltage phase that satisfies this equation must necessarily satisfy:

$$|V_1^*| = |V_2^*|, \quad \angle V_{12}^* = 0 \quad (3.9)$$

However, Equation 3.9 implies that both P_1^* and P_2^* are equal to 0. Therefore, it can be concluded that a steady-state current state satisfying Equation 3.8 does not exist as long as g is not equal to 0. This is because the conductance component (resistance component) of the transmission line causes power loss, and in the setting of Equation 3.8, it indicates that the power supply and demand are not balanced across the entire system. Therefore, it is important to note that for certain values of active and reactive power, there might not exist solutions to Equation 3.7.

Next, let us assume that the conductance g of the transmission line is zero for simplicity. Additionally, assume that the ground capacitance is sufficiently small and the susceptance b is negative. Then:

$$P_1^* = -b|V_1^*||V_2^*| \sin \angle V_{12}^*, \quad P_2^* = b|V_1^*||V_2^*| \sin \angle V_{12}^*$$

In this case, the voltage phasor distribution must be such that $P_1^* = -P_2^*$.

For example, in the case where the value of Equation 3.8 is specified, the absolute value of the voltage phasor can be specified as:

$$|V_1^*| = \sqrt{\frac{2}{|b|}}, \quad |V_2^*| = \sqrt{\frac{2}{|b|}}$$

As a result, the phase difference can be determined as:

$$\angle V_{12}^* = \frac{\pi}{6}$$

Since three or more variables have already been determined, the reactive power is automatically determined as:

$$Q_1^* = 2 - \sqrt{3}, \quad Q_2^* = 2 + \sqrt{3}$$

As shown in Example 3.1, the power flow calculation is a procedure that determines a set of $4N$ constants, given the admittance matrix \mathbf{Y} of the power network and $2N$ simultaneous equations in steady state:

$$P_1^* + jQ_1^* = \sum_{j=1}^N \bar{Y}_{1j} |V_1^*| |V_j^*| e^{j(\angle V_1^* - \angle V_j^*)} \\ \vdots \quad (3.10)$$

$$P_N^* + jQ_N^* = \sum_{j=1}^N \bar{Y}_{Nj} |V_N^*| |V_j^*| e^{j(\angle V_N^* - \angle V_j^*)}$$

$$(P_1^*, Q_1^*, |V_1^*|, \angle V_1^*, \dots, P_N^*, Q_N^*, |V_N^*|, \angle V_N^*) \quad (3.11)$$

where $|V_i^*$ and $\angle V_i^*$ are the magnitude and phase angle of the voltage at bus i in polar form, and P_i^* and Q_i^* are the active and reactive power injections at bus i , respectively. Note that the phase angle of the voltage is only meaningful in a relative sense, so there are effectively only $(4N - 1)$ variables to be determined.

As described in Section 3.1.2, the power flow calculation can be interpreted as a procedure for finding the equilibrium point of a power system model that is capable of balancing demand and supply throughout the system. The characteristics of individual devices, such as generators and loads, are not considered in this process, and only the steady-state values of inputs and outputs at each bus are determined.

More precisely, Step B in Section 3.1.2 is used to calculate the equilibrium point of the internal state of the system of differential-algebraic equations. The calculation of Step B is described in Section 3.3.

3.2.2 Numerical Search Method for Steady-State Power Flow

Generally, the standard models of the Institute of Electrical Engineers in Japan [?], the IEEE 39-bus system model [18], and the IEEE 68-bus system model [19], provide data sheets with standard values for the power supplied by each generator bus and the power consumed by each load bus, in addition to the impedance values of each

transmission line. By specifying $2N$ variables based on these standard values, the remaining variables can be explored numerically.

The data sheets typically provide the values of active and reactive power consumed by each load bus, as well as the active power supplied by each generator bus and the magnitude of the voltage phase at that bus. Therefore, $2N$ steady-state values can be specified in advance using these values. However, as shown in Example 3.1, if all steady-state values of active power at every bus are specified in advance, the remaining variables cannot be set to any value that satisfies the system of equations in 3.4 due to the impact of transmission losses. For instance, if the values of active or reactive power at some load buses are specified at a different steady-state value from that on the data sheet, the steady-state values of active and reactive power that should be supplied to the generator bus change, and as a result, the steady-state values of power flowing through the transmission network and the voltage phase of the bus also change, leading to a change in the total transmission loss for the entire system. Therefore, if steady-state values of active power at every generator bus are specified in advance, the system of equations in 3.4 cannot generally be solved.

A typical solution to this problem is to introduce a special generator bus called the **slack bus** to resolve it. At the slack bus, instead of specifying the active power, the phase of the voltage phase is specified. At this time, only the relative value of the voltage phase at each bus has meaning, so the steady-state value of the phase of the slack bus can be set to 0 without losing generality. As a result, the active power at the slack bus is automatically determined to be consistent with the total transmission loss for the entire system. The above steps can be summarized as follows.

- (a) Based on the data sheet, the value of $(|V_{i_0}^*|, \angle V_{i_0}^*)$ is specified for the slack bus, the value of $(P_i^*, |V_i^*|)_{i \in \mathcal{I}_G \setminus \{i_0\}}$ is specified for other generator buses, and the value of $(P_i^*, Q_i^*)_{i \in \mathcal{I}_L}$ is specified for the load bus bar.
- (b) Other variables are numerically searched to satisfy simultaneous equations of Equation 3.4.

Here, \mathcal{I}_G is the set of indices for generator buses, \mathcal{I}_L is the set of indices for load buses, and $i_0 \in \mathcal{I}_G$ represents the index of the slack bus. Unconnected buses are treated as load buses with zero consumed active and reactive power.

Table 3.1 Data sheet and power flow calculation results (1)

	Bus 1	Bus 2	Bus 3
P_i^*	0.5	-3	
Q_i^*		0	
$ V_i^* $	2		2
$\angle V_i^*$			0

(a) Data sheet

	Bus 1	Bus 2	Bus 3
P_i^*			2.5006
Q_i^*	0.0157		0.1388
$ V_i^* $		1.9969	
$\angle V_i^*$	-0.0490	-0.0596	

(b) Power flow calculation results

Table 3.2 Data sheet and power flow calculation results (2)

	Bus 1	Bus 2	Bus 3
P_i^*		-3	0.5
Q_i^*		0	
$ V_i^* $	2		2
$\angle V_i^*$	0		

(a) Data sheet

	Bus 1	Bus 2	Bus 3
P_i^*	2.5158		
Q_i^*	-0.0347		0.1759
$ V_i^* $		1.9918	
$\angle V_i^*$		-0.0538	-0.0419

(b) Power flow calculation results

Example 3.2 Power flow calculation based on the datasheet Let us consider the electrical power system model consisting of 3 bus bars discussed in Example 2.1. For the admittance matrix of the power grid of Equation 2.10, the admittance values of the two transmission lines are set to be:

$$y_{12} = 1.3652 - j11.6041, \quad y_{23} = -j10.5107 \quad (3.12)$$

Please note that the conductance (real part of y_{23}) of the transmission line that connects bus bar 2 and bus bar 3 is set to zero, so the active power transmission loss on this line is zero.

First, let us consider a case where bus bar 1 is the generator bus, bus bar 2 is the load bus, and bus bar 3 is the slack bus. Specifically, we assume that the values in Table 3.1(a) are specified for each bus bar. In this case, the set of variable satisfying the simultaneous equations in Equation 3.4 can be obtained as shown in Table 3.1(b). The transmission los in this case is:

$$P_1^* + P_2^* + P_3^* = 6.2562 \times 10^{-4}, \quad Q_1^* + Q_2^* + Q_3^* = 1.5450 \times 10^{-1}$$

The ratio of power transmission loss to the consumed power of the load is about 0.02%, which is very small. The reason why the power transmission loss for the active power is small is that most of the active power consumed by the load on bus bar 2 (about 2.5 pu out of 3 pu) is supplied by the generator on bus bar 3, and only 0.5 pu is supplied by the generator on bus bar 1. In other words, most of the active power consumed by the load on bus bar 2 is supplied using the right transmission line, which has no power transmission loss.

Next, consider the case where bus bar 1 is the slack bus, bus bar 2 is the load bus, and bus bar 3 is the generator bus, and specify the variables for each bus bar as shown in Table 3.2(a). The result of the power flow calculation in this case is shown in Table 3.2(b). The power loss in this case is given by:

$$P_1^* + P_2^* + P_3^* = 1.5826 \times 10^{-2}, \quad Q_1^* + Q_2^* + Q_3^* = 1.4120 \times 10^{-1}$$

The ratio of power loss to consumed power of the load in this case is about 0.52%. As compared to the previous example, it can be seen that the power loss due to active

power transmission has increased. This is because the majority of the active power consumed by bus 2 is being supplied using the left transmission line where power losses occur. On the other hand, it can also be seen that the reactive power loss has decreased as compared to the previous example.

From Example 3.2, it can be seen that the magnitude of the overall transmission losses of the system varies depending on the power flow distribution that is obtained. Generally, when supplying power using transmission lines with a large conductance (or resistance) component, the transmission losses of active power increase. As the transmission losses increase, the generation cost, among other economic costs, also increases because a larger amount of generation is required to supply the same amount of consumed active power.

On the other hand, it is important to note that an economically efficient steady-state power flow distribution may not necessarily correspond to a high stability equilibrium point. Therefore, in practical applications, it is important to search for better equilibrium points by considering trade-offs between economic efficiency and stability. The process of searching for such better equilibrium points is called **optimal power flow calculation** in power system engineering. In this book, we discuss the relationship between the selection of equilibrium points and stability in Chapters 4 and 5.

3.2.3 The relationship between the admittance matrix and transmission loss

The following derivation provides a mathematical expression for transmission losses in any power flow distribution for a general power network consisting of N buses. Assuming that the real and imaginary parts of the admittance matrix \mathbf{Y} , which are the conductance matrix G and susceptance matrix B , respectively, are symmetric, appropriate constants $\phi_{ij} = \phi_{ji}$ and $\psi_{ij} = \psi_{ji}$ can be used to represent G_{ij} and B_{ij} , respectively, as follows:

$$G_{ij} = \begin{cases} \sum_{j=1}^N \phi_{ij}, & i = j \\ -\phi_{ij}, & i \neq j \end{cases} \quad B_{ij} = \begin{cases} -\sum_{j=1}^N \psi_{ij}, & i = j \\ \psi_{ij}, & i \neq j \end{cases} \quad (3.13)$$

Here, G_{ij} and B_{ij} denote the (i, j) th element of the conductance matrix G and the susceptance matrix B , respectively. Equation 3.13 is equivalent to defining:

$$\phi_{ii} := \sum_{j=1}^N G_{ij}, \quad \phi_{ij} := -G_{ij}, \quad \psi_{ii} := -\sum_{j=1}^N B_{ij}, \quad \psi_{ij} := B_{ij}$$

Using this expression, the following fact can be shown.

Theorem 3.1 (Expression of transmission loss through bus bar voltage phasor)
For Equation 3.4, the transmission losses of active and reactive power for the entire system are defined as:

$$L_P(t) := P_1(t) + \cdots + P_N(t), \quad L_Q(t) := Q_1(t) + \cdots + Q_N(t) \quad (3.14)$$

These transmission losses are given by:

$$\begin{aligned} L_P(t) &= \sum_{i=1}^N \phi_{ii} |V_i(t)|^2 + \sum_{i=1}^N \sum_{j=i+1}^N \phi_{ij} W(V_i(t), V_j(t)) \\ L_Q(t) &= \sum_{i=1}^N \psi_{ii} |V_i(t)|^2 + \sum_{i=1}^N \sum_{j=i+1}^N \psi_{ij} W(V_i(t), V_j(t)) \end{aligned} \quad (3.15)$$

where the following is used:

$$W(V_i, V_j) := (|V_i| - |V_j|)^2 + 2|V_i||V_j|\{1 - \cos(\angle V_i - \angle V_j)\}$$

Proof For simplification, time t is omitted. Also, we denote $\angle V_i - \angle V_j$ as $\angle V_{ij}$. From Equation 3.4, we have $Y_{ij} = G_{ij} + jB_{ij}$, and $Y_{ij} = Y_{ji}$, therefore:

$$\begin{aligned} \sum_{i=1}^N (P_i + jQ_i) &= \sum_{i=1}^N \bar{Y}_{ii} |V_i|^2 + \sum_{i=1}^N \sum_{j=i+1}^N \bar{Y}_{ij} |V_i| |V_j| (e^{j\angle V_{ij}} + e^{j\angle V_{ji}}) \\ &= \sum_{i=1}^N \bar{Y}_{ii} |V_i|^2 + 2 \sum_{i=1}^N \sum_{j=i+1}^N \bar{Y}_{ij} |V_i| |V_j| \cos \angle V_{ij} \end{aligned}$$

Thus, using the notation of G_{ij} and B_{ij} from Equation 3.13, we obtain:

$$\begin{aligned} L_P &= \sum_{i=1}^N \left(\sum_{j=1}^N \phi_{ij} \right) |V_i|^2 - 2 \sum_{i=1}^N \sum_{j=i+1}^N \phi_{ij} |V_i| |V_j| \cos \angle V_{ij} \\ L_Q &= \sum_{i=1}^N \left(\sum_{j=1}^N \psi_{ij} \right) |V_i|^2 - 2 \sum_{i=1}^N \sum_{j=i+1}^N \psi_{ij} |V_i| |V_j| \cos \angle V_{ij} \end{aligned}$$

where we focus on the first term of L_P . Because $\phi_{ij} = \phi_{ji}$, we have:

$$\sum_{i=1}^N \sum_{j=1}^N \phi_{ij} |V_i|^2 = \sum_{i=1}^N \phi_{ii} |V_i|^2 + \sum_{i=1}^N \sum_{j=i+1}^N \phi_{ij} |V_i|^2 + \sum_{i=1}^N \sum_{j=i+1}^N \phi_{ij} |V_j|^2$$

If we rewrite the first term of L_P using this, we can obtain:

$$\begin{aligned} L_P &= \sum_{i=1}^N \phi_{ii} |\mathbf{V}_i|^2 + \sum_{i=1}^N \sum_{j=i+1}^N \phi_{ij} \left(|\mathbf{V}_i|^2 + |\mathbf{V}_j|^2 - 2|\mathbf{V}_i||\mathbf{V}_j| \cos \angle \mathbf{V}_{ij} \right) \\ &= \sum_{i=1}^N \phi_{ii} |\mathbf{V}_i|^2 + \sum_{i=1}^N \sum_{j=i+1}^N \phi_{ij} \left\{ (|\mathbf{V}_i| - |\mathbf{V}_j|)^2 + 2|\mathbf{V}_i||\mathbf{V}_j|(1 - \cos \angle \mathbf{V}_{ij}) \right\} \end{aligned}$$

Therefore, L_P can be expressed in the form of Equation 3.15. With the same steps, L_Q can be expressed with the format of Equation 3.15.

Theorem 3.1 shows that the discussion of electrical power loss in the electrical power system of two bus bars shown in the Example 3.1 can be generalized to power systems consisting of any number of buses. Here, if we express the admittance matrix \mathbf{Y} as in Section 2.2.3:

$$\mathbf{Y} = \mathbf{Y}_0 + j \operatorname{diag}(b_i)_{i \in \{1, \dots, N\}}$$

In this case, it is known that $\mathbf{Y}_0 \mathbf{1} = 0$, which means that the sum of each row of the real and imaginary parts of \mathbf{Y}_0 is 0. Thus, for all $i \in 1, \dots, N$:

$$\phi_{ii} = 0, \quad \psi_{ii} = -b_i$$

Furthermore, since the conductance of each transmission line is nonnegative and the susceptance is negative, it follows that ϕ_{ij} and ψ_{ij} are nonnegative for all $i \neq j$. Therefore, as long as ϕ_{ij} is not 0, loss will always occur when transmitting active power between a bus bar i and a bus bar j . This implies that the transmission loss of active power $L_P(t)$ is positive at any time t for the entire power system. Similarly, if b_i is sufficiently small; in other words, if the capacitance to ground of a transmission line is sufficiently small, loss of reactive power $L_Q(t)$ is also positive. In other words, connecting devices with capacitive characteristics to the buses reduces the loss of reactive power.

3.3 The steady state of generators achieving desired power supply

In this Section, we explain how to retroactively calculate the steady-state values of the internal states and external inputs of generators, as well as the parameter values of loads, to achieve the power flow state described by the results of the power flow calculation explained in Step B of Section 3.1.2.

3.3.1 The steady state of generators that achieves a desired supply of electric power

Let us consider a generator model that inputs the voltage phasor in Section 2.3.2. For simplicity of notation, subscripts i have been omitted:

$$\begin{aligned}\dot{\delta} &= \omega_0 \Delta\omega \\ M \Delta\dot{\omega} &= -D \Delta\omega - P + P_{\text{mech}} \\ \tau \dot{E} &= -\frac{X}{X'} E + \left(\frac{X}{X'} - 1\right) |V| \cos(\delta - \angle V) + V_{\text{field}}\end{aligned}\tag{3.16}$$

Here, if the active power and reactive power are the outputs:

$$P = \frac{|V|E}{X'} \sin(\delta - \angle V), \quad Q = \frac{|V|E}{X'} \cos(\delta - \angle V) - \frac{|V|^2}{X'}\tag{3.17}$$

The purpose here is to determine the steady-state values of the internal state and external input values of a generator that are consistent with the given constant values of active power, reactive power, and voltage phasor of the bus to which the generator is connected, as the result of power flow calculation. Specifically, let $(P^*, Q^*, |V^*|, \angle V^*)$ denote the given set of active power, reactive power, and absolute value and phase of the voltage phasor. Then, the objective is to determine the steady-state values of the internal state of the generator (δ^*, E^*) and the external input values $(P_{\text{mech}}^*, V_{\text{field}}^*)$ that satisfy the following set of equations:

$$\begin{aligned}p^* &= \frac{|v^*|e^*}{X'} \sin(\delta^* - \angle v^*), \\ q^* &= \frac{|v^*|e^*}{X'} \cos(\delta^* - \angle v^*) - \frac{|v^*|^2}{X'}, \\ 0 &= -p^* + p_{\text{mech}}^*, \\ 0 &= -\frac{X}{X'} e^* + \left(\frac{X}{X'} - 1\right) |v^*| \cos(\delta^* - \angle v^*) + v_{\text{field}}^*\end{aligned}\tag{3.18}$$

The set of equations in 3.18 represents the equilibrium point of the generator model when the steady-state value of the angular frequency deviation $\Delta\omega$ in Equation 3.16 is zero. Also, the given $(P^*, Q^*, |V^*|, \angle V^*)$ corresponds to the input and output values of the generator model for each bus.

The specific values of the steady-state internal states of the generator that satisfy Equation 3.18 are given by:

$$\begin{aligned}\delta^* &= \angle v^* + \arctan\left(\frac{p^*}{q^* + \frac{|v^*|^2}{X'}}\right), \\ e^* &= \frac{X'}{|v^*|} \sqrt{\left(q^* + \frac{|v^*|^2}{X'}\right)^2 + (p^*)^2}\end{aligned}\tag{3.19a}$$

The steady-state values of the mechanical and field inputs are:

$$\begin{aligned} p_{\text{mech}}^* &= p^*, \\ v_{\text{field}}^* &= \frac{\frac{X}{|v^*|} \left\{ \left(q^* + \frac{|v^*|^2}{X'} \right) \left(q^* + \frac{|v^*|^2}{X} \right) + (p^*)^2 \right\}}{\sqrt{\left(q^* + \frac{|v^*|^2}{X'} \right)^2 + (p^*)^2}} \end{aligned} \quad (3.19b)$$

Please refer to Section 3.3.3 for the derivation process of these equations.

3.3.2 Load Parameters for Achieving Desired Power Consumption

In this section, we explain how to set the parameters of the load model described in Section 2.4.1 to achieve the desired power consumption. By eliminating the current phase using Equation 3.3, the fixed impedance model can be expressed as follows:

$$p + jq = -\frac{|v|^2}{z_{\text{load}}^*} \quad (3.20)$$

Here, the subscript i of the bus is omitted for simplicity. This can be interpreted as the fixed impedance model of the load, where the current phase V is the input and the active power P and reactive power Q are the outputs. If the values of the active power and reactive power determined by power flow calculations are represented as P^* and Q^* , respectively, and the absolute value of the voltage phase is represented as $|V^*|$, then the real part (resistance) and imaginary part (reactance) of the load impedance z_{load}^* can be calculated as:

$$\text{Re}[z_{\text{load}}^*] = -\frac{p^*|v^*|^2}{(p^*)^2 + (q^*)^2}, \quad \text{Im}[z_{\text{load}}^*] = -\frac{q^*|v^*|^2}{(p^*)^2 + (q^*)^2} \quad (3.21)$$

Similarly, for the fixed current model, since the equation can be expressed as:

$$p + jq = \bar{i}_{\text{load}}^* |v| \quad (3.22)$$

The real and imaginary parts of the load current parameter can be calculated as:

$$\text{Re}[i_{\text{load}}^*] = \frac{p^*}{|v^*|}, \quad \text{Im}[i_{\text{load}}^*] = -\frac{q^*}{|v^*|}$$

For the fixed power model, since the equation can be expressed as:

$$p + jq = p_{\text{load}}^* + jq_{\text{load}}^* \quad (3.23)$$

Then, clearly, the parameters are:

$$p_{\text{load}}^* = p^*, \quad q_{\text{load}}^* = q^*$$

By setting these parameter values in the load model, the steady-state flow state obtained by power flow calculation can be achieved.

3.3.3 mathematical relationship between generator internal state and input/output

In the following, we mathematically analyze the internal state of the generator, the active and reactive power provided to the bus bar, and voltage phasor of the bus bar. We use the generator model discussed in Section 2.3.7. However, for ease of notation, we omit the subscript i and use the model as follows:

$$\begin{aligned}\dot{\delta} &= \omega_0 \Delta\omega \\ M \Delta\dot{\omega} &= -D \Delta\omega - P + P_{\text{mech}} \\ \tau \dot{E} &= -\frac{X_d}{X'_d} E + \left(\frac{X_d}{X'_d} - 1 \right) |V| \cos(\delta - \angle V) + V_{\text{field}}\end{aligned}\tag{3.24}$$

When the output is given as active and reactive power, we have:

$$\begin{aligned}P &= \frac{|V|E}{X'_d} \sin(\delta - \angle V) - \left(\frac{1}{X'_d} - \frac{1}{X_q} \right) |V|^2 \sin(\delta - \angle V) \cos(\delta - \angle V), \\ Q &= \frac{|V|E}{X'_d} \cos(\delta - \angle V) - |V|^2 \left(\frac{\cos^2(\delta - \angle V)}{X'_d} + \frac{\sin^2(\delta - \angle V)}{X_q} \right)\end{aligned}\tag{3.25}$$

Note that X'_d and X_q are equal to X' , and if we replace X_d with X , this model matches the generator model discussed in Section 3.3.1. When the output is given as current phasors, we have:

$$\begin{aligned}|I| \cos(\delta - \angle I) &= \frac{|V|}{X_q} \sin(\delta - \angle V), \\ |I| \sin(\delta - \angle I) &= \frac{E - |V| \cos(\delta - \angle V)}{X'_d}\end{aligned}\tag{3.26}$$

Note that equations 3.25 and 3.26 are equivalent outputs, meaning that for any given $(\delta, E, |V|, \angle V)$, there exists a one-to-one relationship between (P, Q) and $(|I|, \angle I)$.

The following facts are shown for this generator model.

Lemma 3.1 (Relationship between generator internal states and input/output)

Consider Equation 3.25 as a system of equations in $\delta - \angle V$ and E . The solution is given by:

$$\delta - \angle V = \arctan \left(\frac{P}{Q + \frac{|V|^2}{X_q}} \right), \quad (3.27a)$$

$$E = \frac{\frac{X'_d}{|V|} \left\{ \left(Q + \frac{|V|^2}{X_q} \right) \left(Q + \frac{|V|^2}{X'_d} \right) + P^2 \right\}}{\sqrt{\left(Q + \frac{|V|^2}{X_q} \right)^2 + P^2}} \quad (3.27b)$$

where $|V| \neq 0$.

Conversely, if we consider Equation 3.27 as a system of equations in P and Q , the solution is given by Equation 3.25.

Proof First, we derive Equation 3.27 from Equation 3.25. Multiplying P by $\cos(\delta - \angle V)$ and Q by $\sin(\delta - \angle V)$ and taking the difference, we obtain:

$$P \cos(\delta - \angle V) - Q \sin(\delta - \angle V) = \frac{|V|^2}{X_q} \sin(\delta - \angle V)$$

Dividing both sides by $\cos(\delta - \angle V)$, we obtain Equation 3.27a. Next, we show the relation of Equation 3.27b. Rewriting P and Q in terms of I using the Equation 3.3, Equation 3.25 is equivalently transformed to Equation 3.26. Furthermore, this is equivalent to:

$$|V| e^{j(\delta - \angle V)} = E - X'_d |I| \sin(\delta - \angle I) + j X_q |I| \cos(\delta - \angle I) \quad (3.28)$$

The relationship in Equation 3.27a can be expressed in complex numbers as:

$$\frac{e^{j(\delta - \angle V)} - e^{-j(\delta - \angle V)}}{e^{j(\delta - \angle V)} + e^{-j(\delta - \angle V)}} = \underbrace{\frac{P}{Q + \frac{|V|^2}{X_q}}}_\alpha j$$

Therefore, we obtain:

$$e^{-j(\delta - \angle V)} = \frac{1 - \alpha j}{1 + \alpha j} e^{j(\delta - \angle V)}$$

By considering the complex conjugate of Equation 3.3, it can be transformed into an equivalent form given by:

$$|I| e^{j(\delta - \angle I)} = \frac{P + jQ}{|V|} e^{j(\delta - \angle V)} \quad (3.29)$$

Then, by taking the complex conjugate of the above equation:

$$|I| e^{-j(\delta - \angle I)} = \frac{P - jQ}{|V|} \cdot \frac{1 - \alpha j}{1 + \alpha j} e^{j(\delta - \angle V)} \quad (3.30)$$

From Equations 3.29 and 3.30:

$$\begin{aligned} |\mathbf{I}| \sin(\delta - \angle \mathbf{I}) &= \frac{1}{|\mathbf{V}|} \cdot \frac{\alpha P + Q}{1 + \alpha j} e^{j(\delta - \angle \mathbf{V})}, \\ |\mathbf{I}| \cos(\delta - \angle \mathbf{I}) &= \frac{1}{|\mathbf{V}|} \cdot \frac{P - \alpha Q}{1 + \alpha j} e^{j(\delta - \angle \mathbf{V})} \end{aligned}$$

By substituting these into Equation 3.28 and rewriting \mathbf{I} in terms of P and Q , we can show that when Equation 3.27a holds, Equation 3.25 is equivalent to:

$$E = \frac{X'_d}{|\mathbf{V}|} \left\{ \left(Q + \frac{|\mathbf{V}|^2}{X_q} \right) \left(Q + \frac{|\mathbf{V}|^2}{X'_d} \right) + P^2 \right\} \frac{Q + \frac{|\mathbf{V}|^2}{X_q} - jP}{\left(Q + \frac{|\mathbf{V}|^2}{X_q} \right)^2 + P^2} e^{j(\delta - \angle \mathbf{V})} \quad (3.31)$$

Here, we have used the fact that from Equation 3.27a:

$$Q + \frac{|\mathbf{V}|^2}{X_q} - jP = \left| Q + \frac{|\mathbf{V}|^2}{X_q} - jP \right| e^{-j(\delta - \angle \mathbf{V})}$$

Furthermore, since $|E| = E$ and

$$\left(Q + \frac{|\mathbf{V}|^2}{X_q} \right)^2 + P^2 = \left| Q + \frac{|\mathbf{V}|^2}{X_q} - jP \right|^2$$

Equation 3.27b can be obtained.

We can follow the reverse steps to derive Equation 3.25 from Equation 3.27. Using Equation 3.27a, we can replace the E in Equation 3.27b with the expression in Equation 3.31. As mentioned earlier, when Equation 3.27a holds, Equation 3.31 is equivalent to Equation 3.25. \square

Lemma 3.1 shows that there is a one-to-one relationship between the pairs $(\delta - \angle \mathbf{V}, E)$ and (P, Q) . Specifically, it shows that the internal state of generators (δ, E) can be uniquely determined from the input/output $(|\mathbf{V}|, \angle \mathbf{V})$ or (P, Q) . Please note that the relationship in Equation (3.27) holds at any time t , regardless of whether the system is in steady-state or transient. The following theorem gives a relationship that holds between the input, output, and internal state under a steady state of generators.

Theorem 3.2 (Relationship between generator internal states and input/output in steady state)

Consider the generator model given by Equations 3.24 and 3.25. Let \mathbf{V}^\star , $\Delta\omega^\star$, $\angle \mathbf{V}^\star$, P^\star , and Q^\star be real constants. Let us assume the inputs of mechanical torque and field voltage are constants given by:

$$\begin{aligned} P_{\text{mech}}(t) &= D\Delta\omega^\star + P^\star, \\ V_{\text{field}}(t) &= \frac{\frac{X_d}{|\mathbf{V}^\star|} \left\{ \left(Q^\star + \frac{|\mathbf{V}^\star|^2}{X_q} \right) \left(Q^\star + \frac{|\mathbf{V}^\star|^2}{X_d} \right) + (P^\star)^2 \right\}}{\sqrt{\left(Q^\star + \frac{|\mathbf{V}^\star|^2}{X_q} \right)^2 + (P^\star)^2}} \end{aligned} \quad (3.32a)$$

and the input due to the voltage phase angle of the bus are given by:

$$|V(t)| = |V^*|, \quad \angle V(t) = \omega_0 \Delta \omega^* t + \angle V^* \quad (3.32b)$$

where ω_0 is the nominal frequency. Then, in steady state, the rotor angle, angular frequency deviation, and internal voltage are given by

$$\begin{aligned} \delta(t) &= \angle V(t) + \arctan \left(\frac{P^*}{Q^* + \frac{|V^*|^2}{X_q}} \right), \\ \Delta \omega(t) &= \Delta \omega^*, \\ E(t) &= \frac{\frac{X_d'}{|V^*|} \left\{ \left(Q^* + \frac{|V^*|^2}{X_q} \right) \left(Q^* + \frac{|V^*|^2}{X_d'} \right) + (P^*)^2 \right\}}{\sqrt{\left(Q^* + \frac{|V^*|^2}{X_q} \right)^2 + (P^*)^2}} \end{aligned} \quad (3.33)$$

Furthermore, the active and reactive power supplied to bus bars are constants and given by:

$$P(t) = P^*, \quad Q(t) = Q^* \quad (3.34)$$

Proof First, we demonstrate that Equation 3.34 holds for the output under the assumption that Equation 3.33 is a solution to the differential equation in Equation 3.24 with the input given by Equation 3.32. As shown in Lemma 3.1, considering Equation 3.33 as equations for P^* and Q^* , their solutions are given by

$$\begin{aligned} P^* &= \frac{|V^*|E(t)}{X_d'} \sin(\delta(t) - \angle V(t)) \\ &\quad - \left(\frac{1}{X_d'} - \frac{1}{X_q} \right) |V^*|^2 \sin(\delta(t) - \angle V(t)) \cos(\delta(t) - \angle V(t)), \\ Q^* &= \frac{|V^*|E(t)}{X_d'} \cos(\delta(t) - \angle V(t)) \\ &\quad - |V^*|^2 \left(\frac{\cos^2(\delta(t) - \angle V(t))}{X_d'} + \frac{\sin^2(\delta(t) - \angle V(t))}{X_q} \right) \end{aligned}$$

which implies Equation 3.34.

Next, we verify that Equation 3.33 is a solution to the differential equation in Equation 3.24 with the input given by equation 3.32. The differential equation for δ and $\Delta \omega$ in Equation 3.24 is equivalent to

$$\frac{M}{\omega_0} \ddot{\delta}(t) + \frac{D}{\omega_0} \dot{\delta}(t) + P(t) - P_{\text{mech}}(t) = 0$$

If we substitute the expressions for $P_{\text{mech}}(t)$ from Equation 3.32a, $P(t)$ from Equation 3.34, and $\delta(t)$ from Equation 3.33 into the relationship given by Equation 3.32b, we can see that this differential equation is satisfied. Similarly, by substituting the expressions for $V_{\text{field}}(t)$ from Equation 3.32a, $\delta(t) - \angle V(t)$, and $E(t)$ from Equation 3.33 into Equation 3.24, we can see that the differential equation for E is satisfied. Here, we use the fact that:

$$\cos\left(\arctan\left(\frac{P^*}{Q^* + \frac{|V^*|^2}{X_q}}\right)\right) = \frac{Q^* + \frac{|V^*|^2}{X_q}}{\sqrt{\left(Q^* + \frac{|V^*|^2}{X_q}\right)^2 + (P^*)^2}}$$

From the above, we prove Theorem 3.2.

From Theorem 3.2, we can determine the values of mechanical input P_{mech}^* and field input V_{field}^* that are necessary to achieve the voltage phase, active power, and reactive power of the bus bars determined by power flow calculation, as well as the steady-state behavior of internal states (δ, E) at that time. Note that in Equation 3.32b, the phase of the voltage phasor is not a constant, but the steady-state value of the angular frequency deviation $\Delta\omega^*$, which usually should be set to zero as a constant with practical significance, is determined only by the value of $\angle V^*$ obtained from the power flow calculation. Clearly, when $\Delta\omega^* = 0$,

$$P_{\text{mech}}(t) = P^*, \quad \delta(t) = \angle V^* + \arctan\left(\frac{P^*}{Q^* + \frac{|V^*|^2}{X_q}}\right)$$

From the above discussion, we can see that even if we determine $(P^*, Q^*, |V^*|, \angle V^*)$ by power flow calculation without considering the dynamic characteristics of the generator, we can uniquely calculate $(P_{\text{mech}}^*, V_{\text{field}}^*)$ that are consistent with them. This result leads to Equation (3.19).

Furthermore, the following theorem gives an equivalence relation between the inputs and internal states in steady-state of the generator.

Theorem 3.3 (Equivalence relation between input/output and internal state of generator)

For the generator model given by Equations 3.24 and 3.25, the necessary and sufficient conditions for Equations 3.35 to hold for all $t \geq 0$ are that Equations 3.36 hold for all $t \geq 0$, where

$$\frac{d^2\delta}{dt^2}(t) = 0, \quad \frac{dE}{dt}(t) = 0, \quad \frac{dP_{\text{mech}}}{dt}(t) = 0, \quad \frac{dV_{\text{field}}}{dt}(t) = 0 \quad (3.35)$$

and

$$\frac{dP}{dt}(t) = 0, \quad \frac{dQ}{dt}(t) = 0, \quad \frac{d|V|}{dt}(t) = 0, \quad \frac{d^2\angle V}{dt^2}(t) = 0 \quad (3.36)$$

Moreover, when equations 3.35 or 3.36 hold, the following holds for all $t \geq 0$:

$$\Delta\omega(t) = \frac{1}{\omega_0} \frac{d\angle V}{dt}(t) \quad (3.37)$$

which is a constant.

Proof First, we show that if Equation 3.35 holds, then Equation 3.36 also holds. From Equation 3.24, since $\Delta\omega$, E , P_{mech} , and V_{field} are all constants, we can see that P and $|V| \cos(\delta - \angle V)$ are also constants. Therefore, from the two equations in Equation 3.25, we can see that Q and $|V| \sin(\delta - \angle V)$ are also constants. Additionally,

$$|V|^2 \cos^2(\delta - \angle V) + |V|^2 \sin^2(\delta - \angle V) = |V|^2$$

and since the left-hand side is constant, we can see that $|V|$ is also constant. Furthermore, in the first equation of Equation 3.27, the right-hand side is constant, so the derivatives of $\angle V$ and δ are equal for any order. Therefore, we have

$$\frac{d^2 \angle V}{dt^2} = \frac{d^2 \delta}{dt^2} = 0$$

Next, we show that if Equation 3.36 holds, then Equation 3.35 also holds. From Equation 3.27, we know that E is constant and that the second derivative of δ is 0, which means that $\Delta\omega$ is constant. Therefore, from Equation 3.24, since P and $|V| \cos(\delta - \angle V)$ are constants, we can see that P_{mech} and V_{field} are also constants. Equation 3.37 is obvious from the fact that the derivatives of $\angle V$ and δ are equal. \square

As Theorem 3.3 shows, the fact that the external inputs ($P_{\text{mech}}, V_{\text{field}}$) to the generator are constant and the internal states (δ, E) are in a steady state is equivalent to the input/output ($P, Q, |V|, \angle V$) to the bus being in a steady state. Therefore, the procedures for power flow calculations that determine the active and reactive power and voltage phase angles for each bus are mathematically equivalent to searching for one of the equilibrium points of the power system model, assuming that all internal states and external inputs of the generators are in steady state. This is the steady-state of the entire power system.

3.4 Time Response Calculation of Power System Model

In this Section, we explain a method to calculate the time response of the electric power system model explained as Step C in Section 3.1.2. We will also numerically analyze the behavior of the electrical power system against several disturbances.

3.4.1 Initial Value Response

In this section, we explain the method for calculating the time response of the power system model, which was described as Step C in Section 3.1.2. We also numerically analyze the behavior of the power system model in response to several disturbances.

By following the procedures outlined in Sections 3.2 and 3.3, the equilibrium point of the power system model can be obtained as a steady-state where all generator frequency deviations are zero. Specifically, by using the bus variables determined in the power flow calculation, the initial values of the internal states and external inputs of each generator model, as shown in Theorem 3.2, can be set. In addition, the constants derived in Section 3.3.2 can be set for each load model. By doing so, the differential-algebraic equation system representing the power system model is in equilibrium at the given steady-state power flow condition.

In particular, if the obtained equilibrium point is stable in a meaningful sense, then even if some perturbation occurs in the internal states of the generators, the internal states of the power system model will asymptotically converge to the original steady-state values. We confirm this fact in the following example.

Table 3.3 Steady-state values of generators for flow calculation results of Table 3.1

i	$P_{\text{mech}_i}^*$ [pu]	$V_{\text{filed}_i}^*$ [pu]	δ_i^* [rad]	$\Delta\omega_i^*$ [pu]	E_i^* [pu]
1	0.5000	2.0442	0.0670	0	2.0210
3	2.5006	2.5062	0.3870	0	2.2097

Table 3.4 Steady-state values of generators for flow calculation results of Table 3.2

i	$P_{\text{mech}_i}^*$ [pu]	$V_{\text{filed}_i}^*$ [pu]	δ_i^* [rad]	$\Delta\omega_i^*$ [pu]	E_i^* [pu]
1	2.5158	2.7038	0.5356	0	2.3069
3	0.5000	2.1250	0.0390	0	2.0654

Example 3.3 Initial response of the electrical power system model Let us consider the electrical power system model consisting of three bus bars handled in the Example 3.2. Let us consider a situation where the generator model of Equation 3.16 is connected to bus bar 1 and bus bar 3, and a load model with constant impedance of Equation 3.20 is connected to bus bar 2. For the generator model, we use the constants for generator 1 and generator 2 presented in 2.1.

For the two results of the power flow calculation in 3.1 and 3.2, we calculate the steady values of mechanical torque, field voltage, rotor argument, and interval voltage for generator 1 and generator 2 based on Equation (3.19). The calculated steady values are shown in 3.3 and 3.4. Similarly, if we back calculate the load impedance based on Equation 3.21, it can be obtained as in the first row of 3.5 and 3.6. Please

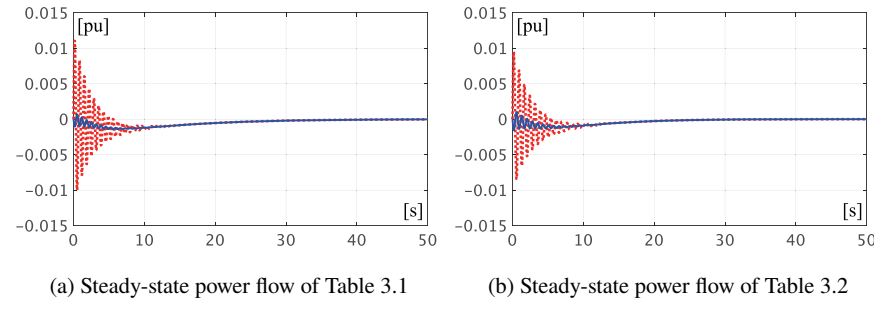


Fig. 3.2 Time response of frequency deviation for initial value disturbance
(Solid blue line: $\Delta\omega_1$, Dashed red line: $\Delta\omega_3$)

note that, depending on the result of the power flow calculation, the internal state of the generators, the steady value of the external input, and the load impedance vary.

Let us perturb the steady value of the internal state of the generators as the initial value. Specifically:

$$\begin{bmatrix} \delta_1(0) \\ \delta_3(0) \end{bmatrix} = \begin{bmatrix} \delta_1^* + \frac{\pi}{6} \\ \delta_3^* \end{bmatrix}, \quad \begin{bmatrix} E_1(0) \\ E_3(0) \end{bmatrix} = \begin{bmatrix} E_1^* + 0.1 \\ E_3^* \end{bmatrix} \quad (3.38)$$

The initial value of the frequency deviation is 0. Figure 3.2 shows the initial value response of the frequency deviation corresponding to the two power flow calculations at this time. The solid blue line represents the frequency deviation of generator 1, while the broken red line is the frequency deviation of generator 3. With either one of the steady power flow distributions, oscillations with a similar frequency were generated. Since the system frequency was set to 60 [Hz], a frequency deviation of 0.015 [pu] is equal to 0.9 [Hz].

Table 3.5 Impedance value of load [pu]

Load	$\text{Re}[z_{\text{load}_2}^*]$	$i[z_{\text{load}_2}^*]$
Steady-state	1.3293	0
Increased load	1.3426	0
Decreased load	1.3160	0

(a) Results of power flow calculation for Table 3.1 (a) Results of power flow calculation for Table 3.2

Table 3.6 Impedance value of load [pu]

Load	$\text{Re}[z_{\text{load}_2}^*]$	$i[z_{\text{load}_2}^*]$
Steady-state	1.3224	0
Increased load	1.3356	0
Decreased load	1.3092	0

3.4.2 Response to Parameter Variations of the Load Model

For a power system model in steady-state, if any of the constants in the load model are changed, the values of the voltage and current phases at all buses generally change. At this point, the power supply and demand in the entire system generally no longer balance, so unless the value of the mechanical input is appropriately modified according to the given excitation input value, the angular frequency deviation of each generator will not converge to zero. Let's verify this in the following example.

Example 3.4 Time Response of Power System Model to Load Impedance Changes

Let us calculate the time response of the angular frequency deviation when the load impedance value changes under the same setting as Example 3.3. Specifically, we calculate the time response by increasing or decreasing the resistance of the load by 1% based on the results of the power flow calculation. The increased and decreased load impedance values are shown in the second and third rows of Tables 3.5 and 3.6, respectively.

The calculation results are shown in Figures 3.3 and 3.4. The solid blue line represents the angular frequency deviation of generator 1, and the dashed red line represents that of generator 3. In all cases, it can be seen that the angular frequency deviations of the two generators change in sync. Also, since increasing the resistance generally increases the consumption of active power, the frequency of the generators decreases. The opposite is true when the resistance is decreased. It should be noted that since the mechanical input of the generators is fixed at the value before the change in resistance, the balance of active power supply and demand is not maintained, and the steady-state value of the angular frequency deviation is nonzero. Furthermore, although the ratio of the change in load resistance is the same in both Figures 3.3 and 3.4, the resulting values of the angular frequency deviation are different. This suggests that the sensitivity (stability) to disturbances changes depending on how the equilibrium point of the power system model is chosen.

In Example 3.4, unlike the result in Example 3.3, the generator's frequency deviation has a non-zero steady-state value. In order to make this frequency deviation zero, it is necessary to adjust the mechanical input or excitation input of the generator group appropriately. On the other hand, to make the steady-state value of the frequency deviation zero, frequency control is generally performed by a control algorithm that adjusts the mechanical input of the generator group to balance the demand and supply of active power. However, it is practically difficult to accurately measure the changes in all loads. Therefore, feedback control that automatically searches for the value of the mechanical input that achieves the demand-supply balance through control operations based on an integrator is necessary. The details of this are described later in Sections 5.1 and 5.2.

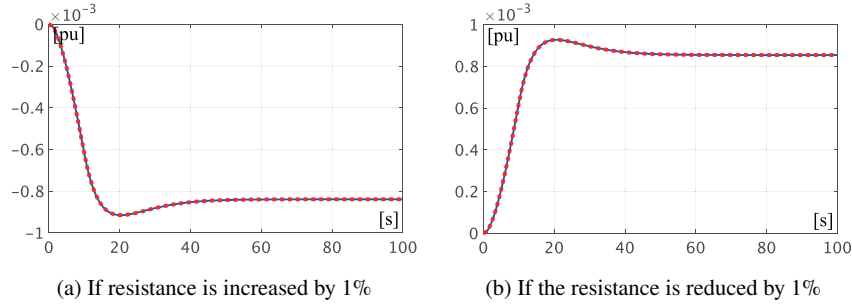


Fig. 3.3 Time response of angular frequency deviation to load change
(Steady-state state of Table 3.1, line type is the same as Figure 3.2.)

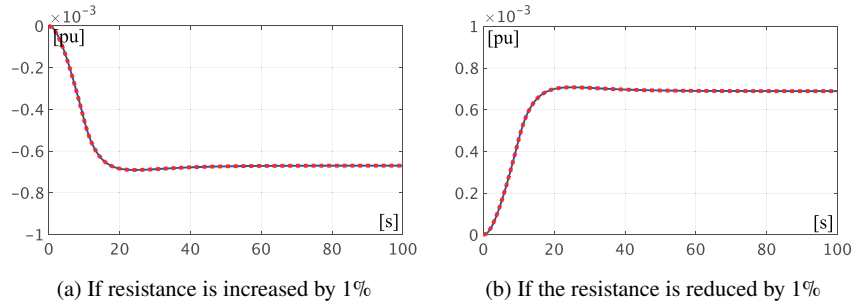


Fig. 3.4 Time response of angular frequency deviation to changes in load
(Steady-state state of Table 3.2, line type is the same as Figure 3.2.)

3.4.3 Response to ground fault

3.4.3.1 What is ground fault?

When an electric circuit comes into contact with the ground due to contact with an object or lightning strike, a phenomenon called **ground fault** occurs, and a large current flows into the ground. Ground fault detection devices quickly operate in power systems to detect the occurrence of ground fault and block the ground fault current. If the ground fault current is removed and the blocking is released, the power system operation before the occurrence of ground fault can be restored.

The time required to detect and remove ground fault is generally about 70 [ms]. During this time, the ground fault current flowing into the ground can cause severe disturbances to the power system operation. Note that the disturbance due to ground fault is not modeled as an external input, but is modeled as a "switching to a different power system model during the time when the ground fault is still present."

3.4.3.2 Formulation of bus bar ground fault

Bus bar ground faults discussed in this book are modeled assuming that the voltage phasor of the bus is constrained to zero during the time the fault persists. Without losing generality, we explain it for the case where a fault occurs on bus bar 1 of a power system model consisting of N bus bars. Additionally, we assume that the fault occurs at time 0 and persists until time t_0 . Under these conditions, the power flow state in Equation 3.2 satisfies the algebraic equation of the normal operating state in Equation 3.1 for $t < 0$ and $t \geq t_0$. However, for the time period when the fault persists, $t \in [0, t_0]$, the power flow state must satisfy the algebraic equation in Equation 3.39, which excludes the equation related to the current phasor of the faulted bus $\mathbf{I}_1(t)$, and the constraint condition on the voltage phasor of the faulted bus:

$$\begin{bmatrix} \mathbf{I}_2(t) \\ \vdots \\ \mathbf{I}_N(t) \end{bmatrix} = \begin{bmatrix} \mathbf{Y}_{22} & \cdots & \mathbf{Y}_{2N} \\ \vdots & \ddots & \vdots \\ \mathbf{Y}_{N2} & \cdots & \mathbf{Y}_{NN} \end{bmatrix} \begin{bmatrix} \mathbf{V}_2(t) \\ \vdots \\ \mathbf{V}_N(t) \end{bmatrix} \quad (3.39a)$$

and the constraint condition on the voltage phase of the faulted bus:

$$|\mathbf{V}_1(t)| = 0 \quad (3.39b)$$

Note that for buses and time periods where a ground fault has not occurred, the voltage and current phasors follow the differential or algebraic equations that represent each equipment's model. This is the same as during normal operation. Therefore, in numerical simulations, it is necessary to switch between the following two models:

- During periods where a ground fault has not occurred, the normal power system model is used.
- During periods where a ground fault is ongoing, the power system model is used with the affected bus and its connected equipment and transmission lines removed.

The current phasor $\mathbf{I}_1(t)$ flowing from device 1 to bus 1 during a ground fault is determined by the dynamic characteristics of the device. Specifically, if the device is a generator, then its internal state evolves over time according to following differential equations for $t \in [0, t_0]$, where $|\mathbf{V}_1(t)|$ is set to 0.

$$\begin{aligned} \dot{\delta}_1 &= \omega_0 \Delta \omega_1 \\ M_1 \Delta \dot{\omega}_1 &= -D_1 \Delta \omega_1 + P_{\text{mech}1} \\ \tau_1 \dot{E}_1 &= -\frac{X_1}{X'_1} E_1 + V_{\text{field}1} \end{aligned} \quad (3.40)$$

In this case, current phasor $\mathbf{I}_1(t)$ is given with the following as an output of generators:

$$|\mathbf{I}_1(t)| = \frac{E_1(t)}{X'_1}, \quad \angle \mathbf{I}_1(t) = \delta_1(t) - \frac{\pi}{2}$$

On the other hand, if device 1 is modeled as a constant impedance load, then $|\mathbf{I}_1(t)|$ is also zero since $|V_1(t)|$ is zero as given by Eq. (2.41a). For other load models, the situation is generally similar, except that for constant power loads, $|\mathbf{I}_1(t)|$ becomes infinite, so numerical instability must be taken into account in simulations. Note that the ground fault current phasor flowing from bus 1 to ground can be expressed as

$$\mathbf{I}'_1(t) := \mathbf{I}_1(t) - \sum_{j=2}^N Y_{1j} V_j(t), \quad t \in [0, t_0)$$

where N is the number of buses.

The value of the ground fault current phasor does not need to be calculated for the purpose of running numerical simulations of power system models. On the other hand, when a generator is connected to the ground fault bus, it is important to calculate the value of the generator's internal state at the time t_0 when the ground fault is cleared, so it is necessary to solve the differential equations in Equation 3.40. For the initial internal states of each generator at the time of the ground fault occurrence, arbitrary values can be set for any flow state. In this book, appropriate values obtained as a result of the power flow calculation for a steady-state flow condition are used. Note that at the time of occurrence and clearance of the ground fault, the internal states of each generator are continuous, but the voltage and current phasors of each bus change discontinuously.

The calculation of the time response for bus-ground faults can be summarized in the following steps:

- (a) Set the variable values at the steady-state condition obtained from the power flow calculation as the initial values of the internal states of each generator.
- (b) Calculate the time evolution using the power system model that excludes the faulted bus and the devices and transmission lines connected to it, for the time interval $t \in [0, t_0]$, where the fault persists.
- (c) If a generator is connected to the faulted bus, set the bus voltage phase to zero for $t \in [0, t_0]$, and calculate the time evolution of its internal state.
- (d) Set the values of the internal states of each generator at time t_0 , and calculate the time evolution of the system after the fault is cleared using the usual power system model with all devices connected.

Let us calculate the time response for bus-ground faults using these steps.

Example 3.5 Time response of power system model to bus bar ground fault

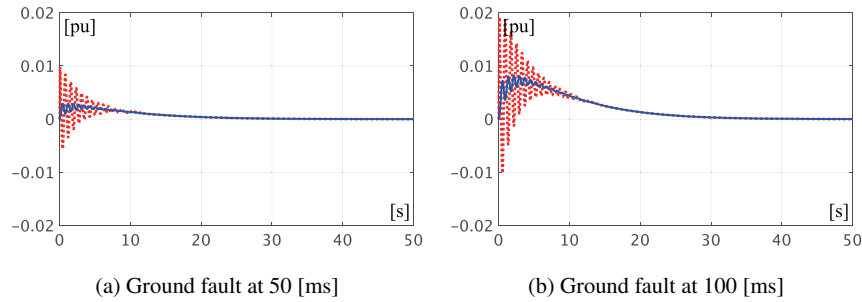


Fig. 3.5 Time response of angular frequency deviation to ground fault
(Steady-state of 3.1, line type is the same as 3.2)

In the same setting as Examples 3.3 and 3.4, let us calculate the time response of the frequency deviation of the bus due to ground fault. Specifically, we set the two steady-state power flow states obtained by power flow calculation as initial values and calculate the time response when a ground fault occurs at bus 1. For comparison, we consider two cases where the time until the fault is cleared is 50 [ms] and 100 [ms], respectively.

The calculation results are shown in Figures 3.5 and 3.6. The solid blue line represents the frequency deviation of generator 1, and the dashed red line represents the frequency deviation of generator 3. From Figure 3.5, it can be seen that the frequency oscillation of generator 3 is large in the steady-state power flow state shown in Table 3.1. In particular, a larger oscillation occurs when the duration of the ground fault is 100 [ms]. The reason why the oscillation of generator 3 is larger is that, as shown in Table 2.1, the inertia constant of generator 1 is large at 100 [s], while that of generator 3 is small at 12 [s]. In other words, the oscillation of the generator with larger inertia causes the larger oscillation of the generator with smaller inertia.

On the other hand, it can be seen from Figure 3.6 that the frequency oscillation for the same ground fault is small in the steady-state power flow state shown in Table 3.2. This is because in the steady-state power flow state of Table 3.1, generator 3 with small inertia supplied most of the active power consumed by the load, while in the steady-state power flow state of Table 3.2, generator 1 with large inertia supplied most of the active power. In general, synchronous generators have the characteristic that their sensitivity to disturbances increases as the supplied power approaches its maximum value. In the steady-state power flow state of Table 3.2, the stability of generator 3 with small inertia is relatively high, so the sensitivity of the frequency deviation to the ground fault is low.

From Example 3.5, it can be seen that the stability of the power system model for ground faults varies depending on the steady-state power flow condition (equilibrium point). In particular, in Example 3.2, the steady-state power flow condition in Table 3.1 was superior from the perspective of transmission loss, while in Example 3.5, the

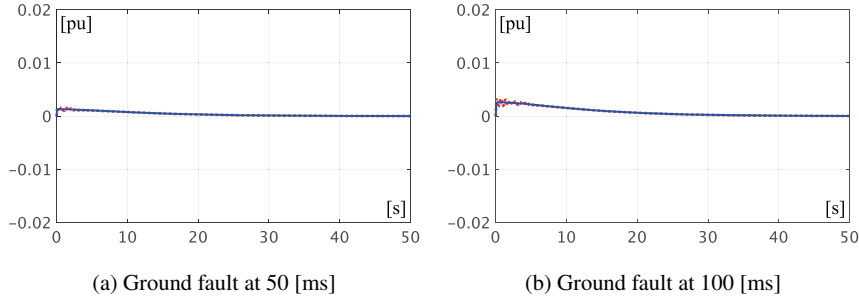


Fig. 3.6 Time response of angular frequency deviation to ground fault
(Steady-state of 3.2, line type is the same as 3.2)

steady-state power flow condition in Table 3.2 was found to be superior in terms of system stability with respect to ground faults. These examples suggest the importance of exploring desirable equilibrium points, taking into account trade-offs between factors such as economic efficiency and stability.

It should be noted that ground faults may occur at various locations and not only on specific buses or transmission lines, so it is necessary to improve the overall stability of the power system in a meaningful way. Control mechanisms for this purpose are explained in Sections 5.3 and 5.4.

Furthermore, from the simulation results of Examples 3.3 to 3.5, it can be observed that when the internal state settles into a steady state without diverging, "all generator frequency deviations have converged to the same value." Similar results are also observed in Example 2.3. This synchronization of frequency in the steady-state power flow condition is a universal phenomenon in power system models. Frequency control, which will be discussed in Sections 5.1 and 5.2, is based on the assumption that the frequency will automatically synchronize in the steady-state power flow condition, and control algorithms are constructed accordingly.

3.5 Synchronization of bus bar voltage in a steady power flow distribution

In this section, we mathematically investigate the frequency synchronization phenomenon observed in Section 3.4 from the perspective of the graph structure of the power transmission network. Based on the results of Theorem 3.3, we introduce the following definition.

Definition 3.1 (Synchronization of the steady power flow distribution and bus bar voltage)

Consider the power system model in which the devices are coupled by the simultaneous equations of Equation 3.4. For all buses i , if the following hold for all $t \geq 0$, the power system is said to be in a **steady-state power flow**.

$$\frac{dP_i}{dt}(t) = 0, \quad \frac{dQ_i}{dt}(t) = 0, \quad \frac{d|V_i|}{dt}(t) = 0, \quad \frac{d^2\angle V_i}{dt^2}(t) = 0 \quad (3.41)$$

²

Moreover, if the power system is in a steady-state power flow and Equation 3.42 holds, the buses i and j are said to be **synchronized** in the steady-state power flow.

$$\frac{d\angle V_i}{dt}(t) = \frac{d\angle V_j}{dt}(t) \quad (3.42)$$

As stated in Theorem 3.3, the validity of Equation 3.41 for the generator bus is equivalent to the internal state of the generator and the external input being in steady state. Moreover, if any selected pair of buses (i, j) are in synchronized in the sense of Definition 3.1, it can be concluded that the angular frequency deviation of all generators converges to the same value. Note that the validity of Equation 3.41 for any bus applies to the current phase I_i .

$$\frac{d|I_i|}{dt}(t) = 0, \quad \frac{d^2\angle I_i}{dt^2}(t) = 0, \quad \frac{d\angle I_i}{dt}(t) = \frac{d\angle V_i}{dt}(t)$$

This means that it can be easily verified by the equations:

$$|P_i(t) + jQ_i(t)| = |V_i(t)||I_i(t)|, \quad \angle(P_i(t) + jQ_i(t)) = \angle V_i(t) - \angle I_i(t)$$

Let \mathcal{N}_i denote the set of adjacent buses connected to bus i via transmission lines. In other words:

$$\mathcal{N}_i := \{j : Y_{ij} \neq 0, \quad j \neq i\}$$

Note that bus i is not included in \mathcal{N}_i . The number of adjacent buses connected to bus i is denoted by $|\mathcal{N}_i|$ and is called the **degree** of bus i .

The number of adjacent buses connected to bus i via transmission lines is denoted as $|\mathcal{N}_i|$, and this is referred to as the **degree** of bus i , which is equal to $|\mathcal{N}_i|$. In addition, the power system model assumes a steady-state condition, which can be expressed as:

$$\angle V_i(t) = \Omega_i t + \phi_i$$

where, Ω_i and ϕ_i are constant.

Under this assumption, the power balance equation for bus i in Equation 3.4 is given by:

² Please note that the mathematical definition of this “steady power flow distribution” is unique to this book and is not typically used in electrical power system engineering.

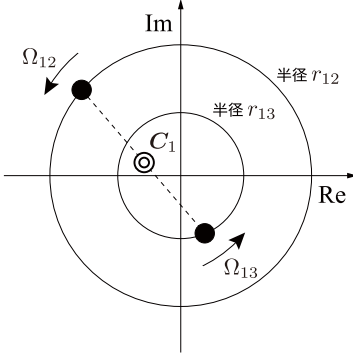


Fig. 3.7 When bus bar 1 is connected to bus bars 2 and 3

$$P_i + jQ_i = \sum_{j=1}^N \bar{Y}_{ij} |V_i| |V_j| e^{j\{(\Omega_i - \Omega_j)t + \phi_i - \phi_j\}}$$

Here, assuming a steady-state condition, the active and reactive power supplied to bus i , as well as the magnitude of the bus voltage phasor, are all constants. If we denote these quantities as P_i^* , Q_i^* , and $|V_i^*|$, respectively, then the power balance equation can be transformed into the following:

$$\underbrace{\frac{1}{|\mathcal{N}_i|} \sum_{j \in \mathcal{N}_i} r_{ij} e^{j(\Omega_{ij}t + \Phi_{ij})}}_{C_i(t)} = z_i \quad (3.43)$$

where $\Omega_{ij} := \Omega_i - \Omega_j$ is the frequency difference between bus i and bus j . The constants r_{ij} , Φ_{ij} , and z_i are defined as:

$$r_{ij} := |V_i^*| |V_j^*| |Y_{ij}|, \quad \Phi_{ij} := \phi_i - \phi_j - \angle Y_{ij},$$

$$z_i := \frac{\{P_i^* - \text{Re}[Y_{ii}]|V_i^*|^2 + j(Q_i^* + i[Y_{ii}]|V_i^*|^2)\}}{|\mathcal{N}_i|}$$

In the following, we consider deriving the equation $\Omega_{ij} = 0$ for all $j \in \mathcal{N}_i$, which represents synchronization with adjacent buses, from the Equation 3.43. Here, the Equation 3.43 represents that the center of gravity $C_i(t)$ of $|\mathcal{N}_i|$ points that move at a constant speed along the circumference of a circle with radius r_{ij} and initial phase Φ_{ij} and angular velocity Ω_{ij} , is invariant at a point z_i on the complex plane.

Figure 3.7 illustrates the relationship when bus 1 is connected to buses 2 and 3. Based on this fact, the following result can be obtained.

Lemma 3.2 (Synchronization of busbars derived from power flow equations)

Consider $\mathbf{C}_i(t)$ in Equation 3.43 for real constants r_{ij} , Ω_i , Ω_j , and Φ_{ij} , where $r_{ij} > 0$. If $|\mathcal{N}_i| = 1$, then $\mathbf{C}_i(t)$ being a constant independent of t is equivalent to Equation ???. If $|\mathcal{N}_i| = 2$, then $\mathbf{C}_i(t)$ being a constant independent of t is equivalent to either Equation ?? being true, or to:

$$\Omega_{j_1} = \Omega_{j_2}, \quad r_{ij_1} = r_{ij_2}, \quad |\Phi_{ij_1} - \Phi_{ij_2}| = \pi \quad (3.44)$$

where $\mathcal{N}_i = \{j_1, j_2\}$. If $|\mathcal{N}_i| = 3$, then $\mathbf{C}_i(t)$ being a constant independent of t is equivalent to Equation ?? holding, or to either of the following:

- For $\mathcal{N}_i = j_1, j_2, j_3$, Equation 3.45 holds, where

$$\Omega_{j_1} = \Omega_{j_2} = \Omega_{j_3}, \quad \sum_{j \in \mathcal{N}_i} r_{ij} e^{j\Phi_{ij}} = 0, \quad (3.45)$$

- $\Omega_i = \Omega_{j_3}$ holds for $j_3 \in \mathcal{N}_i$ and Equation 3.44 holds, where $\mathcal{N}_i \setminus j_3 = j_1, j_2$.

Proof By applying Lemma 3.3 at the end of the chapter, it can be shown that the cases where $|\mathcal{N}_i| = 1$ and $|\mathcal{N}_i| = 2$ hold. Therefore, we consider the case where $|\mathcal{N}_i| = 3$ below.

For simplicity of notation, let $j \in \{1, 2, 3\}$, and denote r_{ij} , Φ_{ij} , Ω_i , and \mathbf{C}_i as r_j , Φ_j , Ω_0 , and \mathbf{C}_0 , respectively. First, we consider the case where $\Omega_j \neq \Omega_0$ for all $j \in \{1, 2, 3\}$. From Lemma 3.3, it follows that when Equation ?? holds, Equation 3.43 is equivalent to

$$\Omega_1 = \Omega_2 = \Omega_3, \quad \sum_{j=1}^3 r_j e^{j\Phi_j} = 0$$

which implies Equation 3.45. However, if $\Omega_1 = \Omega_2 = \Omega_3$, then by the same argument as in the case $|\mathcal{N}_i| = 1$, it follows that $\mathbf{C}_i(t)$ is a constant independent of t , and Equation ?? is equivalent to Equation ??, leading to a contradiction.

Next, we consider the case where Equation ?? does not hold, i.e., there exists $j \in \{1, 2, 3\}$ such that $\Omega_0 = \Omega_j$. Without loss of generality, we may assume that $\Omega_0 = \Omega_3$. In this case, we have

$$\mathbf{C}_0(t) = \frac{1}{3} \left\{ r_3 e^{j\Phi_3} \sum_{j=1}^2 r_j e^{j\{\Omega_0 - \Omega_j\}t + \Phi_j} \right\}.$$

Thus, we can discuss the invariance with respect to t in the same way as the case $|\mathcal{N}_i| = 2$. Therefore, the fact that $\mathbf{C}_0(t)$ is a constant independent of t is equivalent to Equation ?? or:

$$\Omega_1 = \Omega_2, \quad r_1 = r_2, \quad |\Phi_1 - \Phi_2| = \pi.$$

Therefore, the proposition is proved. \square

Lemma 3.2 shows that when the degree of the target bus is 1, i.e., for a bus at the endpoint of a line like in 3.8(a), it synchronizes with its neighboring bus. When the degree of the target bus (the node indicated by a thick line) is 2, i.e., for a bus on

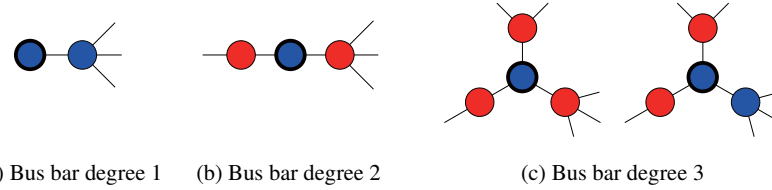


Fig. 3.8 Synchronization with adjacent busbars according to the degree of the busbar

a chain-like path like in 3.8(b), at least its two neighboring buses synchronize. Furthermore, when the degree of the target bus is 3, i.e., for a bus at a node connected by three power lines like in 3.8(c), either the three buses except the target bus synchronize, or at least one of the adjacent buses synchronizes with the target bus. This means that situations where only one of the adjacent buses does not synchronize or situations where no pair of buses synchronize do not occur.

Similar analyses can be performed for cases where the degree of the target bus is greater than or equal to 4. However, deriving equivalent synchronization conditions generally becomes complicated due to higher-order equations involving Ω_i and Ω_j , and multiple combinations of some adjacent buses synchronizing while others do not. Nevertheless, it is generally shown that if any $|\mathcal{N}_i| - 1$ adjacent buses out of the $|\mathcal{N}_i|$ buses adjacent to the target bus i synchronize with bus i , then the remaining one also synchronizes.

By combining the conditions for degrees 3 and below as shown in Lemma 3.2, it is possible to show the synchronization of all buses even when there are buses with degrees greater than or equal to 4 in the power grid. For example, it can be shown for a power grid with a tree structure, which is connected and has no cycles, that all buses synchronize.

It is possible to perform a similar analysis even when the degree of the bus of interest is four or greater. However, because the resulting conditions become higher-order equations in terms of Ω_i and Ω_j , and there are multiple combinations where only certain adjacent buses synchronize, writing down equivalent conditions regarding synchronization generally becomes complicated. However, if any of the $|\mathcal{N}_i| - 1$ adjacent buses to the bus of interest i synchronize, then the remaining one will generally synchronize as well.

By combining the conditions for degrees 3 or lower shown in Lemma 3.2, it is possible to demonstrate synchronization of all buses even when the network contains buses with degree 4 or greater. For example, it can be shown for a power network with a tree structure (i.e., connected with no cycles) that all buses will synchronize.

Theorem 3.4 (Synchronization of Generators in a Tree-Structured Power System) Consider the power system model where the devices are connected by a network of transmission lines represented by a system of simultaneous equations as shown in



Fig. 3.9 Synchronization of bus bars in a power grid with a tree structure

Equation 3.4. When the graph of the power system network has a tree structure, all generators synchronize in steady-state operating conditions.

Proof We focus on the bus at the endpoint indicated by the bold line in 3.9(a). Since the degree of the bus is 1, the adjacent bus is synchronized with the endpoint bus. Next, if the adjacent bus to the endpoint is on a chain path, its degree is 2, so at least the two adjacent buses are synchronized. By repeating this process, as shown in 3.9(a), the synchronization of all buses is demonstrated on the chain path connecting the endpoint and buses of degree 3 or higher.

Similarly, all buses with degree 3 or higher that exist on nodes from another endpoint are synchronized, so all buses on chain paths connecting the buses of the bold nodes in 3.9 are synchronized. By repeating this discussion, it is demonstrated that all buses in the power system tree are synchronized. \square

There is no degree restriction on the buses in the power grid with a tree structure, as stated in Theorem 3.4. Thus, even if there are buses with degree 4 or higher in the power grid, it is sometimes possible to deduce the synchronization of all buses using only the graph structure information. Similarly, the following theorem can be proven:

Theorem 3.5 (Synchronization of Buses in a Ring-Structured Power Grid) Consider a power system model in which a group of devices is connected by a system of power transmission lines described by the set of equations in 3.4. If the power grid has a circular structure and the total number of buses is odd, then all buses will be synchronized in the steady-state power flow.

Proof If we focus on one bus, the synchronization of the two buses at each end of it is shown. By repeating this process, the synchronization of all buses is shown when the total number of buses is odd. \square

Theorem 3.5 demonstrates that for a circular structured power grid with an odd number of transmission lines, all the main lines will synchronize regardless of the admittance values of the power grid. On the other hand, for an even number of transmission lines, it is not possible to conclude the synchronization of all the main lines for a circular structured power grid without additional information such as admittance values.

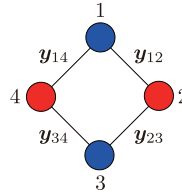


Fig. 3.10 Synchronization of four busbars in a ring-structured transmission network

The following example demonstrates that even when the number of transmission lines is even, the synchronization of all main lines can be inferred with only some information about the admittance values.

Example 3.6 Synchronization of four bus bars in a power grid with a ring structure Let us consider synchronization of bus bars under a steady power flow distribution in a power grid with a ring structure shown in Figure 3.10. Since the number of bus bars is even, synchronization of bus bars cannot be shown using only the information of the graph structure as in Theorem 3.5. However, as it is shown with red and blue in Figure 3.10, synchronization of alternating bus bars is shown by Lemma 3.2. Therefore, for all bus bars to show synchronization, all that is necessary is to show that one of the conditions of Equation 3.44 is not satisfied for at least one bus bar.

Let y_{ij} denote the admittance of the transmission line connecting bus i and bus j . Then, the central condition in Equation 3.44 for each bus can be expressed as follows:

$$\begin{aligned} |V_2^*||y_{12}| &= |V_4^*||y_{14}|, & |V_1^*||y_{12}| &= |V_3^*||y_{23}|, \\ |V_2^*||y_{23}| &= |V_4^*||y_{34}|, & |V_3^*||y_{23}| &= |V_1^*||y_{14}| \end{aligned} \quad (3.46)$$

Expressing this in matrix form, we have:

$$\underbrace{\begin{bmatrix} 0 & |y_{12}| & 0 & -|y_{14}| \\ -|y_{12}| & 0 & |y_{23}| & 0 \\ 0 & -|y_{23}| & 0 & |y_{34}| \\ |y_{14}| & 0 & -|y_{34}| & 0 \end{bmatrix}}_S \begin{bmatrix} |V_1^*| \\ |V_2^*| \\ |V_3^*| \\ |V_4^*| \end{bmatrix} = 0$$

A necessary condition for the existence of a positive vector $(|V_1^*|, \dots, |V_4^*|)$ that satisfies this equation is that the matrix S on the left-hand side is not invertible. However, note that even if S is singular, it does not necessarily mean that there exists a positive vector that is its nullspace. From the sparse structure of the column vectors, it can be seen that S is non-invertible if and only if:

$$|y_{12}||y_{34}| = |y_{14}||y_{23}| \quad (3.47)$$

Therefore, all buses are synchronized unless the admittance matrix satisfies this condition. It is also shown that if Equation 3.47 holds, then a necessary and sufficient condition for the existence of a positive vector that satisfies the central condition in Equation 3.44 is Equation 3.47.

Next, let us consider the right-hand side conditions in Equation 3.44 for buses 1 and 3:

$$|\phi_2 - \phi_4 + \angle y_{12} - \angle y_{14}| = \pi, \quad |\phi_2 - \phi_4 + \angle y_{23} - \angle y_{34}| = \pi$$

Similarly, if we focus on bus bar 2 and bus bar 4, we obtain the following equations:

$$|\phi_1 - \phi_3 + \angle y_{12} - \angle y_{23}| = \pi, \quad |\phi_1 - \phi_3 + \angle y_{14} - \angle y_{34}| = \pi$$

In general, when the ground capacitance is sufficiently small, the real part of the admittance, which is the conductance component, is non-negative, and the imaginary part, which is the susceptance component, is negative. In other words

$$\angle y_{ij} \in \left[-\frac{\pi}{2}, 0 \right]$$

Note that if we satisfy the above conditions, then the necessary and sufficient condition for the existence of (ϕ_1, \dots, ϕ_4) that satisfy the above conditions is:

$$\angle y_{12} - \angle y_{14} = \angle y_{23} - \angle y_{34} \quad (3.48)$$

Therefore, unless the admittance matrix satisfies this condition, all busbars will synchronize.

From the above discussion, it can be seen that the necessary and sufficient conditions for the existence of one or more sets of unsynchronized busbars in steady-state power flow are given by Equations 3.47 and 3.48. These two conditions suggest that only the opposite busbars will synchronize with each other when the power transmission network shown in Figure 3.10 has a specific symmetry with respect to the values of admittance.

From Example 3.6, it can be seen that the condition given by Equation 3.44 represents a specific symmetry with respect to the values of admittance in the power transmission network. In practical applications, it is a universal fact that all busbars will synchronize in steady-state power flow for sparse transmission networks with low degree of each busbar, unless there is a specific symmetry in the graph structure. In fact, to the best of the authors' knowledge, it has been numerically verified that all busbars synchronize in steady-state power flow for any power system model parameters set to realistic values.

3.6 Implementation of Power Flow Calculation

Let us consider building a numerical simulation environment for analyzing and controlling power systems. In order to correctly perform numerical simulations of large and complex power system models, it is useful to employ object-oriented thinking and programming techniques, which allow us to describe them as a group of modules separated by their functions. In this section, we introduce an implementation method of power flow calculation using Matlab, based on this approach. For basic syntax of Matlab, please refer to [?] or [?]. For object-oriented programming with Matlab, please refer to [?], and for general principles of object-oriented programming, please refer to [?] or [20].

3.6.1 Solving Algebraic Equations

In order to perform power flow calculation, it is necessary to solve the algebraic equations in Equation 3.10. In this section, we will show how to use MATLAB to explore the solutions of algebraic equations using a simple example.

Example 3.7 Searching for a solution for algebraic equations

Consider the following set of algebraic equations:

$$x^2 - y = 0 \quad x^2 + y^2 - 2 = 0 \quad (3.49a)$$

We want to find the values of (x, y) that satisfy these equations using numerical computations. Note that the solutions are $(x, y) = (-1, 1)$ and $(1, 1)$. MATLAB provides a convenient command for solving algebraic equations called `fsolve` from the optimization toolbox. To use this command, we need to implement a function $f(x, y)$ such that the algebraic equations in Equation 3.49 can be written in the form $f(x, y) = 0$. We implement the function $f(x, y)$ in Program 3.1.

```

1 function out = func_ex1(x_in)
2
3 x = x_in(1);
4 y = x_in(2);
5
6 out = zeros(2, 1);
7 out(1) = x^2 - y;
8 out(2) = x^2 + y^2 - 2;
9
10 end

```

Program 3.1 func_ex1.m

Next, using this function, we will write a program to explore the solution of the algebraic equation by executing `fsolve`. The program for this is shown in Program 3.2.

```

1 options = optimoptions('fsolve', 'Display', 'iter');
2 x0 = [0.1; 0.5];
3 x_sol = fsolve(@func_ex1, x0, options)

```

Program 3.2 main_ex1.m

Here, the first line's `options` sets the options to be given to `fsolve` to solve the algebraic equation, and in this example, the optimization process is displayed. Also, the second line `x0 = [0.1; 0.5];` represents the initial values for numerically searching for solutions. When this program is executed, the following results are obtained.

execution3.1

Iteration	Func-count	f(x)	(Omitted)
0	3	3.2677	
1	6	0.282554	
(Omitted)			
4	15	3.60447e-14	

The equation is solved

(Omitted)

```

x_sol =
1.0000
1.0000

```

From this result, it can be seen that as the iteration progresses, the value of $f(x)$ decreases, and a solution is found where $f(x)$ is almost 0. The solution found through this search is (1, 1), which is indeed a solution to the algebraic equation. However, it should be noted that numerical solution methods using `fsolve` do not always find all the solutions, and only one of the solutions may be obtained.

Next, let's show the case where the other solution is obtained. When the second line of Program 3.2 is changed to `x0 = [-0.1; 0.5];` and executed, the following result is obtained.

execution3.2

Iteration	Func-count	f(x)
0	3	3.2677
1	6	0.282554
(Omitted)		
4	15	3.60447e-14

The equation has been solved.

(Omitted)

```

x_sol =
-1.0000
1.0000

```

In this execution result, the solution (-1, 1) is obtained. In numerical solution methods for nonlinear algebraic equations, it is important to note that different solutions can be obtained depending on the initial values. As a reference, let's check

the execution result when the initial values set in the second line of 3.2 are set as $x_0 = [-0.1; -0.1]$:

execution3.3			
Iteration	Func-count	f(x)	(Omitted)
0	3	2.8125	
1	6	1.89068	
(Omitted)			
29	62	1.75	
 No solution found.			
(Omitted)			
x_sol =			
 0.0000			
-1.2247			

As seen in this example, depending on the initial values given, even for equations with solutions, correct solutions may not be obtained. In practice, it is important to provide initial values close to the desired solution.

3.6.2 Simple implementation of power flow calculation

Next, we will introduce a simple implementation method for power flow calculation.

Example 3.8 Implementation method for power flow calculations

Consider performing power flow calculations on the power system model consisting of 3 buses in Example 3.2. Since power flow calculation is also a type of calculation that solves algebraic equations, it is necessary to implement the $f(x)$ part of $f(x) = 0$ as in Example 3.7.

If the admittance values of the two transmission lines are set to the values in Equation 3.12, the steady-state power flow state that is consistent with the data sheet in 3.2(a) is as follows.

$$(|I_1^*|, \angle I_1^*, |V_1^*|, \angle V_1^*, |I_2^*|, \angle I_2^*, |V_2^*|, \angle V_2^*, |I_3^*|, \angle I_3^*, |V_3^*|, \angle V_3^*)$$

Given the admittance matrix \mathbf{Y} , the current is uniquely determined by the voltage, so the power flow calculation is essentially a process of determining the set of voltages for the buses. Therefore, we can take the real and imaginary parts of the voltage phasors for all buses and arrange them as variables x in the algebraic equations.³ In this case, the voltage phasors, current phasors, active and reactive power for each bus are all functions of x . Denoting them as $\hat{V}_i(x)$, $\hat{I}_i(x)$, $\hat{P}_i(x)$, and $\hat{Q}_i(x)$, respectively, the algebraic equations to be solved are given by:

³ It is also possible to take the magnitude and phase angle of the voltage phasors as x .

$$\begin{aligned} |V_1^*| - |\hat{V}_1(x)| &= 0 \\ \angle V_1^* - \angle \hat{V}_1(x) &= 0 \\ P_2^* - \hat{P}_2(x) &= 0 \\ Q_2^* - \hat{Q}_2(x) &= 0 \\ P_3^* - \hat{P}_3(x) &= 0 \\ |V_3^*| - |\hat{V}_3(x)| &= 0 \end{aligned}$$

If we implement the functions on the left side, it becomes a program 3.3.

Though this function has five output arguments, with `fsolve`, only the first output argument is used. The remaining arguments were added to confirm the result.

```

1 function [out, Vhat, Ihat, Phat, Qhat] = func_ex2(x)
2 % x: [Real(V1), Imag(V1),
3 %       Real(V2), Imag(V2),
4 %       Real(V3), Imag(V3)]';
5
6 y12 = 1.3652 - 11.6040j;
7 y23 = -10.5107j;
8 Y = [y12, -y12, 0;
9      -y12, y12+y23, -y23;
10     0, -y23, y23];
11
12 V1abs = 2;
13 V1angle = 0;
14
15 P2 = -3;
16 Q2 = 0;
17
18 P3 = 0.5;
19 V3abs = 2;
20
21 V1hat = x(1) + 1j*x(2);
22 V2hat = x(3) + 1j*x(4);
23 V3hat = x(5) + 1j*x(6);
24
25 Vhat = [V1hat; V2hat; V3hat];
26
27 Ihat = Y*Vhat;
28 PQhat = Vhat.*conj(Ihat);
29 Phat = real(PQhat);
30 Qhat = imag(PQhat);
31
32 out = [V1abs-abs(V1hat); V1angle-angle(V1hat);
33          P2-Phat(2); Q2-Qhat(2);
34          P3-Phat(3); V3abs-abs(V3hat)];
35 end

```

Program 3.3 func_ex2.m

As mentioned in Example 3.7, when numerically searching for solutions to algebraic equations, the choice of initial values is important. In power flow calculations,

an initial value called the **flat start** is often used. In the flat start, the initial value of x is set by

$$|\hat{V}_i(x)| = 1, \quad \angle V_i(x) = 0$$

for all buses. This corresponds to setting the real and imaginary parts of V_i to 1 and 0, respectively. The specific program for the flat start is as follows.

```

1 x0 = [1; 0; 1; 0; 1; 0];
2 options = optimoptions('fsolve', 'Display', 'iter');
3 x_sol = fsolve(@func_ex2, x0, options);
4
5 [~, V, I, P, Q] = func_ex2(x_sol);
6 Vabs = abs(V);
7 Vangle = angle(V);
8 display('Vabs:');
9 display('Vangle:');
10 display('P:');
11 display('Q:');

```

Program 3.4 main_ex2.m

The initial value for the flat start is set in the first line of Program 3.4. Then, on the fifth line, the voltage phasors, current phasors, active power, and reactive power are calculated using the solution of the algebraic equation. Finally, on the sixth line and below, the absolute value, phase angle, active power, and reactive power of the voltage phasors are displayed. The result of running Program 3.4 is shown. Note that this result matches the values shown in Table 3.2(b).

execution3.4

Iteration	Func-count	f(x)	(Omitted)
0	7	11.25	
1	14	3.28327	
(Omitted)			
5	42	4.19428e-28	

The equation has been solved.

(Omitted)

Vabs:

2.0000	1.9918	2.0000
--------	--------	--------

Vangle:

0.0000	-0.0538	-0.0419
--------	---------	---------

P:

2.5158	-3.0000	0.5000
--------	---------	--------

Q:

-0.0347	0.0000	0.1759
---------	--------	--------

3.6.3 Implementation of Power Flow Calculation using Separated Modules

In the previous section, a simple implementation of power flow calculation was described. However, in this implementation, it is necessary to rewrite the function corresponding to Program 3.3 every time the admittance matrix is changed. Also, if the number or type of buses is changed, the entire program needs to be rewritten. In this section, to enable power flow calculation for large-scale power systems or implementation by multiple people, we consider dividing the program into a group of modules. This leads to a well-structured implementation.

First, let's consider modularizing the implementation of the admittance matrix in Program 3.3.

Example 3.9 Separation of Implementation of Admittance Matrix

Let's separate the part of Program 3.3 that specifies the admittance matrix. For this purpose, we can make the variable Y an input argument of the function. For example, a modification like Program 3.5 can be considered.

```
1 function [out, Vhat, Ihat, Phat, Qhat] = func_ex3(x, Y)
2 (Same as lines 12 through 34 of program 3-3)
3 end
```

Program 3.5 function_ex2.m

However, since `fsolve` requires a "function with only the parameters to be optimized as arguments", the modified Program 3.5 cannot be used directly. This problem can be solved by using a technique called **currying** of functions. Specifically, program 3.5 can be modified as follows.

```
1 x0 = [1; 0; 1; 0; 1; 0];
2 options = optimoptions('fsolve', 'Display', 'iter');
3
4 y12 = 1.3652 - 11.6040j;
5 y23 = -10.5107j;
6 Y = [y12, -y12, 0;
7      -y12, y12+y23, -y23;
8      0, -y23, y23];
9
10 func_curried = @(x) func_ex3(x, Y);
11
12 x_sol = fsolve(func_curried, x0, options);
13 [~, V, I, P, Q] = func_curried(x_sol);
14 (Same as line 6 and below in program 3-4)
```

Program 3.6 main_ex3.m

The "`@(x)` expression of `x`" used creates a function that returns the value of the expression with argument `x`. This type of function that is created without a name is called an **anonymous function**. When an anonymous function contains variables that are not included in its arguments, such as Y in this case, it uses a constant from the workspace. Therefore, it is possible to generate a new function by fixing some of

the variables among multiple arguments and leaving only the remaining variables as arguments. This technique is called currying. Using currying, a function that takes any number of arguments can be used as a function with a specified number of arguments. This allows for the separation of functionality without using global variables.

Next, let us consider the part of the Program 3.3 that calculates the constraint conditions for each busbar. In the Program 3.3, the constraint conditions for each busbar are directly written, so it is necessary to rewrite the program every time the number of busbars is changed. Furthermore, there is an implicit case distinction depending on the type of busbar, and if the types of busbars are increased, it is necessary to modify the processing of the case distinction.

To write a transparent program without using case distinctions, it is useful to use the concept of **polymorphism** in object-oriented programming. In the following example, we explain the concept of polymorphism through an implementation example.

Example 3.10 Implementation of Power Flow Calculation using Polymorphism

In power flow calculation, different constraint conditions are set depending on the type of busbar, but all busbars have a common property of "having constraint conditions." By implementing this common property as a "method with a common name," a simple program can be created. To understand this, let's define classes corresponding to slack busbars, generator busbars, and load busbars in Program 3.7 as shown in Program 3.10.

```

1 classdef bus_slack
2
3 properties
4     Vabs
5     Vangle
6 end
7
8 methods
9     function obj = bus_slack(Vabs, Vangle)
10        obj.Vabs = Vabs;
11        obj.Vangle = Vangle;
12    end
13
14    function out = get_constraint(obj, Vr, Vi, P, Q)
15        Vabs = norm([Vr; Vi]);
16        Vangle = atan2(Vi, Vr);
17        out = [Vabs-obj.Vabs; Vangle-obj.Vangle];
18    end
19 end
20 end

```

Program 3.7 bus_slack.m

```

1 classdef bus_generator
2
3 properties

```

```

4     P
5     Vabs
6 end
7
8 methods
9     function obj = bus_generator(P, Vabs)
10        obj.P = P;
11        obj.Vabs = Vabs;
12    end
13
14    function out = get_constraint(obj, Vr, Vi, P, Q)
15        Vabs = norm([Vr; Vi]);
16        out = [obj.P-P; Vabs-obj.Vabs];
17    end
18 end
19 end

```

Program 3.8 bus_generator.m

```

1 classdef bus_load
2
3 properties
4     P
5     Q
6 end
7
8 methods
9     function obj = bus_load(P, Q)
10        obj.P = P;
11        obj.Q = Q;
12    end
13
14    function out = get_constraint(obj, Vr, Vi, P, Q)
15        out = [P-obj.P; Q-obj.Q];
16    end
17 end
18 end

```

Program 3.9 bus_load.m

The classes defined here, bus_slack, bus_generator, and bus_load, all have a method called `get_constraint` with a common input and output. In this case, a program that uses these classes can calculate the appropriate constraint conditions by calling `get_constraint` without being aware of what type of busbar it is. Using this idea, Program 3.3 can be rewritten as follows.

```

1 function [out, V, I, P, Q] = func_power_flow(x, Y, a_bus)
2
3 V = x(1:2:end) + 1j*x(2:2:end);
4 I = Y*V;
5 PQhat = V.*conj(I);
6 P = real(PQhat);
7 Q = imag(PQhat);
8
9 out_cell = cell(numel(a_bus), 1);

```

```

10
11 for i = 1:numel(a_bus)
12   bus = a_bus{i};
13   out_cell{i} = bus.get_constraint...
14     real(V(i)), imag(V(i)), P(i), Q(i));
15 end
16 out = vertcat(out_cell{:});
17
18 end

```

Program 3.10 func_power_flow.m

The program 3.10 assumes that the cell array, which is the set of mother lines, is input as `a_bus`. An example of how to use this function is shown in the program 3.11.

```

1 (Same as lines 1-8 in program 3-6)
2
3 a_bus = cell(3, 1);
4 a_bus{1} = bus_slack(2, 0);
5 a_bus{2} = bus_load(-3, 0);
6 a_bus{3} = bus_generator(0.5, 2);
7
8 func_curried = @(x) func_power_flow(x, Y, a_bus);
9
10 x_sol = fsolve(func_curried, x0, options);
11
12 (Same as Program 3-4, line 6 and following)

```

Program 3.11 main_ex4.m

In the program 3.11, the slack bus bar, load bus bar, and generator bus bar are defined respectively and assigned to the cell array `a_bus`. At this time, in the program 3.10, `get_constraint` is executed for each bus bar assigned to `a_bus`. Since `get_constraint` is implemented for each bus line type, the appropriate processing is performed without having to describe the case. Such different processing for similar program calls is called polymorphism, and is one of the important concepts in object-oriented programming.

In an implementation using polymorphism like Program 3.10, it has the advantage of easy adaptability to changes in the number and configuration of buses. Specifically, by changing the number and definition of buses in lines 3-6 of Program 3.11, Program 3.10 can be used without modification.

Moreover, adding new types of buses is also easy. Program 3.10 assumes only that a method called `get_constraint` with appropriate inputs and outputs exists for the bus. In other words, if it has `get_constraint`, it is defined as a bus. This is called "duck typing", a concept that comes from "if it walks like a duck and quacks like a duck, then it must be a duck." This allows module designers to define a new bus class by implementing only `get_constraint` without having to pay attention to the internal processing of Program 3.10. Thus, this approach clarifies the scope of implementation for module designers.

The above has allowed us to prospectively implement a program for calculating the tidal currents given an admittance matrix. Furthermore, let us implement the computation of the admittance matrix by dividing it into a group of modules.

Example 3.11 Calculation of Admittance Matrix using Object-oriented Programming

The admittance matrix is generally defined by multiple power transmission lines. Therefore, we create a class that represents a power transmission line and consider using a collection of its instances. A power transmission line connects two busbars, so it is necessary to identify the numbers of these busbars. Additionally, regardless of the type of power transmission line model, the admittance matrix $\mathbf{Y}_{\text{branch}}$ satisfying

$$\begin{bmatrix} \mathbf{I}_{\text{from}} \\ \mathbf{I}_{\text{to}} \end{bmatrix} = \mathbf{Y}_{\text{branch}} \begin{bmatrix} \mathbf{V}_{\text{from}} \\ \mathbf{V}_{\text{to}} \end{bmatrix} \quad (3.50)$$

is generally determined. Here, \mathbf{V}_{from} and \mathbf{V}_{to} are the voltages of the busbars at both ends of the power transmission line, and \mathbf{I}_{from} and \mathbf{I}_{to} are the currents flowing from the busbars to the power transmission line at both ends. For example, in the simple power transmission line discussed in Example 2.1, we have

$$\mathbf{Y}_{\text{branch}} = \begin{bmatrix} y & -y \\ -y & y \end{bmatrix}$$

In summary, it is sufficient to return the information of the two connected buses and the admittance matrix $\mathbf{Y}_{\text{branch}}$ to define a transmission line. An example implementation of a transmission line based on this idea is as follows.

```

1 classdef branch
2
3 properties
4     y
5     from
6     to
7 end
8
9 methods
10    function obj = branch(from, to, y)
11        obj.from = from;
12        obj.to = to;
13        obj.y = y;
14    end
15
16    function Y = get_admittance_matrix(obj)
17        y = obj.y;
18        Y = [y, -y;
19              -y, y];
20    end
21 end
22 end

```

Program 3.12 branch.m

The function to compute the admittance matrix using this transmission line class is implemented as follows

```

1 function Y = get_admittance_matrix(n_bus, a_branch)
2
3     Y = zeros(n_bus, n_bus);
4
5     for i = 1:numel(a_branch)
6         br = a_branch{i};
7         Y_branch = br.get_admittance_matrix();
8         Y([br.from, br.to], [br.from, br.to]) =...
9             Y([br.from, br.to], [br.from, br.to]) + Y_branch;
10    end
11
12 end
```

Program 3.13 get_admittance_matrix.m

The input argument `n_bus` is the number of bus lines. Also, `a_branch` is a cell array containing the transmission lines. This program can be used as follows:

```

1 a_branch = cell(2, 1);
2 a_branch{1} = branch(1, 2, 1.3652-11.6040j);
3 a_branch{2} = branch(2, 3, -10.5107j);
4
5 Y = get_admittance_matrix(3, a_branch)
```

Program 3.14 main_admittance_matrix.m

In the program 3.13, we only assume that the transmission line has the data `from` and `to` and that it has the method `get_admittance_matrix` and the method `get_admittance_matrix`. Therefore, when considering other transmission line models such as π -type models. When considering other transmission line models, such as π -type models, the variables `to` and `from` and the method `get_admittance_matrix` are also assumed to be used. The program program 3.13 can be used without any modification by simply implementing a class with variables named `to`, `from` and a method named `get_admittance_matrix`.

From the above, the program to calculate tidal currents can be summarized as follows.

Example 3.12 Implementation result of power flow calculation

The program implemented in the above example can be organized as a function for performing power flow calculation, which is shown in Program 3.15.

```

1 function [V, I, P, Q] = calculate_power_flow(a_bus, a_branch)
2
3     n_bus = numel(a_bus);
4     Y = get_admittance_matrix(n_bus, a_branch);
5
6     func_curried = @(x) func_power_flow(x, Y, a_bus);
7
8     x0 = kron(ones(n_bus, 1), [1; 0]);
```

```

9 options = optimoptions('fsolve', 'Display', 'iter');
10 x_sol = fsolve(func_curried, x0, options);
11
12 [~, V, I, P, Q] = func_curried(x_sol);
13
14 end

```

Program 3.15 calculate_power_flow.m

This program takes a set of buses and a set of transmission lines as inputs and performs power flow calculations. It can be used as shown in Program 3.16.

```

1 a_bus = cell(3, 1);
2 a_bus{1} = bus_slack(2, 0);
3 a_bus{2} = bus_load(-3, 0);
4 a_bus{3} = bus_generator(0.5, 2);
5
6 a_branch = cell(2, 1);
7 a_branch{1} = branch(1, 2, 1.3652-11.6040j);
8 a_branch{2} = branch(2, 3, -10.5107j);
9
10 [V, I, P, Q] = calculate_power_flow(a_bus, a_branch);
11
12 display('Vabs:'), display(abs(V))
13 display('Vangle:'), display(angle(V))
14 display('P:'), display(P)
15 display('Q:'), display(Q)

```

Program 3.16 main_power_flow.m

If it is necessary to perform power flow calculations for different power grids, other programs can be used without modification by changing only the definitions of buses and transmission lines in lines 1 to 8 of Program 3.16. Also, if a new type of bus or transmission line is required, a new class implementing the data and methods with predetermined names can be implemented. Therefore, compared to a simple implementation like Example 3.8, this program has high readability and extensibility.

3.7 Implementation method for time response calculation of power system models

In this section, we will explain how to numerically calculate the time response of a power system model using MATLAB . To calculate the time response of a power system model, it is necessary to solve a system of differential-algebraic equations that combine differential equations representing the dynamic characteristics of the equipment and algebraic equations representing the power flow. First, let's look at an example of a simple differential-algebraic equation system and its solution method.

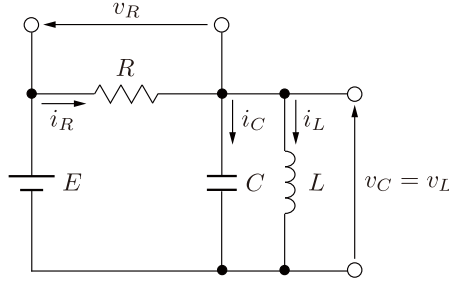


Fig. 3.11 Differential Algebraic Equations Example: LC Parallel Circuit

Example 3.13 Numerical solution method for a simple differential-algebraic equation system

Let us perform a numerical simulation for the case where R , L , C , and E are all equal to 1 in the simple electrical circuit shown in Figure 3.11. The dynamic elements of this circuit are the coil L and the capacitor C , and their differential equations are given by:

$$L\dot{i}_L = v_L \quad (3.51a)$$

$$C\dot{v}_C = i_C \quad (3.51b)$$

where the initial values are set to $i_L(0) = 0$ and $v_C(0) = 0$. Also, the algebraic equations given by Ohm's law and Kirchhoff's law are:

$$v_R = Ri_R \quad (3.52a)$$

$$i_R = i_L + i_C \quad (3.52b)$$

$$v_L = v_C \quad (3.52c)$$

$$E = v_C + v_R \quad (3.52d)$$

Using the algebraic equations in (3.52), redundant variables such as v_R and i_R can be eliminated, resulting in an equivalent system of ordinary differential equations. This operation corresponds to Kron reduction, and the resulting system of ordinary differential equations is given by:

$$\dot{i}_L = \frac{1}{L}v_C \quad (3.53a)$$

$$\dot{v}_C = \frac{1}{RC}(E - v_C) - \frac{1}{C}\dot{i}_L \quad (3.53b)$$

First, let's write a program to solve this system of ordinary differential equations. The `ode45` solver in MATLAB is commonly used for solving systems of ordinary differential equations. By implementing the function $f(t, x)$ for the ordinary differential equation $\dot{x} = f(t, x)$, the solver can compute the solution of the system of ordinary differential equations. Implementing the right-hand side of (3.53), the program becomes as shown in Program 3.17.

```

1 function dx = func_RLC_ode(x, R, C, L, E)
2
3 iL = x(1);
4 vC = x(2);
5
6 diL = vC/L;
7 dvC = (E-vC)/R/C - iL/C;
8
9 dx = [diL; dvC];
10
11 end
```

Program 3.17 func_RLC_ode.m

As a result, when `ode45` is executed and the ordinary differential equation system is solved, the Program 3.18 becomes:

```

1 R = 1;
2 L = 1;
3 C = 1;
4 E = 1;
5
6 func = @(t, x) func_RLC_ode(x, R, C, L, E);
7 x0 = [0; 0];
8 tspan = [0 30];
9
10 [t, x] = ode45(func, tspan, x0);
11
12 plot(t, x)
```

Program 3.18 main_RLC_ode.m

The output variable x in the program 3.18 is a matrix in which the time series of i_L and v_C are arranged vertically. Therefore, note that the time series of other variables such as i_C and i_R need to be additionally calculated using the algebraic equation of the Equation 3.52.

Next, consider directly finding the solution of the system of differential algebra equations without going through Kron reduction. In this case, since the physical algebraic equation can be written down as it is, there is an advantage that the description is easy even if the system becomes complicated. One of the commands that can solve the system of differential algebra with MATLAB is `ode15s`. The target is a system of differential algebraic equations described in the following format.

$$M\dot{x} = f(t, x) \quad (3.54)$$

Applying the expression (3.51) and the expression (3.52):

$$\underbrace{\begin{bmatrix} 0 & L & 0 & 0 & 0 & 0 \\ 0 & 0 & 0 & 0 & C & \\ 0 & 0 & 0 & 0 & 0 & \\ 0 & 0 & 0 & 0 & 0 & \\ 0 & 0 & 0 & 0 & 0 & \\ 0 & 0 & 0 & 0 & 0 & \end{bmatrix}}_M \underbrace{\begin{bmatrix} \dot{i}_R \\ \dot{i}_L \\ \dot{i}_C \\ \dot{v}_R \\ \dot{v}_L \\ \dot{v}_C \end{bmatrix}}_{\dot{x}} = \underbrace{\begin{bmatrix} v_L \\ i_C \\ v_R - R i_R \\ i_R - i_L - i_C \\ v_L - v_C \\ E - v_C - v_R \end{bmatrix}}_{f(t,x)}$$

Note that the order in which the elements on the 3rd to 6th lines on the right side are placed is arbitrary. Implementing this right-hand side results in a Program 3.19.

```

1 function dx = func_RLC_dae(x, R, C, L, E)
2
3 iR = x(1);
4 iL = x(2);
5 iC = x(3);
6 vR = x(4);
7 vL = x(5);
8 vC = x(6);
9
10 diL = vL;
11 dvC = iC;
12
13 con1 = vC-vL;
14 con2 = E-vC-vR;
15 con3 = iR-(iC+iL);
16 con4 = vR-iR*R;
17
18 dx = [diL; dvC; con1; con2; con3; con4];
19 end

```

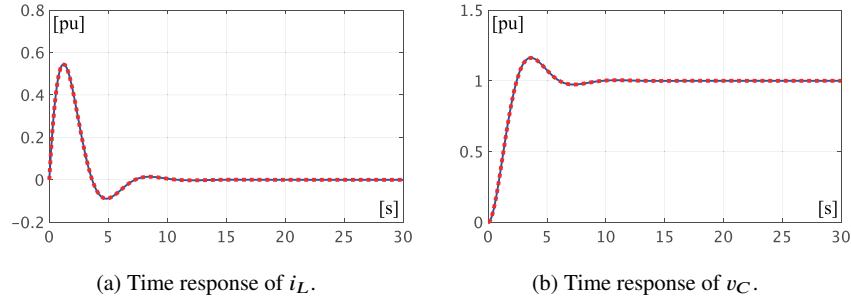
Program 3.19 func_RLC_dae.m

This function can be used to solve a system of differential algebraic equations such as in Program 3.20.

```

1 function dx = func_RLC_dae(x, R, C, L, E)
2
3 iR = x(1);
4 iL = x(2);
5 iC = x(3);
6 vR = x(4);
7 vL = x(5);
8 vC = x(6);
9
10 diL = vL;
11 dvC = iC;
12
13 con1 = vC-vL;
14 con2 = E-vC-vR;
15 con3 = iR-(iC+iL);

```

**Fig. 3.12 Time response of LC parallel circuits**

(Blue solid line: ode45, red dashed line: ode15s)

```

16 con4 = vR-iR*R;
17
18 dx = [diL; dvC; con1; con2; con3; con4];
19 end

```

Program 3.20 main_RLC_dae.m

In this program, M of the expression 3.54 is set in the option on the 13th line. Also, the initial value of the state is set in the 10th line, but only the state of the differential equation, that is, the 2nd and 6th elements, has meaning. The state of the algebraic equation does not need to be calculated and set by the user himself because the value that satisfies the equation is automatically searched by `ode15s`. In fact, the algebraic equation is not satisfied by the initial value with all the elements as 0, but the solution of the system of differential algebraic equations is calculated without any problem. The solution x obtained in the 15th line is a matrix in which the time series of $v_R, v_L, v_C, i_R, i_L, i_C$ are arranged, and all of them are different from the case of equivalent conversion to the ordinary differential equation system. The time series of the variables of is calculated at once.

Figure 3.12 shows the time response of i_L and v_C when the differential algebraic equation system is solved directly and when it is converted to an ordinary differential equation system. In each figure, two lines are displayed: one is the solution obtained by `ode45` (blue solid line) and the other is the solution obtained by `ode15s` (red dashed line). It is clear that the two solutions are equal.

3.7.1 Simple implementation of time response calculations for power system models

The following example describes how to implement a numerical simulation of a power system model.

Example 3.14 Simple implementation of power system simulation

Let us implement a program to numerically compute the time response of the power system model discussed in the Example 3.3. To describe this system, we need the differential equations in Equation 2.21a for bus bars 1 and 3, to which the generators are connected. Also, the algebraic equation of Equation 2.17a holds. A constant-impedance load model is connected to bus bar 2 and the algebraic equation of Equation 2.41a is satisfied. Furthermore, the algebraic system of equations of Kirchhoff's law, Equation 3.1, holds for the entire system at any given time.

Here, we consider describing the vertically arranged vector x of $\delta_1, \Delta\omega_1, E_1, \delta_3, \Delta\omega_3, E_3, V_1, V_2, V_3, I_1, I_2$, and I_3 in the form of:

$$M\dot{x} = f(t, x)$$

An implementation example of the right-hand side function $f(t, x)$ is shown in Program 3.21.

```

1  function dx = func_simulation_3bus(x, Y, parameter)
2
3  delta1 = x(1);
4  omega1 = x(2);
5  E1 = x(3);
6  delta3 = x(4);
7  omega3 = x(5);
8  E3 = x(6);
9  V1 = x(7) + 1j*x(8);
10 V2 = x(9) + 1j*x(10);
11 V3 = x(11) + 1j*x(12);
12 I1 = x(13) + 1j*x(14);
13 I2 = x(15) + 1j*x(16);
14 I3 = x(17) + 1j*x(18);
15
16 omega0 = parameter.omega0;
17
18 X1 = parameter.X1;
19 X1_prime = parameter.X1_prime;
20 M1 = parameter.M1;
21 D1 = parameter.D1;
22 tau1 = parameter.tau1;
23 Pmech1 = parameter.Pmech1;
24 Vfield1 = parameter.Vfield1;
25
26 z2 = parameter.z2;
27
28 X3 = parameter.X3;
29 X3_prime = parameter.X3_prime;
30 M3 = parameter.M3;
31 D3 = parameter.D3;
32 tau3 = parameter.tau3;
33 Pmech3 = parameter.Pmech3;
34 Vfield3 = parameter.Vfield3;
35
```

```

36 P1 = real(V1*conj(I1));
37 P3 = real(V3*conj(I3));
38
39 dx1 = [omega0 * omega1;
40 (-D1*omega1-P1+Pmech1)/M1;
41 (-X1/X1_prime*E1+...
42 (X1/X1_prime-1)*abs(V1)*cos(delta1-angle(V1))+Vfield1)/tau1
    ];
43
44 dx3 = [omega0 * omega3;
45 (-D3*omega3-P3+Pmech3)/M3;
46 (-X3/X3_prime*E3+...
47 (X3/X3_prime-1)*abs(V3)*cos(delta3-angle(V3))+Vfield3)/tau3
    ];
48
49 con1 = I1-(E1*exp(1j*delta1)-V1)/(1j*X1_prime);
50 con2 = V2+z2*I2;
51 con3 = I3-(E3*exp(1j*delta3)-V3)/(1j*X3_prime);
52
53 con_network = [I1; I2; I3] - Y*[V1; V2; V3];
54
55 dx = [dx1; dx3;real(con1); imag(con1); real(con2);
56     imag(con2); real(con3); imag(con3);
57     real(con_network); imag(con_network)];
58
59 end

```

Program 3.21 func_simulation_3bus.m

In this program, the voltage and current phasors included in \mathbf{x} are expressed by arranging their real and imaginary parts. Additionally, the `parameter` structure is used to specify variables collectively. Solving the differential algebraic equation system using Program 3.21 results in Program 3.22.

```

1 a_branch = cell(2, 1);
2 a_branch{1} = branch(1, 2, 1.3652-11.6040j);
3 a_branch{2} = branch(2, 3, -10.5107j);
4 Y = get_admittance_matrix(3, a_branch);
5
6 parameter = struct();
7
8 parameter.M1 = 100;
9 parameter.D1 = 10;
10 parameter.tau1 = 5.14;
11 parameter.X1 = 1.569;
12 parameter.X1_prime = 0.936;
13 parameter.Pmech1 = 2.5158;
14 parameter.Vfield1 = 2.7038;
15
16 parameter.z2 = 1.3224;
17
18 parameter.M3 = 12;
19 parameter.D3 = 10;
20 parameter.tau3 = 8.97;
21 parameter.X3 = 1.220;

```

```

22 parameter.X3_prime = 0.667;
23 parameter.Pmeh3 = 0.5000;
24 parameter.Vfield3 = 2.1250;
25
26 parameter.omega0 = 60*2*pi;
27
28 x0 = [0.5357 + pi/6; 0; 2.3069 + 0.1;...
29     0.0390; 0; 2.0654; zeros(12, 1)];
30 M = blkdiag(eye(6), zeros(12, 12));
31
32 tspan = [0 50];
33
34 options = odeset('Mass', M);
35 func = @(t, x) func_simulation_3bus(x, Y, parameter);
36 [t, x] = ode15s(func, tspan, x0, options);
37
38 plot(t, x(:, [2, 5]))

```

Program 3.22 main_simulation_simple.m

In Program 3.22, the initial value response of the power system model is calculated, and the angular frequency deviations of the two generators are plotted.

3.7.2 Implementation method for time response calculation using a group of partitioned modules

In this section, we explain how to separate the program described in the previous section into functions and modify it into a highly extensible program.

Example 3.15 Modularization of generators and loads The program 3.21 consists of two steps: dividing the input x into the state variables, voltage and current of each device, and computing differential and algebraic equations. Let us consider how to write a program that executes these two steps in a clear view.

First, in order to properly partition the variable x , we need to know the number of states of each device. Also, for all devices, the time derivative of the state $\frac{dx}{dt}$ in the differential equation and $f(x)$ in the algebraic equation $f(x) = 0$ is computed. Using the concept of duck typing, if a device has functions to return the number of states, perform time differentiation, and compute algebraic equations, it can be defined as a device. If we implement a generator and a load as a device with these functions, then we have a Program 3.23 and a Program 3.24.

```

1 classdef generator < handle
2
3 properties
4     omega0
5     X
6     X_prime

```

```
7      M
8      D
9      tau
10     Pmech
11     Vfield
12 end
13
14 methods
15     function obj = generator(omega0, M, D, tau, ...
16         X, X_prime, Pmech, Vfield)
17
18         obj.omega0 = omega0;
19         obj.X = X;
20         obj.X_prime = X_prime;
21         obj.M = M;
22         obj.D = D;
23         obj.tau = tau;
24         obj.Pmech = Pmech;
25         obj.Vfield = Vfield;
26     end
27
28     function nx = get_nx(obj)
29         nx = 3;
30     end
31
32     function [dx, con] = get_dx_constraint(obj, x, V, I)
33         delta = x(1);
34         omega = x(2);
35         E = x(3);
36         P = real(V*conj(I));
37
38         Pmech = obj.Pmech;
39         Vfield = obj.Vfield;
40
41         X = obj.X;
42         X_prime = obj.X_prime;
43         D = obj.D;
44         M = obj.M;
45         tau = obj.tau;
46
47         omega0 = obj.omega0;
48
49         dE = (-X/X_prime*E+...
50             (X/X_prime-1)*abs(V)*cos(delta-angle(V))...
51             +Vfield)/tau;
52         dx = [omega0 * omega;
53             (-D*omega-P+Pmech)/M;
54             dE];
55         con = I-(E*exp(1j*delta)-V)/(1j*X_prime);
56         con = [real(con); imag(con)];
57     end
58 end
59
60 end
```

Program 3.23 generator.m

```

1 classdef load_impedance < handle
2
3 properties
4     z
5 end
6
7 methods
8     function obj = load_impedance(z)
9         obj.z = z;
10    end
11
12    function nx = get_nx(obj)
13        nx = 0;
14    end
15
16    function [dx, con] = get_dx_constraint(obj, x, V, I)
17        dx = [];
18        z = obj.z;
19        con = V+z*I;
20        con = [real(con); imag(con)];
21    end
22 end
23
24 end

```

Program 3.24 load_impedance.m

In these programs, the method `get_nx` returns the number of states and `get_dx_constraint` returns the time derivative of the state and the constraint conditions. With the device defined in this way, the Program3.21 can be rewritten as Program3.25.

```

1 function out = func_simulation(t, x, Y, a_component)
2
3 n_component = numel(a_component);
4 x_split = cell(n_component, 1);
5 V = zeros(n_component, 1);
6 I = zeros(n_component, 1);
7
8 idx = 0;
9 for k = 1:n_component
10     nx = a_component{k}.get_nx();
11     x_split{k} = x(idx+1:idx+nx);
12     idx = idx + nx;
13 end
14
15 for k = 1:n_component
16     V(k) = x(idx+1) + x(idx+2)*1j;
17     idx = idx + 2;
18 end
19
20 for k = 1:n_component
21     I(k) = x(idx+1) + x(idx+2)*1j;

```

```

22     idx = idx + 2;
23 end
24
25 dx = cell(n_component, 1);
26 con = cell(n_component, 1);
27
28 for k = 1:n_component
29     component = a_component{k};
30     xk = x_split{k};
31     Vk = V(k);
32     Ik = I(k);
33     [dx{k}, con{k}] = component.get_dx_constraint(xk, Vk, Ik);
34 end
35
36 con_network = I - Y*V;
37
38 out = vertcat(dx{:});
39 out = [out; vertcat(con{:})];
40 out = [out; real(con_network); imag(con_network)];
41
42 end

```

Program 3.25 func_simulation.m

In the Program3.25, it is assumed that the cell array of the device is input to `a_component`. In addition, the variable `x` is divided in lines 9 through 23. At this time, by obtaining the number of device states in line 10, the division can be performed appropriately. In lines 28 to 34, the time derivative of the states and the constraints are computed. In line 33 of the program, we call `get_dx_constraint`, which is implemented using polymorphism. In line 38 of the Program, `vertcat(dx{:})` vertically combines all the elements of the cell array `dx`. That is, it is equivalent to `[dx{1}; dx{2}; ... ; dx{end}]`.

Let us consider running a numerical simulation using Program 3.25. Specifically, the numerical simulation part of the Program3.22 can be summarized as follows:

```

1 function [t, x, V, I] = ...
2     simulate_power_system(a_component, Y, x0, tspan)
3
4 n_component = numel(a_component);
5 a_nx = zeros(n_component, 1);
6 for k = 1:n_component
7     component = a_component{k};
8     a_nx(k) = component.get_nx();
9 end
10 nx = sum(a_nx);
11
12 M = blkdiag(eye(nx), zeros(n_component*4));
13 options = odeset('Mass', M, 'RelTol', 1e-6);
14
15 y0 = [x0(:); zeros(4*n_component, 1)];
16
17 [t, y] = ode15s(@(t, x) func_simulation(t, x, Y, a_component)
    , ...

```

```

18     tspan, y0, options);
19
20
21 x = cell(n_component, 1);
22 V = zeros(numel(t), n_component);
23 I = zeros(numel(t), n_component);
24
25 idx = 0;
26
27 for k = 1:n_component
28     x{k} = y(:, idx+(1:a_nx(k)));
29     Vk = y(:, nx+2*(k-1)+(1:2));
30     V(:, k) = Vk(:, 1) + 1j*Vk(:, 2);
31     Ik = y(:, nx+2*n_component+2*(k-1)+(1:2));
32     I(:, k) = Ik(:, 1) + 1j*Ik(:, 2);
33     idx = idx + a_nx(k);
34 end
35
36 end

```

Program 3.26 simulate_power_system.m

In the Program3.26, lines 5 to 9 define the matrixM| using the number of states obtained from each device. In line 17, the differential algebraic equations are solved using the program 3.25. In lines 27 to 34, the result is divided into the state variables of each device, the voltage phasors and current phasors of each bus bar, and returned.

Furthermore, rewriting the Program3.22 results in the Program3.27.

```

1 a_branch = cell(2, 1);
2 a_branch{1} = branch(1, 2, 1.3652-11.6040j);
3 a_branch{2} = branch(2, 3, -10.5107j);
4
5 Y = get_admittance_matrix(3, a_branch);
6
7 gen1 = generator(60*2*pi, 100, 10, 5.14, ...
8     1.569, 0.936, 2.5158, 2.7038);
9
10 load2 = load_impedance(1.3224);
11
12 gen3 = generator(60*2*pi, 12, 10, 8.97, ...
13     1.220, 0.667, 0.5000, 2.1250);
14
15 a_component = {gen1; load2; gen3};
16
17 x0 = [0.5357 + pi/6; 0; 2.3069 + 0.1i; 0.0390; 0; 2.0654];
18 tspan = [0 50];
19
20 [t, x, V, I] = simulate_power_system(a_component, Y, x0, tspan);
21
22 plot(t, [x{1}(:, 2), x{3}(:, 2)])

```

Program 3.27 main_simulation_3bus.m

In the Program 3.27, an array `a_component` of devices representing generators and loads is created and the function `simulate_power_system` defined in the Program 3.26 is executed.

When changing the structure of the power transmission network or the devices to be connected in numerical calculations of time response, it is sufficient to change `a_branch` and `a_component` in program 3.27, and it is not necessary to modify programs from 3.23 to 3.26. Moreover, if using other devices than generators and loads in programs 3.23 and 3.24, it is enough to implement a class with `get_nx` and `get_dx_constraint` and use it.

Thanks to this modularization, the resulting program is more readable and extensible compared to the implementation in Example 3.14.

In the execution results of this program, the state of each device is returned in the cell array `x`. Let's confirm that the elements of `x` form a matrix consistent with the number of state variables for each device. Here, the device connected to bus 2 is a load, and the number of states is 0, so `x{2}` is an empty matrix with 0 columns. The program plots the second element of the states of the generators connected to bus 1 and bus 3, i.e., the angular frequency deviation.

In Example 3.15, it is possible to implement time-response calculations of the power system model with clear visibility by modularizing the generator and load modules. However, in Program 3.27, it is necessary to calculate in advance the values of the external input of the generator and the impedance of the load that match the desired equilibrium point. Since these values depend on the dynamic characteristics of each equipment, there is room for improvement from the perspective of functional separation. To solve this problem, let's consider extending the program described in Example 3.15 and making it functionally more separated.

Example 3.16 Adding a Method to Calculate the Steady State of Generators and Loads

In numerical calculations of the time response of power system models, achieving a steady-state flow that realizes the desired power supply is important. At this time, Equation 3.19 and Equation 3.21 must be satisfied for each generator and load, respectively. Since these equations are related to the state equations of each device, it is appropriate to implement them in the classes of `generator` and `load_impedance`. From this perspective, by adding a method to calculate the steady state that achieves the desired power supply to Program 3.23 and Program 3.24, Programs 3.28 and 3.29 are obtained.

```

1 classdef generator < handle
2
3 % (Same as lines 3-12 of program 3-23)
4
5 methods
6
7 % (Same as lines 15-57 in program 3-23)
8
9     function x_equilibrium = set_equilibrium(obj, V, I, P, Q)

```

```

10    Vabs = abs(V);
11    Vangle = angle(V);
12
13    X = obj.X;
14    X_prime = obj.X_prime;
15
16    delta = Vangle + atan(P/(Q+Vabs^2/X_prime));
17    E = X_prime/Vabs*sqrt((Q+Vabs^2/X_prime)^2+P^2);
18
19    x_equilibrium = [delta; 0; E];
20
21    obj.Pmech = P;
22    obj.Vfield = X*E/X_prime ...
23        - (X/X_prime-1)*Vabs*cos(delta-Vangle);
24
25    end
26
27
28 end

```

Program 3.28 generator.m

```

1 classdef load_impedance < handle
2
3 (Same as lines 3-5 in program 3-24)
4
5 methods
6
7 (Same as lines 8 through 21 in Program 3-24)
8
9     function x_equilibrium = set_equilibrium(obj, V, I, P, Q)
10        x_equilibrium = [];
11        obj.z = -V/I;
12
13    end
14
15
16 end

```

Program 3.29 load_impedance.m

In these programs, `set_equilibrium` is a method that takes the voltage phase V , current phase I , active power P , and reactive power Q of the bus in the desired steady state as input and returns the steady state value of the state $x_{equilibrium}$. Theoretically, it is sufficient to provide only V and P without providing I , but I is also provided for convenience. Using the parameters obtained from the power flow calculation, a simulation similar to Example 3.15 can be described as follows.

```

1 a_bus = cell(3, 1);
2 a_bus{1} = bus_slack(2, 0);
3 a_bus{2} = bus_load(-3, 0);
4 a_bus{3} = bus_generator(0.5, 2);
5
6 a_branch = cell(2, 1);

```

```

7 a_branch{1} = branch(1, 2, 1.3652-11.6040j);
8 a_branch{2} = branch(2, 3, -10.5107j);
9
10 gen1 = generator(60*2*pi, 100, 10, 5.14, 1.569, 0.936, [], []);
11 load2 = load_impedance([]);
12 gen3 = generator(60*2*pi, 12, 10, 8.97, 1.220, 0.667, [], []);
13
14 a_component = {gen1; load2; gen3};
15
16 [V, I, P, Q] = calculate_power_flow(a_bus, a_branch);
17 Y = get_admittance_matrix(3, a_branch);
18
19 x_equilibrium = cell(numel(a_component), 1);
20 for k=1:numel(a_component)
21     x_equilibrium{k} = ...
22         a_component{k}.set_equilibrium(V(k), I(k), P(k), Q(k));
23 end
24
25 x0 = vertcat(x_equilibrium{:});
26 x0(1) = x0(1) + pi/6;
27 x0(3) = x0(3) + 0.1;
28 tspan = [0 50];
29
30 [t, x, V, I] = simulate_power_system(a_component, Y, x0, tspan);
31
32 plot(t, [x{1}(:, 2), x{3}(:, 2)])

```

Program 3.30 main_simulation_3bus_equilibrium.m

In Program 3.30, the process of defining the power system model using the classes for the bus, transmission line, generator, and load, and performing power flow calculations to obtain the time response is made clear. Users can execute numerical simulations without paying attention to the internal dynamic characteristics by simply specifying the physical constants of each equipment. In this example, it is assumed that each equipment model has the method `set_equilibrium`. This corresponds to changing the definition of equipment in terms of duck typing.

In the above examples, numerical calculations for the initial value response of the power system model were discussed. Next, we will describe the implementation method for time response calculations for ground faults.

Example 3.17 Numerical calculation of time response to ground fault In order to calculate the response to a ground fault, the voltage at the bus bar where the fault occurred should be fixed at 0 for a certain time, as described in section 3.4.3. This can be implemented as follows by modifying some constraints in line 36 of the Program 3.25.

```

1 function out = func_simulation(x, Y, a_component, bus_fault)
2
3     (Same as lines 3-34 of program 3-25)
4

```

```

5   con_network = I - Y*V;
6   con_network(bus_fault) = V(bus_fault);
7
8   (Same as lines 38 through 40 in program 3-25)
9
10 end

```

Program 3.31 func_simulation.m

In this program, an input argument has been added, and it is assumed that the number of the bus bar where the ground fault occurs is assigned to `bus_fault`. The Program 3.26 is changed to correspond to this change, resulting in Program 3.32.

```

1 function [t, x, V, I] = simulate_power_system(a_component, ...
2 Y, x0, tspan, bus_fault, tspan_fault)
3
4 if nargin < 5
5     bus_fault = [];
6 end
7
8 if nargin < 6
9     tspan_fault = [0, 0];
10 end
11
12 (Same as lines 4-15 of program 3-26)
13
14 if isempty(bus_fault)
15     [t, y] = ode15s(...%
16         @(t, x) func_simulation(t, x, Y, a_component, []),...
17         tspan, y0, options);
18 else
19     [t1, y1] = ode15s(...%
20         @(t, x) func_simulation(t, x, Y, a_component, bus_fault)%
21         ,...,%
22         tspan_fault, y0, options);
23
24     [t2, y2] = ode15s(...%
25         @(t, x) func_simulation(t, x, Y, a_component, []),...
26         [tspan_fault(2), tspan(2)], y1(end, :), options);
27
28     t = [t1; t2];
29     y = [y1; y2];
30 end
31
32 (Same as lines 21 through 34 of program 3-26)
33 end

```

Program 3.32 simulate_power_system.m

In this program, the bus bar and time interval where the ground fault occurs are added to the input arguments. However, lines 4 through 10 set default values if these values are not entered, so the program can be used without specifying a ground fault as in the Program 3.27. Such a property that allows past programs to be used in newer versions is called **backward compatibility**.

In the Program 3.32, a ground fault is specified in lines 19 to 21, and the numerical simulation after the ground fault is cleared is performed in lines 23 to 25. Note that the initial value of the state in the numerical simulation after the ground fault is cleared is the final value of the time response calculation during the ground fault. If a program that numerically simulates the time response to a ground fault is written using this program, it will be Program 3.33.

```

1 (Same as lines 1 through 23 of program 3-30)
2
3 x0 = vertcat(x_equilibrium{:});
4 tspan = [0 50];
5
6 fault_bus = 1;
7 fault_tspan = [0, 50e-3];
8
9 [t, x, V, I] = simulate_power_system(a_component, Y, x0, tspan
10     ,...
11     fault_bus, fault_tspan);
12 plot(t, [x{1}(:, 2), x{3}(:, 2)])

```

Program 3.33 main_simulation_3bus_fault.m

Execution of this program yields results equivalent to 3.6a.

Finally, the calculation of the time response to the input signal is described in the following example.

Example 3.18 Numerical computation of time response to input signals

In the examples we have dealt with so far, we consider performing numerical simulations that vary the mechanical input P_{mech} of the generator or the size of the load, as in Example 3.4.2. To do this, we need to modify the program to consider external inputs.

In order to consider external inputs, it is necessary that the number of inputs received by each device is explicitly stated in the device definitions. Therefore, we add the requirement that each device definition must have a method that returns the number of inputs.

Furthermore, we modify Program 3.28 and 3.29 to reflect external inputs in the calculation of state variable time derivatives and constraint conditions. These modifications result in Program 3.34 and Program 3.35.

```

1 classdef generator < handle
2
3 (Same as lines 3-12 of program 3-23)
4
5 methods
6
7 (Same as lines 15-57 in program 3-23)
8
9     function nu = get_nu(obj)
10        nx = 1;

```

```

11     end
12
13 function [dx, con] = get_dx_constraint(obj, x, V, I, u)
14
15 (Same as lines 33 through 36 of program 3-23)
16
17 Pmech = obj.Pmech + u;
18
19 (Same as lines 39-56 in program 3-23)
20
21 end
22
23 (Same as lines 9 through 24 of program 3-28)
24
25 end
26 end

```

Program 3.34 generator.m

```

1 classdef load_impedance < handle
2
3 (Same as lines 3-5 in program 3-24)
4
5 methods
6
7 (Same as lines 8 through 21 in Program 3-24)
8
9 function nu = get_nu(obj)
10    nu = 2;
11    end
12
13 function [dx, con] = get_dx_constraint(obj, x, V, I, u)
14    dx = [];
15    z = real(obj.z)*(1+u(1)) + 1j*imag(obj.z)*(1+u(2));
16    con = V+z*I;
17    con = [real(con); imag(con)];
18    end
19
20 (Same as lines 9 through 12 in program 3-29)
21
22 end
23
24 end

```

Program 3.35 load_impedance.m

In these programs, the method `get_nu` returns the number of inputs that can be received, and `get_dx_constraint` has been modified to appropriately handle the input `u`.

In this case, the input to the generator represents the increment of P_{mech} , while the input to the load represents the change in the real and imaginary parts of the impedance.

By using these devices, it is possible to calculate input responses. Modifying Program 3.31 and 3.32 to accommodate input responses results in Program 3.36 and 3.37.

```

1 function out = func_simulation(t, x, Y, a_component, ...
2     bus_fault, U, bus_U)
3
4     % (Same as lines 3-26 of program 3-25)
5
6     for k = 1:n_component
7
8         % (Same as lines 29-32 of program 3-25)
9
10        if ismember(k, bus_U)
11            uk = U{bus_U==k}(t);
12        else
13            uk = zeros(component.get_nu(), 1);
14        end
15
16        [dx{k}, con{k}] = component.get_dx_constraint(xk, V_k, I_k, uk)
17        ;
18    end
19
20    % (Same as lines 5-6 in program 3-31)
21
22    % (Same as lines 38 through 40 in program 3-25)
23
24 end

```

Program 3.36 func_simulation.m

```

1
2 function [t, x, V, I] = simulate_power_system(a_component, ...
3     Y, x0, tspan, bus_fault, tspan_fault, U, bus_U)
4
5     % (Same as lines 4 through 10 in program 3-32)
6
7     if nargin < 7
8         U = {};
9         bus_U = [];
10    end
11
12    % (Same as lines 4-15 of program 3-26)
13
14    if isempty(bus_fault)
15        func = @(t, x) func_simulation(t, x, Y, a_component, ...
16            [], U, bus_U);
17        [t, y] = ode15s(func, tspan, y0, options);
18    else
19        func = @(t, x) func_simulation(t, x, Y, a_component, ...
20            bus_fault, U, bus_U);
21        [t1, y1] = ode15s(func, tspan_fault, y0, options);
22    end

```

```

23 func = @(t, x) func_simulation(t, x, Y, a_component, ...
24     [], U, bus_U);
25 [t2, y2] = ode15s(func, ...
26     [tspan_fault(2), tspan(2)], y1(end, :), options);
27
28 t = [t1; t2];
29 y = [y1; y2];
30
31 (Same as lines 21 through 34 of program 3-26)
32
33 end

```

Program 3.37 simulate_power_system.m

In these programs, the input arguments `U` and `bus_U` have been added. Here, `bus_U` is assumed to be assigned the number of the bus that specifies the input signal. In addition, `U` is a cell array with the number of elements specified by the bus. Each element is a function that takes the time `t` as an argument and returns the input signal. Note that in line 11 of Program 3.36, the element corresponding to the k -th bus is selected from `U`.

An example program that uses the modified functions to perform simulations is shown in Program 3.38.

```

1 (Same as lines 1 through 25 of program 3-30)
2
3 tspan = [0 50];
4
5 bus_U = [1; 2];
6 U = {@(t) 0; @(t) [0.05*t/50; 0.05*t/50]};
7
8 [t, x, V, I] = simulate_power_system(a_component, Y, x0, ...
9     tspan, [], [], U, bus_U);
10
11 plot(t, [x{1}(:, 2), x{3}(:, 2)])

```

Program 3.38 main_simulation_3bus_input.m

In Program 3.38, input signals are defined in lines 6 and 7. In this program, the load impedance is increased by 5seconds. The input signal for bus 1 always returns 0, so it has no meaning, but it was added to demonstrate how to specify inputs. In the case of bus 3, no input is specified, so the input is automatically set to 0.

With these changes, time response calculations can be performed for external inputs. Since these changes have been made with backward compatibility in mind, by appropriately modifying Program 3.38, initial value response calculations, ground fault calculations, and time response calculations for various power systems can be performed. Furthermore, the other programs in the program group can be used without any modifications. This is the advantage of implementing the programs as a group of modules.

Mathematical Appendix

Lemma 3.3 For real constants r_i , ω_i , and ϕ_i .

$$C_n(t) := \sum_{i=1}^n r_i e^{j(\omega_i t + \phi_i)}$$

However, $r_i > 0$ and $\phi_i \in [0, 2\pi)$. In this case, the necessary and sufficient condition for C_1 to be a constant independent of t is $\omega_1 = 0$. Also, the necessary and sufficient condition for C_2 to be a constant independent of t is $\omega_1 = \omega_2 = 0$. Besides that,

$$\omega_1 = \omega_2, \quad r_1 = r_2, \quad |\phi_2 - \phi_1| = \pi$$

Furthermore, when ω_1 , ω_2 , and ω_3 are all non-zero, the necessary and sufficient condition for C_3 to be a constant independent of t is

$$\omega_1 = \omega_2 = \omega_3, \quad \sum_{i=1}^3 r_i e^{j\phi_i} = 0$$

Proof First, by setting the derivative of C_1 with respect to t to 0:

$$r_1 \omega_1 e^{j(\omega_1 t + \phi_1)} = 0$$

Therefore, the necessary and sufficient condition for C_1 to be a constant independent of t is that $\omega_1 = 0$. Next, by setting the derivative of C_2 with respect to t to 0:

$$r_1 \omega_1 e^{j(\omega_1 t + \phi_1)} + r_2 \omega_2 e^{j(\omega_2 t + \phi_2)} = 0 \quad (3.55)$$

Multiply both sides by $e^{-j(\omega_1 t + \phi_1)}$ and further differentiate by t .

$$r_2 \omega_2 (\omega_2 - \omega_1) e^{j\{((\omega_2 - \omega_1)t + \phi_2 - \phi_1)\}} = 0$$

This is equivalent to $\omega_2(\omega_2 - \omega_1) = 0$. Thus, $\omega_1 = \omega_2$ is obtained. In particular, if $\omega_1 = \omega_2 = 0$, then the equation 3.55 is satisfied for any r_1 , r_2 , ϕ_1 , ϕ_2 . Also, when ω_1 and ω_2 are non-zero:

$$r_1 e^{j\phi_1} + r_2 e^{j\phi_2} = 0$$

This is equivalent to $r_1 = r_2$ and $|\phi_2 - \phi_1| = \pi$.

Finally, consider C_3 . As before, by setting the derivative of C_2 with respect to t to 0

$$r_1 \omega_1 e^{j(\omega_1 t + \phi_1)} + r_2 \omega_2 e^{j(\omega_2 t + \phi_2)} + r_3 \omega_3 e^{j(\omega_3 t + \phi_3)} = 0 \quad (3.56)$$

Multiply both sides by $e^{-j(\omega_1 t + \phi_1)}$ and further differentiate by t .

$$r_2\omega_2(\omega_2 - \omega_1)e^{j\{(\omega_2 - \omega_1)t + \phi_2 - \phi_1\}} + r_3\omega_3(\omega_3 - \omega_1)e^{j\{(\omega_3 - \omega_1)t + \phi_3 - \phi_1\}} = 0$$

Similarly, multiplying both sides by $e^{-j\{(\omega_2 - \omega_1)t + \phi_2 - \phi_1\}}$ and further differentiating by t yields

$$r_3\omega_3(\omega_3 - \omega_1)(\omega_3 - \omega_2)e^{j\{(\omega_3 - \omega_2)t + \phi_3 - \phi_2\}} = 0$$

This is because $\omega_3 \neq 0$.

$$(\omega_3 - \omega_1)(\omega_3 - \omega_2) = 0 \quad (3.57a)$$

By a similar procedure, from Equation 3.56

$$(\omega_2 - \omega_1)(\omega_3 - \omega_2) = 0, \quad (\omega_3 - \omega_1)(\omega_2 - \omega_1) = 0 \quad (3.57b)$$

Equation 3.57 is equivalent to $\omega_1 = \omega_2 = \omega_3$. In this case, since $\omega_1, \omega_2, \omega_3$ are non-zero, the Equation 3.56 becomes:

$$\sum_{i=1}^n r_i e^{j\phi_i} = 0$$

Chapter 4

Steady-state stability analysis of power system models

In this Chapter, we conduct stability analysis based on the approximate linearization of power system models. The structure of this Chapter is as follows. First, in Section 4.1, we derive a linear approximation model for the power system model described by a system of ordinary differential equations using Kron reduction of the generator buses. Then, in Section 4.2, we explain the method for numerically analyzing the stability of the derived linear approximation model. We also confirm through numerical simulation that the stability of the linear approximation model depends not only on the physical constants of the generators, loads, and transmission lines, but also on the selection of the steady-state power flow. Additionally, in Section 4.3, we explore advanced topics and demonstrate how the stability of the linear approximation model can be analyzed using the concept of passivity in dynamic systems.

COFFEE BREAK

Derivation of the approximate linear system:

Consider the nonlinear system:

$$\dot{x}(t) = f(x(t)) + Bu(t)$$

where $f(0) = 0$. The function $f(x)$ can be expressed near the origin by a Taylor expansion as:

$$f(x) = f(0) + \frac{\partial f}{\partial x}(0)x + \text{Second or higher order term}$$

Here, $f(x)$ and x are expressed as $f_i(x)$ and x_i , respectively, and $\frac{\partial f}{\partial x}(x)$ is the *Jacobian matrix* with the (i, j) element given by $\frac{\partial f_i}{\partial x_j}(x)$. By using this Jacobian matrix, we define:

$$A := \frac{\partial f}{\partial x}(0)$$

Then, when the magnitudes of the state $x(t)$ and input $u(t)$ are sufficiently small, the behavior of the nonlinear system can be approximated by the behavior of the

linear system obtained by neglecting terms of degree 2 or higher in the function f :

$$\dot{x}^{\text{lin}}(t) = Ax^{\text{lin}}(t) + Bu^{\text{lin}}(t)$$

Note that even if $u(t)$ and $u^{\text{lin}}(t)$ are the same, the state $x(t)$ of the nonlinear system and the state $x^{\text{lin}}(t)$ of the approximate linear system may not be exactly the same.

4.1 Stability analysis based on linear approximation

4.1.1 Approximate linearization of the power system model

In this section, we derive an approximate linear model for the power system model where each bus has a generator connected, which is equivalent to the Kron-reduced differential equation system model discussed in Section 2.3.3. We derive the approximate linear model for the steady-state flow state. The differential equation system model is given by:

$$\begin{aligned}\dot{\delta}_i &= \omega_0 \Delta\omega_i \\ M_i \Delta\dot{\omega}_i &= -D_i \Delta\omega_i - f_i(\delta, E) + P_{\text{mechi}} \quad i \in \mathcal{I}_G \\ \tau_i \dot{E}_i &= -\frac{X_i}{X'_i} E_i + (X_i - X'_i) g_i(\delta, E) + V_{\text{field}i}\end{aligned}\tag{4.1}$$

However, δ and E are vectors obtained by vertically arranging δ_i and E_i , respectively. The nonlinear terms representing the interactions between generators are expressed as follows:

$$\begin{aligned}f_i(\delta, E) &:= -E_i \sum_{j=1}^N E_j (B_{ij}^{\text{red}} \sin \delta_{ij} - G_{ij}^{\text{red}} \cos \delta_{ij}), \\ g_i(\delta, E) &:= -\sum_{j=1}^N E_j (B_{ij}^{\text{red}} \cos \delta_{ij} + G_{ij}^{\text{red}} \sin \delta_{ij})\end{aligned}\tag{4.2}$$

In addition, $\delta_{ij} := \delta_i - \delta_j$ is defined. Note that, due to the properties of reduced admittance, the reduced conductance and reduced susceptance satisfy the symmetry condition:

$$G_{ij}^{\text{red}} = G_{ji}^{\text{red}}, \quad B_{ij}^{\text{red}} = B_{ji}^{\text{red}}, \quad \forall (i, j) \in \mathcal{I}_G \times \mathcal{I}_G$$

To obtain the partial derivatives of these nonlinear functions with respect to each variable, we define:

$$\begin{aligned} k_{ij}(\delta_{ij}) &:= -B_{ij}^{\text{red}} \cos \delta_{ij} - G_{ij}^{\text{red}} \sin \delta_{ij}, \\ h_{ij}(\delta_{ij}) &:= -B_{ij}^{\text{red}} \sin \delta_{ij} + G_{ij}^{\text{red}} \cos \delta_{ij} \end{aligned} \quad (4.3)$$

Then, for f_i , we obtain:

$$\begin{aligned} \frac{\partial f_i}{\partial \delta_i} &= E_i \sum_{j=1, j \neq i}^N E_j k_{ij}(\delta_{ij}), & \frac{\partial f_i}{\partial E_i} &= 2E_i h_{ii}(\delta_{ii}) + \sum_{j=1, j \neq i}^N E_j h_{ij}(\delta_{ij}), \\ \frac{\partial f_i}{\partial \delta_j} &= -E_i E_j k_{ij}(\delta_{ij}), & \frac{\partial f_i}{\partial E_j} &= E_i h_{ij}(\delta_{ij}) \end{aligned} \quad (4.4)$$

where $j \neq i$.

Similarly, we can obtain the partial derivatives of g_i as follows:

$$\begin{aligned} \frac{\partial g_i}{\partial \delta_i} &= - \sum_{j=1, j \neq i}^N E_j h_{ij}(\delta_{ij}), & \frac{\partial g_i}{\partial E_i} &= k_{ii}(\delta_{ii}), \\ \frac{\partial g_i}{\partial \delta_j} &= E_j h_{ij}(\delta_{ij}), & \frac{\partial g_i}{\partial E_j} &= k_{ij}(\delta_{ij}) \end{aligned} \quad (4.5)$$

We denote the steady-state values of the internal state of generator i as (δ_i^*, E_i^*) and the steady-state values of external inputs as $(P_{\text{mech}i}^*, V_{\text{field}i}^*)$ for the differential equation system in equation 4.1. Furthermore, we use symbols without the subscript i to represent the vector of these values for all $i \in \mathcal{I}_G$. For example, δ^* denotes the vector $(\delta_i^*)_{i \in \mathcal{I}_G}$. With these steady-state values, we can write the following system of equations:

$$\begin{aligned} 0 &= -f_i(\delta^*, E^*) + P_{\text{mech}i}^* & i \in \mathcal{I}_G \\ 0 &= -\frac{X_i}{X'_i} E_i^* + (X_i - X'_i) g_i(\delta^*, E^*) + V_{\text{field}i}^* \end{aligned} \quad (4.6)$$

Here, note that we assume the steady-state value of the frequency deviation $\Delta\omega_i$ in Eq. 4.1 is zero for all $i \in \mathcal{I}_G$. The validity of Eq. 4.6 corresponds to setting the steady-state values of the external input $(P_{\text{mech}}^*, V_{\text{field}}^*)$ to appropriate values that achieve supply-demand balance. By linearizing the system around this steady state, the approximate linear model is obtained as:

$$\begin{bmatrix} \dot{\delta}^{\text{lin}} \\ M\Delta\dot{\omega}^{\text{lin}} \\ \tau\dot{E}^{\text{lin}} \end{bmatrix} = \begin{bmatrix} 0 & \omega_0 I & 0 \\ -L & -D & -C \\ B & 0 & A \end{bmatrix} \begin{bmatrix} \delta^{\text{lin}} \\ \Delta\omega^{\text{lin}} \\ E^{\text{lin}} \end{bmatrix} + \begin{bmatrix} 0 & 0 \\ I & 0 \\ 0 & I \end{bmatrix} \begin{bmatrix} P_{\text{mech}}^{\text{lin}} \\ V_{\text{field}}^{\text{lin}} \end{bmatrix} \quad (4.7)$$

Note that the state and input variables with the subscript "lin" are vectors consisting of small deviations from the corresponding variables with their steady-state values as the reference. Also,

$$M := \text{diag}(M_i)_{i \in \mathcal{I}_G}, \quad D := \text{diag}(D_i)_{i \in \mathcal{I}_G}, \quad \tau := \text{diag}(\tau_i)_{i \in \mathcal{I}_G}$$

are diagonal matrices where $\text{diag}(\cdot)$ is an operator that creates a diagonal matrix from a vector.

Furthermore, for the functions k_{ij} and h_{ij} defined in Equation 4.3, the (i, j) element of the matrices \hat{L} , \hat{A} , \hat{B} , and \hat{C} , defined as:

$$\begin{aligned}\hat{L}_{ij} &:= \begin{cases} E_i^* \sum_{j=1, j \neq i}^N E_j^* k_{ij}(\delta_{ij}^*), & i = j \\ -E_i^* E_j^* k_{ij}(\delta_{ij}^*), & i \neq j \end{cases} \\ \hat{A}_{ij} &:= \begin{cases} k_{ii}(\delta_{ii}^*) - \frac{X_i}{X'_i(X_i - X'_i)}, & i = j \\ k_{ij}(\delta_{ij}^*), & i \neq j \end{cases} \\ \hat{B}_{ij} &:= \begin{cases} -\sum_{j=1, j \neq i}^N E_j^* h_{ij}(\delta_{ij}^*), & i = j \\ E_j^* h_{ij}(\delta_{ij}^*), & i \neq j \end{cases} \\ \hat{C}_{ij} &:= \begin{cases} \sum_{j=1, j \neq i}^N E_j^* h_{ij}(\delta_{ij}^*), & i = j \\ E_i^* h_{ij}(\delta_{ij}^*), & i \neq j \end{cases}\end{aligned}$$

The matrices L , A , B , and C are then defined as follows:

$$\begin{aligned}L &:= \hat{L}, \\ A &:= \text{diag}(X_i - X'_i)_{i \in \mathcal{I}_G} \hat{A}, \\ B &:= \text{diag}(X_i - X'_i)_{i \in \mathcal{I}_G} \hat{B}, \\ C &:= \text{diag}(2E_i^* h_{ii}(\delta_{ii}^*))_{i \in \mathcal{I}_G} + \hat{C}\end{aligned}\tag{4.8}$$

Note that $\delta_{ij}^* := \delta_i^* - \delta_j^*$. It should be noted that the system matrix (L, A, B, C) is a function of the steady-state values (δ^*, E^*) . The block diagram of this approximate linear model is shown in Figure 4.1. Here, P^{lin} represents the approximately linearized active power supplied by the generators. Note that generally $X_i > X'_i$ for all i .

In power system engineering, the value obtained by differentiating the generator's active power with respect to the rotor angle at the steady-state is called the **synchro-nizing power coefficient** [?, Section 8.4]. That is, the matrix L in the approximate linear model given by equation 4.7 corresponds to the synchronizing power coefficient. However, in power system engineering, it is common to define the synchronizing power coefficient using the one-machine infinite-bus system model explained in Section 2.3.5, so it is a scalar value rather than a matrix.

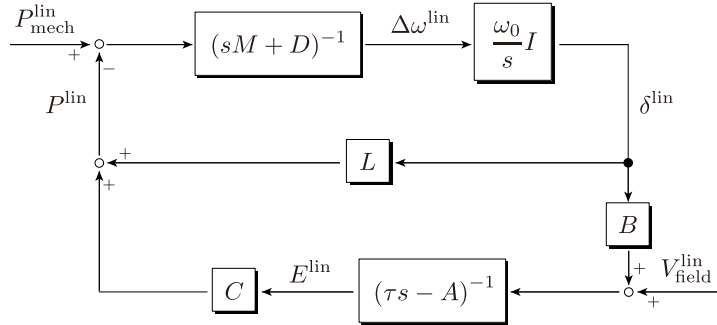


Fig. 4.1 Block Diagram of Approximate Linear Model

4.1.2 Stability analysis of approximate linear models

4.1.2.1 Stability of approximate linear models

In this section, we consider numerically analyzing the stability of the approximate linear model. Whether the approximate linear model of Equation 4.7 is stable or not is characterized by whether the internal states of the generator groups return to the steady state satisfying the simultaneous equations of Equation 4.6 in the event of a small disturbance in the power system, such as temporary minor fluctuations in mechanical input or excitation input of the generators, impedance values of the loads, current or voltage values of the transmission lines, etc., from the reference values at the steady state. In power system engineering, stability against such small fluctuations is called **small signal stability**.

It should be noted that the stability of the approximate linear model of Equation 4.7 depends on the selection of the steady-state values of the internal states of the generator groups (δ^* , E^*) and the steady-state values of external inputs (P_{mech}^* , V_{field}^*). Furthermore, changes in the admittance of the transmission lines or the impedance of the loads alter the reduced conductance G^{red}_{ij} and reduced susceptance B^{red}_{ij} of Equation 4.3. Therefore, the stability of the approximate linear model varies depending on various model parameters mentioned above. The purpose of this section is to numerically examine the relationship between the changes in these model parameters and the stability of the approximate linear model.

4.1.2.2 Stability analysis based on eigenvalues of the system matrix

For the approximate linear model in Equation 4.7, if we appropriately choose the steady-state values (δ^* , E^*) of the internal states as parameters, then the system matrix (L , A , B , C) in Equation 4.8 and the steady-state values (P_{mech}^* , V_{field}^*) of the ex-

ternal inputs satisfying Equation 4.6 are determined dependently. Here, we consider setting

$$P_{\text{mech}i}(t) = P_{\text{mech}i}^*, \quad V_{\text{field}i}(t) = V_{\text{field}i}^*, \quad \forall t \geq 0$$

for all $i \in \mathcal{I}G$ in the nonlinear differential equation system model in Equation 2.29. We then assess the stability of the system using the eigenvalues of the system matrix.

This means that in the approximate linear model of Equation 4.7 the following values are set:

$$P_{\text{mech}}^{\text{lin}}(t) = 0, \quad V_{\text{field}}^{\text{lin}}(t) = 0, \quad \forall t \geq 0$$

In the following, under this assumption, we analyze the stability of an autonomous approximate linear model with input set identically to zero, given by:

$$\begin{bmatrix} \dot{\delta}^{\text{lin}} \\ \Delta\dot{\omega}^{\text{lin}} \\ \dot{E}^{\text{lin}} \end{bmatrix} = \underbrace{\begin{bmatrix} 0 & \omega_0 I & 0 \\ -M^{-1}L & -M^{-1}D & -M^{-1}C \\ \tau^{-1}B & 0 & \tau^{-1}A \end{bmatrix}}_{\Psi} \begin{bmatrix} \delta^{\text{lin}} \\ \Delta\omega^{\text{lin}} \\ E^{\text{lin}} \end{bmatrix} \quad (4.9)$$

Specifically, by examining the sign of the real part of the eigenvalues of the matrix Ψ , we can determine the stability of this approximate linear model. However, it should be noted that Ψ generally has at least one zero eigenvalue. In fact, from the structure of the matrices L and B in equation 4.8, we have:

$$L\mathbb{1} = 0, \quad B\mathbb{1} = 0 \quad (4.10)$$

Therefore, for any model parameters, we have:

$$\Psi v = 0, \quad v := \begin{bmatrix} 1 \\ 0 \\ 0 \end{bmatrix}$$

This means that v is an eigenvector of Ψ corresponding to a zero eigenvalue. If the real parts of all eigenvalues, except for the zero eigenvalue, are negative, then for any initial value, the solution trajectory of Equation 4.9 satisfies:

$$\lim_{t \rightarrow \infty} \delta^{\text{lin}}(t) = c_0 \mathbb{1}, \quad \lim_{t \rightarrow \infty} \Delta\omega^{\text{lin}}(t) = 0, \quad \lim_{t \rightarrow \infty} E^{\text{lin}}(t) = 0 \quad (4.11)$$

Here, c_0 is a constant determined by the initial value. Note that the value of c_0 does not make a significant difference in the analytical results. This is because in the differential equation system model of Equation 4.1, the rotor angle δ_i of a generator has meaning only in relation to the difference between the rotor angle δ_j of other generators. Specifically, if (δ^*, E^*) satisfies the system of equations in equation 4.6 for a certain $(P_{\text{mech}}^*, V_{\text{field}}^*)$, then $(\delta^* + c_0 \mathbb{1}, E^*)$ also satisfies the same system of equations. Therefore, δ^* and $\delta^* + c_0 \mathbb{1}$ are essentially equivalent steady-state values

where all generator rotor angles are rotated by the same amount of c_0 . Equation 4.11 means the asymptotic convergence of solution trajectories to these essentially equivalent steady-state values.

4.2 stability analysis of approximate linear models using numerical calculations

4.2.1 Implementation of approximate linearization using a group of partitioned modules

In this section, we explain the implementation method for obtaining an approximate linear model numerically. Specifically, we describe how to add the functionality of linearization to the program that has been segmented into module groups as explained in Sections 3.6 and 3.7.

In the numerical simulation program of the power system created in Section 3.7, the following state and output equations are implemented for each device as differential and algebraic equations, respectively:

$$\dot{x}_i = f_i^{(1)}(x_i, \mathbf{V}_i, \mathbf{I}_i, u_i), \quad 0 = f_i^{(2)}(x_i, \mathbf{V}_i, \mathbf{I}_i, u_i)$$

In the following, we derive the approximate linear model in the vicinity of the equilibrium point $(x_i^*, \mathbf{V}_i^*, \mathbf{I}_i^*, u_i^*)$ for the device of interest. Specifically, we explain the implementation method of the linear approximation function to the program that has been partitioned into the module group described in Sections 3.6 and 3.7.

For the numerical simulation program of the power system created in Section 3.7, differential equations for the state and algebraic equations for the output are implemented for each device as:

$$\dot{x}_i = f_i^{(1)}(x_i, \mathbf{V}_i, \mathbf{I}_i, u_i), \quad 0 = f_i^{(2)}(x_i, \mathbf{V}_i, \mathbf{I}_i, u_i)$$

We consider the linearization of the functions $f_i^{(1)}$ and $f_i^{(2)}$ as follows:

$$\begin{aligned} f_i^{(1)}(x_i, \mathbf{V}_i, \mathbf{I}_i, u_i) &\approx A_i(x_i - x_i^*) + B_{u_i} u_i \\ &+ B_{\mathbf{V}_i} \begin{bmatrix} \operatorname{Re}[\mathbf{V}_i - \mathbf{V}_i^*] \\ i[\mathbf{V}_i - \mathbf{V}_i^*] \end{bmatrix} + B_{\mathbf{I}_i} \begin{bmatrix} \operatorname{Re}[\mathbf{I}_i - \mathbf{I}_i^*] \\ i[\mathbf{I}_i - \mathbf{I}_i^*] \end{bmatrix} \end{aligned} \quad (4.12)$$

$$\begin{aligned} f_i^{(2)}(x_i, \mathbf{V}_i, \mathbf{I}_i, u_i) &\approx C_i(x_i - x_i^*) + D_{u_i} u_i \\ &+ D_{\mathbf{V}_i} \begin{bmatrix} \operatorname{Re}[\mathbf{V}_i - \mathbf{V}_i^*] \\ i[\mathbf{V}_i - \mathbf{V}_i^*] \end{bmatrix} + D_{\mathbf{I}_i} \begin{bmatrix} \operatorname{Re}[\mathbf{I}_i - \mathbf{I}_i^*] \\ i[\mathbf{I}_i - \mathbf{I}_i^*] \end{bmatrix} \end{aligned} \quad (4.13)$$

A system of simultaneous equations for each machine and algebraic equations for the entire power system can be used to obtain an expression using ordinary differ-

ential equations for the approximate linear model by eliminating all $\mathbf{V}_i - \mathbf{V}_i^*$ and $\mathbf{I}_i - \mathbf{I}_i^*$, where $i \in 1, \dots, N$, as follows:

$$\mathbf{I}_i - \mathbf{I}_i^* = \sum_{j=1}^N Y_{ij}(\mathbf{V}_j - \mathbf{V}_j^*), \quad i \in \{1, \dots, N\}$$

Here, Y_{ij} represents the (i, j) th element of the admittance matrix \mathbf{Y} . Let us check the specific implementation method with the following example.

Example 4.1 (Implementation of Approximate Linear Model)

Equations 4.12 and 4.13 depend on the dynamic characteristics of the device, so it is natural to implement the calculation of coefficient matrices such as A_i and B_{u_i} in the classes of devices such as generators and loads in the implementation example of Section 3.6. For example, in the generator model:

$$A_i = \begin{bmatrix} 0 & \omega_0 & 0 \\ 0 & -\frac{D_i}{M_i} & 0 \\ -\frac{1}{\tau_i} \left(\frac{X_i}{X'_i} - 1 \right) |\mathbf{V}_i^*| \sin(\delta_i^* - \angle \mathbf{V}_i^*) & 0 & -\frac{X_i}{\tau_i X'_i} \end{bmatrix}$$

$$B_{u_i} = \begin{bmatrix} 0 \\ \frac{1}{M_i} \\ 0 \end{bmatrix}, \quad B_{\mathbf{V}_i} = \begin{bmatrix} 0 & 0 \\ -\frac{\text{Re}[I_i^*]}{M_i} & -\frac{i[I_i^*]}{M_i} \\ \frac{1}{\tau_i} \left(\frac{X_i}{X'_i} - 1 \right) \cos \delta_i^* & \frac{1}{\tau_i} \left(\frac{X_i}{X'_i} - 1 \right) \sin \delta_i^* \end{bmatrix}$$

$$B_{\mathbf{I}_i} = \begin{bmatrix} 0 & 0 \\ -\frac{\text{Re}[V_i^*]}{M_i} & -\frac{i[V_i^*]}{M_i} \\ 0 & 0 \end{bmatrix}, \quad C_i = \begin{bmatrix} E_i^* \cos \delta_i^* & 0 & \sin(\delta_i^*) \\ E_i^* \sin \delta_i^* & 0 & -\cos(\delta_i^*) \end{bmatrix}$$

$$D_{u_i} = \begin{bmatrix} 0 \\ 0 \end{bmatrix}, \quad D_{\mathbf{V}_i} = \begin{bmatrix} 0 & -1 \\ 1 & 0 \end{bmatrix}, \quad D_{\mathbf{I}_i} = \begin{bmatrix} -X'_i & 0 \\ 0 & -X'_i \end{bmatrix}$$

If the calculation of these coefficient matrices is added to the generator class as a method named `get_linear_matrix`, the program 4.1 is obtained.

```

1 classdef generator < handle
2
3 properties
4 (Same as lines 4-11 in program 3-23)
5   x_equilibrium
6   V_equilibrium
7   I_equilibrium
8 end
9
10 methods

```

```

11
12 (Same as lines 7 through 21 in program 3-34)
13
14     function x_equilibrium = set_equilibrium(obj, V, I, P, Q)
15
16 (Same as lines 10 through 23 of program 3-28)
17
18     obj.x_equilibrium = x_equilibrium;
19     obj.V_equilibrium = V;
20     obj.I_equilibrium = I;
21     end
22
23     function [A, Bu, BV, BI, C, Du, DV, DI] =...
24         get_linear_matrix(obj)
25
26     X = obj.X;
27     X_prime = obj.X_prime;
28     D = obj.D;
29     M = obj.M;
30     tau = obj.tau;
31
32     omega0 = obj.omega0;
33     delta = obj.x_equilibrium(1);
34     E = obj.x_equilibrium(3);
35     V = obj.V_equilibrium;
36     Vabs = abs(obj.V_equilibrium);
37     Vangle = angle(obj.V_equilibrium);
38     I = obj.I_equilibrium;
39     A = [0, omega0, 0;
40           0, -D/M, 0;
41           -(X/X_prime-1)*Vabs*sin(delta-Vangle)/tau, ...
42           0, -X/X_prime/tau];
43     Bu = [0; 1/M; 0];
44     BV = [0, 0;
45           -real(I)/M, -imag(I)/M;
46           (X/X_prime-1)*cos(delta)/tau, ...
47           (X/X_prime-1)*sin(delta)/tau];
48     BI = [0, 0;
49           -real(V)/M, -imag(V)/M;
50           0, 0];
51     C = [E*cos(delta), 0, sin(delta);
52           E*sin(delta), 0, -cos(delta)];
53     Du = [0; 0];
54     DV = [0, -1; 1, 0];
55     DI = -X_prime*eye(2);
56     end
57
58 end
59
60 end

```

Program 4.1 generator.m

In Program 4.1, lines 18 to 20 in `set_equilibrium` store information about the equilibrium point used in the calculation of the approximate linear model.

If implemented similarly for the constant impedance load model, the program 4.2 is obtained.

```

1 classdef load_impedance < handle
2
3 properties
4     z
5     I_equilibrium
6 end
7
8 methods
9
10 (Same as lines 7 through 18 in program 3-35)
11
12     function x_equilibrium = set_equilibrium(obj, V, I, P, Q)
13         x_equilibrium = [];
14         obj.z = -V/I;
15         obj.I_equilibrium = I;
16     end
17
18     function [A, Bu, BV, BI, C, Du, DV, DI] =...
19         get_linear_matrix(obj)
20
21         A = [];
22         Bu = zeros(0, 2);
23         BV = zeros(0, 2);
24         BI = zeros(0, 2);
25         C = zeros(2, 0);
26         I = obj.I_equilibrium;
27         z = obj.z;
28         Du = [real(z)*real(I), imag(z)*imag(I);
29               real(z)*imag(I), imag(z)*real(I)];
30         DV = eye(2);
31         DI = [real(z), -imag(z); imag(z), real(z)];
32     end
33
34 end
35
36 end

```

Program 4.2 load_impedance.m

By using the class of equipment such as modified generators and loads, the function for obtaining an approximate linear model can be described as shown in Program 4.3.

```

1 function sys = get_linear_model(a_component, Y)
2
3     A = cell(numel(a_component), 1);
4     Bu = cell(numel(a_component), 1);
5     BV = cell(numel(a_component), 1);
6     BI = cell(numel(a_component), 1);

```

```

7   C = cell(numel(a_component), 1);
8   Du = cell(numel(a_component), 1);
9   DV = cell(numel(a_component), 1);
10  DI = cell(numel(a_component), 1);
11
12  for k = 1:numel(a_component)
13    component = a_component{k};
14    [A{k}, Bu{k}, BV{k}, BI{k}, C{k}, Du{k}, DV{k}, DI{k}] =...
15    component.get_linear_matrix();
16  end
17
18  A = blkdiag(A{:});
19  Bu = blkdiag(Bu{:});
20  BV = blkdiag(BV{:});
21  BI = blkdiag(BI{:});
22  C = blkdiag(C{:});
23  Du = blkdiag(Du{:});
24  DV = blkdiag(DV{:});
25  DI = blkdiag(DI{:});
26
27  Ymat = zeros(size(Y, 1)*2, size(Y, 2)*2);
28  Ymat(1:2:end, 1:2:end) = real(Y);
29  Ymat(2:2:end, 1:2:end) = imag(Y);
30  Ymat(1:2:end, 2:2:end) = -imag(Y);
31  Ymat(2:2:end, 2:2:end) = real(Y);
32
33  nx = size(A, 1);
34
35  A11 = A;
36  A12 = [BV, BI];
37  A21 = [C; zeros(size(Ymat, 1), nx)];
38  A22 = [DV, DI; Ymat, -eye(size(Ymat))];
39
40  B1 = Bu;
41  B2 = [Du; zeros(size(Ymat, 1), size(Du, 2))];
42
43
44  Aout = A11 - A12/A22*A21;
45  Bout = B1 - A12/A22*B2;
46  Cout = eye(nx);
47  Dout = 0;
48
49  sys = ss(Aout, Bout, Cout, Dout);
50
51 end

```

Program 4.3 get_linear_model.m

In lines 12 to 16 of Program 4.3, the coefficient matrix of the approximate linear model is obtained from each equipment. Additionally, by eliminating the voltage and current phases of all buses from lines 27 to 47, an expression for the approximate linear model's system of ordinary differential equations is obtained.

The approximate linear model can be used as follows by using Program 4.3.

```

1 (Same as lines 1 through 23 in Program 3-30)
2
3 sys = get_linear_model(a_component, Y);
4
5 sys = sys(2, 1);
6 nyquist(sys)

```

Program 4.4 main_linearization.m

In this example, an approximate linear model is constructed in line 5 with the mechanical input $P_{\text{mech}1}$ of generator 1 as input and the frequency deviation $\Delta\omega_1$ of generator 1 as output. In addition, a Nyquist plot is drawn in line 6.

In the mathematical analysis of Section 4.1.1, an approximate linear model is derived from a nonlinear system of ordinary differential equations where all buses are Kron reduced. On the other hand, in the numerical implementation of this section, the nonlinear differential-algebraic equation system is first linearized, and then Kron reduction is applied to construct the ordinary differential equation system. It should be noted that this is because in the power system model with Kron reduction, expressions generally involve a mixture of information about equipment, buses, and transmission lines.

To increase the readability and expandability of the program, it is important to modularize each element appropriately, as in the implementation of this section.

4.2.2 Numerical analysis of small signal stability

Let us perform a stability analysis based on approximate linearization for an actual electrical power system model consisting of three generators.

Example 4.2 Numerical stability analysis of the linearized model Let us consider an electrical power system model consisting of three generators discussed in the Example 2.3. The constant of the generators and transmission lines are set to the same value as in the Example 2.3, and a linear approximation model for Equation 4.9 is derived with the approximate of the steady value shown in 2.2. Figure 4.2 shows the time response When the initial values are set as follows to correspond to Equation 2.32:

$$\delta^{\text{lin}}(0) = \begin{bmatrix} \frac{\pi}{6} \\ 0 \\ 0 \end{bmatrix}, \quad \Delta\omega^{\text{lin}}(0) = \begin{bmatrix} 0 \\ 0 \\ 0 \end{bmatrix}, \quad E^{\text{lin}}(0) = \begin{bmatrix} 0.1 \\ 0 \\ 0 \end{bmatrix} \quad (4.14)$$

The blue, black, and red lines represent generators 1, 2, and 3, respectively. From this figure, we can see that the internal state of the generator group converges asymptotically as given in (4.11). Moreover, it approximately reproduces the initial value response of the nonlinear model shown in Fig. 2.10.

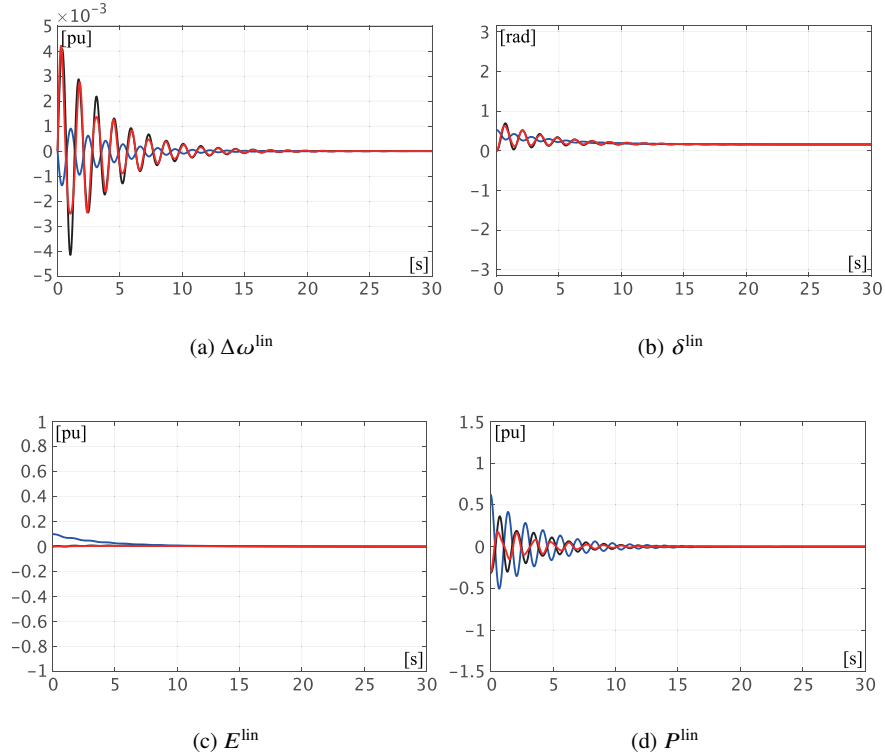


Fig. 4.2 Initial value response of approximate linear model
 (Blue: Generator 1, Black: Generator 2, Red: Generator 3)

Next, we parameterize the constants and steady-state values of the generators and transmission lines to analyze the stability of the resulting approximate linear model. For the generator constants, we compare the cases where all the damping coefficients are set to 10 and where they are set to 0.1, i.e., we consider the two cases:

$$(D_1, D_2, D_3) = (10, 10, 10), \quad (D_1, D_2, D_3) = (0.1, 0.1, 0.1)$$

Other constants are set to the values in Table 2.1. In addition, the steady-state values of the rotor angle differences are expressed in terms of a parameter $\theta_1 \in [0, 1]$ as follows:

$$\delta_{12}^* = -\frac{\pi}{2}\theta_1, \quad \delta_{13}^* = \frac{\pi}{2}\theta_1 \quad (4.15)$$

Here, θ_1 is a parameter that specifies the magnitude of the rotor angle difference in the steady-state. By varying this value, the system matrix in 4.8 changes. Note

that the steady-state values of the internal voltages are not changed from the values in Table 2.2.

The admittance matrix is also modified as follows. Using the admittance values y_{12} and y_{23} in Equation 2.31, the admittance matrix of the power system in Equation 2.10 is constructed. The real part of this admittance matrix, which is the conductance matrix, is denoted as G_0 , and the imaginary part, which is the susceptance matrix, is denoted as B_0 . Specifically,

$$\begin{aligned} G_0 &= \begin{bmatrix} 1.3652 & -1.3652 & 0 \\ -1.3652 & 3.3074 & -1.9422 \\ 0 & -1.9422 & 1.9422 \end{bmatrix}, \\ B_0 &= \begin{bmatrix} -11.6041 & 11.6041 & 0 \\ 11.6041 & -22.1148 & 10.5107 \\ 0 & 10.5107 & -10.5107 \end{bmatrix} \end{aligned} \quad (4.16)$$

Using the parameter $\theta_2 \in [0, 5]$, we express the reference admittance matrix as follows:

$$\mathbf{Y}_0(\theta_2) := \theta_2 G_0 + j B_0 \quad (4.17)$$

Here, θ_2 is a parameter that specifies the size of the real part (conductance matrix). For comparison, we consider two parameterized admittance matrices:

$$\mathbf{Y} = \mathbf{Y}_0(\theta_2), \quad \mathbf{Y} = \frac{\mathbf{Y}_0(\theta_2)}{100}$$

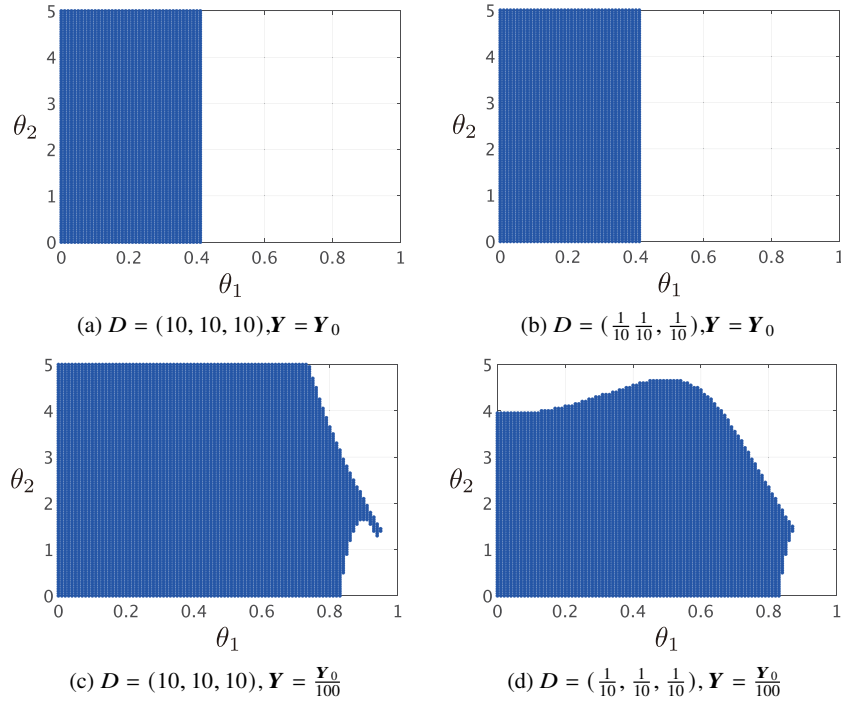
The changes in the admittance matrix are approximately represented in the linearized model by the changes in the values of the reduced conductor B^{red}_{ij} and the reduced susceptance G^{red}_{ij} in equation 4.3. The parameter settings for the comparison are summarized in Table 4.1.

Let us numerically analyze the stability of the approximate linear model by varying the parameters (θ_1, θ_2) for each case (a)-(d) in Table 4.1. Specifically, we will check whether the approximate linear model is stable or not by examining the eigenvalues of Ψ in Equation 4.9 by varying θ_1 and θ_2 on a grid of 100 equidistant points each. The results are shown in Figure 4.3. The blue area represents the parameter region where the approximate linear model is stable. First, in the case of (a), we see that the approximate linear model is stable regardless of the size of the conductance matrix specified by θ_2 , as long as θ_1 is below approximately 0.4, which corresponds to a rotor angle difference of approximately 36° in the steady state. The same result is obtained for case (b), where the generator's damping coefficient is small at 0.1.

Next, we examine the results for cases (c) and (d), where the admittance matrix is multiplied by $\frac{1}{100}$. In this case, we find that when θ_2 is small and the size of the conductance matrix is around 1, the approximate linear model is stable as long as the rotor angle difference in the steady state is below approximately 76° . We also find that as θ_2 increases to 2 or more, the upper limit of the rotor angle difference for stability of the approximate linear model decreases.

Table 4.1 Parameter settings to compare

	$D = (10, 10, 10)$	$D = (0.1, 0.1, 0.1)$
$\mathbf{Y} = \mathbf{Y}_0$	(a)	(b)
$\mathbf{Y} = \mathbf{Y}_0/100$	(c)	(d)

**Fig. 4.3 Area of parameters where the approximate linear model is stable**

4.3 Mathematical stability analysis of the linearized model[‡]

4.3.1 Small signal stability of the linearized model

In this section, we mathematically analyze the stability of the linearized model given in Equation 4.9. The stability is characterized by the eigenvalues of the matrix Ψ . However, as discussed in section 4.2, Ψ is not regular and the eigenspace for the zero eigenvalue is given by

$$\mathcal{M} = \text{span} \left\{ \begin{bmatrix} 1 \\ 0 \\ 0 \end{bmatrix} \right\} \quad (4.18)$$

This eigenspace represents the set of equivalent steady-state values obtained by varying the phase angles of all generators while maintaining their relative values constant. Therefore, it is not a problem which point in the equilibrium set of Equation 4.18 the state of the approximate linear model converges to. Based on this fact, we give the following definition:

COFFEE BREAK

Eigenspace of a square matrix: For a square matrix A and a given eigenvalue λ , the *eigenspace* \mathcal{V}_λ is defined as:

$$\mathcal{V}_\lambda := \ker(\lambda I - A)$$

where \ker denotes the kernel of the matrix. If v_1, \dots, v_k are all linearly independent eigenvectors corresponding to a specific eigenvalue λ , then:

$$\mathcal{V}_\lambda = \text{span}\{v_1, \dots, v_k\}$$

which means that it is a linear space spanned by the eigenvectors associated with a specific eigenvalue.

Definition 4.1 (Small-signal stability of the linear approximation model)

Consider the linearized model given by Equation 4.9. For any initial values, if the internal state converges to one of the equilibrium points in the set \mathcal{M} defined by Equation 4.18, the linearized model is said to be **steady-state stable**.

The small-signal stability in Definition 4.1 means that for any initial condition, Equation 4.11 holds. Note that the value of c_0 in Equation 4.11 is arbitrary, so we express its arbitrariness as "converging to one of the equilibrium points in \mathcal{M} ."

In power system engineering, the term "small-signal stability" is widely used to discuss the stability of a power system against small disturbances using an approximate linear model. However, introducing a mathematical definition like Definition 4.1 is not common practice.

In the following discussion, we assume that the kernel space of Ψ in Equation 4.9 is one-dimensional and that Equation 4.19 holds:

$$\ker \Psi = \mathcal{M} \tag{4.19}$$

It is clear from the structure of the matrix Ψ that \mathcal{M} is a subset of $\ker \Psi$, but it should be noted that we are assuming that $\ker \Psi$ is one-dimensional and that the equality holds. If the kernel space were two-dimensional or greater, the invariant eigenspace would be larger than \mathcal{M} , and the approximate linear model would not be in a steady state stability. Therefore, equation 4.19 is a necessary condition for the steady-state stability of the linear approximation model. In particular, when A is invertible, and using the definition of $L_0 := L - CA^{-1}B$, the necessary condition can be equivalently expressed as:

$$\ker L_0 = \text{span}\{\mathbf{1}\} \tag{4.20}$$

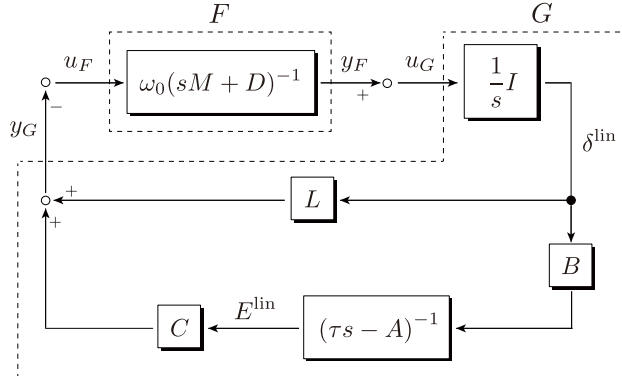


Fig. 4.4 Feedback system representation of approximate linear models

Note that this matrix L_0 plays an important role in the subsequent analysis.

The relationship between equation ?? and equation 4.20 can be verified as follows. Because the $(1, 2)$ block of the matrix Ψ is invertible, the necessary and sufficient condition for the kernel of Ψ to be equal to \mathcal{M} is:

$$\ker \begin{bmatrix} -L & -C \\ B & A \end{bmatrix} = \text{span} \left\{ \begin{bmatrix} 1 \\ 0 \end{bmatrix} \right\}$$

In particular, when A is invertible, we have

$$\begin{bmatrix} -L & -C \\ B & A \end{bmatrix} \begin{bmatrix} x \\ y \end{bmatrix} = 0 \iff L_0 x = 0, \quad y = -A^{-1} B x$$

Thus, the necessary condition is equivalent to equation 4.20.

For the following discussion, we introduce the following fundamental terminology.

Definition 4.2 (Stability of square matrix) For a square matrix A , if all the real parts of its eigenvalues are negative, A is called **stable** or **asymptotically stable**.

4.3.2 Passivity of approximate linear models

4.3.2.1 Representation of Approximate Linear Models with Feedback

Let us consider describing the approximate linear model of Equation 4.9 as a feedback system of two subsystems (Figure 4.4). The first subsystem is described as a system of differential equations for the deviation of the angular frequency:

$$F : \begin{cases} M\Delta\dot{\omega}^{\text{lin}} = -D\Delta\omega^{\text{lin}} + u_F \\ y_F = \omega_0\Delta\omega^{\text{lin}} \end{cases} \quad (4.21)$$

In this book, we refer to this subsystem as the **mechanical subsystem**. The mechanical subsystem is determined solely by the physical constants of the generator set $(M_i, D_i)_{i \in \mathcal{I}G}$ and the reference angular frequency ω_0 , and does not depend on the steady-state values of the internal state (δ^*, E^*) .

The second subsystem is described as a system of differential equations with respect to the rotor angle and internal voltage as follows:

$$G : \begin{cases} \dot{\delta}^{\text{lin}} = u_G \\ \tau\dot{E}^{\text{lin}} = AE^{\text{lin}} + B\delta^{\text{lin}} \\ y_G = CE^{\text{lin}} + L\delta^{\text{lin}} \end{cases} \quad (4.22)$$

We call this subsystem the **electrical subsystem**⁴. The electrical subsystem not only depends on the physical constants of the generator group, $(\tau_i)_{i \in \mathcal{I}G}$, but also on the steady-state values of the internal states, (δ^*, E^*) . In fact, the system matrix (L, A, B, C) in equation 4.8 is a function of (δ^*, E^*) .

If the two subsystems' inputs and outputs are coupled through negative feedback as follows:

$$u_F = -y_G, \quad u_G = y_F \quad (4.23)$$

the approximate linear model of Equation 4.9 is represented. The subsequent analysis of steady-state stability is based on the property called the *passivity* of the mechanical and electrical subsystems. It is well-known that a negative feedback system of a passive subsystem is stable.

4.3.2.2 Passivity of the mechanical subsystem

The mechanical subsystem F in Equation 4.21 has the following strong passivity:

Definition 4.3 (Passivity of linear systems)

Consider the linear system

$$\Sigma : \begin{cases} \dot{x} = Ax + Bu \\ y = Cx \end{cases} \quad (4.24)$$

Using the symmetric matrix P , define the function:

$$W(x) := \frac{1}{2}x^T Px \quad (4.25)$$

⁴ The terms "mechanical subsystem" and "electrical subsystem" introduced here are unique to this book.

For any u , if there exists a semi-positive definite matrix P that satisfies:

$$\frac{d}{dt}W(x(t)) \leq u^T(t)y(t), \quad \forall t \geq 0 \quad (4.26)$$

Then, we call Σ **passive**.

In particular, when there exists a positive definite number ρ such that in addition to the semi-positive definite matrix, the inequality:

$$\frac{d}{dt}W(x(t)) \leq u^T(t)y(t) - \rho \|y(t)\|^2, \quad \forall t \geq 0 \quad (4.27)$$

is satisfied, then we call Σ **strictly passive**.

The function $W(x)$ in Definition 4.3 is generally called the **storage function**. Moreover, the inequality in Equation 4.27 describes a type of passivity that is more strictly called **output-strict passivity**, where the energy represented by the storage function $W(x)$ dissipates more quickly in proportion to the square of the output compared to the passivity in Equation 4.26.

The mechanical subsystem F of Equation 4.21 having strong passivity can be confirmed as follows. First, the subsystem is written as below:

$$F : \begin{cases} \dot{x}_F = A_F x_F + B_F u_F \\ y_F = C_F x_F \end{cases} \quad (4.28)$$

where state x_F represents $\Delta\omega^{\text{lin}}$, and the system matrices are:

$$A_F := -M^{-1}D, \quad B_F := M^{-1}, \quad C_F := \omega_0 I$$

Additionally, we define the symmetric matrix P_F as:

$$P_F := \omega_0 M$$

and since M is positive definite, P_F is also positive definite. Then, the following inequalities hold:

$$A_F^T P_F + P_F A_F \leq -\frac{2 \min\{D_i\}}{\omega_0} C_F^T C_F, \quad P_F B_F = C_F^T$$

Therefore, when the storage function is defined as:

$$W_F(x_F) := \frac{1}{2} x_F^T P_F x_F \quad (4.29)$$

the time derivative along the solution trajectory of F is evaluated as:

$$\begin{aligned}
\frac{d}{dt} W_F(x_F(t)) &= \nabla W_F^\top(x_F) \frac{dx_F}{dt} \\
&= (P_F x_F(t))^\top (A_F x_F(t) + B_F u_F(t)) \\
&= y_F^\top(t) u_F(t) + \frac{1}{2} x_F^\top(t) (A_F^\top P_F + P_F A_F) x_F(t) \\
&\leq y_F^\top(t) u_F(t) - \frac{\min\{D_i\}}{\omega_0} \|y_F(t)\|^2
\end{aligned} \tag{4.30}$$

where $\nabla W_F(x_F)$ is the gradient function obtained by partially differentiating $W_F(x_F)$ with respect to its elements and arranging them vertically. From this, it can be seen that the machine subsystem F in Equation 4.21 is strongly passive for any positive definite $(M_i, D_i)_{i \in \mathcal{I}_G}$. Note that the function $W_F(x_F)$ represents the mechanical kinetic energy of the power system.

4.3.2.3 Passivity of the electrical subsystem

Next, we consider the electrical subsystem G in Equation 4.22. Unlike the mechanical subsystem F , the electrical subsystem G only possesses passivity under limited conditions. While this may seem arbitrary, we consider the case where all reduced conductances in Equation 4.2 are zero, in other words:

$$G_{ij}^{\text{red}} = 0, \quad \forall (i, j) \in \mathcal{I}_G \times \mathcal{I}_G \tag{4.31}$$

Excluding special cases, the condition in Equation 4.31 only holds when the conductance of all transmission lines in the power system is zero, or equivalently, the resistance of all transmission lines is zero. In this case, for the functions $k_{ij}(\delta_{ij})$ and $h_{ij}(\delta_{ij})$ defined in Equation 4.3, the following holds:

$$k_{ij}(\delta_{ij}^*) = k_{ji}(\delta_{ji}^*), \quad h_{ij}(\delta_{ij}^*) = -h_{ji}(\delta_{ji}^*), \quad h_{ii}(\delta_{ii}^*) = 0$$

Therefore, for the system matrix (L, A, B, C) in Equation 4.8, it holds that:

$$L = L^\top, \quad \hat{A} = \hat{A}^\top, \quad C = -\hat{B}^\top \tag{4.32}$$

In the following, we use the symmetric structure of this special system matrix to analyze the passivity of the electrical subsystem.

First, let us express the electrical subsystem G of Equation 4.22 as follows:

$$G : \left\{ \begin{array}{l} \dot{x}_G = A_G x_G + B_G u_G \\ y_G = C_G x_G \end{array} \right. \tag{4.33}$$

where the state x_G is a column vector obtained by concatenating δ^{lin} and E^{lin} , and Ω is a positive definite diagonal matrix defined as follows:

$$\Omega := \text{diag} \left(\sqrt{\frac{X_i - X'_i}{\tau_i}} \right)_{i \in \mathcal{I}_G}$$

The system matrices are expressed as:

$$A_G := \begin{bmatrix} 0 & 0 \\ \Omega^2 \hat{B} & \Omega^2 \hat{A} \end{bmatrix}, \quad B_G := \begin{bmatrix} I \\ 0 \end{bmatrix}, \quad C_G := [L \ -\hat{B}^\top]$$

Furthermore, we define the symmetric matrix P_G as follows:

$$P_G := \begin{bmatrix} L & -\hat{B}^\top \\ -\hat{B} & -\hat{A} \end{bmatrix} \quad (4.34)$$

The following inequalities hold for these matrices:

$$A_G^\top P_G + P_G A_G \leq 0, \quad P_G B_G = C_G^\top \quad (4.35)$$

If we calculated the left of the inequality, it can be expressed as follows using a symmetric matrix $\hat{A}_\Omega := \Omega \hat{A} \Omega$:

$$\frac{A_G^\top P_G + P_G A_G}{2} = \begin{bmatrix} \Omega \hat{B} & 0 \\ 0 & \Omega^{-1} \end{bmatrix}^\top \underbrace{\begin{bmatrix} -I & -\hat{A}_\Omega \\ -\hat{A}_\Omega & -\hat{A}_\Omega^2 \end{bmatrix}}_Y \begin{bmatrix} \Omega \hat{B} & 0 \\ 0 & \Omega^{-1} \end{bmatrix}$$

Here, the top-left block $-I$ of Y is negative definite, and the Schur complement of Y with respect to $-I$ is 0, which implies that Y is negative semi-definite. Therefore, the matrix inequality in Equation 4.35 holds.

COFFEE BREAK

Schur complement:

Let a symmetric matrix M be partitioned as

$$M = \begin{bmatrix} M_{11} & M_{12} \\ M_{12}^\top & M_{22} \end{bmatrix}$$

Then, the **Schur complement** of M with respect to M_{22} is defined as:

$$M/M_{22} := M_{11} - M_{12} M_{22}^{-1} M_{12}^\top$$

Similarly, the Schur complement of M with respect to M_{11} is defined as:

$$M/M_{11} := M_{22} - M_{12}^\top M_{11}^{-1} M_{12}$$

If the matrix M_{22} is positive definite, then M is positive semidefinite if and only if M/M_{22} is positive semidefinite. The same fact holds for the Schur complement of M with respect to M_{11} [21]. The same fact holds if we replace positive semidefinite with positive definite.

Properties of semidefinite matrices:

For any positive semidefinite (or negative semidefinite) matrix $Y \in \mathbb{R}^{n \times n}$ and any matrix $X \in \mathbb{R}^{n \times m}$, the matrix $X^T Y X$ is positive semidefinite (or negative semidefinite). This can be shown from the fact that

$$v^T Y v \geq 0, \quad \forall v \in \mathbb{R}^n \quad \implies \quad (Xw)^T Y (Xw) \geq 0, \quad \forall w \in \mathbb{R}^m$$

By using the relationship given by Equation 4.35, the time derivative of the storage function $W_G(x_G)$ along the solution trajectory of G can be evaluated, where $W_G(x_G)$ is defined by Equation 4.36, similarly to Equation 4.30:

$$W_G(x_G) := \frac{1}{2} x_G^T P_G x_G \quad (4.36)$$

$$\frac{d}{dt} W_G(x_G(t)) \leq y_G^T(t) u_G(t) \quad (4.37)$$

However, to show the passivity of G , P_G in equation 4.34 must be positive semi-definite. If the matrix A in equation 4.8 is stable, then it can be shown that:

$$A = S^2 \hat{A} \quad \iff \quad S^{-1} A S = S \hat{A} S$$

where $S := \text{diag}(\sqrt{X_i - X'_i}) i \in \mathcal{I}G$. Here, \hat{A} is negative definite. Under this condition, the necessary and sufficient condition for P_G in Equation 4.34 to be positive semi-definite is that the Schur complement of $-\hat{A}$ is positive semi-definite, in other words:

$$L_0 = L_0^T \geq 0 \quad (4.38)$$

where L_0 is defined by Equation ?? and can be expressed as $L_0 = L + \hat{B}^T \hat{A}^{-1} \hat{B}$ using Equation 4.32. To summarize the above discussion, the following definition is introduced.

Definition 4.4 (Passive power transmission condition) For the system matrix (L, A, B, C) of Equation 4.8, the following three conditions are together called **passive power transmission conditions**.⁵

- (i) Matrix A is stable.
- (ii) As in Equation 4.31, all reduced conductances are zero.
- (iii) For the matrix L_0 of Equation ??, the matrix inequality of Equation 4.38 holds.

Each of these conditions may be referred to individually as the passive transmission condition (i), and so on.

Based on the above discussions, we can see that the passive power transmission conditions describe the conditions necessary for the electrical system G of Equation

⁵ "Passive power transmission conditions" is a term unique to this book.

4.22 to be passive. Furthermore, these conditions are necessary for the linear approximation model to be statically stable for the passivity of an electrical subsystem and arbitrary physical constant. The details are discussed in Section 4.3.4 and Section 4.3.5. Function $W_G(x_G)$ indicates the electrical potential energy of an electrical power system.

4.3.3 Analysis of small signal stability based on passivity[‡]

4.3.3.1 Stability analysis of feedback systems

In the following, under the passive power transmission conditions defined in Definition 4.4, the small signal stability of the linear approximation model given in Equation 4.9 is analyzed for electric subsystems that are passive. The stability of their feedback systems is also analyzed.

Since the inequalities in Equations 4.30 and 4.37 hold, their sum is given by:

$$\begin{aligned} \frac{d}{dt} \{W_F(x_F(t)) + W_G(x_G(t))\} \\ \leq \underbrace{y_F^\top(t)u_F(t) + y_G^\top(t)u_G(t)}_{\star} - \frac{\min\{D_i\}}{\omega_0} \|y_F(t)\|^2 \end{aligned}$$

By substituting the feedback coupling equation in Equation 4.23 into this inequality, the term indicated by "★" is cancelled out, and the inequality for the entire feedback system can be expressed as:

$$\frac{d}{dt} \{W_F(x_F(t)) + W_G(x_G(t))\} \leq -\frac{\min\{D_i\}}{\omega_0} \|y_F(t)\|^2 \quad (4.39)$$

In other words, the sum of the functions $W_F(x_F)$ and $W_G(x_G)$ is monotonically non-increasing with respect to the time evolution along the feedback system trajectory. Furthermore, since the lower bounds of $W_F(x_F)$ and $W_G(x_G)$ are both 0, their sum asymptotically converges to a certain value as time passes sufficiently. This means that the value of the time derivative on the left-hand side of Equation 4.39 converges to 0. Additionally, since the right-hand side of Equation 4.39 is negative when $y_F(t) \neq 0$ and is only 0 when $y_F(t) = 0$, the following is obtained:

$$\lim_{t \rightarrow \infty} y_F(t) = 0 \quad (4.40)$$

Furthermore, focusing on the output equation of Equation 4.21, since the output y_F is a constant multiple of the internal state $\Delta\omega^{\text{lin}}$, it can be understood that for the mechanical subsystem F :

$$y_F(t) = 0, \quad \forall t \geq 0 \quad \implies \quad \Delta\omega^{\text{lin}}(t) = 0, \quad \forall t \geq 0 \quad (4.41)$$

This is a property called **observability** in system control engineering. Therefore, from Equations 4.40 and 4.41, for the approximated linear model of Equation 4.9, for any initial value $(\Delta\omega^{\text{lin}}(0), \delta^{\text{lin}}(0), E^{\text{lin}}(0))$, the following holds:

$$\lim_{t \rightarrow \infty} \Delta\omega^{\text{lin}}(t) = 0 \quad (4.42)$$

In other words, the internal state of the mechanical subsystem F in Equation 4.21 in the feedback system converges to 0 asymptotically.

COFFEE BREAK

Observability: For a linear system Σ described by Equation 4.24, if the output $y(t)$ is identically zero, then the internal state $x(t)$ is also identically zero, and Σ is said to be **observable** in this case. The necessary and sufficient condition for Σ to be observable is given by Equation 4.43, where n is the dimension of the state.

$$\ker \begin{bmatrix} C \\ CA \\ \vdots \\ CA^{n-1} \end{bmatrix} = \{0\} \quad (4.43)$$

In some contexts, a pair of matrices that satisfies Equation 4.43 is referred to as an observable pair (C, A) .

Controllability: For a linear system Σ described by Equation 4.24, if there exists an input $u(t)$ such that for all initial states $x(0)$, there exists a time $T > 0$ such that $x(T) = 0$, then Σ is said to be **controllable**. The necessary and sufficient condition for Σ to be controllable is given by Equation 4.44, where n is the dimension of the state.

$$\text{im} \left[B \ AB \ \cdots \ A^{n-1}B \right] = \mathbb{R}^n \quad (4.44)$$

Here, im denotes the **image** of the matrix. In some contexts, a pair of matrices that satisfies Equation 4.44 is referred to as a controllable pair (A, B) .

Lyapunov function: Consider the observable linear system Σ described by Equation 4.24, where the input $u(t)$ is identically zero. Let $V(x)$ be a positive semi-definite function that satisfies $V(x) \geq 0$ for all x and $V(0) = 0$. If there exists a positive constant ρ such that the derivative of $V(x)$ along the solution trajectory of Σ satisfies

$$\frac{d}{dt} V(x(t)) = \nabla V^\top(x) \frac{dx}{dt}(t) \leq -\rho \|y(t)\|^2, \quad \forall t \geq 0$$

then the solution trajectory $x(t)$ converges asymptotically to zero for any initial state. Such a function $V(x)$ is called a **Lyapunov function**.

The fact that the value of the Lyapunov function decreases monotonically along the solution trajectory of the system can be interpreted as a type of energy dissipation over time (Figure 4.5). Similar stability analyses based on Lyapunov functions can also be applied to nonlinear systems.

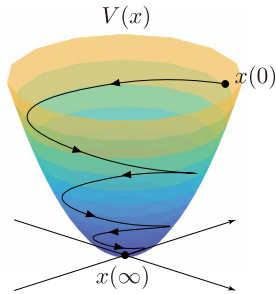


Fig. 4.5 Monotonically decreasing values along the solution trajectory of the Lyapunov function

On the one hand, it is not possible to deduce from the above discussion whether the internal state of the electric subsystem G in Equation 4.22 converges asymptotically to 0. Specifically, from the relation in Equation 4.23 and the asymptotic convergence in Equation 4.42, it can be derived that the input and output of the two subsystems satisfy:

$$\lim_{t \rightarrow \infty} u_F(t) = 0, \quad \lim_{t \rightarrow \infty} u_G(t) = 0, \quad \lim_{t \rightarrow \infty} y_G(t) = 0$$

However, since the electric subsystem is not observable, it cannot be concluded that its internal state converges asymptotically to zero. Assuming that the electric subsystem is observable, it can be concluded that for any initial values:

$$\lim_{t \rightarrow \infty} \delta^{\text{lin}}(t) = 0, \quad \lim_{t \rightarrow \infty} E^{\text{lin}}(t) = 0$$

However, this implies that c_0 must always be equal to 0 in Equation 4.11. This fact contradicts the instability of Equation 4.9 due to the zero eigenvalue of Ψ . It should be noted that except for some special cases, the electric subsystem is controllable.

Example 4.3 Time evolution of stored energy Consider the approximated linear model discussed in the first half of Example 4.2. First, consider the case where the passive transmission condition (ii) is satisfied, i.e., when the conductance of both transmission lines is 0. Specifically, set the admittance values of the transmission lines to:

$$y_{12} = -j11.6041, \quad y_{23} = -j10.5107 \quad (4.45)$$

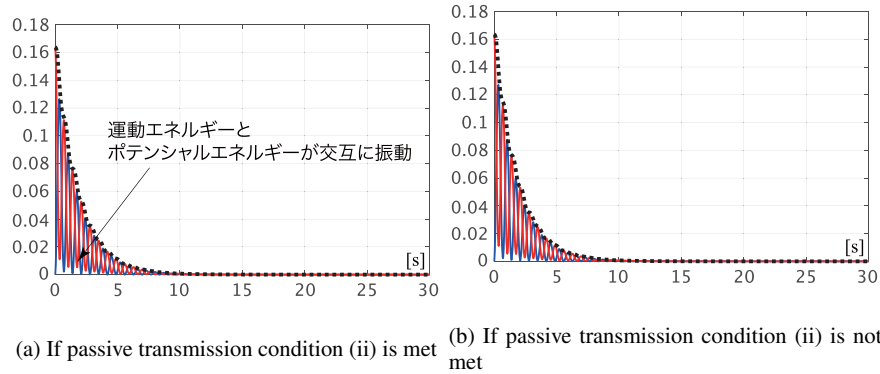


Fig. 4.6 Time variation of the accumulation function according to Example 4.2
(Blue: W_F , Red: W_G , Black: $W_F + W_G$)

This corresponds to setting the parameter θ_2 to 0 in Equation 4.17. In this case, the matrix A becomes stable. Also, all the eigenvalues of L_0 in Equation ?? become non-negative. Thus, the passive transmission conditions (i) and (iii) hold.

Consider the time response of the initial values in Equation 4.14 and calculate the time variation of the kinetic energy $W_F(x_F)$ in Equation 4.29 and the potential energy $W_G(x_G)$ in Equation 4.36. The calculation results are shown in Figure 4.6(a) where the blue and red solid lines represent $W_F(x_F)$ and $W_G(x_G)$, respectively, and the black dashed line represents their sum, which is the total energy of the system. From this figure, it can be seen that while the kinetic and potential energies increase and decrease alternatively, the total energy of the system, which is the sum of these energies, decreases monotonically. The decrease in total energy over time can be interpreted as energy loss due to friction caused by the damping coefficient.

Next, as a reference, let us show the results when the passive power transmission condition (ii) is not satisfied. Specifically, we set $Y_0(1)$ in Equation 4.17 to be the admittance matrix Y by setting θ_2 to 1. This is equivalent to calculating the time variation of the kinetic and potential energies for the initial value response in Figure 4.2. Note that when the passive power transmission condition (ii) is not satisfied, P_G in Equation 4.34 does not become a symmetric matrix, but the potential energy $W_G(x_G)$ can still be calculated using the definition in Equation 4.36. The calculation result in Figure 4.6(b) is almost identical to that in Figure 4.6(a). This fact suggests that even when the conductance of the transmission line is not zero, the electrical potential energy can be approximately calculated based on the definition in Equation 4.36.

4.3.3.2 Basis transformation for separating unobservable state variables

Let us consider deriving an observable subsystem from the electrical subsystem G in Equation 4.22 by removing the common component of unobservable rotor angles. Specifically, we apply a basis transformation to the state δ^{lin} in Equation 4.7 to derive a set of differential equations describing only the deviations of the rotor angles. Note that the following basis transformation is always applicable regardless of whether the passive power delivery condition holds or not.

COFFEE BREAK

Basis transformation of linear systems:

In the state equation:

$$\dot{x}(t) = Ax(t) + Bu(t)$$

each element $x_i(t)$ of the n -dimensional state vector $x(t)$ can be represented as the component of the expansion with respect to the basis e_1, \dots, e_n , such as:

$$x(t) = e_1x_1(t) + \dots + e_nx_n(t)$$

where e_i is an n -dimensional vector with only the i -th element being 1. This basis is called the **standard basis** and represents the time evolution of the "components" of the state vector $x(t)$ in a certain basis. We now consider representing $x(t)$ in another basis v_1, \dots, v_n such that

$$x(t) = v_1\xi_1(t) + \dots + v_n\xi_n(t)$$

where $\xi_i(t)$ is the component of the basis vector v_i . Let us denote the matrix obtained by arranging the vectors v_i horizontally as V and the vector obtained by arranging $\xi_i(t)$ vertically as $\xi(t)$. Then, the linear transformation $x(t) = V\xi(t)$ corresponds to this representation. In this case, the state equation is transformed as:

$$\dot{\xi}(t) = V^{-1}AV\xi(t) + V^{-1}Bu(t)$$

where V_a and V_b are the matrices obtained by arranging the basis vectors of \mathcal{V}_a and \mathcal{V}_b horizontally, respectively, the transformed state equation is obtained as:

$$x(t) = V_a\xi_a(t) + V_b\xi_b(t)$$

where W_a and W_b are matrices that satisfy:

$$\begin{bmatrix} \dot{\xi}_a(t) \\ \dot{\xi}_b(t) \end{bmatrix} = \begin{bmatrix} W_aAV_a & W_aAV_b \\ W_bAV_a & W_bAW_b \end{bmatrix} \begin{bmatrix} \xi_a(t) \\ \xi_b(t) \end{bmatrix}$$

However, V_a and V_b are matrices consisting of the basis vectors of \mathcal{V}_a and \mathcal{V}_b , respectively. W_a and W_b are matrices that satisfy:

$$\begin{bmatrix} W_a \\ W_b \end{bmatrix} = [V_a \ V_b]^{-1} \iff [V_a \ V_b] \begin{bmatrix} W_a \\ W_b \end{bmatrix} = I$$

In this representation, $\xi_a(t)$ represents the component of $x(t)$ with respect to the subspace $\text{span } \mathcal{V}_a$. Similarly, $\xi_b(t)$ represents the component of $x(t)$ with respect to the subspace $\text{span } \mathcal{V}_b$.

The change of basis explained below can be applied regardless of whether passive power transmission conditions hold. δ^{lin} is expanded using a matrix $W \in \mathbb{R}^{N \times (N-1)}$:

$$\delta^{\text{lin}} = W\delta_e^{\text{lin}} + \mathbb{1}\bar{\delta}_e^{\text{lin}} \quad (4.46)$$

Here, $\mathbb{1}$ is a base vector that expresses the common component of δ^{lin} , while W is a matrix with base vectors that express other deviation components. In other words, the common component of δ^{lin} is $\bar{\delta}_e^{\text{lin}}$, and deviation components are δ_e^{lin} . The common component $\bar{\delta}_e^{\text{lin}}$ is one-dimensional, while deviation components δ_e^{lin} are $(N - 1)$ -dimensional.

Next, let us consider the inverse transformation of Equation 4.46. Specifically, let us consider a matrix $W^\dagger \in \mathbb{R}^{(N-1) \times N}$:

$$\delta^{\text{lin}} = \underbrace{\begin{bmatrix} W & \mathbb{1} \end{bmatrix}}_T \begin{bmatrix} \delta_e^{\text{lin}} \\ \bar{\delta}_e^{\text{lin}} \end{bmatrix} \iff \begin{bmatrix} \delta_e^{\text{lin}} \\ \bar{\delta}_e^{\text{lin}} \end{bmatrix} = \underbrace{\begin{bmatrix} W^\dagger \\ \frac{1}{N}\mathbb{1}^\top \end{bmatrix}}_{T^{-1}} \delta^{\text{lin}}$$

For this inverse transformation to exist, the column vector of W must be orthogonal to $\mathbb{1}$. This can be confirmed as follows. From the relationship of inverse transformation, the following must hold:

$$T^{-1}T = \begin{bmatrix} W^\dagger W & W^\dagger \mathbb{1} \\ \frac{1}{N}\mathbb{1}^\top W & \frac{1}{N}\mathbb{1}^\top \mathbb{1} \end{bmatrix} = \begin{bmatrix} I & 0 \\ 0 & 1 \end{bmatrix}$$

In other words, W and W^\dagger are matrices that satisfy:

$$\mathbb{1}^\top W = 0, \quad W^\dagger W = I, \quad W^\dagger \mathbb{1} = 0$$

Therefore, from the first equation, we can see that the column vectors of W must be orthogonal to $\mathbb{1}$. Note that W and W^\dagger can be constructed using an appropriate matrix $U \in \mathbb{R}^{N \times (N-1)}$ that satisfies $\mathbb{1}^\top U = 0$ and $U^\top U$ is invertible, as follows:

$$W = U(U^\top U)^{-1}, \quad W^\dagger = U^\top$$

In this case, the product WW^\dagger can be expressed as the **orthogonal projection matrix** onto the orthogonal complement of $\text{span } \mathbb{1}$:

$$WW^\dagger = I - \frac{1}{N}\mathbb{1}\mathbb{1}^\top \quad (4.47)$$

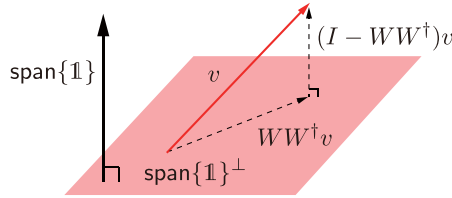


Fig. 4.7 Conceptual diagram of orthogonal projection

The pseudoinverse of W obtained in this way is called the **Moore-Penrose pseudoinverse** [21].

In Figure 4.7, the subspace $\text{span } \mathbf{1}$ is shown by a black arrow, and the orthogonal complement space $\text{span } \mathbf{1}^\perp$ is shown as a plane perpendicular to it. When a vector v is multiplied by the orthogonal projection matrix WW^\dagger , the projection of v onto $\text{span } \mathbf{1}^\perp$, which is the shadow cast by v in the direction perpendicular to $\text{span } \mathbf{1}$, is obtained as $WW^\dagger v$. Furthermore, the complementary relationship, shown below, indicates that it is the orthogonal projection matrix onto $\text{span } \mathbf{1}$'s orthogonal complement, that is, $\text{span } \mathbf{1}$.

$$I - WW^\dagger = \frac{1}{N} \mathbf{1} \mathbf{1}^\top$$

We apply the above-mentioned change of basis to the electrical subsystem G of Equation 4.22. First, if we substitute Equation 4.46 into a differential equation related to $\dot{\delta}_e^{\text{lin}}$, the following is obtained:

$$W\dot{\delta}_e^{\text{lin}} + \mathbf{1}\dot{\delta}_e^{\text{lin}} = u_G$$

By multiplying the left-hand side of this differential equation by W^\dagger or $\frac{1}{N} \mathbf{1}^\top$, we obtain:

$$\dot{\delta}_e^{\text{lin}} = W^\dagger u_G, \quad \dot{\delta}_e^{\text{lin}} = \frac{1}{N} \mathbf{1}^\top u_G$$

Next, noting that the relationship in Equation 4.10 holds for matrices L and B , the differential equation and output equation with respect to E^{lin} can be rewritten as:

$$\tau \dot{E}^{\text{lin}} = AE^{\text{lin}} + BW\delta_e^{\text{lin}}, \quad y_G = CE^{\text{lin}} + LW\delta_e^{\text{lin}}$$

Therefore, the transformed electric subsystem is given by:

$$G : \begin{cases} \dot{\delta}_e^{\text{lin}} = \frac{1}{N} \mathbf{1}^\top u_G \\ \dot{\delta}_e^{\text{lin}} = W^\dagger u_G \\ \tau \dot{E}^{\text{lin}} = AE^{\text{lin}} + BW\delta_e^{\text{lin}} \\ y_G = CE^{\text{lin}} + LW\delta_e^{\text{lin}} \end{cases} \quad (4.48)$$

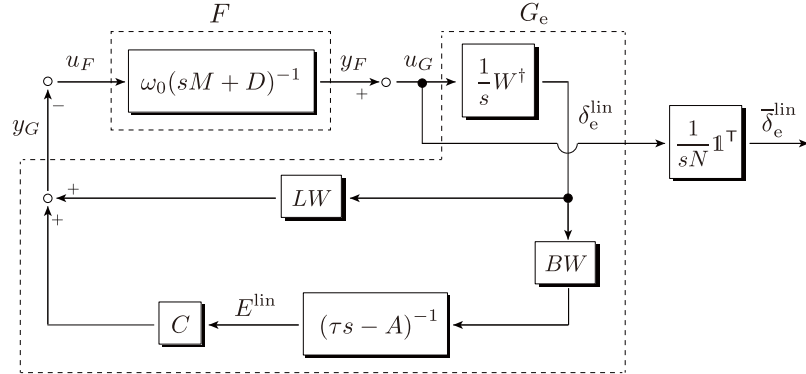


Fig. 4.8 Basis-transformed approximate linear model

One notable point about this system representation is that the common component of δ_e^{lin} , represented by $\bar{\delta}_e^{\text{lin}}$, is affected by the input u_G but has no effect on the output y_G . In other words, $\bar{\delta}_e^{\text{lin}}$ is an unobservable state variable.

By removing the differential equation of $\bar{\delta}_e^{\text{lin}}$ from Equation 4.48, $(N - 1)$ -dimensional controllable and observable subsystem is obtained as:

$$G_e : \begin{cases} \dot{\delta}_e^{\text{lin}} = W^\dagger u_G \\ \tau \dot{E}^{\text{lin}} = AE^{\text{lin}} + BW\delta_e^{\text{lin}} \\ y_G = CE^{\text{lin}} + LW\delta_e^{\text{lin}} \end{cases} \quad (4.49)$$

Here, please note that from observability of G_e , the following holds.

$$y_G(t) = 0, \quad \forall t \geq 0 \quad \Rightarrow \quad \begin{bmatrix} \delta_e^{\text{lin}}(t) \\ E^{\text{lin}}(t) \end{bmatrix} = 0, \quad \forall t \geq 0 \quad (4.50)$$

The fact mentioned above is important for the analysis of the steady-state stability of the approximate linear model in equation 4.9. As a reference, the block diagram of the approximate linear model transformed by the change of basis is shown in Figure 4.8.

It should be noted that it is a necessary and sufficient condition for G_e to be controllable and observable that the pair $(\tau^{-1}A, \tau^{-1}B)$ is controllable and the pair $(C, \tau^{-1}A)$ is observable. In the following, we assume controllability and observability. Note that an exact proof is not always easy, but assuming that the rank of B and C is $(N - 1)$ or higher in most situations, there are no practical obstacles to analysis.

4.3.3.3 Small signal stability analysis based on passivity

In the following, assuming the passive power transfer condition defined in Definition 4.4, we show the passivity of G_e in Equation 4.49 using the same procedure as that of the electrical subsystem G in Equation 4.22. To this end, we express G_e in the form of:

$$G_e : \begin{cases} \dot{x}_{G_e} = A_{G_e}x_{G_e} + B_{G_e}u_G \\ y_G = C_{G_e}x_{G_e} \end{cases} \quad (4.51)$$

where x_{G_e} is a vector composed of δ_e^{lin} and E^{lin} , and:

$$A_{G_e} := \begin{bmatrix} 0 & 0 \\ \Omega^2 \hat{B}W & \Omega^2 \hat{A} \end{bmatrix}, \quad B_{G_e} := \begin{bmatrix} W^\dagger \\ 0 \end{bmatrix}, \quad C_{G_e} := [LW \ -\hat{B}^\top]$$

Additionally, we define the positive semidefinite matrix P_{G_e} as:

$$P_{G_e} := \begin{bmatrix} W & 0 \\ 0 & I \end{bmatrix}^\top \underbrace{\begin{bmatrix} L & -\hat{B}^\top \\ -\hat{B} & -\hat{A} \end{bmatrix}}_{P_G} \begin{bmatrix} W & 0 \\ 0 & I \end{bmatrix} \quad (4.52)$$

Note that if P_G in Equation 4.34 is positive semi-definite, then P_{G_e} is also positive semi-definite. In this case, by noting that $\hat{B}WW^\dagger = \hat{B}$ and $LWW^\dagger = L$ from the relationship in Equation 4.47, we can see that the following equation holds:

$$A_{G_e}^\top P_{G_e} + P_{G_e} A_{G_e} \leq 0, \quad P_{G_e} B_{G_e} = C_{G_e}^\top \quad (4.53)$$

Note that the left matrix inequality is shown from the same equation as 4.35:

$$\frac{A_{G_e}^\top P_{G_e} + P_{G_e} A_{G_e}}{2} = \underbrace{\begin{bmatrix} \Omega \hat{B}W & 0 \\ 0 & \Omega^{-1} \end{bmatrix}^\top \begin{bmatrix} -I & -\hat{A}_\Omega \\ -\hat{A}_\Omega & -\hat{A}_\Omega^2 \end{bmatrix} \begin{bmatrix} \Omega \hat{B}W & 0 \\ 0 & \Omega^{-1} \end{bmatrix}}_Y$$

Therefore, the time derivative along the solution trajectory of G_e of the storage function:

$$W_{G_e}(x_{G_e}) := \frac{1}{2} x_{G_e}^\top P_{G_e} x_{G_e}$$

can be evaluated as:

$$\frac{d}{dt} W_{G_e}(x_{G_e}(t)) \leq y_G^\top(t) u_G(t) \quad (4.54)$$

Thus, G_e in Equation 4.49 is passive. Note that this inequality is equivalent to the inequality in Equation 4.37, and the values of the two storage functions satisfy:

$$W_G(x_G(t)) = W_{G_e}(x_{G_e}(t)), \quad \forall t \geq 0$$

By considering the observability of G_e shown by Equation 4.50, the following is true for the arbitrary initial value of the solution trajectory of the linear approximation model of Equation 4.9:

$$\lim_{t \rightarrow \infty} \Delta\omega^{\text{lin}}(t) = 0, \quad \lim_{t \rightarrow \infty} \begin{bmatrix} \delta_e^{\text{lin}}(t) \\ E^{\text{lin}}(t) \end{bmatrix} = 0 \quad (4.55)$$

Therefore, from the relationship of the change of basis of Equation 4.46, we can see that Equation 4.11 holds for the arbitrary initial value. In other words, the linear approximation model of Equation 4.9 is statically stable. Also:

$$c_0 = \lim_{t \rightarrow \infty} \bar{\delta}_e^{\text{lin}}(t)$$

and state variables $\bar{\delta}_e^{\text{lin}}$ follow the differential equation of Equation 4.48.

We summarize the previous discussion in the following theorem.

Theorem 4.1 (Small signal stability of the linear approximation model based on passivity) *For any steady-state value (δ^*, E^*) that satisfies the passive power transfer condition defined in Definition 4.4, the electrical subsystem G given in equation 4.22 is passive. Additionally, for any positive constants $(M_i, D_i, \tau_i)_{i \in \mathcal{I}_G}$, the approximate linear model given in equation 4.9 is steady-state stable.*

As discussed in Theorem 4.1, under the passive power transmission conditions, the linear approximation model is statically stable for combinations of all physical constants $(M_i, D_i, \tau_i)_{i \in \mathcal{I}_G}$. Analysis based on passivity allows stability independent of model parameters.

4.3.4 Necessary conditions for the approxiamte linear model to be passive[‡]

4.3.4.1 Passivity and positive realness

It is known that the passivity of a linear system is mathematically equivalent to the property called positive realness of its transfer function. In this section, we consider the necessity of the passive power transmission condition defined in Definition 4.4 from the viewpoint of the passivity of the electrical subsystem based on this equivalence.

COFFEE BREAK

Transfer function: For a linear system:

$$\begin{cases} \dot{x}(t) = Ax(t) + Bu(t) \\ y(t) = Cx(t) + Du(t) \end{cases}$$

its **transfer function** is defined as:

$$Q(s) := C(sI - A)^{-1}B + D$$

When the Laplace transform of the input $u(t)$ is $U(s)$ and the Laplace transform of the output $y(t)$ is $Y(s)$, the transfer function relates to the system as $Y(s) = Q(s)U(s)$. The input-output behavior of a linear system is characterized by its transfer function.

The transfer function from the input u_G to the output y_G of the electrical subsystem G in Equation 4.22 is given by:

$$G(s) := -\frac{1}{s} \underbrace{\left\{ -C(\tau s - A)^{-1}B - L \right\}}_{H(s)} \quad (4.56)$$

Note that since unobservable state variables are not relevant to the input-output characteristics, the transfer function of G_e in Equation 4.49 is also equal to $G(s)$. Hereafter, we consider the case where the transfer function $H(s)$ in Equation 4.56 is stable. The stability of the transfer function is defined as follows.

Definition 4.5 (Stability of a transfer function) When the real part of all poles of the transfer function $Q(s)$ is negative, $Q(s)$ is called **stable**.

The poles of a transfer function are the zeros of the denominator polynomial. It is known that $H(s)$ in equation 4.56 being stable is equivalent to all the real parts of the eigenvalues of the matrix $\tau^{-1}A$ being negative.

Furthermore, the **Positive realness** of a transfer function is defined as follows.

Definition 4.6 (Positive realness of a transfer function) For a square transfer function $Q(s)$, the following is defined:

$$\Omega_0 := \{\omega_0 \in \mathbb{R} : \text{The pure imaginary number } j\omega_0 \text{ is a pole of } Q(s)\} \quad (4.57)$$

$Q(s)$ is called **positive real** if the following three conditions are satisfied.

- The real part of all poles of $Q(s)$ is nonpositive.
- For all $\omega \in [0, \infty) \setminus \Omega_0$, $Q(j\omega) + Q^T(-j\omega)$ is positive semi-definite.
- When there are poles of a pure imaginary number, their multiplicity is 1, and the following is true for the remaining number:

$$\lim_{s \rightarrow j\omega_0} (s - j\omega_0)Q(s) = \lim_{s \rightarrow j\omega_0} \{(s - j\omega_0)Q(s)\}^* \geq 0, \quad \forall \omega_0 \in \Omega_0$$

In Definition 4.6, the two most important conditions are the first and second ones. The first condition expresses the stability of the transfer function. However, it also includes the case where the real part of the pole is 0. The second condition concerns the positive definiteness of the complex symmetric part of the transfer function evaluated on the imaginary axis. In particular, if $Q(s)$ is a scalar, that is, both the input

and output are scalars, the second condition expresses that the real part of $Q(j\omega)$ is non-negative for all $\omega \in [0, \infty) \setminus \Omega_0$. However, it should be noted that for matrix-valued $Q(s)$, in general,

$$Q(j\omega) + Q^T(-j\omega) \neq 2 \operatorname{Re}[Q(j\omega)]$$

Also, for $Q(s)$ with real coefficients, $Q^T(-j\omega)$ is equal to $Q(j\omega)^*$. The third condition is exceptional in the case when $Q(s)$ has pure imaginary poles. However, it is necessary to analyze transfer functions with poles at the origin, such as $G(s)$ in Equation 4.56.

COFFEE BREAK

Complex Symmetric and Skew Hermitian Parts of a Square Matrix: Any square matrix M can be decomposed as:

$$M = \frac{M + M^*}{2} + \frac{M - M^*}{2}$$

where $\frac{M+M^*}{2}$ is called the **complex symmetric part** (Hermitian part) of M , and $\frac{M-M^*}{2}$ is called the **complex skew-symmetric part** (skew Hermitian part) of M .

In system control engineering, it is known that passivity in Definition 4.3 and positive realness in Definition 4.6 are equivalent. If we apply Lemma 4.2 at the end of this chapter to the discussion in this section, the necessary and sufficient condition for $G(s)$ in Equation 4.56 to be positive real is the existence of a positive definite matrix P_{G_e} that satisfies Equation 4.55 for the controllable and observable state space realization G_e in Equation 4.51. This is equivalent to the passivity of G_e defined by the inequality in Equation 4.54. Furthermore, the positive realness of P_{G_e} in Equation 4.52 is shown by the fact that both the Schur complements with respect to $-\hat{A}$ and $-\hat{A}$ of the matrix $W^T (L + \hat{B}^T \hat{A}^{-1} \hat{B}) W$ are positive definite, where $W^T L_0 W$ satisfies Equation 4.20 and the column vectors of W in Equation 4.46 are orthogonal to 1.

4.3.4.2 Necessary condition for the transfer function of the electrical subsystem to be positive-real

As a mathematical preparation for deriving necessary conditions, we introduce the concept of **negative imaginarity** of transfer functions, which is similar to positive-realness [22, 23].

Definition 4.7 (Negative imaginarity of a transfer function) For a square transfer function $Q(s)$ without a pole at the origin, we define Ω_0 of Equation 4.57. When the following three conditions are satisfied, $Q(s)$ is called **negative imaginary**.

- The real part of all poles of $Q(s)$ is nonpositive.
- For all $\omega \in (0, \infty) \setminus \Omega_0$, $j \{Q(j\omega) - Q^T(-j\omega)\}$ is positive semi-definite.

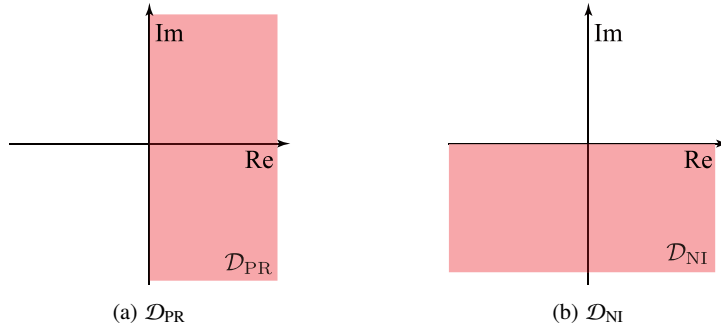


Fig. 4.9 Positive realms and negative imaginary realms

- When there is a pole of a pure imaginary number, their multiplicity is 1, and the following holds for the remaining numbers:

$$\lim_{s \rightarrow j\omega_0} (s - j\omega_0)jQ(s) = \lim_{s \rightarrow j\omega_0} \{(s - j\omega_0)jQ(s)\}^* \geq 0, \quad \forall \omega_0 \in \Omega_0$$

While Definition 4.6 defines positive-realness based on the positive-definiteness of the complex symmetric part of a transfer function, Definition 4.7 defines negative-imaginaryness based on the positive-semidefiniteness of the complex anti-symmetric part of the transfer function multiplied by the imaginary unit. Note that since the eigenvalues of a complex anti-symmetric matrix are purely imaginary, their product with the imaginary unit is real. In particular, when $Q(s)$ is a scalar transfer function, the second condition implies that the imaginary part of $Q(j\omega)$ is non-positive for all $\omega \in (0, \infty) \setminus \Omega_0$. Furthermore, in the following discussion, we focus only on the second condition to consider the negative-imaginaryness of stable transfer functions. Similar to positive-realness, negative-imaginaryness can also be characterized as the solvability of matrix inequalities, as described in Lemma 4.3 at the end of this chapter.

COFFEE BREAK

Nyquist plot: The plot of the frequency response function $Q(j\omega)$ for $\omega \in \mathbb{R}$ on the complex plane is called the **Nyquist plot**. It is often used in geometric analysis of stability for feedback systems. The analysis method is called the **Nyquist stability criterion**. Note that when $Q(s)$ is a scalar and the coefficients of the numerator and denominator polynomials are real, the plot of $Q(j\omega)$ for negative ω is symmetrical to the plot for positive ω with respect to the real axis.

The relationship of positive realness and negative imaginarity is explained with Figure 4.9. If the transfer function $Q(s)$ is scalar, $Q(s)$ being positive real can be understood as the trajectory related to non-negative ω of the frequency response function $Q(j\omega)$ is included in the range \mathcal{D}_{PR} shown in 4.9(a).

$$\mathcal{D}_{\text{PR}} = \mathbf{j} \mathcal{D}_{\text{NI}}$$

and $-\frac{1}{j} = \mathbf{j}$ for $G(s)$ and $H(s)$ of Equation 4.56, the following is derived:

$$G(j\omega) \in \mathcal{D}_{\text{PR}}, \quad \forall \omega > 0 \quad \iff \quad H(j\omega) \in \mathcal{D}_{\text{NI}}, \quad \forall \omega > 0$$

Therefore, a negative imaginarity analysis of $H(s)$ is equivalent to a positive realness analysis of $G(s)$. To be accurate, $G(j\omega)$ and $H(j\omega)$ are complex matrices; thus, \mathcal{D}_{PR} and \mathcal{D}_{NI} should be redefined with a set of positive semi-definite matrices.

Therefore, a negative imaginarity analysis of $H(s)$ is equivalent to a positive realness analysis of $G(s)$. Based on this fact, the passive power transmission conditions (ii) and (iii) are necessary conditions for $G(s)$ to be positive real.

Theorem 4.2 *Positive realness of electrical subsystem transfer function* For any (δ^*, E^*) where the transfer function $H(s)$ given by Equation 4.56 is stable, a necessary and sufficient condition for $H(s)$ to be negative imaginary is that the passive power transmission condition (ii) in Definition 4.4 holds. Furthermore, a necessary and sufficient condition for the transfer function $G(s)$ given by Equation 4.56 to be positive real is that both passive power transmission conditions (ii) and (iii) in Definition 4.4 hold.

Proof First, we show that if $H(s)$ is negative imaginary for any (δ^*, E^*) where $H(s)$ is stable, then the passive power transmission condition (ii), which is expressed in equation 4.31, holds true. Now, since:

$$\lim_{\omega \rightarrow \infty} \mathbf{j} \{H(j\omega) - H^T(-j\omega)\} = \mathbf{j} (-L + L^T) \geq 0$$

L must be symmetric for $H(s)$ to be negative imaginary. Therefore, we obtain $k_{ij}(\delta_{ij}^*) = k_{ji}(\delta_{ji}^*)$.

Therefore, L must be symmetric for $H(s)$ to be negative vacuity. Thus, we have $K_{IJ}(\delta_{IJ}^*) = K_{JI}(\delta_{JI}^*)$.

In other words:

$$G_{ij}^{\text{red}} \sin \delta_{ij}^* = 0, \quad \forall (i, j) \in \mathcal{I}_G \times \mathcal{I}_G$$

This implies $\delta_i^* \neq \delta_j^*$ for (i, j) where $G_{ij}^{\text{red}} = 0$. Also, even in the case where $\delta_i^* = \delta_j^*$, there exists a sufficiently small $\gamma > 0$ such that $\tau^{-1}A$ is stable for $\delta^* + \gamma e_i$ due to the continuity of the eigenvalue parameter variation for matrices with parameters. Here, e_i represents a vector with only the i -th element being 1 and the others being 0. Therefore, we obtain:

$$G_{ij}^{\text{red}} = 0, \quad \forall i \neq j \tag{4.58}$$

Furthermore, if $H(s)$ is negative imaginary, then L_0 in equation ?? must also be symmetric, because we have:

$$\lim_{\omega \rightarrow 0} j \{ H(j\omega) - H^T(-j\omega) \} = j \left(-L_0 + L_0^T \right) \geq 0$$

When equation 4.58 holds, it should be noted that L_0 can be expressed as follows:

$$C = \text{diag} \left(2E_i^\star G_{ii}^{\text{red}} \right) - \hat{B}^T$$

Note that L_0 is given by:

$$L_0 = \underbrace{L + \hat{B}^T \hat{A}^{-1} \hat{B}}_{L_1} - \underbrace{\text{diag}(2E_i^\star G_{ii}^{\text{red}}) \hat{A}^{-1} \hat{B}}_{L_2}$$

where \hat{A} is a symmetric matrix defined in equation 4.8. Therefore, L_1 is symmetric. On the other hand, for L_2 to be symmetric for any E^\star , it must be the case that $G_{ii}^{\text{red}} \neq 0$ for all i . From this, it follows that if $H(s)$ is negative imaginary for any (δ^\star, E^\star) such that $H(s)$ is stable, then equation 4.31 holds.

Next, we will show that if Equation 4.31 holds, then $H(s)$ is negative imaginary for any (δ^\star, E^\star) that makes $H(s)$ stable. For this purpose, it is enough to show that there exists a positive definite matrix P that satisfies L is symmetric and

$$\tilde{A}^T P + P \tilde{A} \leq 0, \quad P \tilde{A}^{-1} \tilde{B} = C^T \quad (4.59)$$

$$\tilde{A} := \tau^{-1} A, \quad \tilde{B} := \tau^{-1} B$$

Note that if equation 4.31 holds, then

$$k_{ij}(\delta_{ij}^\star) = k_{ji}(\delta_{ji}^\star), \quad h_{ij}(\delta_{ij}^\star) = -h_{ji}(\delta_{ji}^\star), \quad h_{ii}(\delta_{ii}^\star) = 0$$

which implies that L is symmetric. Moreover, since $H(s)$ is stable, we have

$$\tilde{A} = \text{diag} \left(\frac{X_i - X'_i}{\tau_i} \right) \hat{A}$$

and since $X_i > X'_i$, the matrix \hat{A} in Equation 4.8 is negative definite. Therefore, we can choose $P = -\hat{A}$ as a positive definite matrix that satisfies Equation 4.59, which implies that $H(s)$ is negative imaginary.

Next, we show the equivalence of $G(s)$. Since $H(s)$ is stable, the poles of $G(s)$ on the imaginary axis are only at the origin and have a multiplicity of 1. Therefore, the necessary and sufficient condition for $G(s)$ to be positive real is:

$$G(j\omega) + G^T(-j\omega) \geq 0, \quad \forall \omega \in \mathbb{R} \setminus \{0\} \quad (4.60)$$

Then the following can be established:

$$\lim_{s \rightarrow 0} sG(s) = \lim_{s \rightarrow 0} \{sG(s)\}^T \geq 0 \quad (4.61)$$

When the Equation 4.31 holds, then the Equation 4.60 holds.

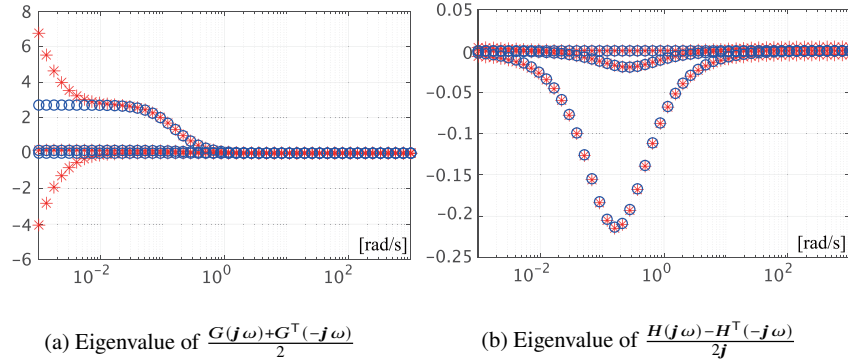


Fig. 4.10 Positive realness of $G(s)$ and negative imaginariness of $H(s)$
(Blue: passive transmission condition (ii) is satisfied, Red: not satisfied)

$$G(j\omega) + G^\top(-j\omega) = \frac{j}{\omega} \{H(j\omega) - H^\top(-j\omega)\}, \quad \forall \omega \in \mathbb{R} \setminus \{0\} \quad (4.62)$$

It is shown from $H(s)$ that $H(s)$ is negative imaginary. Moreover:

$$\lim_{s \rightarrow 0} sG(s) = L - C\tilde{A}^{-1}\tilde{B} = L - CA^{-1}B$$

Therefore, the positive semi-definiteness of equation 4.61 is equivalent to the passive transmission condition (iii), i.e., the condition of Equation 4.38. Note that when the passive transmission condition (ii) holds, L is symmetric and:

$$C\tilde{A}^{-1}\tilde{B} = CP^{-1}C^\top$$

is also symmetric, which also shows the symmetry of the expression 4.61.

On the contrary, if either the passive power transmission condition (ii) or (iii) is not satisfied, it indicates that $G(s)$ is not positive real. As for the latter, it is evident from the fact that the condition in Equation 4.38 is equivalent to the condition in Equation 4.61. Additionally, when the passive power transmission condition (ii) is not satisfied, $H(s)$ is not purely imaginary, and there exist some point $\omega_0 \geq 0$ and sufficiently small $\epsilon > 0$ such that:

$$\lambda_{\min} [j \{H(j(\omega_0 + \alpha)) - H^\top(-j(\omega_0 + \alpha))\}] < 0, \quad \forall \alpha \in (0, \epsilon]$$

where λ_{\min} denotes the minimum eigenvalue. Therefore, for all non-zero $\omega \in (\omega_0, \omega_0 + \epsilon]$, the complex symmetric part of $G(j\omega)$ is not semi-positive definite. \square

Let us confirm the result of Theorem 4.2 with the following example.

Example 4.4 Transmission loss and positive realness of transfer function of electrical subsystem

Let's examine the positive realness of $G(s)$ and the negative imaginary property of $H(s)$ for the power system model composed of three generators that we dealt with in Example 4.2. We will calculate these properties in two cases: when the passive power transmission condition (ii) is satisfied and when it is not, for comparison purposes. Specifically, as in Example 4.3, we set two types of $Y_0(0)$ and $Y_0(1)$ as the admittance matrix Y of the transmission network. The eigenvalues of the complex symmetric part of $G(j\omega)$ and the imaginary parts of the eigenvalues of the complex skew-symmetric part of $H(j\omega)$ are plotted against the frequency ω on the horizontal axis in Figure 4.10(a) and Figure 4.10(b), respectively. The blue circles indicate when the passive power transmission condition (ii) is satisfied, and the red asterisks indicate when it is not. From this figure, we can see that if the conductance of the transmission lines is non-zero, the complex symmetric part of $G(j\omega)$ is not semi-positive definite in the low-frequency band.

The meaning of the passive power transmission condition (iii), which appeared as a condition for P_G in Equation 4.34 to be semi-positive definite, can also be explained as follows. Consider the state equation of the internal voltage in the electrical subsystem G given in Equation 4.22:

$$\tau \dot{E}^{\text{lin}} = AE^{\text{lin}} + B\delta^{\text{lin}}$$

Let us focus on the limit where the time constant $(\tau_i)_{i \in I_G}$ tends to 0. This corresponds to considering the limit where "the time it takes for the internal voltage to reach a steady state is much shorter than the variation of δ^{lin} ." In this case, the following approximation holds:

$$E^{\text{lin}}(t) \simeq -A^{-1}B\delta^{\text{lin}}(t), \quad \forall t \geq 0 \quad (4.63)$$

However, if A is unstable, i.e., if the passive power transmission condition (i) does not hold, the state E^{lin} diverges. Systems with state variables that have different time scales are called **singularly perturbed systems** [24] in the field of control engineering. A differential equation system with sufficiently small time constants can be approximated by an algebraic equation system. In fact, the dynamic characteristics of internal voltage often have smaller time constants than the mechanical turbine dynamics.

Assuming that equation 4.63 holds as an equality, substituting it into the output equation of equation 4.22 yields a low-dimensional approximation of the electrical subsystem as follows:

$$\hat{G} : \begin{cases} \dot{\hat{\delta}}^{\text{lin}} = u_G \\ y_G = L_0 \hat{\delta}^{\text{lin}} \end{cases} \quad (4.64)$$

However, to indicate that this is an approximation, the state variable is distinguished as $\hat{\delta}^{\text{lin}}$.

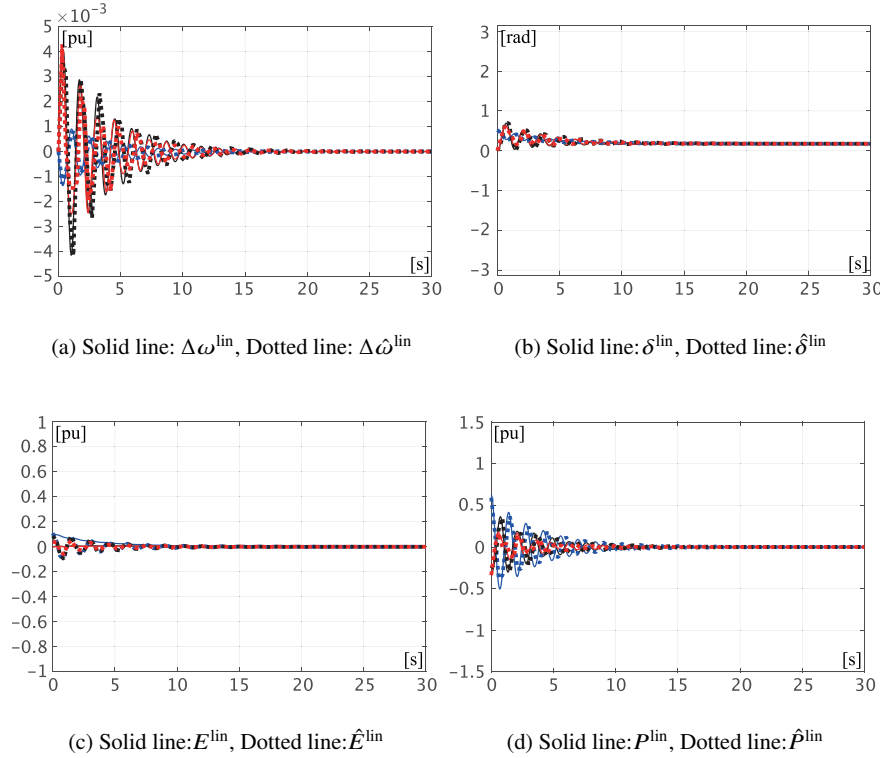


Fig. 4.11 Time response when low-dimensional approximation is applied
(Blue: Generator 1, Black: Generator 2, Red: Generator 3)

Using the low-dimensional approximation of this singular perturbation system, the entire approximate linear model of equation 4.9 is approximated as a system of coupled differential equations with two second-order oscillators:

$$M\ddot{\delta}^{\text{lin}} + D\dot{\delta}^{\text{lin}} + \omega_0 L_0 \delta^{\text{lin}} = 0 \quad (4.65)$$

From this result, it can be understood that the passive power transmission condition (iii) represents the "semi-positive definiteness of the spring constant matrix" in the case of small time constants. Furthermore, the electrical subsystem G of Equation 4.22 can be interpreted as corresponding to a dynamic spring constant.

Example 4.5 Low-dimensional approximation for an approximate linear model As a reference, the time response of the second-order oscillator system of Equation 4.65 for the approximate linear model discussed in Example 4.2 is shown in Figure 4.11. The solid lines represent the response of the original approximate linear model, while the dashed lines represent the response of the second-order oscillator system obtained

by applying the low-dimensional approximation of the singular perturbation system. In addition,

$$\Delta\hat{\omega}^{\text{lin}} := \omega_0^{-1}\dot{\hat{\delta}}^{\text{lin}}, \quad \hat{E}^{\text{lin}} := -A^{-1}B\hat{\delta}^{\text{lin}}, \quad \hat{P}^{\text{lin}} := L\hat{\delta}^{\text{lin}} + CE^{\text{lin}}$$

The initial values for the approximate linear model are given by:

$$\hat{\delta}^{\text{lin}}(0) = \begin{bmatrix} \frac{\pi}{6} \\ 0 \\ 0 \end{bmatrix}, \quad \Delta\hat{\omega}^{\text{lin}}(0) = \begin{bmatrix} 0 \\ 0 \\ 0 \end{bmatrix}$$

From Figure 4.11, it can be seen that the time response of both systems matches well in terms of the peak values and decay rates of the oscillations.

4.3.5 Necessary condition for the steady-state stability of the approximate linear model \ddagger

In the following, we discuss the necessity of the passive power transmission condition (iii) for the steady-state stability of the approximate linear model in equation 4.9. Specifically, we show that the passive power transmission condition (iii) is a necessary condition for the steady-state stability of the approximate linear model regardless of the physical constants of the generator group.

Note that as shown in section 4.3.4, the passive power transmission condition (i) is a necessary condition for the stability of the approximate linear model even in the limit where the time constants $(\tau_i)_{i \in \mathcal{I}G}$ are sufficiently small. This can be verified by the fact that if the matrix A is unstable, the low-dimensional approximation of the singular perturbation system in equation 4.63 cannot be applied, and the internal voltage diverges.

When the passive power transmission condition (ii) does not hold, L_0 is generally not symmetric, so a generalized version of the passive power transmission condition (iii) was introduced to apply it to non-symmetric L_0 as well:

$$\Lambda(L_0) \subseteq [0, \infty) \tag{4.66}$$

Here, $\Lambda(L_0)$ denotes the set of eigenvalues of L_0 . The condition in Equation 4.66 represents that all eigenvalues of L_0 are "non-negative real numbers". In the following, we refer to this generalized condition as the passive electrical condition (iii)', defined in Definition 4.4. Note that when L_0 is symmetric, the passive electrical conditions (iii) and (iii)' are equivalent. The following lemma is proven.

Lemma 4.1 (Necessary condition for the small signal stability of a second-order oscillator system) Consider the second-order oscillator system given by Equation 4.65. For any initial conditions and any positive definite $(M_i, D_i)_{i \in \mathcal{I}G}$, the necessary condition for the existence of a constant c_0 such that Equation 4.67 holds as $t \rightarrow \infty$ is that the passive power condition (iii)' holds.

$$\lim_{t \rightarrow \infty} \hat{\delta}^{\text{lin}}(t) = c_0 \mathbf{1} \quad (4.67)$$

Proof If the passive transmission condition (iii)' does not hold, we show that there exist positive constants $(M_i, D_i)_{i \in \mathcal{I}_G}$ such that Equation 4.67 does not hold. For this purpose, we discuss the following two cases:

- (a) There exist eigenvalues of L_0 with negative real part or purely imaginary part.
- (b) There exist eigenvalues of L_0 with positive real part and nonzero imaginary part.

First, let us consider case (a). In what follows, we choose the constant matrices $M = \omega_0 I$ and $D = \omega_0 d I$. Then, the eigenvalue equation for Equation 4.65 is given by:

$$\begin{bmatrix} 0 & I \\ -L_0 & -dI \end{bmatrix} \begin{bmatrix} v \\ w \end{bmatrix} = \lambda \begin{bmatrix} v \\ w \end{bmatrix}$$

Eliminating w by substitution from this equation, we obtain:

$$(\lambda^2 I + d\lambda I + L_0) v = 0$$

This eigenvalue equation implies that v is an eigenvector of L_0 , and for its eigenvalue κ , we have:

$$\lambda^2 + d\lambda + \kappa = 0 \iff \lambda = \frac{-d \pm \sqrt{d^2 - 4\kappa}}{2} \quad (4.68)$$

Therefore, to show that the real part of $\sqrt{d^2 - 4\kappa}$ is greater than d in case (a), it suffices to prove that $\sqrt{d^2 - 4\kappa}$ has a larger real part than d in the case where the real part of κ is negative or the real part of κ is zero and the imaginary part of κ is nonzero. In general, for any complex number z , we have:

$$\operatorname{Re}[z] = \sqrt{\operatorname{Re}[z^2] + (\operatorname{i}[z])^2}$$

Using this formula with $z = \sqrt{d^2 - 4\kappa}$, we obtain:

$$\operatorname{Re}\left[\sqrt{d^2 - 4\kappa}\right] = \sqrt{d^2 - 4 \operatorname{Re}[\kappa] + (\operatorname{i}[\kappa])^2}$$

This value is always greater than d in case (a), where the real part of κ is negative or the real part of κ is zero and the imaginary part of κ is nonzero. Therefore, the 2-degree-of-freedom oscillator system in equation 4.65 is unstable in case (a).

Next, consider the case (b). Below, it is shown that there exists a positive definite number d such that the eigenvalue λ of Equation 4.68 becomes purely imaginary. If the real matrix L_0 has complex eigenvalues, there must be at least one with a negative imaginary part. Denote this eigenvalue by $\kappa = \alpha + \beta j$, where $\alpha > 0$ and $\beta < 0$. It is shown that there exist some $\omega \neq 0$ and $d > 0$ that satisfy

$$-d + \sqrt{d^2 - 4\kappa} = \omega j$$

Moving $-d$ to the left-hand side and squaring both sides gives:

$$-4(\alpha + \beta j) = 2d\omega j - \omega^2$$

This equation is satisfied if we choose $\omega = 2\sqrt{\alpha}$ and $d = -\frac{\beta}{\sqrt{\alpha}}$. Therefore, the second-order oscillator system has a steady-state oscillatory solution, and Equation 4.67 does not hold. \square

Lemma 4.1 shows that the passive power transfer condition (iii)' is a necessary condition for the steady-state stability of an approximate linear model for any generator group's physical parameters in the limit of small internal voltage time constants. Furthermore, Theorem 4.1 demonstrates that when the passive power transfer conditions (i)–(iii) hold, the approximate linear model is stable for any physical parameters. Based on these facts, the conclusion of this section is summarized in the following theorem.

Theorem 4.3 (Small signal stability of linearized models) *For any positive parameters $(M_i, D_i, \tau_i)_{i \in IG}$, the necessary condition for the steady-state stability of the linearized model in Equation 4.9 is that the passive power transmission conditions (i) and (iii)' in Definition 4.4 hold.*

In particular, if the passive power transmission condition (ii) holds, then the necessary and sufficient condition for the above steady-state stability is that the passive power transmission conditions (i) and (iii)' hold.

We present an analytical example of the small signal stability of the linear approximate model using Theorem 4.3.

Example 4.6 Small signal stability analysis based on the passive power transmission conditions

Using Theorem 4.3, let's analyze the small signal stability of the approximate linear model consisting of three generators discussed in Example 4.2. The physical constants of the generators are set to the same values as in Example 4.2. Since the passive power transmission condition (i) is satisfied for all parameters, the region of parameters where passive power transmission condition (iii)' is not satisfied is overlaid on Figure 4.12. However, the red region shows eigenvalues of L_0 in which the real part is negative, while the purple region shows eigenvalues of L_0 that are complex. The region on the horizontal axis where θ_2 is zero represents the case where the passive power transmission condition (ii) holds.

Theorem 4.3 shows that the red and purple regions are "dangerous parameter regions where the approximate linear model will always become unstable for a certain setting of physical constants." Additionally, when the passive power transmission condition (ii) holds, i.e., for parameters on the horizontal axis where θ_2 is zero, it is shown that the approximate linear model will always be steady-state stable regardless of the values of these constants as long as θ_1 is set to a non-red value.

The noteworthy point from the result in Figure 4.12 is that the red parameter region accurately captures part or all of the boundary of the blue parameter region,

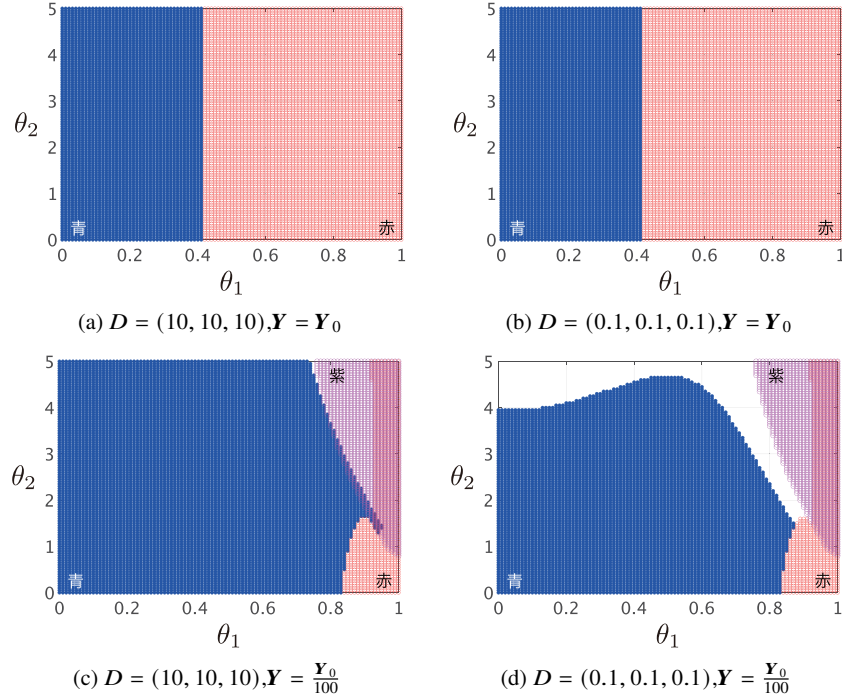


Fig. 4.12 Regions of parameters for which the approximate linear model is stable

where the model is steady-state stable under the physical constants mentioned above. The necessity of the passive power transmission condition (iii)' shown in Theorem 4.3 implies that there is at least one setting of physical constants for which the approximate linear model becomes unstable. Therefore, it is not always possible to accurately capture the parameter region that ensures steady-state stability for specific constants set in Example 4.2. On the other hand, the fact that part of the boundary of the blue region is accurately captured suggests that the approximate linear model is often unstable when L_0 has eigenvalues with negative real parts.

Also, in cases (a) and (b), it can be seen that there is no purple region. That is, for all the explored parameters, the eigenvalues of L_0 are real numbers. Generally, unless θ_2 is zero, L_0 is an asymmetric matrix, so it is not obvious that L_0 only has real eigenvalues. On the other hand, in cases (c) and (d) where the admittance matrix is multiplied by $\frac{1}{100}$, it is also known that L_0 has complex eigenvalues when θ_1 and θ_2 are relatively large. However, in realistic settings, it has been confirmed that L_0 mostly has real eigenvalues.

Mathematical Appendix

Lemma 4.2 Consider a stable and square transfer function:

$$Q(s) = C(sI - A)^{-1}B + D$$

where (A, B) is controllable and (C, A) is observable. The necessary and sufficient condition for $Q(s)$ to be positive real is the existence of a positive definite symmetric matrix P such that:

$$\begin{bmatrix} A^T P + PA & PB - C^T \\ B^T P - C & -(D + D^T) \end{bmatrix} \leq 0$$

The proof can be found in [25, Theorem 5.31] or [26, Theorem 3], among others. Also, [27] provides a detailed overview of related results.

Lemma 4.3 Consider a stable and square transfer function

$$Q(s) = C(sI - A)^{-1}B + D$$

where (A, B) is controllable and (C, A) is observable. The necessary and sufficient condition for $Q(s)$ to be negative imaginary is that D is symmetric and there exists a positive definite symmetric matrix P such that:

$$A^T P + PA \leq 0, \quad -PA^{-1}B = C^T$$

The proof can be found in [23, Lemma 7], among others.

Chapter 5

Stabilization control of power system models

In this Chapter, we will explain frequency stabilization control and transient stabilization control of power system models. The structure of this chapter is as follows. First, in Section 5.1, we outline the automatic generation control, which is a representative example of frequency stabilization control, to suppress the deviation of angular frequency caused by load variations, and confirm through numerical simulations that the steady-state power flow state changes by adjusting the parameters of the controller. Next, in Section 5.2, as an advanced topic, we perform mathematical stability analysis of frequency stabilization control. In particular, based on passivity that does not depend on equilibrium points for nonlinear systems, we show the relationship between the stability region of the power system model and the convex region of potential energy function. Furthermore, in Section 5.3, we explain the configuration and functions of standard automatic voltage regulators and power system stabilizers used for transient stabilization control. Finally, in Section 5.4, as an advanced topic, we explain the design methodology of power system stabilizers based on retrofit control theory.

5.1 Frequency stabilization control

5.1.1 Automatic generation control using broadcast-type PI controller

5.1.1.1 Overview of Automatic Generation Control

In this section, we will explain the principle of **Automatic Generation Control (AGC)** which adjusts the generation output appropriately in response to unknown load variations. Automatic Generation Control adjusts the generation output by performing control actions such as increasing the generation output when the power supply is insufficient compared to the demand, and decreasing the generation output when the power supply is excessive, based on the observed frequency devia-

tions of multiple generators. This control action is based on the general characteristic of power systems that negative frequency deviations occur when the power supply is insufficient compared to the demand, and positive frequency deviations occur when the power supply is excessive. In power system engineering, the overall control to asymptotically converge the frequency deviation to zero is generally referred to as **Frequency Stabilization Control**. Automatic Generation Control is one of the methods for Frequency Stabilization Control.

In actual power system operation, the central dispatch center performs Automatic Generation Control. Although the basic operating principle is common, there are several methods depending on the objectives. The target is to maintain the frequency within a range of about $\pm 0.2\text{Hz}$ with respect to the reference frequency of 50Hz or 60Hz. Note that the frequency deviation of the voltage phasor at a nearby substation is often observed instead of the frequency deviation of the generator, because the frequency of the voltage phasor at the substation is generally close to that of the generator. Also, one of the challenges of Automatic Generation Control is that there are many unknown constants and variables in the actual power system. For example, it is possible to roughly predict the total amount of load in a time scale of about 30 minutes, but it is not possible to accurately grasp the values of individual loads that change every moment. It is also difficult to accurately know all the constants such as the impedance of each transmission line. Therefore, it is necessary to design control algorithms that can be applied without knowing the accurate model of the entire power system. In actual power system operation, weather forecast information, temperature data, historical data, and other information are used to predict changes in total demand for certain areas to some extent. The size of the area and the method used vary, but it is impossible to predict the demand completely.

On the other hand, as confirmed in the numerical examples in Section 3.4, when the supply-demand balance is not maintained, various problems such as frequency deviation and tie-line power flow deviation may occur. Therefore, it is important to establish an effective Automatic Generation Control method that can mitigate the impact of unknown load variations and maintain the stability of the power system. In this section, we will explain the principle of Automatic Generation Control using a broadcast-type PI controller, which is one of the methods for Frequency Stabilization Control. Therefore, it is necessary to design a control algorithm that can be applied without knowing the accurate model of the entire power system. In actual power system operation, weather forecast information, temperature data, historical data, and other information are used to predict changes in total demand for certain areas to some extent. The size of the area and the method used vary, but it is impossible to predict the demand completely.

5.1.1.2 Formulation of automatic generation control

In the following, we consider a generator model with the bus voltage phasor as the input, as discussed in Section 2.3.2. The dynamic characteristics of the generator are restated as follows:

$$\begin{aligned}\dot{\delta}_i &= \omega_0 \Delta \omega_i \\ M_i \Delta \dot{\omega}_i &= -D_i \Delta \omega_i - P_i + P_{\text{mechi}} \\ \tau_i \dot{E}_i &= -\frac{X_i}{X'_i} E_i + \left(\frac{X_i}{X'_i} - 1 \right) |V_i| \cos(\delta_i - \angle V_i) + V_{\text{field}i}\end{aligned}\quad (5.1a)$$

When considering active power and reactive power as outputs, we have:

$$\begin{aligned}P_i &= \frac{E_i |V_i|}{X'_i} \sin(\delta_i - \angle V_i), \\ Q_i &= \frac{E_i |V_i|}{X'_i} \cos(\delta_i - \angle V_i) - \frac{|V_i|^2}{X'_i}\end{aligned}\quad (5.1b)$$

According to this expression, the load model for inputting the phase of the busbar voltage and outputting the active and reactive powers is also shown again. The constant impedance model is given by:

$$P_i = -\frac{|V_i|^2}{\operatorname{Re}[\bar{z}_{\text{load}i}^*]}, \quad Q_i = -\frac{|V_i|^2}{i \operatorname{Im}[\bar{z}_{\text{load}i}^*]} \quad (5.2a)$$

where $\bar{z}_{\text{load}i}^*$ is a constant representing the impedance of the load.

Similarly, the constant current model is expressed as:

$$P_i = |V_i| \operatorname{Re}[I_{\text{load}i}^*], \quad Q_i = -|V_i| i [I_{\text{load}i}^*] \quad (5.2b)$$

where $I_{\text{load}i}^*$ is a constant representing the current phase of the load.

The constant power model is given by:

$$P_i = P_{\text{load}i}^*, \quad Q_i = Q_{\text{load}i}^* \quad (5.2c)$$

where $P_{\text{load}i}^*$ and $Q_{\text{load}i}^*$ are constants.

These generator models and load models are combined to describe the entire power system using a differential-algebraic equation (DAE) model, as shown in the algebraic equation system:

$$\begin{aligned}P_1 + jQ_1 &= \sum_{j=1}^N \bar{Y}_{1j} |V_1| |V_j| e^{j(\angle V_1 - \angle V_j)} \\ &\vdots \\ P_N + jQ_N &= \sum_{j=1}^N \bar{Y}_{Nj} |V_N| |V_j| e^{j(\angle V_N - \angle V_j)}\end{aligned}\quad (5.3)$$

where the generator bus indices are denoted by the set \mathcal{IG} and the load bus indices are denoted by the set \mathcal{IL} , and without loss of generality, we can define:

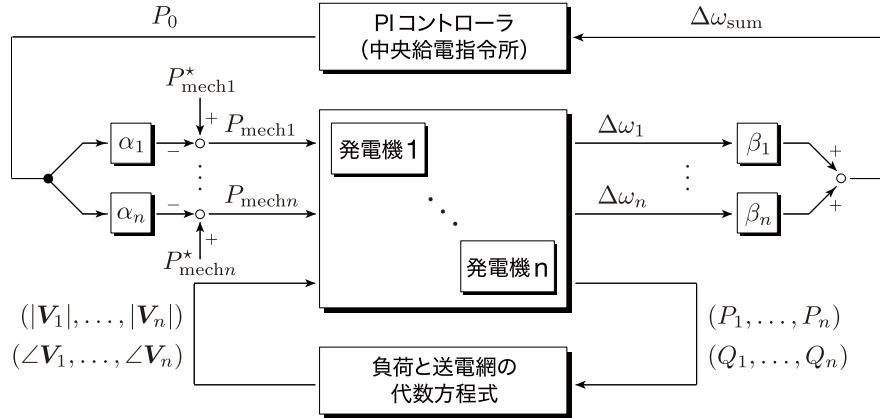


Fig. 5.1 Signal transmission structure for automatic power generation control

$$\mathcal{I}_G := \{1, \dots, n\}, \quad \mathcal{I}_L := \{n+1, \dots, n+m\}$$

where n represents the total number of generator buses and m represents the total number of load buses. Furthermore, N represents the total number of buses, which is equal to $n + m$.

The automatic generation control (AGC) is a control algorithm that adjusts the mechanical input $P_{\text{mech}i}$ in Equation (5.1). Here, we consider a broadcast-type PI controller that observes the weighted sum of frequency deviations for all generators and sends a control input with appropriate weighting to all generators. Specifically, for each $i \in \mathcal{I}_G$, we set:

$$P_{\text{mech}i}(t) = P_{\text{mech}i}^* - \alpha_i \underbrace{\left(k_P \Delta\omega_{\text{sum}}(t) + k_I \int_0^t \Delta\omega_{\text{sum}}(\tau) d\tau \right)}_{P_0(t)} \quad (5.4a)$$

where $P_{\text{mech}i}^*$ is a constant representing the standard setting value of the mechanical input. Moreover, α_i is a non-negative constant specifying the contribution of generator i , and:

$$\Delta\omega_{\text{sum}}(t) := \sum_{i=1}^n \beta_i \Delta\omega_i(t)$$

is the weighted sum of frequency deviations with non-negative weights β_i . Furthermore, k_P and k_I are positive constants representing the gains of the PI controller. This AGC controller has a structure where the generated signal $P_0(t)$, which is produced by a single PI controller with weighting of α_i and β_i , is simultaneously broadcasted to all generators (Figure 5.1). Note that Equation 5.4a can be expressed as a differential equation as follows:

$$\begin{aligned}\dot{\xi} &= \Delta\omega_{\text{sum}} \\ P_{\text{mech}i} &= P_{\text{mech}i}^* - \alpha_i (k_p \Delta\omega_{\text{sum}} + k_I \xi)\end{aligned}\quad (5.4b)$$

In electric power systems engineering, the non-negative constant α_i is referred to as the **participation factor** of generator i . It should be noted that in real-world thermal power generation and nuclear power generation, there is a **prime mover** that generates mechanical input by rotating a turbine using high-pressure steam generated by thermal or nuclear power. The prime mover incorporates a **governor** that automatically controls the rotation speed of the generator. In order to analyze more realistic automatic generation control, it is necessary to consider a prime mover model that takes input from the central dispatch center as setpoint and outputs mechanical input to the generator [?, Chapter 3].

By changing the ratio of participation factors, it is possible to adjust the values of effective power supplied by each generator in a balanced steady-state load flow condition. From the perspective of system control engineering, this can be interpreted as "moving the stable equilibrium point of the power system model by switching controllers." As analyzed in Chapter 4, the stability of the power system depends on the choice of equilibrium point. The total generation cost and transmission loss of the power system also depend on the choice of equilibrium point. Therefore, appropriately switching the participation factors according to the distribution of load can lead to improved system stability and reduced economic costs.

In actual power system operation, the updating of participation factors is typically done at intervals of several minutes to several tens of minutes [15, Section 11.1]. In the terminology of power system engineering, the scheme for updating these participation factors is called **economic load dispatching control** (EDC). The control algorithm that uses the participation factors as constants during the updating interval is called **load frequency control** (LFC). However, it should be noted that there may be cases where there is no clear distinction between economic load dispatching control and load frequency control in the literature, or where economic load dispatching control is considered as a different scheme, so caution is necessary.

5.1.2 Numerical simulation of frequency stabilization control

Let's verify the effectiveness of frequency stabilization control using a simple example.

Example 5.1 Frequency stabilization by Automatic Generation Control Consider the power system model consisting of 3 busbars as discussed in Examples 2.1, 3.2, and 3.3. The physical constants of the generators and transmission lines are set to the same values as in Example 3.3, and the initial values of the internal states of the generators are set to the steady-state values shown in Table 3.4. In addition, the field input is assumed to be constant at the values shown in Table 3.4.

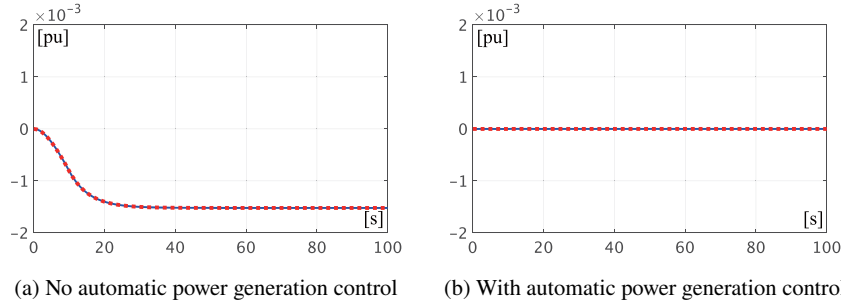


Fig. 5.2 Time response of angular frequency deviation to power consumption increase
(Blue solid line: $\Delta\omega_1$, Red dashed line: $\Delta\omega_3$)

The load at busbar 2 is set to a constant power model, and we consider a case where the consumption of active power increases by 1% from the initial steady-state load flow condition. First, we show the time response of the frequency deviation when there is no automatic generation control and the mechanical input of the generators is constant at the values shown in Table 3.4, as shown in Figure 5.2(a). It can be seen that the steady-state value of the frequency deviation does not become zero because the supply and demand are not balanced due to the increased power consumption by the load.

Next, we show the results when the broadcast-type PI controller of Equation 5.4 is incorporated as automatic generation control, with the parameters of the controller set to the values shown in Table 5.1(a), as shown in Figure 5.2(b). From this figure, it can be seen that the frequency deviation hardly occurs even when the consumption of load power changes, due to the effectiveness of automatic generation control.

Table 5.1 Controller Parameter Setting

Setup	k_P	k_I	α_1	α_3	β_1	β_3
(a)	100	500	1	3	1	3
(b)	100	500	1	1	1	1
(c)	100	500	3	1	3	1

Next, let us confirm the change in steady-state power flow conditions by adjusting the contribution coefficients of the broadcast-type PI controller in Equation 5.4 to achieve supply-demand balance.

Example 5.2 Change in steady-state power flow conditions by adjusting contribution coefficients Consider a power system model consisting of two generators and one load, similar to Example 5.1. Here, we confirm that the ratio of active power

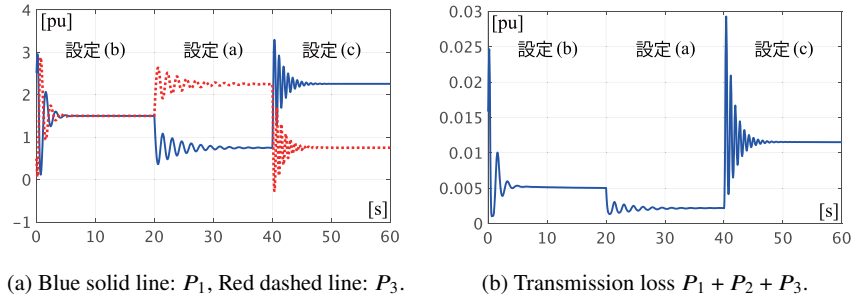


Fig. 5.3 Time response of effective power to changes in contribution factor

supplied by Generator 1 and Generator 3 changes by varying the contribution coefficients of the broadcast-type PI controller in Equation 5.4. Specifically, we switch the contribution coefficients as follows:

- Parameters of 5.1 (b) are set for 0 [s] to 20 [s].
- Parameters of 5.1 (a) are set for 20 [s] to 40 [s].
- Parameters of 5.1 (c) are set for 40 [s] to 60 [s].

The resulting time response is shown in Figure 5.3(a). The solid blue line represents the value of active power supplied by Generator 1 (P_1), and the dashed red line represents the value of active power supplied by Generator 3 (P_3). From this result, it can be seen that the ratio of P_1 and P_3 in the steady-state power flow conditions matches the ratio of contribution coefficients α_1 and α_3 .

Next, the time response of the total active power transmission loss $P_1 + P_2 + P_3$, which represents the power transmission loss due to active power, is shown in Figure 5.3(b). Note that P_2 is the active power consumed by the load and its value is constant at -3.

From this figure, it can be seen that the magnitude of active power transmission loss varies depending on the realized steady-state power flow conditions. In particular, when the parameters of the broadcast-type PI controller are set to the values in Table 5.1 (a), i.e., when power is mainly supplied using the lossless transmission line between Bus 2 and Bus 3, the total power transmission loss of the entire power system is smaller, which is consistent with the discussion in Example 3.2. The admittance of the transmission lines is set to the values in Equation (3.12).

As shown in Example 5.2, by adjusting the contribution coefficients of a broadcast-type PI controller, it is possible to change the steady-state power flow condition. At the same time, the magnitude of transmission losses and the required generation cost for each steady-state power flow condition also change. Therefore, by appropriately controlling the contribution coefficients, it is possible to achieve more economical system operation. However, it should be noted that a steady-state power flow condition with lower economic costs is not necessarily a highly stable equilibrium point,

so it is important to carefully consider trade-offs between economic efficiency and stability.

5.2 Mathematical stability analysis of frequency stabilization control system

5.2.1 Power system model under consideration

5.2.1.1 Assumptions on Power System Model and Automatic Generation Control

In Section 4.1, an approximate linear model was derived under the assumption that the power system model is in the vicinity of steady-state power flow conditions, and necessary and sufficient conditions for steady-state stability were analyzed. In this section, using the concept of passivity for nonlinear systems, we analyze the frequency stability of the power system model described as a system of differential-algebraic equations, taking into consideration the stability of the entire feedback control system with automatic generation control. Specifically, we conduct stability analysis under the following assumptions.

- All generators are expressed with the generator model of Equation (5.2). However, it is assumed that the field voltage of each generator is set to a constant.
- All loads are expressed with the constant power model of Equation 5.2c.
- For algebraic equations for the power grid of Equation 5.3, conductance of all transmission lines is assumed to be 0.
- For the broadcast-type PI controller of Equation (5.4), automatic generation control is performed. However, it is assumed that α_i and β_i are equal for all $i \in \mathcal{I}_G$ for the weight of the participation factor and frequency deviation.

The first and second assumptions refer to considering a standard model for the generator and load in the power system. The third assumption regarding the transmission network implies that transmission losses are assumed to be zero, which is essential for conducting stability analysis mathematically. In reality, it is not possible to completely eliminate transmission losses in a power system, but reducing transmission losses can be achieved by transmitting power at higher voltages with lower currents. The discussion in this section assumes that transmission losses can be approximately considered as zero due to high-voltage transmission. The fourth assumption is necessary for the input-output characteristics of the broadcast-type PI controller to be passive. However, it should be noted that even if some coefficients are zero, as long as at least one contribution coefficient α_i for $i \in \mathcal{I}_G$ is positive, it is acceptable.

Furthermore, as shown in the analysis of Section 3.5:

- The frequency deviation of all generators become equalize under a steady power flow distribution.

The following frequency stability analysis is based on this fact. Specifically, in order for the integral controller in the broadcast-type PI controller to make the steady-state angular frequency deviations of all generators zero, it is necessary for the above-mentioned angular frequency deviations to automatically synchronize with each other. Note that this requires the characteristic of automatic synchronization among the angular frequency deviations using only one integrator included in the broadcast-type PI controller.

5.2.1.2 Representation of power system with automatic generation control as a feedback system

Similar to the discussion in Section 4.3.2, we consider representing the power system model as a feedback system consisting of two subsystems. The first subsystem is described by the following equations:

$$\begin{aligned} \mathbb{F} : \quad M\Delta\dot{\omega} &= -D\Delta\omega + u_{\mathbb{F}} + P_{\text{mech}}^* \\ y_{\mathbb{F}} &= \omega_0\Delta\omega \end{aligned} \quad (5.5)$$

However, $\Delta\omega$ is a vector composed of $\Delta\omega_i$ stacked vertically, and M and D are matrices formed by diagonally arranging M_i and D_i . Also, P_{mech}^* is a constant vector composed of $P_{\text{mech}i}^*$. This \mathbb{F} is equivalent to the mechanical subsystem in Section 4.3.2, except for the difference in the constant vector P_{mech}^* . The second subsystem is represented by the nonlinear differential-algebraic equation system of the electrical subsystem in Section 4.3.2, given by:

$$\begin{aligned} \dot{\delta}_i &= u_{G_i} \\ G_i : \tau_i \dot{E}_i &= -\frac{X_i}{X'_i} E_i + \left(\frac{X_i}{X'_i} - 1 \right) |V_i| \cos(\delta_i - \angle V_i) + V_{\text{field}i}^* \\ y_{G_i} &= \frac{E_i |V_i|}{X'_i} \sin(\delta_i - \angle V_i) \end{aligned} \quad (5.6a)$$

The voltage phasor of the bus in Equation 5.6a satisfies a set of simultaneous equations for all generator buses as follows:

$$\begin{aligned} P_i &= \sum_{j=1}^N B_{ij} |V_i| |V_j| \sin(\angle V_i - \angle V_j) & i \in \mathcal{I}_G \\ Q_i &= -\sum_{j=1}^N B_{ij} |V_i| |V_j| \cos(\angle V_i - \angle V_j) \end{aligned} \quad (5.6b)$$

and a set of coupled equations for all load bus bars given by:

$$\begin{cases} P_{\text{load}i}^{\star} = \sum_{j=1}^N B_{ij} |V_i| |V_j| \sin(\angle V_i - \angle V_j) \\ Q_{\text{load}i}^{\star} = - \sum_{j=1}^N B_{ij} |V_i| |V_j| \cos(\angle V_i - \angle V_j) \end{cases} \quad i \in \mathcal{I}_L \quad (5.6c)$$

In addition, the active power P_i and reactive power Q_i in Equation (5.6b) are defined by Equation (5.1b). Also, B_{ij} represents the (i, j) element of the susceptance matrix B , which is the imaginary part of the admittance matrix Y . In the following, we consider the combination of Equations (5.6a) to (5.6c) for all generator buses $i \in \mathcal{I}_G$ as one subsystem, and denote it as the electrical subsystem \mathbb{G} .

Furthermore, the dynamic characteristics of the broadcast-type PI controller in Equation (5.4) are represented as follows:

$$\mathbb{K} : \begin{cases} \dot{\xi} = h^T u_{\mathbb{K}} \\ y_{\mathbb{K}} = h \left(k_p h^T u_{\mathbb{K}} + k_I \xi \right) \end{cases} \quad (5.7)$$

where h is a column vector consisting of α_i .

In this case, the inputs and outputs of the aforementioned subsystems \mathbb{F} , \mathbb{G} , and controller \mathbb{K} are interconnected as follows:

$$u_{\mathbb{F}} = -y_{\mathbb{K}} + v_{\mathbb{F}}, \quad u_{\mathbb{K}} = \frac{1}{\omega_0} y_{\mathbb{F}} \quad (5.8a)$$

$$u_{\mathbb{G}} = y_{\mathbb{F}}, \quad v_{\mathbb{F}} = -y_{\mathbb{G}} \quad (5.8b)$$

This represents the entire feedback control system incorporating automatic generation control. However, it should be noted that the "power balance equation" block includes unknown model parameters such as load consumption power and transmission line admittance. The block diagram of the entire feedback control system is shown in Figure 5.4. Please note that the block representing the "power balance equation" includes unknown model parameters such as load consumption power and transmission line admittance.

5.2.2 Equilibrium-independent passivity of power system models

5.2.2.1 Equilibrium-independent passivity

The discussion in Section 4.3.2 was based on an approximate linear model, and the convergence to zero of the internal state represented the asymptotic convergence to a specific steady-state power flow condition in the original nonlinear model. On the other hand, in power system models represented as nonlinear differential-algebraic equation systems, the internal state does not necessarily converge to zero even at steady-state power flow conditions where power supply and demand are balanced.

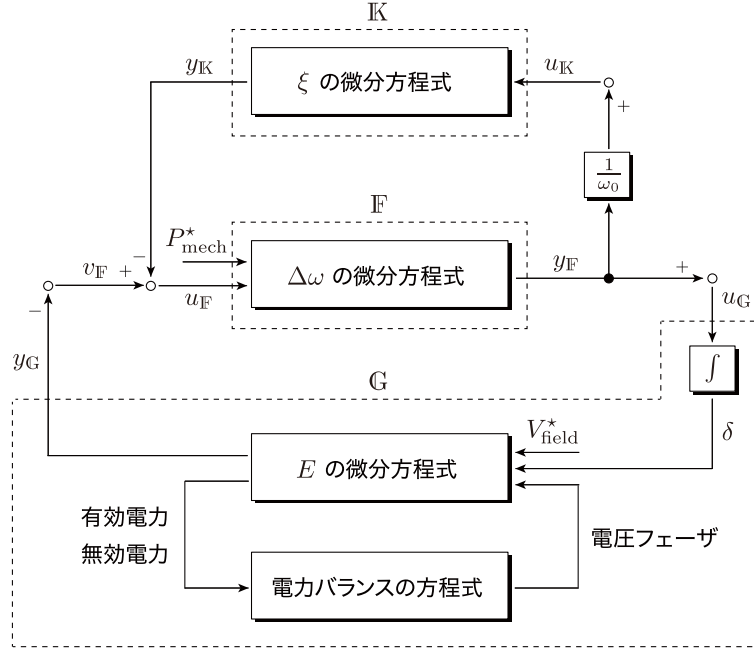


Fig. 5.4 Feedback control system incorporating automatic power generation control

Furthermore, the steady-state power flow condition itself can change depending on set values such as mechanical inputs. Therefore, it is desirable to conduct stability analysis that does not depend on the selection of individual steady-state power flow conditions (equilibrium points). A concept proposed in control engineering for such analysis is called **equilibrium-independent passivity** [28, 29]. Note that in some literature, it is also referred to as **shifted passivity** [30]. Its definition is given as follows.

Definition 5.1 (Equilibrium-independent passivity) Let us consider a nonlinear system:

$$\Sigma : \begin{cases} E\dot{x} = f(x) + Bu + Rd^* \\ y = h(x) \end{cases} \quad (5.9)$$

where $f : X \rightarrow \mathbb{R}^n$ and $h : X \rightarrow \mathbb{R}^m$ are smooth functions, and $B \in \mathbb{R}^{n \times m}$, $E \in \mathbb{R}^{n \times n}$, $R \in \mathbb{R}^{n \times p}$ are matrices. Also, $d^* \in \mathbb{R}^p$ is a constant vector. Here, X represents the admissible state space.

The set of achievable equilibrium points by constant inputs is denoted as:

$$\mathcal{E}_\Sigma := \{x^* \in X : \text{there exists } u^* \text{ satisfying } 0 = f(x^*) + Bu^* + Rd^*\}$$

For each equilibrium point $x^* \in \mathcal{E}\Sigma$, if there exists a differentiable positive semi-definite function $W_{x^*} : \mathcal{X} \rightarrow \mathbb{R}_{\geq 0}$ such that $W_{x^*}(x^*) = 0$ and for any input u , the following inequality holds for all $t \geq 0$:

$$\frac{d}{dt} W_{x^*}(x(t)) \leq (u(t) - u^*)^\top (y(t) - y^*), \quad \forall t \geq 0$$

then Σ is called **equilibrium-independent passive**. Here, u^* and y^* denote the steady-state input and output at the equilibrium point, respectively, and are defined as:

$$u^* := -(B^\top B)^{-1} B^\top \{f(x^*) + R d^*\}, \quad y^* := h(x^*)$$

In particular, if there exists a positive constant ρ such that the following inequality holds for all $t \geq 0$:

$$\frac{d}{dt} W_{x^*}(x(t)) \leq (u(t) - u^*)^\top (y(t) - y^*) - \rho \|y(t) - y^*\|^2, \quad \forall t \geq 0$$

then Σ is called **equilibrium-independent strictly passive**.

In Definition 5.1, the passivity of the system is defined with respect to the equilibrium point $x^* \in \mathcal{E}\Sigma$ as a reference. In the context of linear systems, it is known that this definition of passivity is equivalent to the definition of passivity in Section 4.3.2, unless the system has a zero eigenvalue [28]. Note that the function $W_{x^*}(x)$ mentioned above is called the storage function, similar to conventional passivity definitions. It should be noted that this storage function $W_{x^*}(x)$ is an implicit function of the equilibrium point x^* .

COFFEE BREAK

Descriptor representation: The matrix E in Equation 5.9 is introduced to represent the electrical subsystem \mathbb{G} of the differential-algebraic equation system given by Equation (5.6). Specifically, by setting:

$$E = \begin{bmatrix} I & 0 \\ 0 & 0 \end{bmatrix}$$

the system Σ in Equation 5.9 represents the following differential-algebraic equation system:

$$\begin{cases} \dot{x}_1 = f_1(x_1, x_2) + B_1 u + R_1 d^* \\ 0 = f_2(x_1, x_2) \\ y = h(x_1, x_2) \end{cases}$$

When applied to the electrical subsystem \mathbb{G} , x_1 is a vector containing all δ_i and E_i , and x_2 is a vector containing all $|V_i|$ and $\angle V_i$. On the other hand, when

E is regular, it represents a differential equation system like the mechanical subsystem \mathbb{F} given by Equation 5.5. This type of system representation is called the **descriptor representation**.

In reference [29], it is shown that when a system is passive regardless of its equilibrium point, its storage function can be expressed in the form of Equation 5.10 using a certain function $U(x)$:

$$W_{x^*}(x) = U(x) - U(x^*) - \nabla U^\top(x^*)(x - x^*) \quad (5.10)$$

In Definition 5.1, it is a requirement that the storage function $W_{x^*}(x)$ in Equation 5.10 is a positive semi-definite function. Specifically, the condition is that Equation 5.11 holds:

$$U(x) \geq U(x^*) + \nabla U^\top(x^*)(x - x^*) \quad (5.11)$$

If this inequality holds for any pair $(x, x^*) \in \mathcal{X} \times \mathcal{X}$, then for each equilibrium point $x^* \in \mathcal{E}\Sigma$, $W_{x^*}(x)$ is a positive semi-definite function. The inequality in Equation 5.11 expresses the convexity of the function $U(x)$. As will be explained later, the region \mathcal{X} where $U(x)$ is convex plays an important role in stability analysis using passivity that does not depend on the equilibrium point.

COFFEE BREAK

Convex function: A function $f(x)$ is called **convex** if, for any two points (x, y) in its domain and any $\theta \in [0, 1]$, the following inequality holds:

$$f(\theta x + (1 - \theta)y) \leq \theta f(x) + (1 - \theta)f(y), \quad \forall \theta \in [0, 1]$$

In particular, if $f(x)$ is differentiable, a necessary and sufficient condition for $f(x)$ to be convex is that, for any two points (x, y) ,

$$f(x) \geq f(y) + \nabla f^\top(y)(x - y)$$

This inequality means that the graph of $f(x)$ is always above the tangent line to $f(x)$ at the point $x = y$.

Bregman Distance: In statistics, the quantity on the right-hand side of equation 5.10 for a convex function $U(x)$ is called the **Bregman distance** [31] between x and x^* with respect to $U(x)$. If $U(x)$ is chosen to be $|x|^2$, then the Bregman distance $W_{x^*}(x)$ reduces to the Euclidean distance $|x - x^*|^2$.

5.2.2.2 Analysis of the mechanical subsystem

As shown in Section 4.3.2, the mechanical subsystem \mathbb{F} is strongly passive. Similarly, we confirm that \mathbb{F} in Equation 5.5 is also strongly passive regardless of the equilibrium point. First, the mechanical subsystem is represented in the form:

$$\mathbb{F} : \begin{cases} \dot{x}_{\mathbb{F}} = A_{\mathbb{F}}x_{\mathbb{F}} + B_{\mathbb{F}}u_{\mathbb{F}} + R_{\mathbb{F}}d_{\mathbb{F}}^{\star} \\ y_{\mathbb{F}} = C_{\mathbb{F}}x_{\mathbb{F}} \end{cases} \quad (5.12)$$

Here, the state $x_{\mathbb{F}}$ is a vector consisting of $\Delta\omega_i$, and $u_{\mathbb{F}}$ and $y_{\mathbb{F}}$ are vectors consisting of $u_{\mathbb{F}i}$ and $y_{\mathbb{F}i}$, respectively. Also, $d\mathbb{F}^{\star}$ represents P_{mech}^{\star} , and the system matrices are:

$$A_{\mathbb{F}} := -M^{-1}D, \quad B_{\mathbb{F}} := M^{-1}, \quad R_{\mathbb{F}} := M^{-1}, \quad C_{\mathbb{F}} := \omega_0 I$$

Note that the matrices M and D are diagonal matrices composed of M_i and D_i . For an arbitrarily selected equilibrium point $x^{\star}\mathbb{F} \in \mathcal{EF}$, the storage function is chosen as:

$$W_{x_{\mathbb{F}}^{\star}}(x_{\mathbb{F}}) = \frac{\omega_0}{2}(x_{\mathbb{F}} - x_{\mathbb{F}}^{\star})^T M(x_{\mathbb{F}} - x_{\mathbb{F}}^{\star}) \quad (5.13)$$

Here, $(x^{\star}\mathbb{F}, u^{\star}\mathbb{F}, y^{\star}\mathbb{F})$ with respect to the equilibrium point satisfies:

$$0 = A_{\mathbb{F}}x_{\mathbb{F}}^{\star} + B_{\mathbb{F}}u_{\mathbb{F}}^{\star} + R_{\mathbb{F}}d_{\mathbb{F}}^{\star}, \quad y_{\mathbb{F}}^{\star} = C_{\mathbb{F}}x_{\mathbb{F}}^{\star} \quad (5.14)$$

If expressed in the form of Equation 5.10, the storage function can be written as:

$$U_{\mathbb{F}}(x_{\mathbb{F}}) := \frac{\omega_0}{2}x_{\mathbb{F}}^T M x_{\mathbb{F}}$$

Therefore, the storage function can be expressed as:

$$W_{x_{\mathbb{F}}^{\star}}(x_{\mathbb{F}}) = U_{\mathbb{F}}(x_{\mathbb{F}}) - U_{\mathbb{F}}(x_{\mathbb{F}}^{\star}) - \nabla U_{\mathbb{F}}^T(x_{\mathbb{F}}^{\star})(x_{\mathbb{F}} - x_{\mathbb{F}}^{\star})$$

The gradient function of this storage function can be expressed as:

$$\nabla W_{x_{\mathbb{F}}^{\star}}(x_{\mathbb{F}}) = \omega_0 M(x_{\mathbb{F}} - x_{\mathbb{F}}^{\star})$$

Hence, the time derivative of the storage function can be evaluated as:

$$\begin{aligned} \frac{d}{dt}W_{x_{\mathbb{F}}^{\star}}(x_{\mathbb{F}}(t)) &= \nabla W_{x_{\mathbb{F}}^{\star}}^T(x_{\mathbb{F}}(t)) \dot{x}_{\mathbb{F}}(t) \\ &= \nabla W_{x_{\mathbb{F}}^{\star}}^T(x_{\mathbb{F}}(t)) \{A_{\mathbb{F}}(x_{\mathbb{F}}(t) - x_{\mathbb{F}}^{\star}) + B_{\mathbb{F}}(u_{\mathbb{F}}(t) - u_{\mathbb{F}}^{\star})\} \\ &\leq (y_{\mathbb{F}}(t) - y_{\mathbb{F}}^{\star})^T(u_{\mathbb{F}}(t) - u_{\mathbb{F}}^{\star}) - \frac{\min\{D_i\}}{\omega_0} \|y_{\mathbb{F}}(t) - y_{\mathbb{F}}^{\star}\|^2 \end{aligned} \quad (5.15)$$

Here, the derivation of the second equality used the relationship in Equation 5.14.

5.2.2.3 Analysis of feedback system for mechanical subsystem and automatic power generation controller

Similar to the mechanical subsystem, the passivity of the broadcast-type PI controller in equation 5.7 can also be demonstrated. By defining the storage function as:

$$W_{\xi^*}(\xi) := \frac{1}{2}k_I(\xi - \xi^*)^2 \quad (5.16)$$

its time derivative can be evaluated as:

$$\begin{aligned} \frac{d}{dt} W_{\xi^*}(\xi(t)) &= (y_K - y_K^*)^\top (u_K - u_K^*) - k_P u_K^\top h h^\top u_K \\ &\leq (y_K - y_K^*)^\top (u_K - u_K^*) \end{aligned} \quad (5.17)$$

where (ξ^*, u_K^*, y_K^*) represents the equilibrium point and Equation 5.18 is used.

$$\begin{cases} 0 = h^\top u_K^* \\ y_K^* = h(k_P h^\top u_K^* + k_I \xi^*) \end{cases} \quad (5.18)$$

In system control engineering, it is known that a negative feedback system between two passive systems becomes passive again. Based on this fact, a feedback connection is made between the mechanical subsystem \mathbb{F} in Equation 5.5 and the broadcast-type PI controller \mathbb{K} in Equation 5.7, resulting in the system:

$$\mathbb{F}_+ : \begin{cases} M\Delta\dot{\omega} = -D\Delta\omega - h(k_P h^\top \Delta\omega + k_I \xi) + P_{\text{mech}}^* + v_F \\ \dot{\xi} = h^\top \Delta\omega \\ y_F = \omega_0 \Delta\omega \end{cases} \quad (5.19)$$

which is strongly passive regardless of the equilibrium point. In fact, adding the inequalities in Equation 5.15 and Equation 5.17, we obtain:

$$\begin{aligned} \frac{d}{dt} \left\{ W_{x_F^*}(x_F(t)) + \omega_0 W_{\xi^*}(\xi(t)) \right\} \\ \leq (y_F(t) - y_F^*)^\top (v_F(t) - v_F^*) - \frac{\min\{D_i\}}{\omega_0} \|y_F(t) - y_F^*\|^2 \end{aligned} \quad (5.20)$$

where Equation 5.8a is used for the input-output relationship.

Furthermore, by using the input-output relationship in equation 5.8b, combining the machine subsystem \mathbb{F}_+ in equation 5.19 with \mathbb{G} in equation 5.6 represents the entire feedback control system incorporating automatic generation control. Based on this fact, we analyze the passivity of \mathbb{G} independent of the equilibrium point below.

5.2.2.4 Analysis of the electrical subsystem

We analyze the passivity of the electrical subsystem \mathbb{G} in equation (5.6) independent of its equilibrium point. Here, we represent the column vector containing the time-varying variables δ_i , E_i , $|V_i|$, and $\angle V_i$ related to the generator bus and load bus of \mathbb{G} as $x_{\mathbb{G}}$. Under this notation, we define the potential energy function as follows:

$$\begin{aligned} U_{\mathbb{G}}(x_{\mathbb{G}}) := & \sum_{i=1}^n \left\{ \frac{X_i E_i^2}{2X'_i(X_i - X'_i)} - \frac{E_i |V_i|}{X'_i} \cos(\delta_i - \angle V_i) + \frac{|V_i|^2}{2X'_i} \right\} \\ & - \sum_{i=n+1}^{n+m} \{P_{\text{load}_i}^* \angle V_i + Q_{\text{load}_i}^* \ln |V_i|\} \\ & - \sum_{i=1}^N \sum_{j=1}^N \frac{B_{ij}}{2} |V_i| |V_j| \cos(\angle V_i - \angle V_j) \end{aligned} \quad (5.21)$$

This potential energy function has been used, for example, in the stability analysis of power systems consisting of a single-axis generator model and a constant power load model, as described in [11, 12, 14]. Based on the expression in Equation (5.10), a candidate storage function is constructed as follows:

$$W_{x_{\mathbb{G}}^*}(x_{\mathbb{G}}) = U_{\mathbb{G}}(x_{\mathbb{G}}) - U_{\mathbb{G}}(x_{\mathbb{G}}^*) - \nabla U_{\mathbb{G}}^T(x_{\mathbb{G}}^*)(x_{\mathbb{G}} - x_{\mathbb{G}}^*) \quad (5.22)$$

Its gradient function is:

$$\nabla W_{x_{\mathbb{G}}^*}(x_{\mathbb{G}}) = \nabla U_{\mathbb{G}}(x_{\mathbb{G}}) - \nabla U_{\mathbb{G}}(x_{\mathbb{G}}^*)$$

To calculate the time derivative of the storage function, we need to find the gradient function of the potential energy function. First, we calculate the partial derivatives of $U_{\mathbb{G}}(x_{\mathbb{G}})$ with respect to δ_i and E_i , which are given by:

$$\begin{aligned} \frac{\partial U_{\mathbb{G}}}{\partial \delta_i}(x_{\mathbb{G}}) &= \frac{E_i |V_i|}{X'_i} \sin(\delta_i - \angle V_i), \\ \frac{\partial U_{\mathbb{G}}}{\partial E_i}(x_{\mathbb{G}}) &= -\frac{1}{X_i - X'_i} \left\{ -\frac{X_i}{X'_i} E_i + \left(\frac{X_i}{X'_i} - 1 \right) |V_i| \cos(\delta_i - \angle V_i) \right\} \end{aligned}$$

Therefore, if each variable follows the differential-algebraic equation of Equation (5.6), because of Equation 5.6a, the following is true for all $i \in \mathcal{I}_{\mathbb{G}}$:

$$\frac{\partial U_{\mathbb{G}}}{\partial \delta_i}(x_{\mathbb{G}}) = y_{\mathbb{G}_i}, \quad \frac{\partial U_{\mathbb{G}}}{\partial E_i}(x_{\mathbb{G}}) = \frac{V_{\text{field}_i}^* - \tau_i \dot{E}_i}{X_i - X'_i}$$

The partial derivatives of the potential energy function with respect to the voltage phase variables for $i \in \mathcal{I}_{\mathbb{G}}$ are given by:

$$\begin{aligned}\frac{\partial U_{\mathbb{G}}}{\partial |\mathbf{V}_i|}(x_{\mathbb{G}}) &= - \sum_{j=1}^N B_{ij} |\mathbf{V}_j| \cos(\angle \mathbf{V}_i - \angle \mathbf{V}_j) - \frac{Q_i}{|\mathbf{V}_i|} \\ \frac{\partial U_{\mathbb{G}}}{\partial \angle \mathbf{V}_i}(x_{\mathbb{G}}) &= \sum_{j=1}^N B_{ij} |\mathbf{V}_i| |\mathbf{V}_j| \sin(\angle \mathbf{V}_i - \angle \mathbf{V}_j) - P_i\end{aligned}$$

Therefore, from Equation 5.6b, it can be seen that these are equal to 0. Similarly, from Equation 5.6c, for $i \in \mathcal{I}_{\text{L}}$, it can be seen that:

$$\begin{aligned}\frac{\partial U_{\mathbb{G}}}{\partial |\mathbf{V}_i|}(x_{\mathbb{G}}) &= - \sum_{j=1}^N B_{ij} |\mathbf{V}_j| \cos(\angle \mathbf{V}_i - \angle \mathbf{V}_j) - \frac{Q_{\text{loadi}}^*}{|\mathbf{V}_i|} \\ \frac{\partial U_{\mathbb{G}}}{\partial \angle \mathbf{V}_i}(x_{\mathbb{G}}) &= \sum_{j=1}^N B_{ij} |\mathbf{V}_i| |\mathbf{V}_j| \sin(\angle \mathbf{V}_i - \angle \mathbf{V}_j) - P_{\text{loadi}}^*\end{aligned}$$

Therefore, it can be seen that for all $i \in \mathcal{I}_{\mathbb{G}} \cup \mathcal{I}_{\text{L}}$:

$$\frac{\partial U_{\mathbb{G}}}{\partial |\mathbf{V}_i|}(x_{\mathbb{G}}) = 0, \quad \frac{\partial U_{\mathbb{G}}}{\partial \angle \mathbf{V}_i}(x_{\mathbb{G}}) = 0$$

Next, consider the set $(x_{\mathbb{G}}^*, u_{\mathbb{G}}^*, y_{\mathbb{G}}^*)$ related to the steady-state of \mathbb{G} with respect to $\nabla U_{\mathbb{G}}(x^* \mathbb{G})$. From the equilibrium condition, there exists a set of voltage phasors $(|\mathbf{V}_i^*|, \angle \mathbf{V}_i^*)_{i \in \mathcal{I}_{\mathbb{G}} \cup \mathcal{I}_{\text{L}}}$ such that:

$$\begin{cases} 0 = u_{\mathbb{G}_i}^* \\ 0 = -\frac{X_i}{X'_i} E_i^* + \left(\frac{X_i}{X'_i} - 1\right) |\mathbf{V}_i^*| \cos(\delta_i^* - \angle \mathbf{V}_i^*) + V_{\text{fieldi}}^* \\ P_i^* = \sum_{j=1}^N B_{ij} |\mathbf{V}_i^*| |\mathbf{V}_j^*| \sin(\angle \mathbf{V}_i^* - \angle \mathbf{V}_j^*) \\ Q_i^* = -\sum_{j=1}^N B_{ij} |\mathbf{V}_i^*| |\mathbf{V}_j^*| \cos(\angle \mathbf{V}_i^* - \angle \mathbf{V}_j^*) \end{cases} \quad (5.23a)$$

However, $i \in \mathcal{I}_{\mathbb{G}}$ and the steady-state values of active and reactive power are:

$$P_i^* := \frac{E_i^* |\mathbf{V}_i^*|}{X'_i} \sin(\delta_i^* - \angle \mathbf{V}_i^*), \quad Q_i^* := \frac{E_i^* |\mathbf{V}_i^*|}{X'_i} \cos(\delta_i^* - \angle \mathbf{V}_i^*) - \frac{|\mathbf{V}_i^*|^2}{X'_i}$$

In addition, $y_{\mathbb{G}_i}^*$ represents P_i^* . Therefore, the following holds for $i \in \mathcal{I}_{\mathbb{G}}$:

$$\frac{\partial U_{\mathbb{G}}}{\partial \delta_i}(x_{\mathbb{G}}^*) = y_{\mathbb{G}_i}^*, \quad \frac{\partial U_{\mathbb{G}}}{\partial E_i}(x_{\mathbb{G}}^*) = \frac{V_{\text{fieldi}}^*}{X_i - X'_i}$$

Similarly, since the following holds for all $i \in \mathcal{I}_{\text{L}}$:

$$\begin{cases} P_{\text{load}i}^* = \sum_{j=1}^N B_{ij} |V_i^*| |V_j^*| \sin(\angle V_i^* - \angle V_j^*) \\ Q_{\text{load}i}^* = - \sum_{j=1}^N B_{ij} |V_i^*| |V_j^*| \cos(\angle V_i^* - \angle V_j^*) \end{cases} \quad (5.23b)$$

The partial differential related to the voltage phasor variables of the bus bars becomes:

$$\frac{\partial U_G}{\partial |V_i|}(x_G^*) = 0, \quad \frac{\partial U_G}{\partial \angle V_i}(x_G^*) = 0$$

for all $i \in \mathcal{I}_G \cup \mathcal{I}_L$.

Based on the above calculation results, the time derivative along the solution trajectory of the storage function for G can be evaluated as follows:

$$\begin{aligned} \frac{d}{dt} W_{x_G^*}(x_G(t)) &= \nabla W_{x_G^*}^\top(x_G(t)) \dot{x}_G(t) \\ &= \sum_{i=1}^n \left((u_{G_i} - u_{G_i}^*)(y_{G_i} - y_{G_i}^*) - \frac{\tau_i}{X_i - X'_i} \dot{E}_i^2 \right) \\ &\leq (y_G - y_G^*)^\top (u_G - u_G^*) \end{aligned} \quad (5.24)$$

where we used $u_G^* = 0$ from equation 5.23a. This implies that the function $W_{x_G^*}(x_G)$ in Equation 5.22 is a passive storage function independent of the equilibrium point of the electrical subsystem G . Note that the domains of x_G and x_G^* are limited to the region where $W_{x_G^*}(x_G)$ is a semi-positive definite function, that is, the region where the potential energy function $U_G(x_G)$ in Equation 5.21 is a convex function. This will be discussed in the next section.

5.2.3 Stability analysis of frequency stabilization control system

5.2.3.1 Stability analysis of unknown equilibrium points based on passivity

In the following, we analyze the stability of a feedback control system with automatic generation control, using passivity-based stability analysis of the linearized model as in Section 4.3, but assuming that the value of the storage function given by equation 5.22, $W_{x_G^*}(x_G(t))$, is non-negative for all times t , for the trajectory $x_G(t)$ of the electrical subsystem G . We discuss this assumption in the next subsection.

Using the relationship of Equation 5.8b to the sum of inequalities in Equation 5.20 and Equation 5.24, we obtain the following for the entire feedback control system.

$$\frac{d}{dt} \left\{ W_{x_F^*}(x_F(t)) + \omega_0 W_{\xi^*}(\xi(t)) + W_{x_G^*}(x_G(t)) \right\} \leq -\frac{\min\{D_i\}}{\omega_0} \|y_F(t) - y_F^*\|^2$$

From this inequality, it can be seen that the sum of the storage functions is monotonically non-increasing. Moreover, since the lower bound is 0, the sum asymptotically converges to a certain value as time passes. That is, the time derivative of the left-hand side asymptotically approaches 0. Therefore, it follows that:

$$\lim_{t \rightarrow \infty} y_F(t) = y_F^*$$

Furthermore, focusing on the output equation of equation 5.5, the output y_F is a constant multiple of the internal state $\Delta\omega$, and therefore for the mechanical subsystem F , the following holds:

$$y_F(t) = y_F^*, \quad \forall t \geq 0 \quad \implies \quad \Delta\omega(t) = \frac{1}{\omega_0} y_F^*, \quad \forall t \geq 0 \quad (5.25)$$

Furthermore, as analyzed in Section 3.5, the frequency derivation of all generators converges on the same value. This fact implies that there exists a constant γ_0 such that:

$$y_F^* = \gamma_0 \mathbb{1}$$

On the other hand, from the first equation of Equation 5.18, we have:

$$0 = h^\top u_K^* = \frac{1}{\omega_0} h^\top y_F^* = \frac{\gamma_0}{\omega_0} h^\top \mathbb{1}$$

Here, since $h^\top \mathbb{1}$ is not zero, it is inferred that γ_0 is zero. Therefore, it is shown that the angular frequency deviation of all generators converges to zero asymptotically, that is:

$$\lim_{t \rightarrow \infty} \Delta\omega(t) = 0$$

Additionally, it is also understood that, for all $i \in \mathcal{I}_G$, the following holds:

$$\lim_{t \rightarrow \infty} P_{\text{mech}i}(t) = \lim_{t \rightarrow \infty} P_i(t)$$

However, the convergence values of the mechanical inputs and effective power are generally impossible to calculate in advance because the power consumption of loads and the impedance of transmission lines, etc., are unknown in reality. Similarly, the internal states of the electrical subsystem G and the voltage phase variables of the busbars in Equation 5.6 also converge to unknown values asymptotically.

Example 5.3 Time variation of stored energy Consider a power system model consisting of two generators and a constant power load model, as in Examples 5.1 and 5.2. The admittance value of the transmission line is set to the value in Equation 4.45

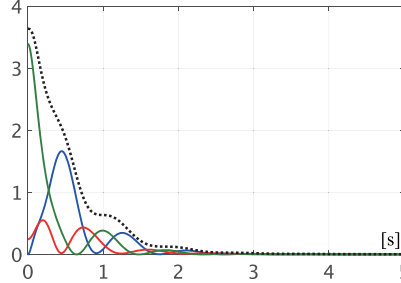
Table 5.2 Temporal change of accumulated energy

	Bus 1	Bus 2	Bus 3
P_i^*	2.5000	-3	0.5
Q_i^*	0.1044	0	0.0365
$ V_i^* $	2	1.9984	2
$\angle V_i^*$	0	-0.0539	-0.0420

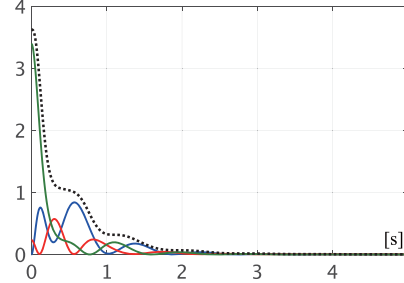
(a) Steady-state power flow state 1

	Bus 1	Bus 2	Bus 3
P_i^*	0.5	-3	2.5000
Q_i^*	0.0432	0	0.1111
$ V_i^* $	2	1.9983	2
$\angle V_i^*$	-0.0488	-0.0595	0

(b) Steady-state power flow state 2



(a) Initial values corresponding to steady-state condition 1

**Fig. 5.5 The time variation of the storage function for the initial value response**(Blue: $W_{x_F^*}$, Red: $W_{x_G^*}$, Green: W_{ξ^*} , Black: Total sum)

with the conductance component set to 0. The physical constants of the generators are set as in Examples 5.1 and 5.2. The broadcast-type PI controller in Equation 5.4 is set with the parameters in Table 5.1 (b).

For the initial values of the generators, the steady-state values corresponding to the two steady-state flow states shown in Table 5.2 are set. The time response of the power system until the steady-state flow state in which the active power of generators 1 and 3 are equal is achieved is then calculated. The values of $W_{x_F^*}(x_F)$ in Equation 5.13, $W_{\xi^*}(\xi)$ in Equation 5.16, and $W_{x_G^*}(x_G)$ in Equation 5.22 are calculated for the time response, and the results are shown in Figure 5.5 (a) and (b). The blue, red, and green solid lines represent $W_{x_F^*}(x_F)$, $W_{x_G^*}(x_G)$, and $W_{\xi^*}(\xi)$, respectively. The black dashed line represents their sum. From these figures, it can be seen that while exchanging energy among the three components, the total energy of the entire power system monotonically decreases.

5.2.3.2 The range where the potential energy function is convex

In the following, we show that the conditions for the potential energy function $U_G(x_G)$ in Equation 5.21 to be a convex function correspond to the passive power

transmission conditions (i) and (iii) discussed in Definition 4.4 in the analysis of the passive properties of the linear approximation model. Note that assumption (ii) of the passive power transmission conditions is assumed in this section.

We consider the case where generators are connected to all buses, in accordance with the setting of the linear approximation model in Section 4.3.2. That is, the subscripts for the generator buses and load buses are

$$\mathcal{I}_G = \{1, \dots, N\}, \quad \mathcal{I}_L = \emptyset$$

In this case, applying the Kron reduction to the generator buses allows us to obtain an equivalent system of ordinary differential equations for the electrical subsystem G in Equation 5.6, with respect to $i \in \mathcal{I}_G$, given by:

$$G_i : \begin{cases} \dot{\delta}_i = u_{G_i} \\ \tau_i \dot{E}_i = -\frac{X_i}{X'_i} E_i - (X_i - X'_i) \sum_{j=1}^N E_j B_{ij}^{\text{red}} \cos \delta_{ij} + V_{\text{field}i}^* \\ y_{G_i} = -E_i \sum_{j=1}^N E_j B_{ij}^{\text{red}} \sin \delta_{ij} \end{cases}$$

where δ_{ij} denotes $\delta_i - \delta_j$. Also, the reduced susceptance B_{ij}^{red} is defined as the (i, j) -th element of the matrix B^{red} , which is obtained by combining the susceptance matrix B of the power network in Eq. (5.6), and is defined as follows:

$$B^{\text{red}} := -\{\text{diag}(X') - \text{diag}(X'_i) B \text{diag}(X'_i)\}^{-1} \quad (5.26)$$

The potential energy function corresponding to the representation of this system of ordinary differential equations is given by Equation 5.21. It is expressed as follows in Equation 5.27:

$$U_G^{\text{red}}(z_G) := \frac{1}{2} \sum_{i=1}^N \left\{ \frac{X_i E_i^2}{X'_i (X_i - X'_i)} + E_i \sum_{j=1}^N E_j B_{ij}^{\text{red}} \cos \delta_{ij} \right\} \quad (5.27)$$

where the vector with all δ_i and E_i is expressed as z_G . If we calculate the partial differential related to the internal state, the following is obtained:

$$\frac{\partial U_G^{\text{red}}}{\partial \delta_i}(z_G) = y_{G_i}, \quad \frac{\partial U_G^{\text{red}}}{\partial E_i}(z_G) = \frac{V_{\text{field}i}^* - \tau_i \dot{E}_i}{X_i - X'_i}$$

Similarly, for the steady state, we have:

$$\frac{\partial U_G^{\text{red}}}{\partial \delta_i}(z_G^*) = y_{G_i}^*, \quad \frac{\partial U_G^{\text{red}}}{\partial E_i}(z_G^*) = \frac{V_{\text{field}i}^*}{X_i - X'_i}$$

Therefore, if we define the corresponding storage function as:

$$W_{z_G^*}^{\text{red}}(z_G) = U_G^{\text{red}}(z_G) - U_G^{\text{red}}(z_G^*) - \{\nabla U_G^{\text{red}}(z_G^*)\}^\top (z_G - z_G^*)$$

Then, similarly to Equation 5.24, its time derivative can be bounded as:

$$\frac{d}{dt} W_{z_G^*}^{\text{red}}(z_G(t)) \leq (y_G - y_G^*)^\top (u_G - u_G^*)$$

Note that all elements of the reduced susceptance matrix B^{red} in Equation 5.26 are non-positive. This fact can be shown as follows. From the discussion in the Section 2.2.3, the susceptance matrix B is a negative definite matrix with non-diagonal elements that are nonnegative. Therefore:

$$B_- := \text{diag}(X'_i) - \text{diag}(X'_i) B \text{diag}(X'_i)$$

is a positive definite matrix with non-positive off-diagonal elements, known as an **M-matrix**. It is known that all elements of the inverse of an M-matrix are non-negative [?]. Therefore, all elements of $B^{\text{red}} = -B_-^{-1}$ are non-positive.

COFFEE BREAK

Hessian matrix: A condition necessary for a twice-differentiable function $f : \mathbb{R}^n \rightarrow \mathbb{R}$ to be a convex over a certain range \mathcal{X} is that the following matrix is positive semi-definite for all $x \in \mathcal{X}$:

$$\nabla^2 f(x) := \begin{bmatrix} \frac{\partial^2 f}{\partial x_1^2}(x) & \cdots & \frac{\partial^2 f}{\partial x_1 \partial x_n}(x) \\ \vdots & \ddots & \vdots \\ \frac{\partial^2 f}{\partial x_n \partial x_1}(x) & \cdots & \frac{\partial^2 f}{\partial x_n^2}(x) \end{bmatrix}$$

This matrix is called the **Hessian matrix** of the function f [32].

The convexity of the potential energy function $U_G^{\text{red}}(z_G)$ in Equation 5.27 is characterized by the positive semidefiniteness of its Hessian matrix $\nabla^2 U_G^{\text{red}}(z_G)$. Computing this Hessian matrix yields to:

$$\nabla^2 U_G^{\text{red}}(z_G) = \begin{bmatrix} L(z_G) & -\hat{B}^\top(z_G) \\ -\hat{B}(z_G) & -\hat{A}(z_G) \end{bmatrix} \quad (5.28)$$

However, the matrix constituting each block has the element (i, j) given by:

$$\begin{aligned} L_{ij}(z_G) &:= \frac{\partial^2 U_G^{\text{red}}}{\partial \delta_i \partial \delta_j}(z_G) = \begin{cases} -E_i \sum_{j=1, j \neq i}^N E_j B_{ij}^{\text{red}} \cos(\delta_{ij}), & i = j \\ E_i E_j B_{ij}^{\text{red}} \cos(\delta_{ij}), & i \neq j \end{cases} \\ \hat{A}_{ij}(z_G) &:= -\frac{\partial^2 U_G^{\text{red}}}{\partial E_i \partial E_j}(z_G) = \begin{cases} -\left(B_{ii}^{\text{red}} + \frac{X_i}{X'_i(X_i - X'_i)}\right), & i = j \\ -B_{ij}^{\text{red}} \cos(\delta_{ij}), & i \neq j \end{cases} \\ \hat{B}_{ij}(z_G) &:= -\frac{\partial^2 U_G^{\text{red}}}{\partial E_i \partial \delta_j}(z_G) = \begin{cases} \sum_{j=1, j \neq i}^N E_j B_{ij}^{\text{red}} \sin(\delta_{ij}), & i = j \\ -E_j B_{ij}^{\text{red}} \sin(\delta_{ij}), & i \neq j \end{cases} \end{aligned}$$

The Hessian matrix evaluated at the equilibrium point in Equation 5.28, $\nabla^2 U_G^{\text{red}}(z_G^*)$, is identical to the matrix P_G in Equation 4.34, which appeared in the passive analysis of the linearized electric subsystem in Section 4.3.2. Note that the positive semi-definiteness of P_G guarantees that the accumulation function for demonstrating the passivity of the linearized model of G is a positive semi-definite function. Therefore, it is understood that the necessary and sufficient condition for $U_G^{\text{red}}(z_G^*)$ to be a convex function is equivalent to the necessary and sufficient condition for P_G to be positive semi-definite, which is equivalent to the passive power transmission conditions (i) and (iii) being satisfied.

In combination with the results from Section 4.3, it can be understood that the region defined as the convex set of the potential energy function $U_G^{\text{red}}(z_G)$ given in Equation 5.27:

$$\mathcal{E}_G := \{z_G^* : \nabla^2 U_G^{\text{red}}(z_G^*) \geq 0\}$$

is also the "maximum" set of equilibrium points that can demonstrate frequency stability based on passivity.

The reason for this is that the passive power transmission conditions are necessary conditions for the linearized electric subsystem to be passive in the vicinity of a specific equilibrium point, as shown in Section 4.3.4. Therefore, for equilibrium points z_G^* where $\nabla^2 U_G^{\text{red}}(z_G^*)$ is not positive semi-definite, the electric subsystem G cannot be passive.

On the other hand, if the initial value of the electrical subsystem $z_G(0)$ is set in the vicinity of a certain equilibrium point z_G^* belonging to the set \mathcal{E}_G , then for all combinations of physical parameters $(M_i, D_i, \tau_i)_{i \in \mathcal{I}_G}$, the entire feedback control system will asymptotically converge to a steady-state power flow state where demand and supply are balanced.

For example, consider a situation where the power consumption of a certain load changes in a stepwise and small manner from a steady-state power flow state where demand and supply are balanced. In this case, since the equilibrium point of the electrical subsystem G undergoes a small variation from the original steady-state power flow state to the new one, the initial time can be regarded as the time when the power consumption changes and the initial value of G can be set in the vicinity of the equilibrium point.

From the above analytical result, it can be concluded that as long as the time variation of model parameters such as loads and controller parameters is sufficiently gradual and the power system state remains in the region where the potential energy function becomes a convex function, frequency stability is maintained by automatic generation control.

5.3 Transient stability control

5.3.1 Decentralized control of generators with excitation system

In power system engineering, the term **transient stability** is widely used when discussing the size and stability of the stability region of the equilibrium point. In this section, we outline the mathematical models and characteristics of **excitation systems** implemented for the purpose of increasing the transient stability of the power system. Excitation systems are generally local controllers implemented "individually" for each generator, which perform control operations that automatically adjust the field input by locally measuring the voltage phase or current phase of the bus to which the generator is connected, as well as the internal state of the generator. The main element of an excitation system is the **Automatic Voltage Regulator** (AVR), a control device that maintains the bus voltage at the desired value. In addition, to suppress oscillations caused by the AVR, additional control algorithms called **Power System Stabilizers** (PSS) may also be incorporated. In Sections 5.3.2 to 5.3.5, we will explain these standard models and control effects.

5.3.2 Standard Automatic Voltage Regulator model

There are many standardized models for automatic voltage regulators. For example, the IEEE's standardization report [33] lists more than 40 standard models. Automatic voltage regulator models are broadly classified into direct current (DC), alternating current (AC), and static types. In the following, we describe representative models of DC and static types.

First, we describe the **IEEE Type DC1 excitation system model**, which is a direct current (DC) model of the automatic voltage regulator. For detailed modeling, please refer to [4, Section 7.9.2] or [15, Section 8.6.3]. Here, we discuss the automatic voltage regulator for a generator connected to bus i . To simplify the notation, we omit the subscript i . Specifically, we use the generator model discussed in Section 2.3.2:

$$\begin{cases} \dot{\delta} = \omega_0 \Delta\omega \\ M \Delta\dot{\omega} = -D \Delta\omega - P + P_{\text{mech}} \\ \tau \dot{E} = -I_{\text{field}} + V_{\text{field}} \end{cases} \quad (5.29)$$

However, for the sake of the following discussion, we define the value of the excitation current of the generator in the units of pu as:

$$I_{\text{field}} := \frac{X}{X'} E - \left(\frac{X}{X'} - 1 \right) |V| \cos(\delta - \angle V) \quad (5.30)$$

The active and reactive powers output by the generator are given by:

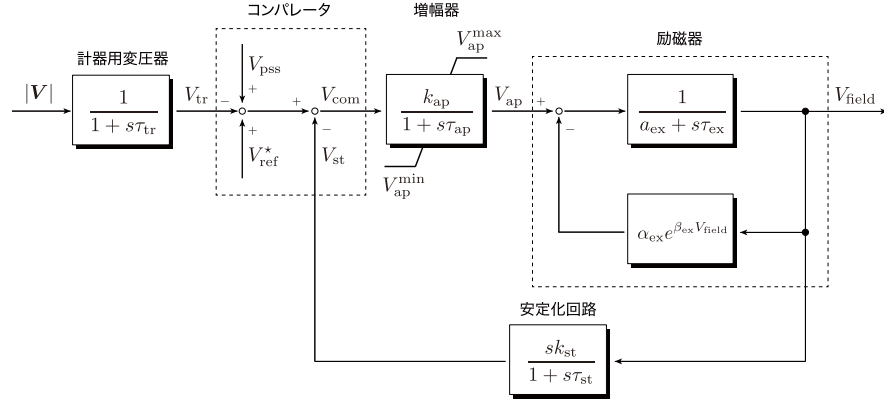


Fig. 5.6 IEEE DC1 type model of automatic voltage regulator

$$P = \frac{E|V|}{X'} \sin(\delta - \angle V), \quad Q = \frac{E|V|}{X'} \cos(\delta - \angle V) - \frac{|V|^2}{X'}$$

It should be noted that for the salient-pole generator model discussed in section 2.3.7, we replace X' and X in Equation 5.30 with X'_d and X_d , respectively, to define I_{field} .

As shown in Figure 5.6, the IEEE DC1 model of the automatic voltage regulator is a controller that takes the magnitude $|V|$ of the bus voltage phasor as input and outputs the field excitation input V_{field} of the generator. However, as additional input signals, a reference signal V_{ref}^* for adjusting the magnitude of the bus voltage phasor to the desired value and a control signal V_{pss} output by the power system stabilizer are applied. The IEEE DC1 model of the automatic voltage regulator consists of four basic devices: a voltage transformer, a comparator, an amplifier, and an exciter, as well as an auxiliary stabilizing circuit. In the following, we will explain the dynamic characteristics of each device.

5.3.2.1 Voltage transformer

The voltage transformer is a device that reduces the bus voltage to a voltage that can be used by the control circuit, and its dynamic characteristics is modeled as a first-order lag filter:

$$\tau_{\text{tr}} \dot{V}_{\text{tr}} = -V_{\text{tr}} + |V| \quad (5.31a)$$

Generally, the time constant τ_{tr} is sufficiently small, and the output V_{tr} of the voltage transformer is almost equal to the absolute value of the bus voltage $|V|$.

5.3.2.2 Comparator

The comparator is a device that outputs the difference between the output V_{tr} of the voltage transformer and the reference signal V_{ref}^* . The output V_{pss} of the power system stabilizer mentioned later is applied as a signal to adjust the constant V_{ref}^* . In addition, when incorporating a stabilizing circuit for the excitation system, its output V_{st} is also fed back. That is, the comparator is modeled as

$$V_{\text{com}} = V_{\text{ref}}^* + V_{\text{pss}} - V_{\text{tr}} - V_{\text{st}} \quad (5.31\text{b})$$

As mentioned above, since V_{tr} is almost equal to $|V|$ because the time constant τ_{tr} is usually very small, if the output V_{pss} of the power system stabilizer and the output V_{st} of the stabilizing circuit are zero, the output V_{com} of the comparator is almost equal to the difference between the reference signal and the absolute value of the bus voltage phase $V_{\text{ref}}^* - |V|$.

5.3.2.3 Amplifier

The amplifier is a device that amplifies the output V_{com} of the comparator to drive the excitation system. There are various types, such as rotary and electromagnetic types, but in many cases, it is modeled as:

$$\tau_{\text{ap}} \dot{V}_{\text{ap}} = \begin{cases} -V_{\text{ap}} + k_{\text{ap}} V_{\text{com}}, & V_{\text{ap}}^{\min} < V_{\text{ap}} < V_{\text{ap}}^{\max} \text{ or } V_{\text{ap}} V_{\text{com}} \leq 0 \\ 0, & \text{otherwise} \end{cases} \quad (5.31\text{c})$$

where the time constant τ_{ap} and gain k_{ap} are non-negative constants, and the saturation that constrains the internal state V_{ap} to the range $[V_{\text{ap}}^{\min}, V_{\text{ap}}^{\max}]$ is expressed by the conditional branching. Note that in some cases, saturation is applied to the output instead of the internal state, and in transient states with large disturbances such as ground faults, the width of the saturation limits may be set large [3, Section 4.3].

5.3.2.4 Exciter

The exciter is a device that generates the field input V_{field} from the output $V_{\text{ap}}^{\text{sat}}$ of the amplifier, modeled as a nonlinear first-order system given by:

$$\tau_{\text{ex}} \dot{V}_{\text{field}} = - \left(a_{\text{ex}} + \underbrace{\alpha_{\text{ex}} e^{\beta_{\text{ex}} V_{\text{field}}}}_{*} \right) V_{\text{field}} + V_{\text{ap}} \quad (5.31\text{d})$$

Here, τ_{ex} is a positive constant, but the sign of a_{ex} may vary depending on the literature. The term denoted by "*" represents the nonlinearity due to magnetic saturation and other effects within the exciter, and α_{ex} and β_{ex} are both non-negative

constants. These constants are typically set to ensure stable dynamic behavior of the exciter in the vicinity of the normal operating point.

5.3.2.5 Stabilizing circuit

The stabilizing circuit is a circuit that is implemented to enhance the stability of the excitation system. In the IEEE DC1 model, it is represented as a mechanism that feeds back the differential value of the field input. That is, its dynamic characteristics are expressed as:

$$\tau_{st} \dot{V}_{st} = -V_{st} + k_{st} \dot{V}_{field} \quad (5.31e)$$

where the time constant τ_{st} and gain k_{st} are non-negative constants. The output V_{st} of this stabilization circuit is fed back to the comparator in Equation 5.31b.

The IEEE Type DC1 excitation system model of AVR is a combination of Equation 5.31a to Equation 5.31e discussed above. The reference values of each parameter are summarized in 5.3 and 5.4. The unit of the time constant is [s] while other units are [pu].

Table 5.3 Parameter example of IEEE DC1 type model

	τ_{tr}	τ_{ap}	k_{ap}	V_{ap}^{\max}	V_{ap}^{\min}
Example 1 [4, Table D.3. Unit F2]	0.00	0.05	57.1	1.00	-1.00
Exampme 2 [3, Table 7.3]		0.00	0.2	20	$-\infty$

Table 5.4 Parameter example of IEEE DC1 type model (continued)

	τ_{ex}	a_{ex}	α_{ex}	β_{ex}	τ_{st}	k_{st}
Example 1 [4, Table D.3. Unit F2]	0.50	-0.045	0.0012	1.21	1.00	0.08
Example 2 [3, Table 7.3]		0.314	1.0	0.0039	1.555	0.35

Next, we will explain the **IEEE Type ST1 excitation system model** which has a similar structure to the IEEE DC1 type but is a static model with faster response. In this automatic voltage regulator model, the excitation system time constant is sufficiently small, and the excitation system model in Equation 5.31d is expressed as a static relationship:

$$V_{field} = \text{sat}(V_{ap}; V_{field}^{\min}, V_{field}^{\max})$$

where sat is the output saturation function defined by:

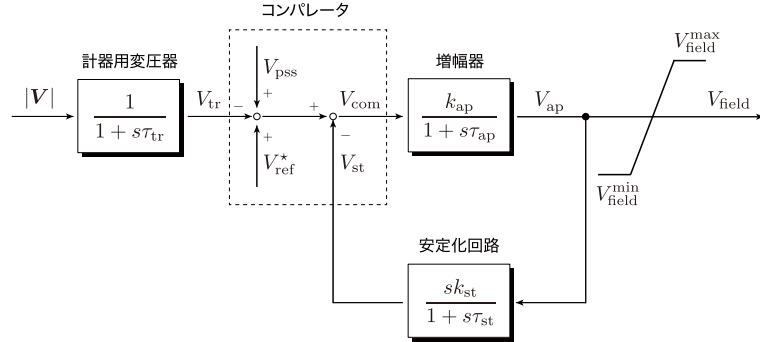


Fig. 5.7 IEEE ST1 type model of automatic voltage regulator

$$\text{sat}(x; \underline{\alpha}, \bar{\alpha}) := \begin{cases} \underline{\alpha}, & x \leq \underline{\alpha} \\ x, & \underline{\alpha} < x \leq \bar{\alpha} \\ \bar{\alpha}, & x > \bar{\alpha} \end{cases}$$

Additionally, the upper and lower limits of output saturation are modeled to mainly depend on the absolute value of the bus voltage phase angle [15, Section 8.63]. Specifically, using $|V|$ and I_{field} in Equation 5.29, they are given by

$$V_{field}^{\min} = \gamma_- |V|, \quad V_{field}^{\max} = \gamma_+ |V| - k_0 I_{field}$$

where γ_- , γ_+ , and k_0 are non-negative constants. The block diagram of this model is shown in Figure 5.7. Note that during a ground fault on the bus, $|V|$ becomes 0, and the excitation input V_{field} is not outputted from the AVR.

Since the excitation response of the IEEE ST1 model is fast enough, stabilizing circuits are often unnecessary. When the amplifier time constant τ_{ap} is small enough that its dynamic characteristics can be ignored, a simplified first-order model given by Equation 5.32 is used. For example, this model is used in [15, Section 12.4] and [34, Section 4.2.2]. Examples of parameters are shown in Examples 1 and 2 of Table 5.5.

$$\begin{cases} \tau_{tr} \dot{V}_{tr} = -V_{tr} + |V| \\ V_{ap} = k_{ap}(V_{ref}^* + V_{pss} - V_{tr}) \\ V_{field} = \text{sat}\left(V_{ap}; V_{field}^{\min}, V_{field}^{\max}\right) \end{cases} \quad (5.32)$$

When the time constant of the amplifier τ_{ap} is not zero, but the time constant of the instrument transformer τ_{tr} is zero or a model that excludes output saturation is often used [1, 3, 35], the following equation can be used:

$$\begin{cases} \tau_{ap} \dot{V}_{ap} = -V_{ap} + k_{ap}(V_{ref}^* + V_{pss} - |V|) \\ V_{field} = V_{ap} \end{cases} \quad (5.33)$$

Table 5.5 IEEE ST1 type model parameter example

	τ_{tr}	τ_{ap}	k_{ap}	γ_+	γ_-	k_0	τ_{st}	k_{st}
Example 1 [15, Section 8.6.3]	0.015	0	200	7.00	-6.40	0.04	0	0
Example 2 [33, Table H.23]	0.02	0	210	6.43	-6.00	0.038	0	0
Example 3 [35, Section V]	0	0.076	36.66	∞	$-\infty$	0	0	0
Example 4 [1, Table 4]	0	0.05	20	∞	$-\infty$	0	0	0

Parameter examples of this model are shown in Example 3 and Example 4 of Table 5.5.

Note that when the desired steady-state value of the excitation input V_{field}^* and the absolute value of the bus voltage $|V^*|$ are given, the reference signal V_{ref}^* for the reference is determined as follows:

$$V_{\text{ref}}^* = \frac{V_{\text{field}}^*}{k_{\text{ap}}} + |V^*| \quad (5.34)$$

However, in actual power system operation, the steady-state values of bus voltage and excitation input are unknown and can vary due to load distribution, and other factors, so the value of the reference signal V_{ref}^* is specified using standard values for bus voltage and excitation input.

5.3.3 Control effectiveness of AVR

Let's analyze the control effectiveness of the Automatic Voltage Regulator (AVR) using a simple power system model.

Example 5.4 Effect of automatic voltage regulator on steady-state and transient stability

Consider the three-bus power system model discussed in Examples 2.1, 3.2, and 3.3. The physical constants of the generator and transmission lines are set to the same values as in Example 3.3. Furthermore, the load connected to bus 2 is modeled as a constant impedance, and the impedance value is set to the first row of Table 3.5. The automatic voltage regulator is set to the IEEE ST1 type model in Equation 5.32. The automatic voltage regulator incorporated in generators 1 and 3 is identical, and the parameter values are those of Example 1 in Table 5.5.

First, let us examine the change in the set of steady-state stable equilibrium points due to the presence or absence of the automatic voltage regulator. Specifically, the steady-state stability of the corresponding power system is determined based on the approximate linearization by varying the difference in steady-state values of the rotor angle, $\delta_3^* - \delta_1^*$, while fixing the steady-state values of the internal voltage of the generators, E_1^* and E_3^* , to the values in the rightmost column of Table 3.3. By calculating the range of $\delta_3^* - \delta_1^*$ where the approximate linear model is stable, it is found

that without the automatic voltage regulator, the range is as shown in (i) of Table 5.6, while with the automatic voltage regulator, the range is as shown in (ii) of Table 5.6. From this result, it is understood that the set of stable equilibrium points tends to decrease due to the automatic voltage regulator.

Note that without loss of generality, δ_1^* or δ_3^* can be set to zero. In addition, if the steady-state values of the internal states of each generator are determined, the corresponding steady-state values of the mechanical and field inputs can be determined by

$$\begin{cases} P_{\text{mech}i}^* = f_i(\delta^*, E^*) \\ V_{\text{field}i}^* = \frac{X_i}{X'_i} E_i^* - (X_i - X'_i) g_i(\delta^*, E^*) \end{cases} \quad i \in \{1, 3\}$$

where δ^* and E^* are vectors with δ_i^* and E_i^* , and functions f_i and g_i are defined by Equation ??.

Furthermore, the steady-state value of the voltage phase of the generator bus can be obtained using Equation 2.23 as follows:

$$\begin{bmatrix} V_1^* \\ V_3^* \end{bmatrix} = \left(\begin{bmatrix} \frac{1}{jX'_1} & 0 \\ 0 & \frac{1}{jX'_3} \end{bmatrix} + Y_{\text{Kron}} \right)^{-1} \begin{bmatrix} \frac{e^{j\delta_1^*}}{jX'_1} & 0 \\ 0 & \frac{e^{j\delta_3^*}}{jX'_3} \end{bmatrix} \begin{bmatrix} E_1^* \\ E_3^* \end{bmatrix}$$

Here, Y_{Kron} is the admittance matrix obtained by Kron reduction of the load bus defined in equation 2.44. The value of the reference signal $V_{\text{ref}i}^*$ is determined by equation 5.34.

Table 5.6 Steady value of rotor declination that stabilizes the state
(AVR: automatic voltage regulator, PSS: system stabilizer)

	(i) Without AVR	(ii) With AVR	(iii) With AVR and PSS
$\delta_3^* - \delta_1^*$ Upper limit [rad]	1.03	0.87	1.32
$\delta_3^* - \delta_1^*$ Lower limit [rad]	-0.90	-0.30	-1.10

COFFEE BREAK

\mathcal{L}_2 norm: The \mathcal{L}_2 norm of a function $y : [0, \infty) \rightarrow \mathbb{R}^n$ is defined as

$$\|y\|_{\mathcal{L}_2} := \sqrt{\int_0^\infty \|y(\tau)\|^2 d\tau}$$

This value can be interpreted as the energy of a time-varying signal. Unless the signal's amplitude decays over time, the \mathcal{L}_2 norm will generally be infinite. The letter " \mathcal{L} " comes from the name of Henri Lebesgue, who is known for his work on the theory of Lebesgue integration.

Next, let us confirm the improvement of transient stability by the automatic voltage regulator. Specifically, we will conduct the following analysis. First, regardless

of the presence of the automatic voltage regulator, we consider a steady-state stability with a steady-state value of the rotor angle difference $\delta_3^* - \delta_1^*$ equal to $-\frac{\pi}{6}$ [rad]. The steady-state value of the internal voltage is set to the above value. Next, we change the initial values of the power system model as parameters and calculate $\|\Delta\omega\|_{\mathcal{L}_2}$ for the time response of the obtained angular frequency deviation. Here, $\Delta\omega$ is a vector consisting of $\Delta\omega_1$ and $\Delta\omega_3$. Similarly, we calculate $\|V - V^*\|_{\mathcal{L}_2}$ for the time response of the main bus voltage phase deviation. Here, $|V|$ is a vector consisting of $\|V - V^*\|_{\mathcal{L}_2}$ is a vector consisting of $|V_1^*|$ and $|V_3^*|$. Note that when the initial value is given inside the stable region of the equilibrium point of interest, the \mathcal{L}_2 norm values of the angular frequency deviation and the main bus voltage phase deviation are finite. Moreover, it is known that the higher the \mathcal{L}_2 norm values of these quantities, the higher the transient stability of the equilibrium point for the given initial values. On the other hand, when the initial value is given outside the stable region, the \mathcal{L}_2 norm values become infinite.

The analysis results of the transient stability are shown in Figure 5.8. The horizontal axis represents the initial value of $\delta_3 - \delta_1$ set, and the vertical axis represents the \mathcal{L}_2 norm value of the angular frequency deviation and the main bus voltage phase deviation generated for the set initial value. The case without the automatic voltage regulator corresponding to (i) in Table 5.6 is represented by a solid blue line, and the case with the automatic voltage regulator corresponding to (ii) is represented by a dashed black line. Note that the plots are shown for the range of initial values for which the \mathcal{L}_2 norm values are finite. The initial values of the internal voltage E_1 and E_3 are set to the same value as their steady-state value E_1^* and E_3^* , respectively. The initial values of the angular frequency deviation $\Delta\omega_1$ and $\Delta\omega_3$ are both set to 0. From this result, it can be seen that the transient stability of the angular frequency deviation and the main bus voltage phase deviation has improved by incorporating the automatic voltage regulator. It can also be seen that the

As a reference, the time response of the angular frequency deviation that occurs when the initial value of $\delta_3 - \delta_1$ is set to -1 and $-\frac{\pi}{2}$, respectively, is shown in Figures 5.9 and 5.10. (a) represents the case without automatic voltage regulator and (b) represents the case with automatic voltage regulator. From these results, it can be seen that incorporating an automatic voltage regulator tends to make the low-frequency component (the center value) of the oscillation of the angular frequency deviation converge to 0 more quickly. On the other hand, it is also found that there is no significant change in the decay rate of the high-frequency component of the oscillation, regardless of the presence or absence of the automatic voltage regulator.

From Example 5.4, it can be seen that incorporating an automatic voltage regulator tends to destabilize some of the equilibrium points that were stable before implementation, while suppressing the low-frequency components of the oscillation of the angular frequency deviation. This means that the transient stability of the power system has improved. The system stabilization device described in the next section has the effect of suppressing the high-frequency components of the oscillation that could not be suppressed by the automatic voltage regulator.

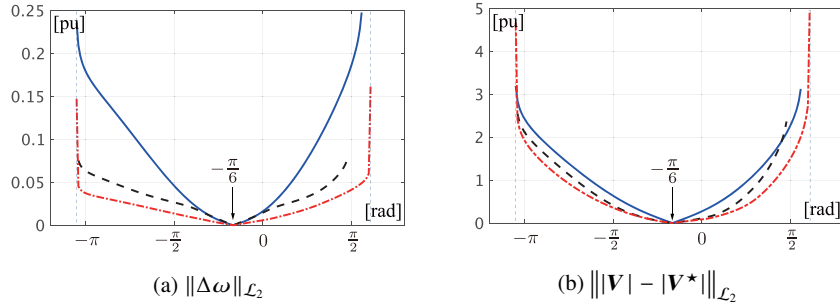


Fig. 5.8 Transient stability evaluation for the initial value of the rotor declination difference
(Blue solid line: (i), Black dashed line: (ii), Red chain line: (iii))

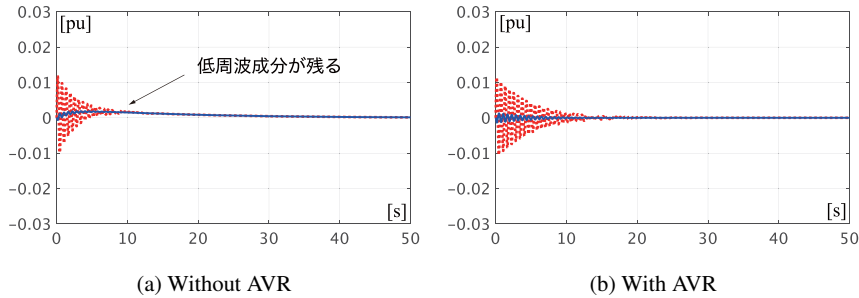


Fig. 5.9 Initial value response of angular frequency deviation
(Blue solid line: $\Delta\omega_1$, red dashed line: $\Delta\omega_3$)

5.3.4 Power System Stabilizer

A power system stabilizer (PSS) is a device that outputs an additional control signal V_{pss} as shown in Figures 5.6 and 5.7. Generally, measurements such as generator's angular frequency deviation, active power, and bus voltage phase are fed back to the PSS. Here we explain the model of a standard PSS called the **IEEE Type PSS1 power system stabilizer model** [33, Section 9.2]. This model mainly consists of two parts: a **washout filter** and a **phase-lead compensator**. The block diagram is shown in Figure 5.11.

5.3.4.1 Washout filter

The washout filter is a high-pass filter used in the power system stabilizer to maintain a steady-state gain of 0. It takes the generator's angular frequency deviation $\Delta\omega$,

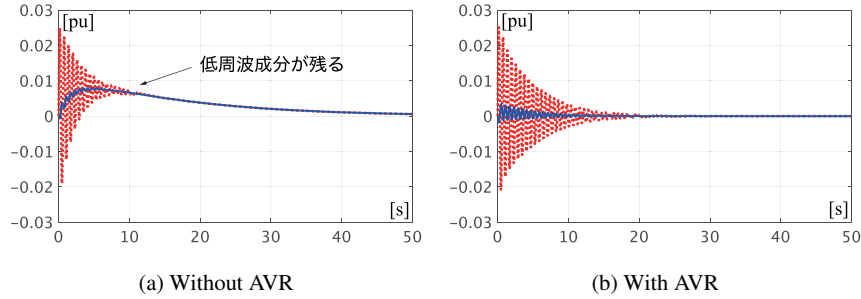


Fig. 5.10 Initial value response of angular frequency deviation
(Blue solid line: $\Delta\omega_1$, Red dashed line: $\Delta\omega_3$)

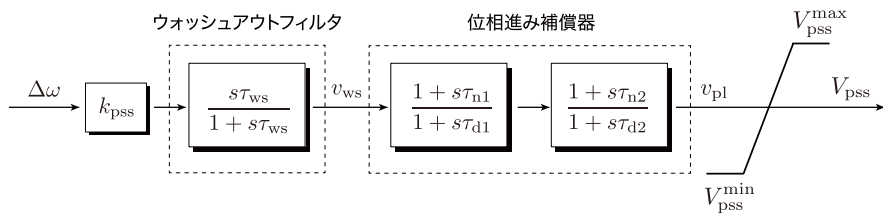


Fig. 5.11 IEEE PSS1 type model of system stabilizer

which is multiplied by a constant gain k_{pss} , as input, and its dynamic characteristics are expressed by the following differential equation:

$$\begin{cases} \tau_{ws}\dot{\xi}_{ws} = -\xi_{ws} + k_{\text{pss}}\Delta\omega \\ v_{ws} = k_{\text{pss}}\Delta\omega - \xi_{ws} \end{cases} \quad (5.35a)$$

The steady-state output v_{ws}^* of the washout filter is zero when the input $\Delta\omega$ is constant. The function of the filter is to extract the angular frequency deviation of the power system in the transient state. The time constant τ_{ws} is typically set between 1 and 20 seconds, considering the settling time of the angular frequency deviation [15, 12.5].

5.3.4.2 Phase-lead compensator

The phase-lead compensator is incorporated to alleviate the phase lag from the bus voltage phase to the generator's active power. Typically, one or two phase lead compensators are connected in series to achieve the desired phase lead. Specifically, the dynamic characteristics of the compensator with input v_{ws} from the washout filter is given by:

$$\begin{cases} \tau_{d1}\dot{\xi}_1 = -\xi_1 + \left(1 - \frac{\tau_{d1}}{\tau_{n1}}\right)v_{ws} \\ v_1 = \frac{\tau_{n1}}{\tau_{d1}}(v_{ws} - \xi_1) \end{cases} \quad \begin{cases} \tau_{d2}\dot{\xi}_2 = -\xi_2 + \left(1 - \frac{\tau_{d2}}{\tau_{n2}}\right)v_1 \\ v_{pl} = \frac{\tau_{n2}}{\tau_{d2}}(v_1 - \xi_2) \end{cases} \quad (5.35b)$$

Finally, the output of the power system stabilizer can be obtained by applying the output v_{pl} of the phase-lead compensator to a saturation function:

$$V_{pss} = \text{sat}\left(v_{pl}; V_{pss}^{\min}, V_{pss}^{\max}\right) \quad (5.35c)$$

An example of the parameters for this model is shown in Table 5.7. However, it should be noted that the parameters for the power system stabilizer need to be determined by considering various factors such as the dynamic characteristics of each generator, automatic voltage regulator, load distribution, and characteristics of the transmission network, and that the desired system stability may not necessarily be achieved by the parameter settings shown in the example. In addition, the standard design guidelines for power system stabilizers are often based on the one-machine infinite-bus system model explained in Section 2.3.5, and caution is required regarding the results when multiple generators are interconnected. For example, in [15, Section 12.5], design guidelines for parameters based on classical control theory using the one-machine infinite-bus system model are presented. In [35], design guidelines based on modern control theory are also explained.

Table 5.7 IEEE PSS1 type model parameter example

	k_{pss}	τ_{ws}	τ_{d1}	τ_{n1}	τ_{d2}	τ_{n2}	V_{pss}^{\min}	V_{pss}^{\max}
Example 1 [15, Section 12.5]	9.50	1.4	0.033	0.154	0.00	0.00	$-\infty$	∞
Example 2 [15, Section 12.8]	20.0	10.0	0.02	0.05	5.40	3.00	$-\infty$	∞
Example 3 [35, Section III]	1.57	10.0	0.03	0.34	0.03	0.34	$-\infty$	∞
Example 4 [33, Table H.3]	3.15	10.0	0.01	0.76	0.01	0.76	-0.09	0.09

5.3.5 Control Effect of Power System Stabilization Device

Let's analyze the control effect of the power system stabilization device using a simple power system model.

Example 5.5 Changes in the small signal stability and the transient stability due to PSS

Let us consider incorporating a power system stabilization device into the system along with an automatic voltage regulator under the same conditions as Example 5.4. The power system stabilization devices installed in generators 1 and 3 are identical,

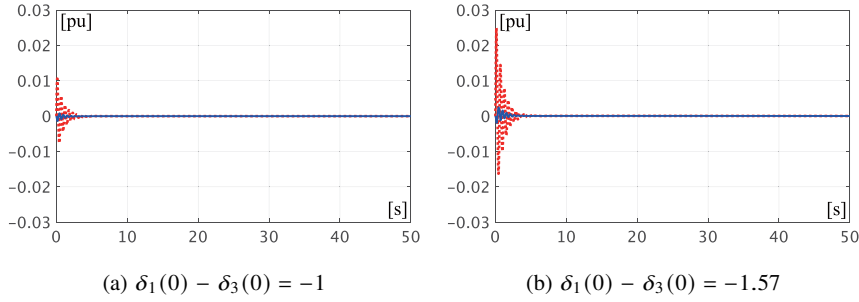


Fig. 5.12 Initial value response of angular frequency deviation
(There is a system stabilizer, and the line type is the same as ??)

and the parameters use the values of Example 2 in Table 5.7. First, let us confirm the change in the set of stable equilibrium points due to the presence of the power system stabilization device, which is shown in the range of (iii) in Table 5.6. From this result, it can be seen that the set of stable equilibrium points has expanded by incorporating the power system stabilization device.

5.4 PSS based on the retrofit control theory

5.4.1 Power system model used in the design of PSS

5.4.1.1 Features of PSS based on the retrofit control theory

In this section, we describe the design methodology of the power system stabilizer based on retrofit control theory [36–40]. The power system stabilizer designed using this methodology can maintain the steady-state power flow condition in a stable manner even when multiple generators are simultaneously incorporated. In particular, each power system stabilizer has the following features:

- Distributed design is possible with just a mathematical model of generators and AVR that incorporates it.
- Distributed implementation is possible with just the local measurement signal of the voltage phasor and current phasor of generator buses.

Next, we consider the case where the IEEE ST1 type AVR model in Equation 5.32 is incorporated into the generator model in Equation 5.29. However, for the sake of simplicity, we exclude saturation of the AVR. Note that the same discussion applies not only to the case with saturation but also to the case where other types of AVRs

are incorporated, the case where existing power system stabilizers are incorporated, and the case where a more detailed generator model is used.

5.4.1.2 Localized linear subsystem

By designing the interaction inputs appropriately, we consider representing the local subsystem, which is coupled with an AVR of the target generator, as a linear system in the form of:

$$G : \begin{cases} \dot{x} = Ax + Bu + Lv \\ w = \Gamma x \\ y = Cx \end{cases} \quad (5.36)$$

where the state vector x is a concatenation of the states of the generator model δ , $\Delta\omega$, E , and the AVR model V_{tr} .

In addition, the input u represents the output V_{pss} of the PSS, and the input-output interactions v and w are defined as:

$$v := \begin{bmatrix} P_{\text{mech}} - \frac{E|V|}{X'} \sin(\delta - \angle V) \\ k_{\text{ap}} V_{\text{ref}}^* + \left(\frac{X}{X'} - 1 \right) |V| \cos(\delta - \angle V) \end{bmatrix}, \quad w := \begin{bmatrix} \delta \\ \Delta\omega \\ E \end{bmatrix} \quad (5.37)$$

Note that the interaction input v in Equation 5.37 contains the non-linear terms of the generator and the variables of the bus voltage phase. It should be noted that the system matrix in Equation 5.36 is defined in accordance with the definitions of these signals as follows:

$$\begin{aligned} A &:= \begin{bmatrix} 0 & \omega_0 & 0 & 0 \\ 0 & -\frac{D}{M} & 0 & 0 \\ 0 & 0 & -\frac{X}{\tau X'} & -\frac{k_{\text{ap}}}{\tau} \\ 0 & 0 & 0 & -\frac{1}{\tau_{\text{tr}}} \end{bmatrix}, \quad B := \begin{bmatrix} 0 \\ 0 \\ \frac{k_{\text{ap}}}{\tau} \\ 0 \end{bmatrix}, \quad C := I \\ L &:= \begin{bmatrix} 0 & 0 & 0 \\ \frac{1}{M} & 0 & 0 \\ 0 & \frac{1}{\tau} & 0 \\ 0 & 0 & \frac{1}{\tau_{\text{tr}}} \end{bmatrix}, \quad \Gamma := \begin{bmatrix} 1 & 0 & 0 & 0 \\ 0 & 1 & 0 & 0 \\ 0 & 0 & 1 & 0 \end{bmatrix} \end{aligned} \quad (5.38)$$

The G in Equation 5.36 is called a **local linear subsystem**. It should be noted that the nonlinear terms of the generator and the variables of the bus voltage phase are included in the interaction input v in Equation 5.37. The system matrix of Equation 5.38 is defined for the local linear subsystem. The model parameters of the local linear subsystem, i.e., the system matrix parameters in Equation 5.38, are assumed to be known and available for the design and implementation of the power system stabilizer.

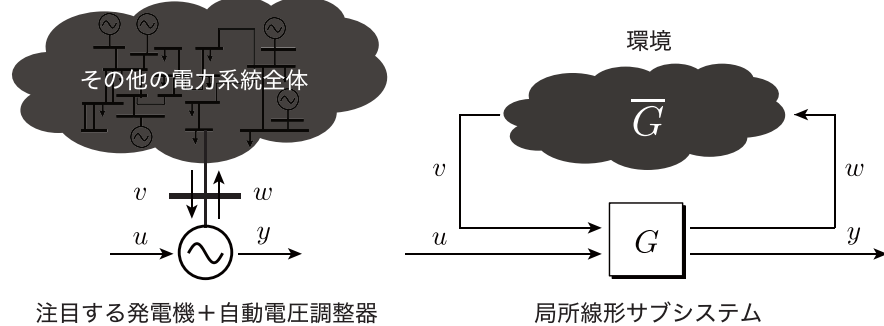


Fig. 5.13 Coupling system of local linear subsystem and environment

5.4.1.3 Environment and approximate linear environment model

Let us consider designing a local controller K for the power system stabilization device, under the assumption that the output y and interaction input/output v and w are measurable.

$$K : (y, v, w) \mapsto u$$

In the following, we call this controller K a **retrofit controller**, which derives from the words retroactive and refit and refers to performing partial expansion or reconstruction of an existing system.

In designing and implementing the retrofit controller, not only the model of the local linear subsystem G is used, but also a linear model that estimates the interaction input v from the interaction output w is utilized. We call this estimation model an **approximate linear environment model**.

To explain the approximate linear environment model, we introduce a nonlinear subsystem called the **environment**, which represents the global subsystem of the entire system except for the local linear subsystem. The environment is a nonlinear system that takes the interaction output w of the local linear subsystem as input and outputs the interaction input v . Formally, we represent the dynamic input-output relationship of the environment as:

$$\bar{G} : w \mapsto v$$

In this case, the feedback coupling system between the local linear subsystem G and the environment \bar{G} represents the entire power system from the perspective of the generator under consideration, as shown in Figure 5.13.

Considering that the environment \bar{G} includes numerous elements such as power transmission networks, loads, and other generators, it is not practical to assume that the complete nonlinear model of the environment is available for the design and implementation of a system stabilizing device for a specific generator. Taking this fact

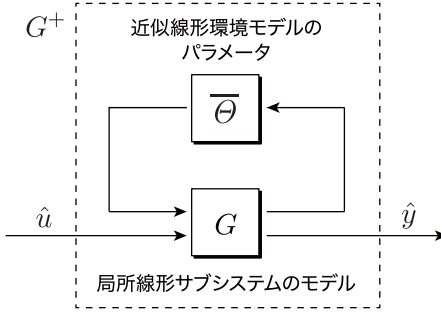


Fig. 5.14 Model used for controller design

into consideration, let us assume a situation where only an approximate linear model of the environment is available. For simplicity, we will describe the approximate linear environment model using a static input-output relationship. However, it is also possible to use a dynamic approximate linear environment model. For further details, please refer to [39].

When the steady-state values of the input-output interaction in the steady-state power flow state of interest are denoted as (v^*, w^*) , the approximated linearized environmental model is parameterized as follows:

$$\bar{G}_{\text{apx}} : v_{\text{apx}} = v^* + \bar{\Theta}(w - w^*) \quad (5.39)$$

Here, $\bar{\Theta}$ is a matrix representing the parameters of the model. The approximated linearized environmental model \bar{G}_{apx} in Equation 5.39 generates the predicted value v_{apx} of the impact of the interaction output w on the interaction input v in the vicinity of their steady-state values (v^*, w^*) by linear prediction.

The power system model used for retrofit controller design is constructed by feed-back coupling the parameters of this approximated linearized environmental model $\bar{\Theta}$ with the model of a local linear subsystem G as shown in Figure 5.14. Specifically, it is given by:

$$G^+ : \begin{cases} \dot{\hat{\xi}} = (A + L\bar{\Theta}\Gamma)\hat{\xi} + B\hat{u} \\ \hat{y} = C\hat{\xi} \end{cases} \quad (5.40)$$

Here, \hat{u} and \hat{y} are virtual input-output signals used for controller design, and are distinguished from u and y by the use of a hat symbol. Note that since C is the identity matrix in Equation 5.38, the output \hat{y} is equal to the internal state $\hat{\xi}$ of G^+ .

5.4.2 PSS design based on the retrofit control theory

5.4.2.1 Design method of retrofit controller

Assuming that the approximate linear environment parameter $\bar{\Theta}$ in Equation 5.39 is identified by an appropriate method, we explain the design method of the retrofit controller. The specific construction method of the approximate linear environment model is described in the next section.

The design of the retrofit controller corresponding to the system stabilization device can utilize the standard control system design method in the field of system control engineering. For instance, let us apply the design method of the **Linear Quadratic Regulator** (LQR) [41, Section 5.3] to the controller design model G^+ in Equation 5.40. In LQR, we use a state-feedback form control algorithm that minimizes the cost function on state and input as follows:

$$J(\hat{\xi}, \hat{u}) := \int_0^\infty \left(\hat{\xi}^\top(t) Q \hat{\xi}(t) + \hat{u}^\top(t) R \hat{u}(t) \right) dt$$

Using the state feedback form in equation 5.41:

$$\hat{u} = \underbrace{-R^{-1}B^\top P(\bar{\Theta})\hat{\xi}}_{\hat{K}(\bar{\Theta})} \quad (5.41)$$

Here, Q is a semi-positive definite matrix, R is a positive definite matrix, and the matrix $P(\bar{\Theta})$ satisfies the **Algebraic Riccati Equation** as follows:

$$(A + L\bar{\Theta}\Gamma)^\top P + P(A + L\bar{\Theta}\Gamma) - PBR^{-1}B^\top P + Q = 0$$

This equation has a positive definite solution. Then, using the gain matrix $\hat{K}(\bar{\Theta})$ in Equation 5.41, the retrofit controller is constructed as follows:

$$K : \begin{cases} \dot{\hat{x}} = A\hat{x} + L \left\{ v - \bar{\Theta}(w - \Gamma\hat{x}) \right\} \\ u = \hat{K}(\bar{\Theta})(y - C\hat{x}) \end{cases} \quad (5.42)$$

Based on this retrofit control theory, the system stabilization device has the following characteristics for any matrix $\bar{\Theta}$:

- When the power system is in steady-state, the input u becomes zero.
- The stability of the steady-state (equilibrium point) does not change before and after implementation.

The first item means that the retrofit controller does not change the steady-state condition, while the second item means that the implementation of the retrofit controller does not change an asymptotically stable equilibrium point to an unstable one. The objective of retrofit control theory is to improve stability while maintaining the asymptotic stability of the equilibrium point and using indicators such as robustness

to disturbances and the size of the stability region. Note that this method cannot asymptotically stabilize an unstable equilibrium point before controller implementation.

Furthermore, it has been shown that the larger the predictive accuracy of the interaction signal by the approximate linear environmental model, the greater the improvement in system stability. Note that if the control algorithm in equation 5.41 stabilizes G^+ in equation 5.40, it is not necessary to use the linear quadratic regulator (LQR) method introduced in section 5.3 of [41]. Additionally, $\hat{K}(\bar{\Theta})$ can be a dynamic control algorithm, and it does not need to be static [39].

5.4.2.2 Construction method of approximate linear environmental model

One practical approach for identifying the parameter $\bar{\Theta}$ in Equation 5.39 is to estimate the relationship between the signals w and v using linearization. Specifically, the partial derivatives of v with respect to each element of w are calculated as:

$$\begin{aligned}\frac{\partial v}{\partial \delta} &= \begin{bmatrix} -\frac{E|V|}{X'} \cos(\delta - \angle V) \\ -\left(\frac{X}{X'} - 1\right) |V| \sin(\delta - \angle V) \\ 0 \end{bmatrix}, & \frac{\partial v}{\partial \Delta\omega} &= \begin{bmatrix} 0 \\ 0 \\ 0 \end{bmatrix} \\ \frac{\partial v}{\partial E} &= \begin{bmatrix} -\frac{|V|}{X'} \sin(\delta - \angle V) \\ 0 \\ 0 \end{bmatrix}\end{aligned}\quad (5.43)$$

Therefore, assuming that the internal state of the generator and the voltage phase of the generator bus are in the vicinity of the steady-state conditions, we obtain:

$$\bar{\Theta}^{\text{int}} := \begin{bmatrix} -\frac{E^*|V^*|}{X'} \cos(\delta^* - \angle V^*) & 0 & -\frac{|V^*|}{X'} \sin(\delta^* - \angle V^*) \\ -\left(\frac{X}{X'} - 1\right) |V^*| \sin(\delta^* - \angle V^*) & 0 & 0 \\ 0 & 0 & 0 \end{bmatrix} \quad (5.44)$$

Here, the steady-state values of the internal state (δ^*, E^*) of the generator and the steady-state value of the bus voltage phase ($|V^*|, \angle V^*$) are the same as those of (v^*, w^*) in Equation 5.39 under the steady-state conditions. By using the matrix $\bar{\Theta}^{\text{int}}$ in Equation 5.44, we can model the "local feedback structure that the internal state of the generator itself exerts". Since the normal power system is operated in the vicinity of the steady-state conditions, the steady-state values required for modeling can be identified based on measured data.

Next, let's consider estimating the indirect effect that signal w has on signal v through automatic generation control. The partial derivative of v with respect to the input P_{mech} of automatic generation control is given by:

$$\frac{\partial v}{\partial P_{\text{mech}}} = \begin{bmatrix} 1 \\ 0 \\ 0 \end{bmatrix}$$

When the broadcast-type PI controller in Equation 5.4 is incorporated as automatic generation control, the time integral of $\omega_0 \Delta \omega$ corresponds to δ , so we have:

$$\frac{\partial P_{\text{mech}}}{\partial \delta} = -\frac{\alpha \beta k_I}{\omega_0}, \quad \frac{\partial P_{\text{mech}}}{\partial \Delta \omega} = -\alpha \beta k_P, \quad \frac{\partial P_{\text{mech}}}{\partial E} = 0$$

Therefore, by the chain rule of differentiation, the effect of signal w on signal v through the broadcast-type PI controller can be modeled as:

$$\overline{\Theta}^{\text{agc}} := -\alpha \beta \begin{bmatrix} \frac{k_I}{\omega_0} & k_P & 0 \\ 0 & 0 & 0 \\ 0 & 0 & 0 \end{bmatrix} \quad (5.45)$$

Note that to obtain this parameter, it is necessary to obtain the values of the controller gains for automatic generation control through an appropriate method.

Similarly, let us consider estimating the indirect effect of signal w on signal v through the bus voltage phasor \mathbf{V} . The partial derivatives of v with respect to the voltage phasor variables ($|V|$, $\angle V$) are given by:

$$\begin{aligned} \frac{\partial v}{\partial |V|} &= \begin{bmatrix} -\frac{E}{X'} \sin(\delta - \angle V) \\ (\frac{X}{X'} - 1) \cos(\delta - \angle V) \\ 1 \end{bmatrix} \\ \frac{\partial v}{\partial \angle V} &= \begin{bmatrix} \frac{E|V|}{X'} \cos(\delta - \angle V) \\ (\frac{X}{X'} - 1) |V| \sin(\delta - \angle V) \\ 0 \end{bmatrix} \end{aligned} \quad (5.46)$$

On the other hand, as analyzed in Section 2.3.3, the bus voltage phase not only depends on the internal state of the connected generator but also on the internal states of all other generators. Specifically, let $\bar{\delta}$ and \bar{E} denote the vector of internal states of all generators except the one of interest. Then, the four partial derivatives $\frac{\partial |V|}{\partial \delta}$, $\frac{\partial \angle V}{\partial \delta}$, $\frac{\partial |V|}{\partial E}$, and $\frac{\partial \angle V}{\partial E}$ depend on the vector z_G that combines the internal states of all generators as:

$$z_G := (\delta, \bar{\delta}, E, \bar{E})$$

While it is difficult to obtain analytical expressions for these partial derivatives for general power system models, if we can measure the numerical values of the following matrix in the neighborhood of the steady-state power flow z_G^* using measurement data:

$$\theta := \begin{bmatrix} \frac{\partial |V|}{\partial \delta}(z_G^*) & 0 & \frac{\partial |V|}{\partial E}(z_G^*) \\ \frac{\partial \angle V}{\partial \delta}(z_G^*) & 0 & \frac{\partial \angle V}{\partial E}(z_G^*) \end{bmatrix} \quad (5.47)$$

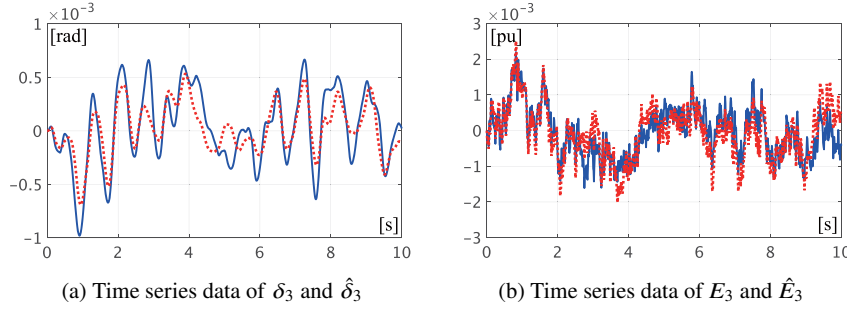


Fig. 5.15 Time response to random excitation input
(Blue solid line: δ_3, E_3 , Red dashed line: $\hat{\delta}_3, \hat{E}_3$)

then we can model the indirect effect of signal w on signal v through the bus voltage phase \mathbf{V} as:

$$\bar{\Theta}^{\text{ext}} := \begin{bmatrix} -\frac{E^*}{X'} \sin(\delta^* - \angle V^*) & \frac{E^* |V^*|}{X'} \cos(\delta^* - \angle V^*) \\ \left(\frac{X}{X'} - 1\right) \cos(\delta^* - \angle V^*) & \left(\frac{X}{X'} - 1\right) |V^*| \sin(\delta^* - \angle V^*) \\ 1 & 0 \end{bmatrix} \hat{\theta} \quad (5.48)$$

where z_G^* in Equation 5.47 denotes the steady-state value of z_G .

The 0 element in the second column corresponds to $\frac{\partial |V|}{\partial \Delta \omega}$ and $\frac{\partial \angle V}{\partial \Delta \omega}$. Furthermore, $\hat{\theta}$ in Equation 5.48 represents the identified value of θ . $\bar{\Theta}^{\text{ext}}$ in Equation 5.48 models the "global feedback structure that the internal state of the generator exerts on itself," in contrast to $\bar{\Theta}^{\text{int}}$ in Equation 5.44, which models the local feedback structure.

It is necessary to identify the parameter $\hat{\theta}$ using data measured during operation, as the power system must always be operated stably. In control engineering, identifying subsystems within an operating feedback system is called "closed-loop identification" [42]. Closed-loop identification is often more difficult than identification when input excitation is possible, as it is generally not possible to freely excite the input of the system being identified.

When using all the estimates obtained from the aforementioned linearization approximations simultaneously, the model parameters in Equation 5.39 are composed of:

$$\bar{\Theta} = \bar{\Theta}^{\text{int}} + \bar{\Theta}^{\text{agc}} + \bar{\Theta}^{\text{ext}} \quad (5.49)$$

As previously explained, the retrofit controller in Equation 5.42 does not change the stability of the steady-state power flow for any matrix $\bar{\Theta}$. However, to maintain the predicted accuracy of the interaction signals obtained from the linearized environment model, it is desirable to update $\bar{\Theta}$ at appropriate intervals to respond to changes in the power flow state.

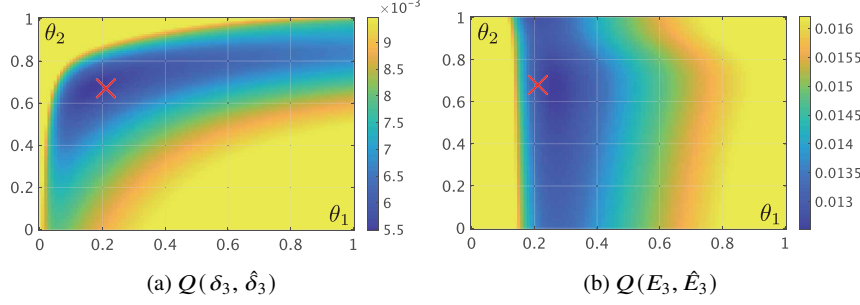


Fig. 5.16 Approximation error of internal state with respect to identification parameter

Example 5.6 Identification of approximate linear environment model based on measurement data

Similar to Example 5.4, we consider a power system model consisting of three buses, with the same AVR incorporated into generators 1 and 3. We also assume that a broadcast-type PI controller with parameter values given in Table 5.1(b) is incorporated as automatic generation control according to Equation (5.4). The steady-state power flow condition corresponds to the results of the power flow calculation in Table 3.2.

In the following, we focus on generator 3 and identify the values of partial derivatives of θ_3 in Equation 5.47 from measurement data. However, the magnitudes of $\frac{\partial|\mathbf{V}^3|}{\partial\delta_3}(zG^\star)$ and $\frac{\partial\angle\mathbf{V}^3}{\partial\delta_3}(zG^\star)$ are relatively small, so we identify only two values of θ_1 and θ_2 from the data, where:

$$\theta_1 := \frac{\partial|\mathbf{V}_3|}{\partial E_3}(z_G^\star), \quad \theta_2 := \frac{\partial\angle\mathbf{V}_3}{\partial\delta_3}(z_G^\star)$$

At this time, $\overline{\Theta}_3^{\text{ext}}$ in Equation 5.48 is parameterized as:

$$\overline{\Theta}_3^{\text{ext}} = \begin{bmatrix} \frac{E_3^\star|\mathbf{V}_3^\star|}{X'_3}\Delta_3^{\cos\theta_2} & 0 & -\frac{E_3^\star}{X'_3}\Delta_3^{\sin\theta_1} \\ \left(\frac{X_3}{X'_3}-1\right)|\mathbf{V}_3^\star|\Delta_3^{\sin\theta_2} & 0 & \left(\frac{X_3}{X'_3}-1\right)\Delta_3^{\cos\theta_1} \\ 0 & 0 & \theta_1 \end{bmatrix} \quad (5.50)$$

where Δ_3^{\sin} and Δ_3^{\cos} are constants defined by:

$$\Delta_3^{\sin} := \sin(\delta_3^\star - \angle\mathbf{V}_3^\star), \quad \Delta_3^{\cos} := \cos(\delta_3^\star - \angle\mathbf{V}_3^\star)$$

The optimization of the parameters (θ_1, θ_2) is carried out using the following procedure. Time series data of (δ_3, E_3) obtained by randomly exciting the input $V_{\text{pss}3}$ of the AVR is obtained from the power system model. Furthermore, a controller design model G_3^+ for the feedback system of the local linear subsystem G_3 and the approximate linear environmental model parameters $\overline{\Theta}_3$ of Equation 5.36 is constructed for

generator 3 using Equation 5.40. Here, $\bar{\Theta}_3$ is defined by Equation 5.49. Then, time series data of $(\hat{\delta}_3, \hat{E}_3)$ are obtained as the first and third elements of \hat{y}_3 when the signal used to excite $V_{\text{pss}3}$ is applied as the input \hat{u}_3 of Equation 5.40. The parameters (θ_1, θ_2) are optimized such that for all time instants t in the time interval where the data is obtained, $\hat{\delta}_3(t)$ and $\hat{E}_3(t)$ are good approximations of $\delta_3(t)$ and $E_3(t)$, respectively.

The time series data of (δ_3, E_3) is shown for the period from 0 [s] to 10 [s] when $V_{\text{pss}3}$ is randomly excited, as indicated by the blue line in Figure 5.15. However, the deviations from the steady-state values (δ_3^*, E_3^*) are also shown. The results of an exhaustive search for the optimal parameters (θ_1, θ_2) on an evenly spaced grid with a width of 0.01 for this data are shown in Figure 5.16. The horizontal and vertical axes represent the values set for θ_1 and θ_2 , respectively, and the colors in regions (a) and (b) represent the values of the error functions $Q(\delta_3, \hat{\delta}_3)$ and $Q(E_3, \hat{E}_3)$, respectively.

Here, the error function $Q(x, \hat{x})$ is defined as follows:

$$Q(x, \hat{x}) := \sum_{k=1}^{1000} \left\| x \left(\frac{k}{100} \right) - \hat{x} \left(\frac{k}{100} \right) \right\|^2$$

It evaluates the error of the continuous-time signal $x(t)$ for $t \in [0, 10]$ with respect to the discrete-time signal $\hat{x}(t)$ sampled at 1,000 points with a period of 0.01 [s].

Based on these results, the parameter values are set to $(0.215, 0.675)$. Note that this parameter value corresponds to the "x" mark in Figure 5.16. The time series data of $(\hat{\delta}_3, \hat{E}_3)$ for this parameter setting is shown as the red dashed line in Figure 5.15. It can be seen that the behavior of the internal state of generator 3 is captured by the obtained approximate linear environment model.

In Example 5.6, the parameters of the approximate linear environment model are identified as the index of the precision by which the internal state of the generators is approximated. The effect of the retrofit control based on this identification method is presented in Chapter 6.

Chapter 6

Numerical simulation examples of a large-scale model

In this Chapter, we apply the fundamentals explained so far to perform numerical simulations of a standard large-scale model called the IEEE 68-bus system model. The structure of this chapter is as follows. First, in Section 6.1, we organize the numerical data of transmission lines, loads, and generators in the IEEE 68-bus system model. Next, in Section 6.2, we analyze the effect of automatic generation control on load fluctuations. Specifically, we analyze the changes in generator and bus variables when the load impedance changes gradually over a few hours. Finally, in Section 6.3, we analyze the transient stability of the system with respect to bus grounding. In particular, we demonstrate that incorporating system stabilizing devices independently designed for each generator based on retrofit control theory can significantly improve system stability.

6.1 Power system model under consideration

6.1.1 IEEE68 bus system model

In this section, we present numerical simulation results using the IEEE68 bus power system model (Figure 6.1). This model consists of 68 buses, with generators connected to 16 buses and loads connected to 35 buses. The "Area 1" in Figure 6.1 represents the power system in the northeastern United States, while "Area 2" represents the power system in the state of New York. In addition, Areas 3 to 5 represent the power systems around New York State, each represented by one set of generators and loads.

The transmission lines are modeled considering the ground capacitance as explained in Section 2.2.2. The constants of each transmission line are set to the values shown in Table 6.1. The first column shows the bus numbers at both ends of the transmission line, and the second, third, and fourth columns show the resistance, reactance, and ground capacitance values of the transmission line, respectively. These

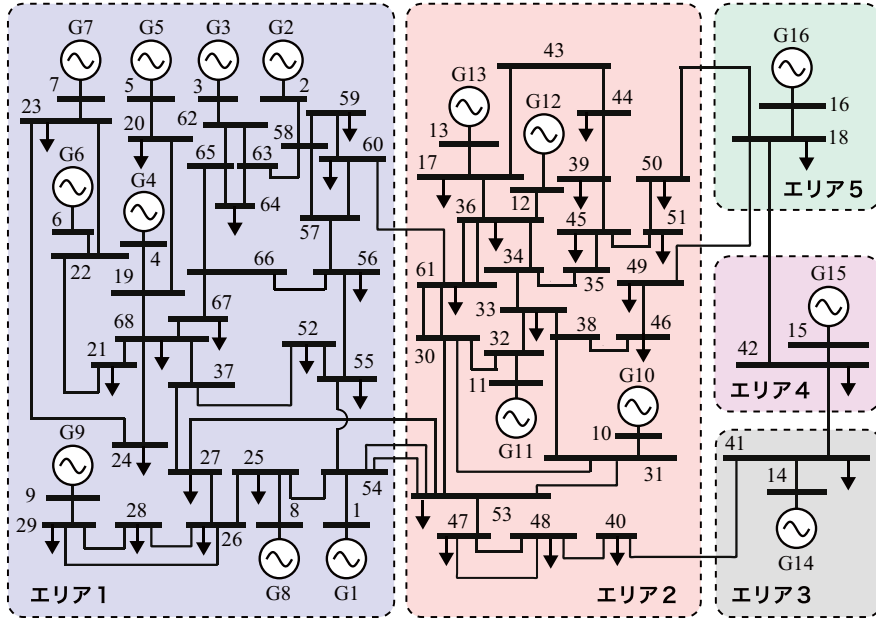


Fig. 6.1 IEEE68 bus system model

are standard values shown in [34, Appendix A]. Furthermore, we use the salient-pole generator model explained in Section 2.3.7 for the generators. The constants for each generator are set to the values shown in Table 6.2, which are also shown in the aforementioned literature.

6.1.2 Data sheet for power flow calculation

The data sheets for the generator buses used in power flow calculations are shown in Table 6.3. Similarly, the data sheet for the load buses is shown in Table 6.4. These values are also cited from [34, Appendix A].

6.1.3 Load model

The constant impedance load model described in Section 2.4.1 is adopted for the load model. The impedance values of the loads determined from the power flow calculation results for the data sheets in Table 6.3 and Table 6.4 are shown in Table

6.5. Note that bus 16 is set as the slack bus, and the value of P_{16}^* is calculated as 33.68.

6.2 Frequency stability analysis for load fluctuations

6.2.1 Load fluctuation settings

In this section, we observe the time response of the angular frequency deviation when the impedance values of the loads are changed. The impedance values of the loads are increased linearly by 10% per hour based on the values in Table 6.5. That is, the impedance of each load is set as:

$$z_{\text{load}i}(t) = \left(1 + \frac{1}{36000}t\right) (r_{\text{load}i} + jx_{\text{load}i}) \quad (6.1)$$

where t is the time in [s].

6.2.2 When the machine input and field input of the generator are constant

Consider the case where both the mechanical and excitation inputs to the generator, which are external inputs, are constant. From the steady-state power flow solution given in the data sheets of Table 6.3 and Table 6.4, the time response of the frequency deviation for all generators is shown in Figure 6.2(a) when the impedance of the load changes according to Equation 6.1. In this case, since the load disturbance causes an imbalance in supply and demand, the frequency deviation does not converge to zero. Moreover, due to the increase in power consumption as the impedance of the load increases, the frequency deviation initially increases in the negative direction for about 7 seconds, and then diverges in the positive direction as the power system model becomes unstable.

6.2.3 Case where the Mechanical Input is Constant

Consider the case where an automatic voltage regulator that controls the excitation input of the generator and a power system stabilizer are installed in all generators. The automatic voltage regulator is set to the IEEE ST1 model described in Section 5.3.2. Specifically, for all generator buses i , it is set to:

$$\begin{aligned} 0.015\dot{V}_{\text{tri}} &= -V_{\text{tri}} + |V_i| \\ V_{\text{field}i} &= 20(V_{\text{ref}i}^* + V_{\text{pssi}} - V_{\text{tri}}) \end{aligned}$$

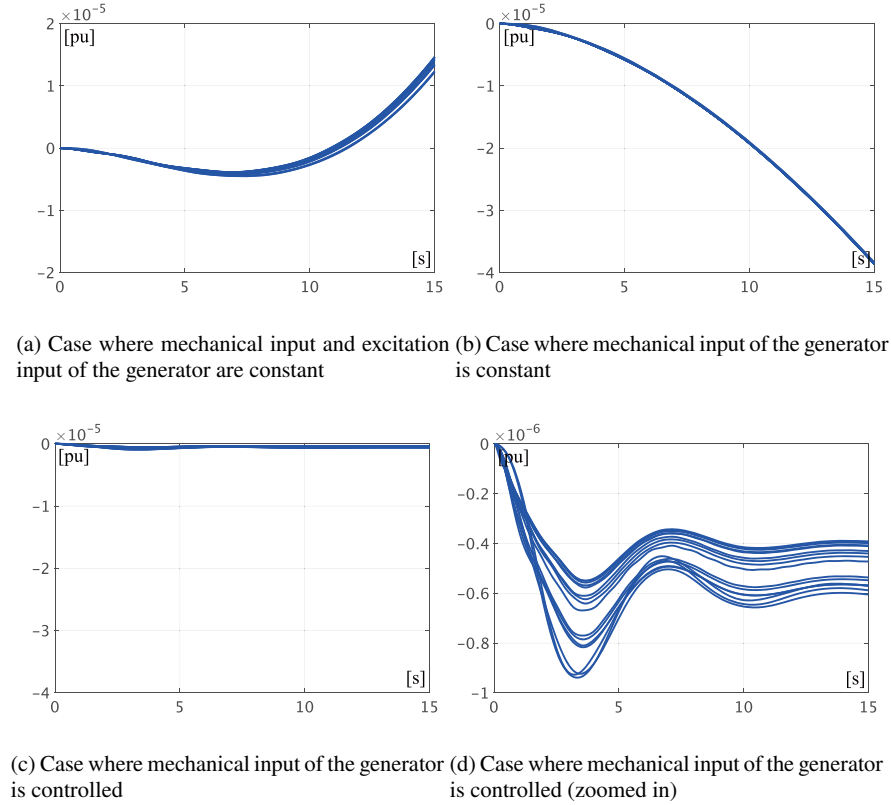


Fig. 6.2 Time response of angular frequency deviation to load variation

In addition, the power system stabilizer is set to the IEEE PSS1 model described in Section 5.3.4. Specifically, for all generator buses i , it is set to:

$$\begin{aligned} 1.4\dot{\xi}_{wsi} &= -\xi_{wsi} + 9.5\Delta\omega_i 0.033\dot{\xi}_i = -\xi_i + 0.79v_{wsi} \\ v_{wsi} &= 9.5\Delta\omega_i - \xi_{wsi} \quad V_{pssi} = 4.67(v_{wsi} - \xi_i) \end{aligned}$$

The time response of the frequency deviation in this case is shown in Figure 6.2(b). Similar to Figure 6.2(a), it can be seen that due to load fluctuations, the supply-demand balance is not satisfied, and the frequency deviation does not become zero. Note that the mechanical input of the generator is also set to be constant for all generators, as described in Section 6.2.2.

6.2.4 Case where machine input is controlled by an automatic generation controller

Consider incorporating an automatic generator control to control the mechanical input of a generator. Here, for each area in Figure 6.1, we will incorporate the broadcast-type PI controller explained in Section 5.1.1. Specifically, let $\mathcal{I}_G^{(l)}$ denote the index set of generator buses in area l . Then, for the automatic generator control in area l , we set:

$$\begin{aligned}\dot{\xi}^{(l)} &= \Delta\omega_{\text{ave}}^{(l)} \\ P_{\text{mech}i} &= P_i^* - \frac{P_i^*}{P_{\text{ave}}^*} \left(100\Delta\omega_{\text{ave}}^{(l)} + 500\xi^{(l)} \right), \quad i \in \mathcal{I}_G^{(l)}\end{aligned}$$

where we define the average of the deviation of angular frequency and the average of the active power in steady-state for the generators in area l as follows:

$$\Delta\omega_{\text{ave}}^{(l)}(t) := \frac{1}{|\mathcal{I}_G^{(l)}|} \sum_{i \in \mathcal{I}_G^{(l)}} \Delta\omega_i(t), \quad P_{\text{ave}}^* := \frac{1}{16} \sum_{i=1}^{16} P_i^*$$

It is assumed that each generator is equipped with an automatic voltage regulator as explained in Section 6.2.3.

The time response of the frequency deviation in this case is shown in Figure 6.2(c). Note that Figure 6.2(d) is an enlarged version of the y-axis scale. As a result of the automatic generation control, it can be seen that the frequency deviation is maintained around 0. Although the impedance value of the load continues to change, the frequency deviation does not become exactly 0, but remains at a small value of about -1×10^{-6} [pu].

Next, the changes in generator variables and bus variables from the initial time to 3 hours later are shown in Figure 6.3. Figures 6.3(a)-(d) represent the changes in $E_i e^{j\delta_i}$, V_i , I_i , and $P_i + jQ_i$, respectively, on a polar coordinate plane. The circle marks indicate the values at the initial time $t = 0$, and the square marks indicate the values at the final time $t = 10800$. The following can be observed from this figure:

- Figure 6.3(a):The internal voltage of all generators is maintained at around 0.7 to 1.5 [pu], and the rotor angle changes gradually in a clockwise direction.
- Figure 6.3(b):The absolute value of the bus voltage is maintained around 1 [pu], and its phase changes gradually in a clockwise direction like the rotor angle.
- Figure 6.3(c):The absolute value of the bus current increases as the consumption power increases with the increase in the impedance value of the load.
- Figure 6.3(d):As the impedance value of the load increases, the supplied active power and reactive power to the bus increase.

From these results, it can be seen that frequency stabilization is appropriately achieved by automatic generation control. In addition, for gradual load changes, it can be seen that the internal state of the generators changes gradually without oscillation, i.e., the entire power system is in a quasi-steady state.

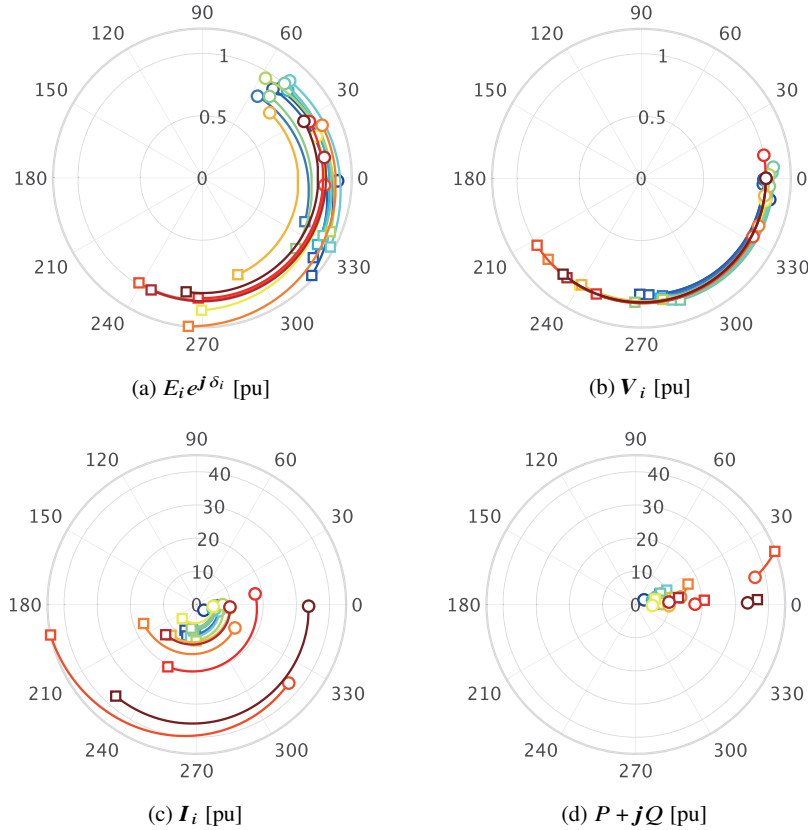


Fig. 6.3 Changes in generator and bus variables due to load variations.
(Circle: initial time, square: end time)

6.3 Transient stability analysis for bus ground faults

6.3.1 Setting of ground fault

In this section, we conduct a transient stability analysis of bus grounding. The transient stability of a power system is evaluated as follows: Let $\Delta\omega_i^{(k)}$ denote the angular frequency deviation of generator i at bus k caused by a ground fault. Then, the sensitivity of the angular frequency deviation of the entire power system to the grounding of bus k is evaluated by the \mathcal{L}_2 -norm of $\Delta\omega^{(k)}$, where $\Delta\omega^{(k)}$ is a vector consisting of the angular frequency deviations $\Delta\omega_1^{(k)}, \dots, \Delta\omega_{16}^{(k)}$ of all generators at bus k . Furthermore, we define the sets of $\|\Delta\omega^{(k)}\|_{\mathcal{L}2}$ for all generator buses and load buses, respectively, as

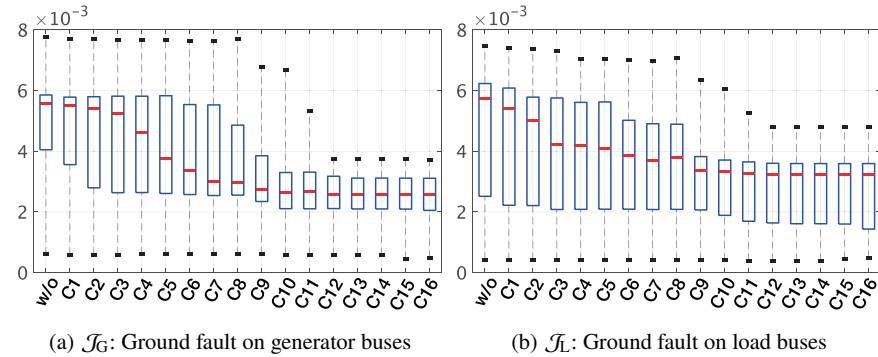


Fig. 6.4 Evaluation of system stability with respect to bus ground fault

$$\mathcal{J}_G := \left\{ \|\Delta\omega^{(k)}\|_{\mathcal{L}_2} \right\}_{k \in \{1, \dots, 16\}}, \quad \mathcal{J}_L := \left\{ \|\Delta\omega^{(k)}\|_{\mathcal{L}_2} \right\}_{k \in \{17, \dots, 68\}}$$

Considering that a ground fault can occur at any bus, not just a specific bus, the transient stability of bus grounding can be evaluated by considering the smallness of the data sets \mathcal{J}_G and \mathcal{J}_L in an appropriate sense. In this section, we use the maximum value, minimum value, and quartiles of \mathcal{J}_G and \mathcal{J}_L shown in box plots to compare the transient stability, in order to visualize the size of the data dispersion. Note that the duration of the ground fault is set to 70 [ms] for all buses.

First, we analyze the transient stability when all generators are equipped with standard automatic voltage regulators and system stabilizers. The parameter settings are the same as in Section 6.2.3. The results of the obtained data sets \mathcal{J}_G and \mathcal{J}_L displayed as boxplots are shown in the first column of Figure 6.4. Figure 6.4(a) shows \mathcal{J}_G regarding the ground fault on the generator bus, and Figure 6.4(b) shows \mathcal{J}_L regarding the ground fault on the load bus. Subsequently, we evaluate the improvement of transient stability due to the addition of local controllers based on these values as a reference.

6.3.2 Effect of power system stabilizers bassed on retrofit control theory

We analyze the transient stability when power system stabilizers based on the retrofit control theory explained in Section 5.4 are incorporated into each generator. The retrofit controllers incorporated into each generator use the parameters of the approximate linear environment model identified from measurement data using the procedure described in Example 5.6. In addition to the automatic voltage regulator,

the model of the power system stabilizer is also used in the local linear subsystem G_i . Furthermore, the controller that stabilizes each design model G_i^+ is designed based on the linear quadratic regulator design method explained in Section 5.4.2.

In this case, we show the results of displaying the obtained data sets \mathcal{J}_G and \mathcal{J}_L as box-and-whisker plots in the second to seventeenth columns of Figure 6.4. The horizontal axis "C*i*" represents the case where retrofit controllers are incorporated into all generators from generator 1 to generator *i*. From these results, we can see that the transient stability gradually improves as the number of retrofit controllers incorporated increases.

Table 6.1 Physical constants of transmission lines

$i-j$	r_{ij}	x_{ij}	c_{ij}	$i-j$	r_{ij}	x_{ij}	c_{ij}
1–54	0	0.0181	0	33–34	0.0011	0.0157	0.2020
2–58	0	0.0250	0	33–38	0.0036	0.0444	0.6930
3–62	0	0.0200	0	34–35	0.0001	0.0074	0
4–19	0.0007	0.0142	0	34–36	0.0033	0.0111	1.4500
5–20	0.0009	0.0180	0	35–45	0.0007	0.0175	1.3900
6–22	0	0.0143	0	36–61	0.0022	0.0196	0.3400
7–23	0.0005	0.0272	0	36–61	0.0022	0.0196	0.3400
8–25	0.0006	0.0232	0	37–52	0.0007	0.0082	0.1319
9–29	0.0008	0.0156	0	37–68	0.0007	0.0089	0.1342
10–31	0	0.0260	0	38–46	0.0022	0.0284	0.4300
11–32	0	0.0130	0	39–44	0	0.0411	0
12–36	0	0.0075	0	39–45	0	0.0839	0
13–17	0	0.0033	0	40–41	0.0060	0.0840	3.1500
14–41	0	0.0015	0	40–48	0.0020	0.0220	1.2800
15–42	0	0.0015	0	41–42	0.0040	0.0600	2.2500
16–18	0	0.0030	0	43–44	0.0001	0.0011	0
17–36	0.0005	0.0045	0.3200	44–45	0.0025	0.0730	0
17–43	0.0005	0.0276	0	45–51	0.0004	0.0105	0.7200
18–42	0.0040	0.0600	2.2500	46–49	0.0018	0.0274	0.2700
18–49	0.0076	0.1141	1.1600	47–48	0.0025	0.0268	0.4000
19–20	0.0007	0.0138	0	47–48	0.0025	0.0268	0.4000
19–68	0.0016	0.0195	0.3040	47–53	0.0013	0.0188	1.3100
21–22	0.0008	0.0140	0.2565	50–51	0.0009	0.0221	1.6200
21–68	0.0008	0.0135	0.2548	52–55	0.0011	0.0133	0.2138
22–23	0.0006	0.0096	0.1846	53–54	0.0035	0.0411	0.6987
23–24	0.0022	0.0350	0.3610	54–55	0.0013	0.0151	0.2572
24–68	0.0003	0.0059	0.0680	55–56	0.0013	0.0213	0.2214
25–26	0.0032	0.0323	0.5310	56–57	0.0008	0.0128	0.1342
25–54	0.0070	0.0086	0.1460	56–66	0.0008	0.0129	0.1382
26–27	0.0014	0.0147	0.2396	57–58	0.0002	0.0026	0.0434
26–28	0.0043	0.0474	0.7802	58–59	0.0006	0.0092	0.1130
26–29	0.0057	0.0625	1.0290	57–60	0.0008	0.0112	0.1476
27–37	0.0013	0.0173	0.3216	59–60	0.0004	0.0046	0.0780
27–53	0.0320	0.3200	0.4100	60–61	0.0023	0.0363	0.3804
28–29	0.0014	0.0151	0.2490	58–63	0.0007	0.0082	0.1389
30–31	0.0013	0.0187	0.3330	62–63	0.0004	0.0043	0.0729
30–32	0.0024	0.0288	0.4880	62–65	0.0004	0.0043	0.0729
30–53	0.0008	0.0074	0.4800	63–64	0.0016	0.0435	0
30–61	0.0019	0.0183	0.2900	64–65	0.0016	0.0435	0
30–61	0.0019	0.0183	0.2900	65–66	0.0009	0.0101	0.1723
31–38	0.0011	0.0147	0.2470	66–67	0.0018	0.0217	0.3660
31–53	0.0016	0.0163	0.2500	67–68	0.0009	0.0094	0.1710
32–33	0.0008	0.0099	0.1680				

References

1. T. Sadamoto, A. Chakrabortty, T. Ishizaki, and J.-i. Imura. Dynamic modeling, stability, and control of power systems with distributed energy resources: Handling faults using two control

Table 6.2 Physical constants of generators

i	M_i	D_i	τ_i	X_{di}	X_{qi}	X'_{di}
1	42.0	4.00	10.20	0.100	0.069	0.031
2	30.2	9.75	6.56	0.295	0.282	0.070
3	35.8	10.00	5.70	0.250	0.237	0.053
4	28.6	10.00	5.69	0.262	0.258	0.044
5	26.0	3.00	5.40	0.330	0.310	0.066
6	34.8	10.00	7.30	0.254	0.241	0.050
7	26.4	8.00	5.66	0.295	0.292	0.049
8	24.3	9.00	6.70	0.290	0.280	0.057
9	34.5	14.00	4.79	0.211	0.205	0.057
10	31.0	5.56	9.37	0.169	0.115	0.046
11	28.2	13.60	4.10	0.128	0.123	0.018
12	92.3	13.50	7.40	0.101	0.095	0.031
13	248.0	33.00	5.90	0.030	0.029	0.006
14	300.0	100.00	4.10	0.018	0.017	0.003
15	300.0	100.00	4.10	0.018	0.017	0.003
16	225.0	50.00	7.80	0.036	0.033	0.007

Table 6.3 Datasheet for tidal current calculations (generator bus bar)

i	P_i^*	$ V_i^* $	i	P_i^*	$ V_i^* $	i	P_i^*	$ V_i^* $
1	2.50	1.045	7	5.60	1.063	13	35.91	1.011
2	5.45	0.980	8	5.40	1.030	14	17.85	1.000
3	6.50	0.983	9	8.00	1.025	15	10.00	1.000
4	6.32	0.997	10	5.00	1.010	16	40.00	1.000
5	5.05	1.011	11	10.00	1.000			
6	7.00	1.050	12	13.50	1.016			

- methods in tandem. *IEEE Control Systems Magazine*, Vol. 39, No. 2, pp. 34–65, 2019.
2. M. Mesbahi and M. Egerstedt. *Graph theoretic methods in multiagent networks*. Princeton University Press, 2010.
 3. P. W. Sauer, M. A. Pai, and J. H. Chow. *Power system dynamics and stability: with synchrophasor measurement and power system toolbox*. John Wiley & Sons, 2017.
 4. P. M. Anderson and A. A. Fouad. *Power system control and stability*. John Wiley & Sons, 2008.
 5. Y. Kuramoto. Self-entrainment of a population of coupled non-linear oscillators. In *International symposium on mathematical problems in theoretical physics*, pp. 420–422. Springer, 1975.
 6. Y. Kuramoto. *Chemical oscillations, waves, and turbulence*. Courier Corporation, 2003.
 7. F. Dorfler and F. Bullo. Synchronization and transient stability in power networks and nonuniform Kuramoto oscillators. *SIAM Journal on Control and Optimization*, Vol. 50, No. 3, pp. 1616–1642, 2012.
 8. F. Dörfler, M. Chertkov, and F. Bullo. Synchronization in complex oscillator networks and smart grids. *Proceedings of the National Academy of Sciences*, Vol. 110, No. 6, pp. 2005–2010, 2013.
 9. M. Nagata, N. Fujiwara, G. Tanaka, H. Suzuki, E. Kohda, and K. Aihara. Node-wise robustness against fluctuations of power consumption in power grids. *The European Physical Journal Special Topics*, Vol. 223, No. 12, pp. 2549–2559, 2014.
 10. T. Nishikawa and A. E. Motter. Comparative analysis of existing models for power-grid synchronization. *New Journal of Physics*, Vol. 17, No. 1, p. 015012, 2015.

Table 6.4 Datasheet used for tidal current calculations (load bus bar)

i	P_i^*	Q_i^*	i	P_i^*	Q_i^*	i	P_i^*	Q_i^*
17	-60.00	-3.00	35	0	0	53	-2.52	-1.19
18	-24.70	-1.23	36	-1.02	0.19	54	0	0
19	0	0	37	0	0	55	-3.22	-0.02
20	-6.80	-1.03	38	0	0	56	-2.00	-0.74
21	-2.74	-1.15	39	-2.67	-0.13	57	0	0
22	0	0	40	-0.65	-0.24	58	0	0
23	-2.48	-0.85	41	-10.00	-2.50	59	-2.34	-0.84
24	-3.09	0.92	42	-11.50	-2.50	60	-2.09	-0.71
25	-2.24	-0.47	43	0	0	61	-1.04	-1.25
26	-1.39	-0.17	44	-2.68	-0.05	62	0	0
27	-2.81	-0.76	45	-2.08	-0.21	63	0	0
28	-2.06	-0.28	46	-1.51	-0.29	64	-0.09	-0.88
29	-2.84	-0.27	47	-2.03	-0.33	65	0	0
30	0	0	48	-2.41	-0.02	66	0	0
31	0	0	49	-1.64	-0.29	67	-3.20	-1.53
32	0	0	50	-1.00	1.47	68	-3.29	-0.32
33	-1.12	0	51	-3.37	1.22			
34	0	0	52	-1.58	-0.30			

Table 6.5 Load impedance

i	$r_{\text{load}i}$	$x_{\text{load}i}$	i	$r_{\text{load}i}$	$x_{\text{load}i}$	i	$r_{\text{load}i}$	$x_{\text{load}i}$
17	-60.00	-3.00	35	0	0	53	-2.52	-1.19
18	-24.70	-1.23	36	-1.02	0.19	54	0	0
19	0	0	37	0	0	55	-3.22	-0.02
20	-6.80	-1.03	38	0	0	56	-2.00	-0.74
21	-2.74	-1.15	39	-2.67	-0.13	57	0	0
22	0	0	40	-0.65	-0.24	58	0	0
23	-2.48	-0.85	41	-10.00	-2.50	59	-2.34	-0.84
24	-3.09	0.92	42	-11.50	-2.50	60	-2.09	-0.71
25	-2.24	-0.47	43	0	0	61	-1.04	-1.25
26	-1.39	-0.17	44	-2.68	-0.05	62	0	0
27	-2.81	-0.76	45	-2.08	-0.21	63	0	0
28	-2.06	-0.28	46	-1.51	-0.29	64	-0.09	-0.88
29	-2.84	-0.27	47	-2.03	-0.33	65	0	0
30	0	0	48	-2.41	-0.02	66	0	0
31	0	0	49	-1.64	-0.29	67	-3.20	-1.53
32	0	0	50	-1.00	1.47	68	-3.29	-0.32
33	-1.12	0	51	-3.37	1.22			
34	0	0	52	-1.58	-0.30			

11. N. Tsolas, A. Arapostathis, and P. Varaiya. A structure preserving energy function for power system transient stability analysis. *IEEE Transactions on Circuits and Systems*, Vol. 32, No. 10, pp. 1041–1049, 1985.
12. P. Varaiya, F. F. Wu, and R.-L. Chen. Direct methods for transient stability analysis of power systems: Recent results. *Proceedings of the IEEE*, Vol. 73, No. 12, pp. 1703–1715, 1985.
13. H.-D. Chang, C.-C. Chu, and G. Cauley. Direct stability analysis of electric power systems using energy functions: theory, applications, and perspective. *Proceedings of the IEEE*, Vol. 83,

- No. 11, pp. 1497–1529, 1995.
14. H.-D. Chiang. *Direct methods for stability analysis of electric power systems: theoretical foundation, BCU methodologies, and applications*. John Wiley & Sons, 2011.
 15. P. Kundur. *Power system stability and control*. Tata McGraw-Hill Education, 1994.
 16. G. Kron. Tensor analysis of networks. *New York*, 1939.
 17. F. Dorfler and F. Bullo. Kron reduction of graphs with applications to electrical networks. *Circuits and Systems I: Regular Papers, IEEE Transactions on*, Vol. 60, No. 1, pp. 150–163, 2013.
 18. T. Athay, R. Podmore, and S. Virmani. A practical method for the direct analysis of transient stability. *IEEE Transactions on Power Apparatus and Systems*, No. 2, pp. 573–584, 1979.
 19. A. K. Singh and B. C. Pal. IEEE PES task force on benchmark systems for stability controls report on the 68-bus 16-machine 5-area system. *IEEE Power Energy Soc*, Vol. 3, , 2013.
 20. S. Metz. *Ruby* ., 9 2016.
 21. D. S. Bernstein. *Matrix mathematics: theory, facts, and formulas*. Princeton University Press, 2009.
 22. I. R. Petersen and A. Lanzon. Feedback control of negative-imaginary systems. *IEEE Control Systems Magazine*, Vol. 30, No. 5, pp. 54–72, 2010.
 23. J. Xiong, I. R. Petersen, and A. Lanzon. A negative imaginary lemma and the stability of interconnections of linear negative imaginary systems. *IEEE Transactions on Automatic Control*, Vol. 55, No. 10, pp. 2342–2347, 2010.
 24. P. Kokotović, H. K. Khalil, and J. O’reilly. *Singular perturbation methods in control: analysis and design*, Vol. 25. Society for Industrial Mathematics, 1987.
 25. A. C. Antoulas. *Approximation of large-scale dynamical systems*. Society for Industrial and Applied Mathematics, Philadelphia, PA, USA, 2005.
 26. B. D. Anderson. A system theory criterion for positive real matrices. *SIAM Journal on Control*, Vol. 5, No. 2, pp. 171–182, 1967.
 27. N. Kottenstette and P. J. Antsaklis. Relationships between positive real, passive dissipative, & positive systems. In *American Control Conference (ACC), 2010*, pp. 409–416. IEEE, 2010.
 28. G. H. Hines, M. Arcak, and A. K. Packard. Equilibrium-independent passivity: A new definition and numerical certification. *Automatica*, Vol. 47, No. 9, pp. 1949–1956, 2011.
 29. J. W. Simpson-Porco. Equilibrium-independent dissipativity with quadratic supply rates. *IEEE Transactions on Automatic Control*, Vol. 64, No. 4, pp. 1440–1455, 2019.
 30. N. Monshizadeh, P. Monshizadeh, R. Ortega, and A. v. d. Schaft. Conditions on shifted passivity of port-hamiltonian systems. *Systems & Control Letters*, Vol. 123, pp. 55–61, 2019.
 31. L. M. Bregman. The relaxation method of finding the common point of convex sets and its application to the solution of problems in convex programming. *USSR computational mathematics and mathematical physics*, Vol. 7, No. 3, pp. 200–217, 1967.
 32. S. Boyd and L. Vandenberghe. *Convex optimization*. Cambridge university press, 2004.
 33. I.-S. S. Board. Ieee recommended practice for excitation system models for power system stability studies. 2016.
 34. B. Pal and B. Chaudhuri. *Robust control in power systems*. Springer Science & Business Media, 2006.
 35. J. H. Chow, G. E. Boukarim, and A. Murdoch. Power system stabilizers as undergraduate control design projects. *IEEE Transactions on power systems*, Vol. 19, No. 1, pp. 144–151, 2004.
 36. T. Ishizaki, T. Sadamoto, J.-i. Imura, H. Sandberg, and K. H. Johansson. Retrofit control: Localization of controller design and implementation. *Automatica*, Vol. 95, pp. 336–346, 2018.
 37. T. Sadamoto, A. Chakrabortty, T. Ishizaki, and J.-i. Imura. Retrofit control of wind-integrated power systems. *Power Systems, IEEE Transactions on*, Vol. 33, No. 3, pp. 2804–2815, 2018.
 38. H. Sasahara, T. Ishizaki, T. Sadamoto, T. Masuta, Y. Ueda, H. Sugihara, N. Yamaguchi, and J.-i. Imura. Damping performance improvement for PV-integrated power grids via retrofit control. *Control Engineering Practice*, Vol. 84, pp. 92–101, 2019.
 39. T. Ishizaki, T. Kawaguchi, H. Sasahara, and J.-i. Imura. Retrofit control with approximate environment modeling. *Automatica*, Vol. 107, pp. 442–453, 2019.

Contents	227
----------	-----

40. T. Ishizaki, H. Sasahara, M. Inoue, T. Kawaguchi, and J.-i. Imura. Modularity-in-design of dynamical network systems: Retrofit control approach. *IEEE Transactions on Automatic Control*, 2021.
41. F. W. Fairman. *Linear control theory: the state space approach*. John Wiley & Sons, 1998.
42. L. Ljung. System identification. In *Signal analysis and prediction*, pp. 163–173. Springer, 1998.